Identification and Characterization of Novel Anti-leishmanial Compounds

Bilal Zulfiqar

Master of Philosophy, Doctor of Pharmacy

Discovery Biology

Griffith Institute for Drug Discovery

School of Natural Sciences

Griffith University

Submitted in fulfilment of the requirements of the degree of

Doctor of Philosophy

October 2017

ABSTRACT

Leishmaniasis is characterized as a parasitic disease caused by the trypanosomatid protozoan termed *Leishmania*. Leishmaniasis is endemic in 98 countries around the globe with increased cases of morbidity and mortality emerging each day. The mode of transmission of this disease is via the bite of a sand fly, genus *Phlebotomus* (Old World) and *Lutzomyia* (New World). The life cycle of *Leishmania* parasite exists between the sand fly (promastigote form) and the mammalian host (amastigote form). Leishmaniasis can be characterized as cutaneous, muco-cutaneous or visceral leishmaniasis based on clinical manifestations exhibited in infected individuals. Although leishmaniasis is treatable, it faces challenges largely due to emerging resistance and extensive toxicity for current drugs. Therapeutic efficacy varies depending upon the species, symptoms and geographical regions of the *Leishmania* parasite.

The drug discovery pipeline for neglected trypanosomatid diseases remains sparse. In particular, the field of leishmaniasis drug discovery has had limited success in translating potential drug candidates into viable therapies. Currently there are few compounds that are clinical candidates for leishmaniasis, it is therefore essential that new compounds that are active against *Leishmania* are identified and evaluated for their potential to progress through the drug discovery pipeline. In order to identify new therapeutics, it is imperative that robust, biologically relevant assays be developed for the screening of anti-leishmanial compounds. The currently available assays have low predictive compatibility and high attrition rate in the identification of the compounds.

In an aim to identify compounds with activity against *L. donovani* (MHOM/IN/80/DD8) promastigotes, a phenotypic, high-throughput, resazurin based 384-well viability based assay was successfully developed to estimate the effect of compound treatment on *L. donovani* DD8 parasites. Complementary cytotoxicity assays were also established to access the toxicological profile of the compounds. The assays developed are robust and reproducible, using standard statistical parameters to assess assay quality and suitability for use in high throughput screening (HTS) based drug discovery.

To identify compounds active against *L. donovani* DD8 parasites, two compound collections were evaluated, a synthetic scaffold and a natural product (NP) based library. A primary screen of the open scaffold library constituting 5560 structurally

diverse synthetic compounds was undertaken. Screening incorporated a promastigote viability assay (extracellular form) and a high-content intracellular amastigote imaging assay. Confirmation of activity was performed together with cytotoxicity studies against both THP-1 (host cell) and HEK-293 cell lines. The second library, Davis open access natural product-based (DOANP) library was tested against kinetoplastids (*Leishmania donovani* DD8, *Trypanosoma brucei brucei* and *Trypanosoma cruzi*) using high-throughput phenotypic assays. This library currently consists of 472 distinct compounds, the majority of which are natural products that have been obtained from Australian natural sources, such as endophytic fungi, plants, macrofungi and marine invertebrates.

The confirmed hits were prioritized based on structure activity relationships to identify potential analogues. Then the activities of these analogues were evaluated to access the *in vitro* effect of these compounds. Based on the anti-leishmanial activity and selectivity, two compounds identified from the synthetic scaffold library were selected to be taken further for characterization and biological profiling. Of these two compounds, the first compound **BZ1** exhibited an IC_{50} value of 0.59 ± 0.13 µM against the intracellular form (amastigote) of the parasite and IC_{50} value of 2.37 ± 0.85 µM against the extracellular form (promastigote) of *L. donovani* DD8 (Old World - Indian strain) parasites. The second compound **BZ1-I** demonstrated to have an IC_{50} of 0.57 ± 0.17 µM against intracellular amastigotes and an IC_{50} value of 0.60 ± 1.12 µM against promastigotes.

The two compounds were subjected to additional assays which included cidal/static effect, time to kill and pre-incubation studies. The mechanism of action studies were also conducted to assess whether the compounds induce apoptosis in parasites and their effect on mitochondrial morphology. Resistance was generated and confirmed for both the compounds in order to determine the target protein using whole genome sequencing technique. Compounds cytotoxicity was also determined against a cytotoxicity panel constituting of THP-1, HEK-293, HepG2, J774.1, Raw-264.1 cell lines to establish the safety profile. The lead molecules were subsequently progressed to Drug Metabolism and Pharmacokinetics (DMPK) and pH stability studies. In addition to the activity against the *L. donovani* DD8 (Old World - Indian strain) parasite, compounds also showed activity against other species and strains of the Old World and New World

parasites, namely *L. infantum* (Old World), *L. donovani* (Old World - Sudanese strain) and *L. infantum* (New World) amastigotes. The compounds were also shown to have *in vitro* activity against *T. brucei* species, *T. cruzi* and *Plasmodium falciparum* strains. Screening against the extracellular and intracellular forms of the parasite, as well as across a panel of leishmanial species, provides a unique activity profile for prioritizing the identified hits. These hit compounds provide urgently needed starting points for the development of novel lead series for future anti-leishmanial therapeutics.

STATEMENT OF ORIGINALITY

This work has not previously been submitted for a degree or diploma in any university. To the best of my knowledge and belief, the thesis contains no material previously published or written by another person except where due reference is made in the thesis itself.

Bilal Zulfiqar

TABLE OF CONTENTS

LIST OF FIGURES

LIST OF TABLES

PUBLICATIONS

Publications arising from research undertaken as part of this Ph.D. are listed below:

1. Zulfiqar, B., Shelper, T. B., & Avery, V. M. (2017). Leishmaniasis drug discovery: recent progress and challenges in assay development. *Drug Discovery Today*. *22*(10), 1516-1531.

2. Zulfiqar, B., Jones, A. J., Sykes, M. L., Shelper, T. B., Davis, R. A., & Avery, V. M. (2017). Screening a Natural Product-Based Library against Kinetoplastid Parasites. *Molecules*, *22*(10), 1715.

ORAL AND POSTER PRESENTATIONS

Zulfiqar, B; Shelper, T.B; Jones, A.J; Avery, V.M. ASMR Queensland Postgraduate Student Conference held on 31st May, 2017 in Brisbane, Australia (Oral).

Zulfiqar, B; Shelper, T.B; Jones, A.J; Avery, V.M. International Student Research Forum (ISRF) hosted by University of Nebraska Medical Center (UNMC), Omaha Nebraska USA from 4th to 8th June, 2017 (Oral).

Zulfiqar, B; Shelper, T.B; Jones, A.J; De Rycker, M; Maes, L; Freitas-Junior, L.H Avery, V.M. 6th World Congress on Leishmaniasis held in Toledo, Spain from 16th to 20th May, 2017 (Poster).

Zulfiqar, B; Shelper, T.B; Jones, A.J; Avery, V.M. Griffith Institute for Drug Discovery (GRIDD) Student Symposium help on 6th and 7th April, 2016 at GRIDD Griffith University, Brisbane, Australia (Oral).

Zulfiqar, B; Jones, A.J; Shelper, T.B; Avery, V.M. SLAS2017 6th Annual International Conference and Exhibition from February 4th to 8th, 2017 in Washington, DC. USA (Poster).

Zulfiqar, B; Jones, A.J; Shelper, T.B; Avery, V.M. Eskitis/SIMM Symposium on 1st and 2nd November 2016 held in Shanghai, China (Oral).

Zulfiqar, B; Jones, A.J; Shelper, T.B; Avery, V.M. International Congress for Tropical Medicine and Malaria held on 18th September, 2016 in Brisbane, Australia (Oral).

Zulfiqar, B; Jones, A.J; Shelper, T.B; Avery, V.M. Eskitis Student Symposium Student Symposium help on 14th and 15th April, 2016 at Eskitis Institute for Drug Discovery, Griffith University, Brisbane, Australia (Oral).

Zulfiqar, B; Jones, A.J; Shelper, T.B; Avery, V.M. Sao Paulo School of Advanced Science on Neglected Diseases Drug Discovery–focus on Kinetoplastids (SPSAS-ND3), Brazilian Centre for Research in Energy and Materials (CNPEM), Campinas, Brazil , from June 14th to 24th , 2015 (Poster).

Zulfiqar, B; Jones, A.J; Shelper, T.B; Avery, V.M. Eskitis Student Symposium Student Symposium help on 26th and 27th March, 2015 at Eskitis Institute for Drug Discovery, Griffith University, Brisbane, Australia (Oral).

AWARDS

1. 3rd Prize Oral Presentation at ASMR Queensland Postgraduate Student Conference held on 31st May, 2017 in Brisbane, Australia (AUD $200)

2. The Screening and Lab Automation (SLAS) Best Academic Poster Award, at SLAS2017 6th Annual International Conference and Exhibition, which was held in February 4th – 8th, 2017 in Washington, DC. USA. (USD $500)

3. Selected to represent Griffith University at International Student Research Forum (ISRF) hosted by University of Nebraska Medical Center (UNMC), Omaha Nebraska USA from 4th to 8th June, 2017. Airfares, accommodation and meals are all provided. (AUD $2500)

4. Received Tony. B travel award (all expenses paid) to present at SLAS2017 6th Annual International Conference and Exhibition, which was held in February 4th – 8th, 2017 in Washington, DC. USA (USD $2500)

5. Awarded all-expense paid travel bursary to attend Eskitis/SIMM Symposium on 1st and 2nd November 2016 held in Shanghai, China (AUD $2500)

6. Awarded a Griffith University International Experience Incentive Scheme (IEIS) Travel Grant on 27th October, 2016 for an overseas program at University of Antwerp, Belgium. (AUD $1500)

7. Awarded 2016 ASP student conference travel grant to attend International Congress for Tropical Medicine and Malaria held on 18th September, 2016 in Brisbane, Australia (AUD $750)

8. Awarded all-expense paid scholarship to attend "Sao Paulo School of Advanced Science on Neglected Diseases Drug Discovery–focus on Kinetoplastids (SPSAS-ND3)" taking place at The Brazilian Centre for Research in Energy and Materials (CNPEM), Campinas- Brazil, from June 14th to 24th, 2015. (USD $3000)

9. Griffith University International Postgraduate Research Scholarship [GUIPRS] (2014-2017). (AUD $92,400)

10. Griffith University Postgraduate Research Scholarship [GUPRS] (2014-2017). (AUD $88,872)

STATEMENT ACKNOWLEDGING THE EXTENT AND NATURE OF ANY ASSISTANCE RECEIVED IN THE PURSUIT OF THE RESEARCH

I would like to acknowledge the co-authors of the publications resulting from the research undertaken of this Ph.D. project. The design and development of this Ph.D. has been completed in consultation with my Ph.D. supervisor Professor Vicky Avery. The contributions of other to this work are detailed below:

I acknowledge my co-authors Dr. Todd Shelper and Professor Vicky Avery for their contribution to the publication "***Leishmaniasis drug discovery: recent progress and challenges in assay development***." This review provides an overview of the disease, current treatment options and compares the various technologies and assay formats currently available for anti-leishmanial drug discovery. The literature review from Chapter 1 was incorporated into the published review.

I acknowledge the contributions of the co-authors Dr. Amy Jones, Dr. Melissa Sykes, Dr. Todd Shelper, Associate Professor Rohan Davis and Professor Vicky Avery to the publication "***Screening a Natural Product-Based Library against Kinetoplastid Parasites***." The results from screening the Davis Open Access Natural Product (DOANP) library are described in the research completed as part of Chapter Four of this thesis and were incorporated into the manuscript.

I acknowledge the contributions of Dr. Amy Jones and Dr. Todd Shelper, who developed the intracellular amastigote assay that was used in the *in vitro* profiling of compound collections described in Chapter Four. I acknowledge the contribution or Associate Professor Rohan Davis for providing the DOANP library and Dr. Wendy Loa for her assistance with pH stability studies of compounds **BZ1** and **BZ1-I** using high-resolution liquid chromatography coupled with Fourier Transform Mass Spectrometry (HRLC/FT-MS).

I acknowledge the contributions of our collaborators; Professor Louis Maes from Laboratory for Microbiology, Parasitology and Hygiene (LMPH), University of Antwerp, Belgium, Professor Lucio H. Freitas-Junior from National Laboratory of Biosciences, National Center for Research on Energy and Materials, Campinas, São

Paulo, Brazil, Dr. Manu De Rycker from Drug Discovery Unit, University of Dundee, Dundee, Scotland for *in vitro* testing of compounds **BZ1** and **BZ1-I** for anti-leishmanial, anti-trypanosomal and anti-malarial activities conducted on our behalf.

I also acknowledge the contributions of Professor Susan Charman from Centre for Drug Candidate Optimization (CDCO), Monash University, Melbourne, Australia for the performing the Drug Metabolism and Pharmacokinetics (DMPK) studies on our behalf.

ACKNOWLEDGEMENTS

This project was carried out in the Discovery Biology laboratory at Griffith Institute for Drug Discovery (GRIDD), Griffith University.

First and foremost, I would like to express my sincere gratitude to my supervisor, Professor Vicky Avery for her constant guidance, encouragement and support throughout my Ph.D. I am profoundly grateful to her for providing me with the freedom to carry out this project on my own. I would also like to thank my co-supervisors Dr. Todd Shelper and Dr. Amy Jones for their contribution of time, ideas, moral support and effort to make my research experience productive and stimulating.

I would like to thank Ms. Angela Hillsdon for the administrative assistance and valuable feedback. I would also like to thank the past and present members of the Discovery Biology laboratory for their generous assistance, gracious co-operation and skillful advice throughout my research work. Many thanks to Dr. Melissa Sykes, Sandra Duffy, Dr. Tayner Rodriquez, Dr. Joshua Wingerd, Dr. Carrie Lovitt, Dr. Catalina Carrasco, Dr. Elke Kaemmerer, Dr. Leonardo Lucantoni, Aaron Lock, Elouise Gaylard, Kate Parsons, Thilini Perera and Mahreen Rasheed for their assistance.

I would like to thank Griffith University for awarding me the Griffith University International Postgraduate Research Scholarship and Griffith University Postgraduate Research Scholarship. I also wish to express gratitude to the following organizations; FAPESP, ASP, SLAS, GRIDD, ISRF and ASMR for awarding funding for me to attend national and international conferences and workshops, which contributed immensely to my professional development.

I owe my deepest gratitude to Thalita Camelo da Silva Ferreira and Bui Thi My Linh for all their moral support. Without their encouragement it would have been impossible for me to finish this work.

Lastly, I would like to thank my family and friends, particularly my mother for her prayers, support and frequent motivation in seeing me continue my research for such a good cause.

ABBREVIATIONS

ACR2	Arsenate reductase
ADME	Absorption, Distribution, Metabolism, and Elimination
AO	Acridine orange
AQP1	Aquaglyceroporin 1
ANOVA	Analysis of variance
BLA	β lactamase reporter assay
CL	Cutaneous leishmaniasis
cLogP	Logarithm of partition coefficient between n-octanol and water
CCL4	C-C motif ligand 4
CFSE	5-,6-carboxyfluorescein diacetate succinimidyl ester
CMI	Cell-mediated immune
CO_2	Carbon dioxide
CPRG	5-bromo-4-chloro-3-indolyl- β-Dgalactopyranoside
CXCL10	C-X-C motif ligand 10
DALYs	Disability adjusted life years
DHFR	Dihydrofolate reductasez
DHODH	Dihydroorotate dehydrogenase
DNA	Deoxyribonucleic acid
DMPK	Drug Metabolism and Pharmacokinetics
DMSO	Dimethyl sulfoxide

DMEM	Dulbecco's Modified Eagle Medium
DND*i*	Drugs for Neglected Diseases Initiative
DOANP	Davis open access natural product-based library
ECG	Electrocardiogram
EMEA	European Medicines Agency
FDA	Food and drug administration
FoxP3	Forkhead box protein 3
GFP	Green fluorescent protein
GHIT	Global Health Innovative Technology Fund
GNF	Genomic Institute of the Novartis Research Foundation
gp63	Glycoprotein 63
GPI	Glycosylphosphatidylinositol
GSH	Glutathione
GSK	GlaxoSmithKline
HAT	Human African trypanosomiasis
HCA	High content analysis
HCI	High content imaging
HCl	Hydrochloric Acid
HCS	High content screening
HEK-293	Human embryonic kidney cell line
HIFBS	Heat inactivated foetal bovine serum

HIV	Human immunodeficiency virus
HTS	High-throughput screening
IC_{50}	Half maximal inhibitory concentration
IFN-γ	Interferon gamma
IFNGR1	Interferon gamma receptor 1
IL-10	Interleukin 10
IPK	Institute Pasteur Korea
iRFP	Infrared fluorescent protein
L-AmB	Liposomal amphotericin B
L.	*Leishmania*
LdMT	*Leishmania* donovani miltefosine transporter
LdRos3	Beta subunit of LdMT
LOD	Limit of detection
LPG	Lipophosphoglycan
LYST	Lysosomal trafficking
luc	Luciferase
MCL	Mucocutaneous leishmaniasis
MDR1	Multidrug-resistant protein 1
MeOH	Methanol
MIC	Minimum inhibitory concentration
mL	Millilitre

mM	Millimolar
MMV	Medicines for Malaria Venture
MOA	Mechanism of action
MOI	Multiplicity of infection
MTT	3-(4,5-dimethylthiazol-2-yl)-2,5-diphenyltetrazolium bromide
nM	Nanomolar
NTDs	Neglected tropical diseases
ºC	Degree Celsius
OD	Optical density
PBS	Phosphate buffer saline
PCR	Polymerase chain reaction
PFA	Paraformaldehyde
PMA	Phorbol myristate acetate
PNPP	P-nitrophenyl phosphate
PKC	Protein kinase C
PKDL	Post-kala-azar dermal leishmaniasis
PPG	Proteophosphoglycan
PS	Phosphatidylserine
PSA	Polar surface area
PTR1	Pteridine reductase 1
PV	Parasitophorous vacuole

QFAB	Queensland Facility of Advanced Bioinformatics
RFP	Red fluorescent protein
RFU	Relative florescence intensity units
ROS	Reactive oxygen species
RPMI	Roswell Park Memorial Institute
SAG:	Sodium antimony gluconate
SAR	Structure–activity relationship
SbIII	Trivalent antimonials
SbV	Pentavalent antimonials
SCC	Saline-sodium-citrate
SD	Standard deviation
SEM	Standard error of mean
SI	Selectivity index
SSG	Sodium stibogluconate
TCP	Target candidate profile
TDR1	Thiol-dependent reductase
THP-1	Human acute monocytic leukemia cell line
TNF	Tumor necrosis factor
TPP	Target product profile
TR	Trypanothione reductase
Triton X	t-Octylphenoxylpolyethoxylethanol

USA	United States of America
v/v	Volume per volume
V.	*Viannia*
VL	Visceral leishmaniasis
w/v	Weight per volume
WHO	World Health Organization
WT	Wild type
%	Percentage
µl	Microliter
µM	Micromolar
µm	Microns

Chapter 1: General introduction

1.1. *Leishmania* - the parasite

Leishmaniasis is a parasitic disease caused by the trypanosomatid protozoans of the genus *Leishmania*. Leishmaniasis dates back to 2,500 B.C., with depictions of facial deformities and skin lesions observed on the pottery excavated from different regions of Peru and Ecuador, presumably from the pre-Incan period (Akhoundi, *et al.*, 2016). Alexander Russel in 1756 reported the first case of leishmaniasis in a Turkish patient and called it *Aleppo boil* (Hawgood, 2001). Aleppo is the city in Syria where ulcerative skin lesions were first observed in diseased individuals hence the name, *Aleppo boil*. In 1882, Cunningham identified the parasite for the first time in skin lesions of an Indian patient with *Delhi boil*, which were fixed in alcohol and stained with gentian violet (Cunningham, 1885). Later in 1900, *Leishmania* parasites were discovered by Sir William Leishman in the spleen smears of a dead soldier in Dum Dum, a populated municipality near Calcutta, India. He published his findings in 1903 (Leishman, 1903); Charles Donovan subsequently identified the same parasite in a human spleen biopsy (Donovan, 1903). The parasite *Leishmania donovani* was named in their honour and the amastigote forms of the parasite are commonly called Leishman-Donovan bodies.

1.1.1. Classification

Leishmania parasites are classified as: Kingdom *Protista*, Phylum *Euglenozoa*, Class *Kinetoplastea*, Subclass *Metakinetoplastina*, Order *Trypanosomatida*, Family *Trypanosomatidae*, Subfamily *Leishmaniinae*, and Genus *Leishmania* (Akhoundi, *et al.*, 2016). There are at least 29 species of the genus *Leishmania* which are identified based on genetic and biochemical differences. The *Trypanosomatidae* family is known mainly by two genera, *Trypanosoma* and *Leishmania*. *Trypanosoma* and *Leishmania* are digenetic parasites, whichmeans their life cycles involves two hosts, within a vertebrate host and an invertebrate vector (hematophagous insects) following zoonotic or anthroponotic transmission patterns (Handman and Bullen, 2002; Gluenz, *et al.*, 2010; Duque and Descoteaux, 2015). The parasite *Trypanosoma cruzi* is responsible for

Chagas disease, while *Trypanosoma brucei* is the causative agent of human African trypanosomiasis (HAT) (Field, *et al.*, 2017; Kaufer, *et al.*, 2017). According to the geographical area and clinical manifestations present in patients, *Leishmania* are classified as either Old World or New World (Lewis, 1971) (Figure 1.1). The disease distribution areas have been classified as "New World" when located in the Americas, and "Old World" referring to Africa, Asia and Europe (Kevric, *et al.*, 2015).

1.1.2. Parasite biology

The *Leishmania* parasite exists in two forms; promastigotes and amastigotes (Figure 1.2) (Handman, 1999). The promastigotes are morphologically different to amastigotes and are classified into 5 stages: procyclic, nectomonad, leptomonad, haptomonad and metacyclic promastigotes (Gossage *et al.*, 2003). Metacyclic promastigotes are regarded as the infective stage and have high adaptability for successful transmission within the human host (Kamhawi, 2006). As illustrated in Figure 1.2a, promastigotes are elongated with a nucleus in the centre and have a kinetoplast anteriorly positioned (Rodgers, *et al.*, 1990). Kinetoplast is a complex of maxi/mini DNA circles which lies within an extension of the mitochondrion. The promastigotes possess a flagellum which is used for propulsion of the parasite and attachment to the microvilli in the gut of the sand fly (Chang, 1979). Flagellum shape and size varies greatly between the different promastigotes stages, ranging from 8 to 12 μm in length (Rogers, *et al.*, 2002). In contrast, amastigotes (Figure 1.2b) are rounded and intracellular (Bates, 1993); residing within macrophages and other mononuclear phagocytic cells e.g. dendritic cells (Ambit, *et al.*, 2011), neutrophils (Ritter, *et al.*, 2009) and fibroblasts (Bogdan, *et al.*, 2000). Amastigotes have a short flagellum which extends from the basal body to the opening of the flagellar pocket and reside within host immune cells, from which they ultimately egress and invade neighbouring host immune cells, such as macrophages or dendritic cells (Sacks and Perkins, 1984).

The precise manner and mechanisms *Leishmania* parasites use to divide remains the source of great debate, as for years it was assumed that promastigotes and the amastigotes repeatedly divided longitudinally by binary fission (Tibayrenc, *et al.*, 1993). Rougeron *et al* proposed possible inbreeding between parasites leading to clonal/sexual reproduction (Rougeron, *et al.*, 2009). Genetic exchange has also been

demonstrated in sand fly species co-infected with two strains of *L. major* (Akopyants, *et al.*, 2009), and naturally occurring hybrid genotypes of *L. Vianni* subgenus have also been shown to coexist in field isolates (Banuls, *et al.*, 2007). Sequencing studies with *L. major* have depicted that genes involved in meiosis are conserved in the parasite (El-Sayed, *et al.*, 2005; Ivens, *et al.*, 2005), suggesting an extant cryptic sexual cycle also exists in *Leishmania* parasites (Heitman, 2006).

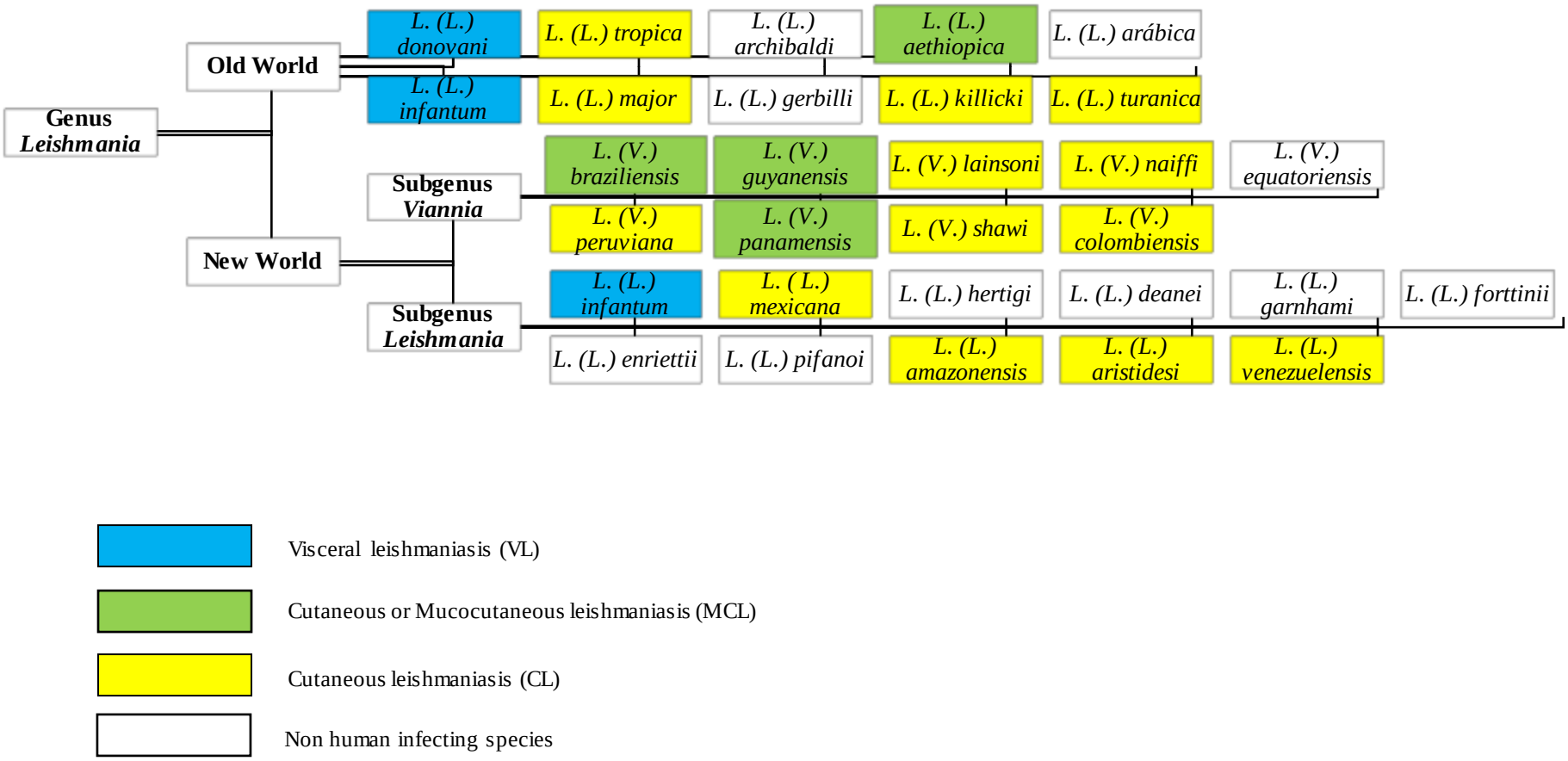

Figure 1.1: Known species of genus *Leishmania* (L) parasites. Subgenus *Leishmania* (L) and *Viannia* (V) found in the Old and New Worlds. Adapted from Akhoundi *et al*., 2016, PLoS neglected tropical diseases, 10, e0004349".

The rate of proliferation of the parasite depends on the parasite form (promastigote or amastigote), the species/strain and the experimental conditions (*in vitro* or *in vivo*). There are several reports with different doubling times; usually promastigotes multiply faster, followed by axenic amastigotes and intracellular amastigotes (Somanna, *et al.*, 2002; Debrabant, *et al.*, 2004; Wheeler, *et al.*, 2011). Kloehn *et al.* reported doubling times for *Leishmania mexicana* in different conditions: 0.37 days (~9 hours) for exponentially growing promastigotes; 4.19 days for axenic amastigotes; and ~12 days during *in vivo* infection in BALB/c mice (Kloehn, *et al.*, 2015). The culture conditions also modify doubling time of the parasite as *Leishmania major* promastigotes grow slower in RPMI medium with a doubling time of ~30 hours but exhibits a doubling time of ~9 hours in M199 medium (Mandell and Beverley, 2017).

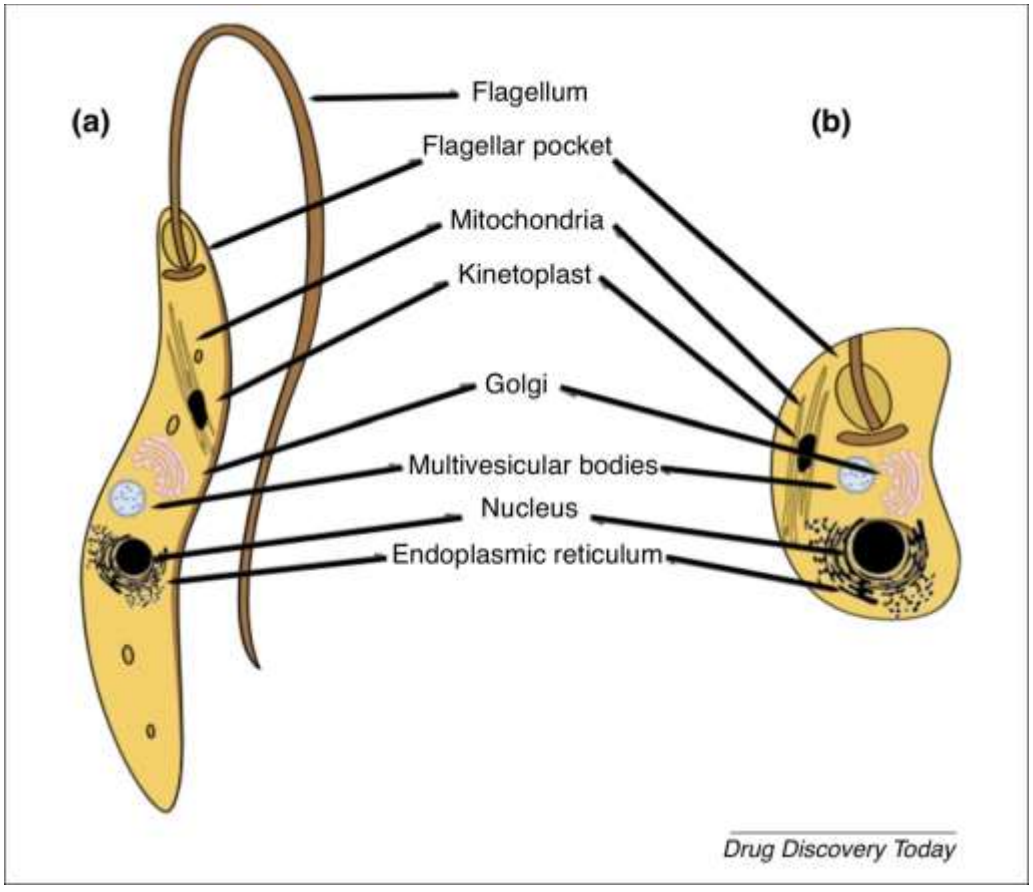

Figure 1.2: Diagram showing the intracellular components of Leishmania promastigotes on the left and the Leishmania amastigote on the right. Reproduced from "Leishmaniasis drug discovery: recent progress and challenges in assay development" *Drug Discovery Today*. 22(10), 1516-1531 (Zulfiqar, *et al.*, 2017), copyright (2017) with permission from Elsevier.

1.1.3. Biochemistry of the parasite

The cell biology and biochemistry of *Leishmania* parasites (Figure 1.3) is similar to other kinetoplastids (Stuart, *et al.*, 2008). Both promastigotes and amastigotes differ in terms of biochemical components (glycolytic enzymes and pathways (Meade, *et al.*, 1984; Castilla, *et al.*, 1995), utilization of fatty acids (Hart and Coombs, 1982), gene expression (Charest and Matlashewski, 1994), protein phosphorylation (Assefa, *et al.*, 1995), nucleases (Bates, 1993) and proteinases (Pral, *et al.*, 1993). The parasite coat for both the forms is made of glycosylated molecules and proteins are anchored by glycosylphosphatidylinositol (GPI) (Ralton, *et al.*, 2002; Kamhawi, 2006). In promastigotes, the most abundant surface molecule is lipophosphoglycan (LPG) (Kamhawi, 2006). Its structure varies from one *Leishmania* species to another but is mainly composed of repeating units of disaccharides and phosphates supported by GPI (Turco, *et al.*, 2001; Kamhawi, 2006). Species are differentiated from one another by the presence of side chains, composition and the position of glycans in the base structure of the LPG (Turco, *et al.*, 2001). The LPG in *L. major* is highly branched compared to *L. donovani* (McConville, *et al.*, 1995). The second largest molecule in the promastigote is the glycoprotein, gp63 (Yao, *et al.*, 2003). This is a metalloproteinase which requires the presence of zinc and has a wide variety of substrates including albumin, gelatin, fibrinogen, casein and haemoglobin (McMaster, *et al.*, 1994). The parasites are also able to secrete molecules such as acid phosphatases and proteophosphoglycans (PPG) (Handman and Bullen, 2002). The acid phosphatases function as hydrolytic enzymes that appear to play a role in the parasites resistance to available drugs, as well as in its pathogenicity (Croft, *et al.*, 2006; Duque and Descoteaux, 2015).

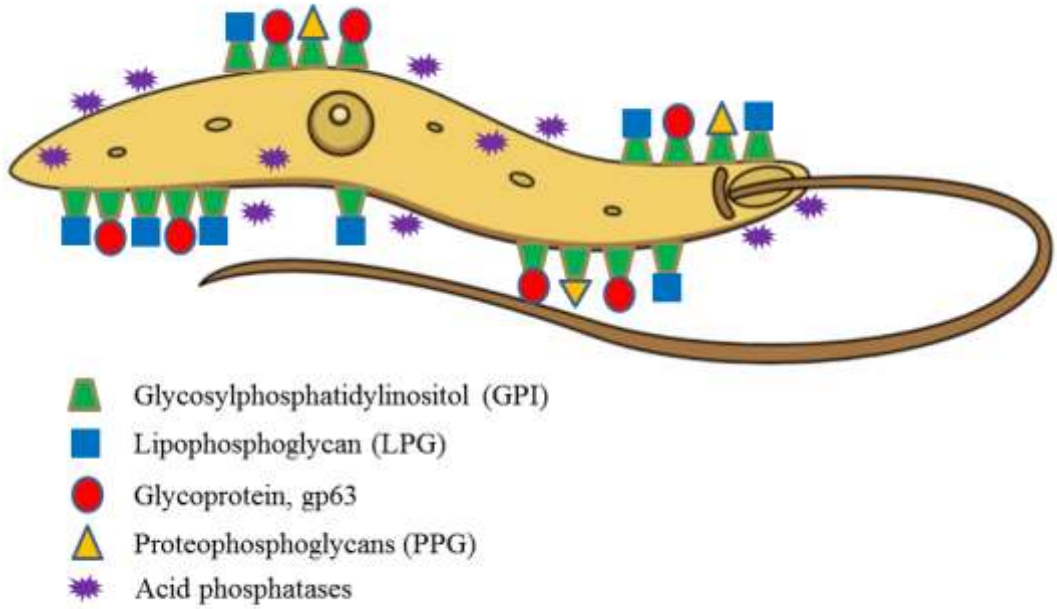

Figure 1.3: *Leishmania* promastigotes showing GPI, LPG, gp63, PPG and acid phosphatases.

1.1.4. Life cycle

The mode of transmission of the parasites responsible for leishmaniasis is via the bite of a sand fly, genus *Phlebotomus* in the old world and *Lutzomyia* in the new world (Stockdale and Newton, 2013). However, it is important to note that not all sand flies serve as vector reservoirs for the transmission of the *Leishmania* parasite (Akhoundi, *et al.*, 2016). The life cycle of *Leishmania* is digenetic (Handman and Bullen, 2002; Gluenz, *et al.*, 2010; Duque and Descoteaux, 2015), as illustrated in Figure 1.4.

The life cycle stages can be categorized as a) host infective stage in which the sand fly takes a blood meal, injecting the metacyclic promastigotes into the mammalian host. The first cells recruited to and infected in the dermal site of inoculation are neutrophils, followed by macrophages (Peters, *et al.*, 2008). The metacyclic promastigotes are then phagocytized by macrophages, initiating the b) host diagnostic stage, where the metacyclic promastigotes transform into amastigotes inside macrophages. Macrophages also uptake parasites released from apoptotic neutrophils and engulf infected cells,

which may inhibit the activation of infected macrophages in the inflammatory site (Ribeiro-Gomes and Sacks, 2012). Within the macrophage phagolysosome, which is a cytoplasmic body formed by fusion of phagosomes and lysosomes, metacyclic promastigotes transform into non-motile amastigotes. Amastigotes multiply and egress from macrophages subsequently invading new cells such as dendritic cells, neutrophils and fibroblasts, perpetuating parasite replication. When a sand fly takes a blood meal from an infected mammalian host, the macrophages infected with the amastigotes are ingested. The amastigotes are subsequently released from the cells, transforming into promastigotes in the mid gut of the sand fly. Promastigotes multiply in the midgut and migrate to the proboscis of the sand fly, where they transform into infective metacyclic promastigotes. Eventually metacyclic promastigotes are injected into the mammalian host and the cycle continues.

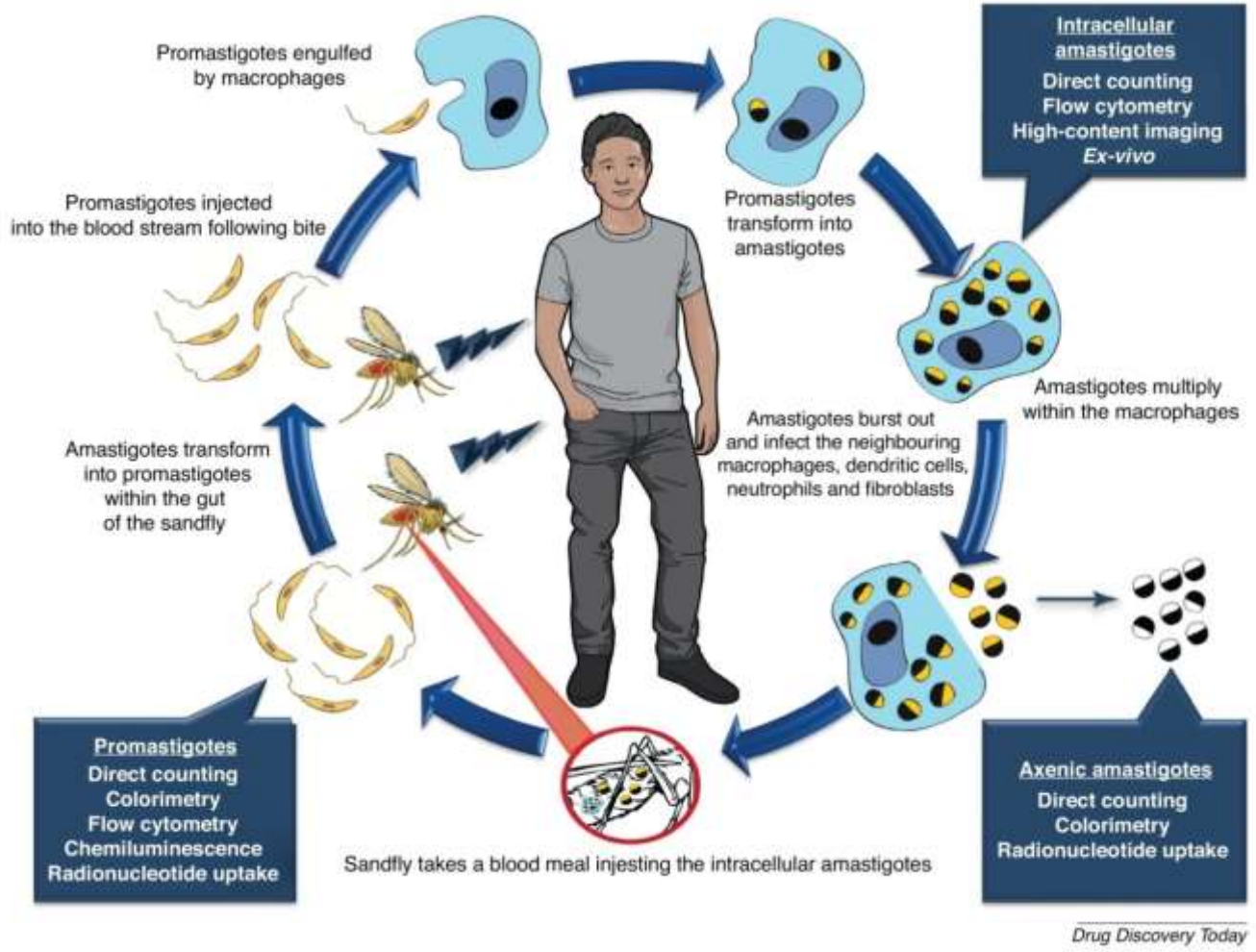

Figure 1.4: Life cycle of *Leishmania* parasite. Reproduced from "Leishmaniasis drug discovery: recent progress and challenges in assay development" *Drug Discovery Today*. 22(10), 1516-1531 (Zulfiqar, *et al*., 2017), copyright (2017) with permission from Elsevier.

1.2. Leishmaniasis - the disease

Leishmaniasis is endemic in approximately 98 countries across the globe with more than 350 million people are at risk of acquiring the disease (WHO, 2015; Hailu, *et al.*, 2016). Around 1.3 million new cases of the disease are reported every year with a mortality rate of 30,000/year (WHO, 2014; Copeland and Aronson, 2015). Humanleishmaniasis is prevalent in all continents except Antarctica and Oceania and is regarded as the third most common parasitic disease after schistosomiasis and malaria on the basis of morbidity and disability adjusted life years (DALYs) (WHO, 2010).

1.2.1. Types of leishmaniasis

According to the clinical manifestations exhibited in infected individuals, leishmaniasis can be classified into the following types:

1.2.1.1. Visceral leishmaniasis

This form of leishmaniasis is caused by *L. donovani* and *L. infantum* (Kevric, *et al.*, 2015). This disease is commonly referred to as kala-azar in areas of the Indian subcontinent (Sundar, *et al.*, 2015). *L. infantum* is the prevalent species in the Mediterranean Basin, Latin and South Americas visceral leishmaniasis (Millán, *et al.*, 2014). In South Americas, *L. infantum* is known as *L. infatum chagasi* and was probably introduced around five hundred years ago, during the Portuguese and Spanish colonization, through infected domestic dogs (Killick-Kendrick 1985; Rioux *et al.*, 1990). *L. donovani* affects people of all ages, whereas *L. infantum*, as the names suggests, primarily affects children (Chappuis, *et al.*, 2007), and occasionally adults who are immunosuppressed, such as in the case of human immunodeficiency virus (HIV) or fungal infections. *L. infantum* is also a causative agent of canine leishmaniasis (Dantas-Torres, *et al.*, 2012), an extremely important disease from a "One Health" point of view, as by addressing the disease in domestic animals, a reservoir is also reduced.

1.2.1.1.1. Distribution and epidemiology

Alvar *et al* reported that visceral leishmaniasis infects 0.2-0.4 million people per annum (Alvar, *et al.*, 2012; WHO, 2016) (Figure 1.5). The total number of deaths from visceral leishmaniasis ranges from 20,000 to 30,000 annually (Ready, 2014; WHO, 2016). Due to the increased frequency in remote areas, and lack of surveillance, it is difficult to estimate the exact number of cases and the fatalities associated with this disease.

1.2.1.1.2. Pathology

Symptoms include anaemia, progressive cachexia, intermittent fever, hepatomegaly and splenomegaly as shown in Figure 1.6 (Ashkan and Rahim, 2008). The incubation period varies from 2 weeks to 18 months for the parasite depending upon immune status of the patient (Ready, 2014), with emergence of initial skin lesion leading to gross inflammation of the viscera (liver and spleen) (Barrett and Croft, 2012). Other symptoms, such as lymphadenopathy and persistent diarrhoea, are also common (Ashkan and Rahim, 2008). The disease is diagnosed using microscopic, biochemical, serological and molecular techniques. Microscopic technique involves identifying the amastigote form via light microscope using Giemsa or haematoxylin and eosin staining (John, *et al.*, 2006; Barrett and Croft, 2012). Biochemical diagnosis is conducted via isoenzyme analysis (WHO, 2010), while serological testing includes using dipsticks e.g. rK39 rapid immunochromatographic test (ICT) (Vaish, *et al.*, 2012), this is the most widely used method used to diagnose visceral leishmaniasis (Ghosh, *et al.*, 2015). In tertiary care hospitals, quantitative polymerase chain reaction (PCR) followed for restriction fragment length polymorphism (RFLP) is used to diagnose a patient (Srivastava, *et al.*, 2013). As the *Leishmania* parasites directly affect macrophages and other cells of the phagocytic mononuclear system, the disease progresses to cause alterations in the patient immunity due to accumulation of dysfunctional T cells resulting in an inability to generate a cell-mediated immune (CMI) response against previously encountered antigens making the patient susceptible to superinfections (Stanley and Engwerda, 2007). As the macrophages are abundant in the liver and spleen, enlargement of these organs occurs due to inflammation. The parasites infect the bone marrow leading to pancytopenia (decreased production of red blood

cells, white cells, and platelets) (Stanley and Engwerda, 2007). CD4+ and CD8+ T cells are important for resistance to visceral leishmaniasis, and they are involved in the production of IL-2, IFN-γ, and IL-12. The latter acts independently of IFN-γ and is linked to the production of transforming growth factor beta (TGF-β). Susceptibility involves IL-10 (but not IL-4) and B cells (Goto and Lindoso, 2004; Engwerda and Kaye, 2004; Faleiro, *et al*., 2014; Rodrigues, *et al*., 2016).

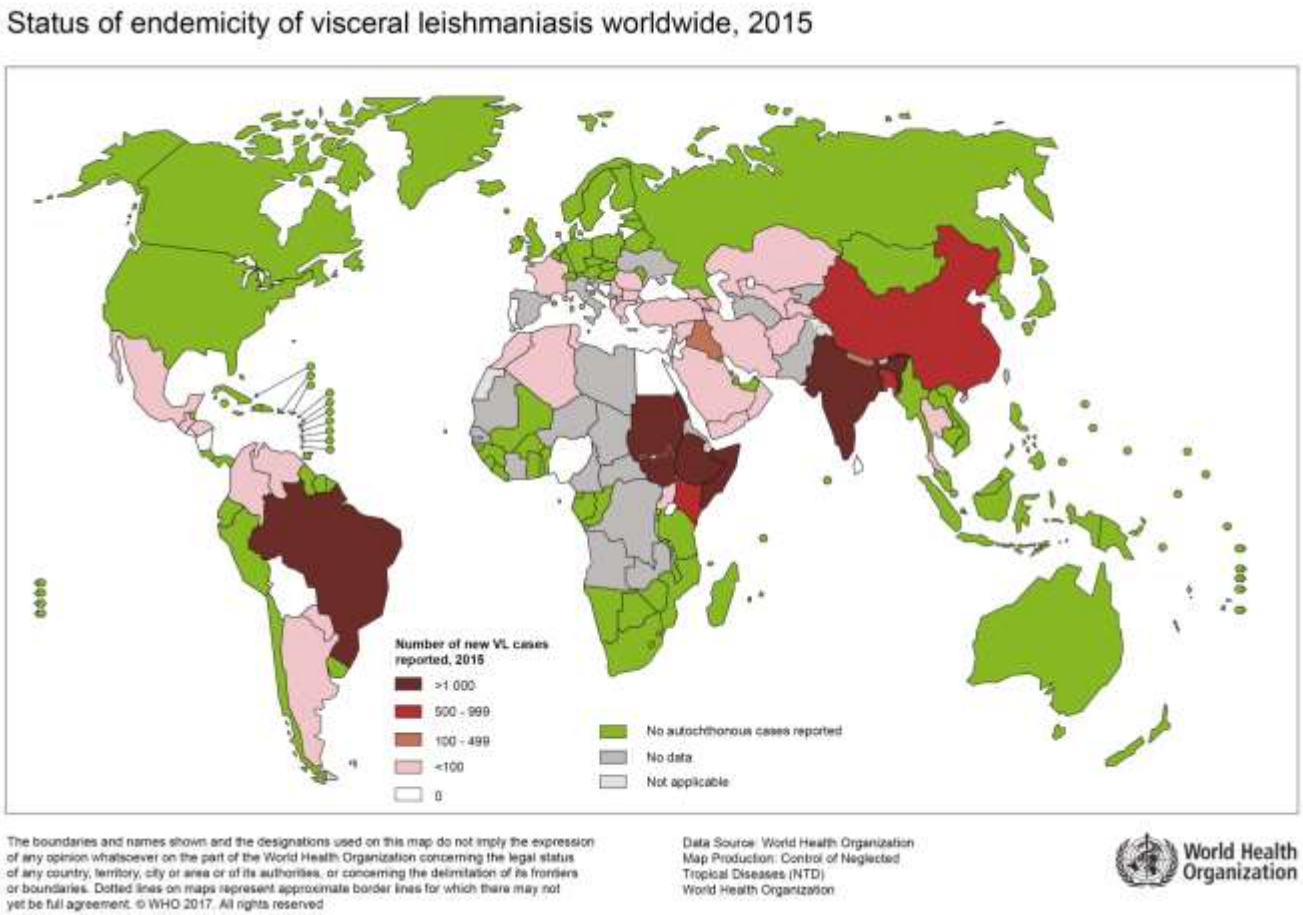

Figure 1.5: Worldwide epidemiology of visceral leishmaniasis, adapted from leishmaniasis epidemiological situation, WHO. Retrieved on October 9th, 2017, available at: www.who.int/leishmaniasis/burden/en/.

1.2.1.2. Post-Kala Azar dermal leishmaniasis (PKDL)

Post-kala-azar dermal leishmaniasis (PKDL) is a skin condition that usually develops following treatment for visceral leishmaniasis (Mukhopadhyay, *et al.*, 2014). The symptoms of PKDL include lymphadenopathy and parakeratosis of the rete pegs (epithelial extensions in mucous membrane and skin underlying the connective tissue) with appearance of maculopapular, macular and nodular rash (Ramesh, *et al.*, 2007). It is common in areas endemic for visceral leishmaniasis caused by *L. donovani*, approximately 50% of the cases of visceral leishmaniasis treated in Sudan develop PKDL, against 10-20% in India, but the incidence of PKDL is not exactly known because systematic follow up of visceral leishmaniasis patients after treatment is rare (WHO, 2010; Hailu, *et al.*, 2016). PKDL may also sporadically occur in *L. infantum* endemic areas, mainly the Mediterranean countries and Latin America (Antinori, *et al.*, 2007; Desjeux and Ramesh, 2011). Patients with PKDL act as reservoirs for parasites, playing an important role in transmission (anthroponotic transmission) (Molina, *et al.*, 2017). The interval between visceral leishmaniasis cure and PKDL varies according to the endemic area: in India, PKDL usually occurs within 5 year following cure from visceral leishmaniasis (Das, *et al.*, 2012), while in Sudan the majority of cases develop lesions during or within the same year of visceral leishmaniasis treatment (Zijlstra, *et al.*, 2003). The emergence of PKDL occurs after treatment with all the currently available therapies: sodium antimony gluconate (SAG), miltefosine, paromomycin, AmBisome and even in combination of miltefosine and paromomycin (Das, *et al.*, 2017). PKDL is often described in three grades. In grade one the lesions are scattered but restricted to the face, grade two is characterised by lesions on the face and upper trunk and grade three is described with lesions all over the body (Desjeux, *et al.*, 2013). Spontaneous healing has been observed and patients with grade one and mild grade two PKDL are left untreated with careful follow-up (Zijlstra, *et al.*, 2003).

The potential reasons for PKDL are still unknown but a number of different mechanisms have been proposed including genetic predisposition (Ganguly, *et al.*, 2010), response to sodium stibogluconate treatment (Croft, 2008), environmentally acquired traits related to high concentrations of arsenic in drinking water (Perry, *et al.*, 2013; Perry, *et al.*, 2015; Perry, *et al.*, 2015; Das, *et al.*, 2016) or a combination of

these. Previous treatment of visceral leishmaniasis with inadequate dosage of drug and the drug used, parasite resistance and genetic factors may play a role (Zijlstra, 2016).

In PKDL, the immune response to *Leishmania* parasites changes from a Th2 dominated response to a mixed Th1/Th2 response, changing the cytokine profile (Zijlstra, 2016). The precise understanding of PKDL immunopathogenesis is still obscure (Zijlstra, 2016). Evidence suggests that the pathogenesis is immunologically mediated as abnormal levels of interleukin 10 (IL-10) have been monitored in the peripheral blood of visceral leishmaniasis patients (Zijlstra, *et al.*, 2003), IL-10 plays an important role in regulating the Th1/Th2 response by limiting T cell differentiation and activation (Couper, *et al.*, 2008). The laboratories of Ganguly and Katara have both demonstrated that in lesion skin tissues not only enhanced IL-10 production is observed but forkhead box protein 3 (FoxP3) expression is also elevated (Ganguly, *et al.*, 2010; Katara, *et al.*, 2011). FoxP3 is a master regulator for regulatory T cells, naturally occurring $CD4^+CD25^+Foxp3^+$ regulatory T cells (Fontenot, *et al.*, 2003). There is also low expression of Interferon gamma (IFN-γ) and its receptor IFNGR1 (Salih, *et al.*, 2014; Salotra, *et al.*, 2016). IFN-γ, like IL-10, is also produced by $CD4^+CD25^+Foxp3^+$ regulatory T cells. It has been shown that blockade of IL-10 in *ex vivo* assays results in increased IFN-γ (Singh, *et al.*, 2012; Faleiro, *et al.*, 2014). Polymorphisms in the IFNGR1 receptor have been found in Sudanese populations, which can possibly be a factor for the increased number of cases in Sudan (Salih, *et al.*, 2007). Despite our belief how PKDL may have evolved, we still know very little. Instances have also been reported where the individuals developed PKDL without previous visceral leishmaniasis (Hasnain, *et al.*, 2016), for which clear explanations have yet to be forthcoming.

Figure 1.6: Pathophysiology of visceral leishmaniasis. (a) A child in Ethiopia suffering from visceral leishmaniasis showing signs of an enlarged spleen and liver. (b) A child in South Sudan suffering from post-kala-azar dermal leishmaniasis. (c) A patient from Ethiopia suffering from post kala Azar dermal leishmaniasis PKLD. Retrieved on Oct 9th, 2017availabe at: www.who.int/campaigns/world-health-day/2014/photos/leishmaniasis/en/.**Cutaneous leishmaniasis**

In the Old World (India, Ethiopia, Sudan, Syria, Iraq and Iran), cutaneous leishmaniasis (CL) is mostly caused by *L. aethiopica*, *L. major* and *L. tropica*. A small number of cases are due to infection with *L. infantum* (del Giudice, *et al.*, 1998; Kroidl, *et al.*, 2014; Ben-Shimol, *et al.*, 2016). In the New World (central and south American countries) multiple species; *L. peruviana*, *L. braziliensis*, *L. amazonensis*, *L. guyanesis*, *L. venezuelensis*, *L. panamensis*, *L. mexicana*, and *L. peruviana* (Showler and Boggild, 2015) are the causative agents of the disease. The names have been given based on the geographical area and clinical manifestations present in patients.

1.2.1.3.1. Distribution and epidemiology

Between 0.7 to 1.2 million cases of CL are reported annually around the globe (Showler and Boggild, 2015; WHO, 2016). About 95% of cutaneous leishmaniasis cases occur in

the Middle East, Americas, Central Asia and the Mediterranean basin. The majority of the cases in the Americas are reported in Brazil. The countries most affected in the Middle East are Syria and Iraq, whereas Afghanistan and Kazakhstan are the countries mostly affected in Central Asia (Showler and Boggild, 2015) (Figure 1.7).

1.2.1.3.2. Pathology

A lesion begins at the site of the sand fly bite, which enlarges in size accompanied by redness. The characteristic features of this disease are plaques, papules and nodule formation with the addition of skin thickening at multiple sites on the facial skin and the outer surface of the membranous tissue (Figure 1.8) (Machado, *et al.*, 2015). The lesion size can vary from a few millimetres to centimetres in diameter and at times multiple lesions can be observed in the same individual at multiple locations (Machado, *et al.*, 2015). The lesion heals with timehealing time may range from years to some months and may illicit permanent damage (Machado, *et al.*, 2015). A minor lesion at the site of bite can be observed in cases of *L. tropica*, *L. aethopica* and *L. peruviana*. Depending upon the parasite and the site of the lesion, cutaneous leishmaniasis can take different forms such as verrucous, nodular, zosteriform, and psoriaform like lesions (Showler and Boggild, 2015) The verrucous and psoriaform lesions are difficult to treat and alternative approaches to conventional drugs have been used including cryotherapy, thermotherapy, carbon dioxide (CO_2) laser, dynamic phototherapy and electrotherapy (Masmoudi, *et al.*, 2013). The immunological spectrum ranges from individuals with a strong T cell response, characterized by delayed-type hypersensitivity (DTH) and high levels of interferon γ (IFNγ), to individuals who lack a DTH response but may have high levels of antibodies (Carvalho, *et al.* 1994; Scott and Novais, 2016). *Leishmania* parasites are phagocytosed and killed by IFNγ-activated macrophages, thus individuals with a strong DTH response have few parasites in their lesions and develop a severe disease phenotype known as mucosal leishmaniasis (Bacellar, *et al.* 2002). In contrast, those individuals with only a humoral response are unable to control the parasite load, since *Leishmania* parasites are not neutralized by antibodies. These patientsdevelop a severe disease called diffuse cutaneous leishmaniasis. Between these extremes are patients who develop lesions that may self-heal or become chronic, with intermediate levels of T cell and antibody responses (Scott and Novais, 2016).

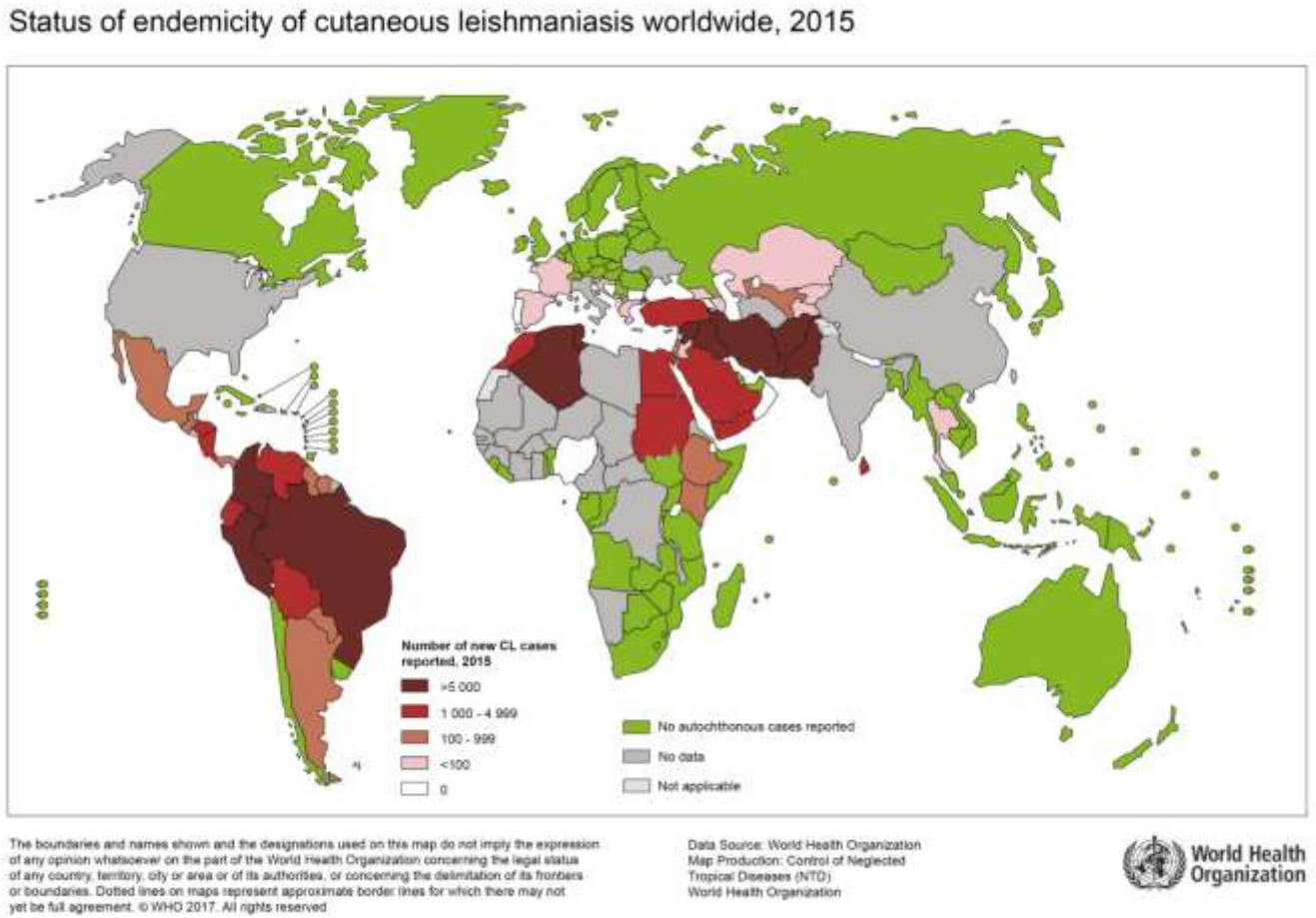

Figure 1.7: Worldwide epidemiology of cutaneous leishmaniasis, adapted from leishmaniasis epidemiological situation, WHO. Retrieved on October 9th, 2017, available at: www.who.int/leishmaniasis/burden/en/.

Figure 1.8: Pathophysiology of cutaneous leishmaniasis. (a) Intra-lesion injection administered to a patient in Afghanistan suffering from cutaneous leishmaniasis. (b) Child in Afganistan suffering from cutaneous leishmaniasis. Retrieved on October 9th, 2017, available at: www.who.int/leishmaniasis/burden/en/.

1.2.1.4. Mucocutaneous leishmaniasis

1.2.1.4.1. Distribution and epidemiology

In various regions within Peru, Bolivia and Brazil approximately 35,000 cases of mucocutaneous leishmaniasis are reported annually (WHO, 2016). The disease is caused by *L. braziliensis*, *L. panamensis* and *L. amazonensis* (Guerra, *et al.*, 2011). A few cases have been reported where the disease is caused by *L. guyanensis* (Naiff, *et al.*, 1988). Intermittent migration and colonization of areas where forest associated activities, such as excavation of gold or extraction of wood and oil, by human settlers has led to the spread of the infection (WHO, 2016).

1.2.1.4.2. Pathology

Individuals with mucocutaneous leishmaniasis develop metastatic lesions, in which the amastigotes disseminate through the blood and lymphatic system from the skin to the naso-oropharyngeal mucosa and cause mucosal leishmaniasis (Figure 1.9) (Berman, 1997; Goto and Lindoso, 2010). This results in the progressive destruction of the nasal mucosa, as well as the soft and hard palate, and eventually the nasal septum. The disfigurement of the face and crippling injuries results in social discrimination

encompassing both the general community and workplace (Kassi, *et al.*, 2008). Although little is known about the risk factors associated with this disease, it has been proposed that it is linked to the possession of certain alleles of tumor necrosis factor alpha (TNF- α) and lymphotoxin alpha (previously known as TNF- β) (Aggarwal *et a*l., 1985), which may act as the predisposing factor for this disease (Amato, *et al.*, 2009). TNF α and β are the important cytokines belonging to tumour necrosis factor superfamily. Both of these cytokines are produced by activated macrophages and are involved in regulation of cell proliferation, differentiation, survival and apoptosis functions (Engwerda, *et al.*, 2004). TNF β is specifically inhibited by IL-10 which functions to regulating the Th1/Th2 cell immune response (Awasthi, *et al.*, 2004). The anti-inflammatory TNFα inhibitor pentoxyphylline has been used in combination with antimonials and was found to be more effective than antimonials alone (Lessa, *et al.*, 2001). The elevated levels of C-X-C motif ligand 10 (CXCL10) and C-C motif ligand 4 (CCL4) have also been reported to be a predisposing factor for the disease (Vargas-Inchaustegui, *et al.*, 2010). CXCL10 is a chemokine of the CXC family, which binds to the receptor, CXCR3 to modulate T cell migration, adhesion molecule expression and monocyte stimulation (Dufour, *et al.*, 2002). CCL4, also a chemotactic cytokine is mainly produced by macrophages which functions as a chemoattractant for monocytes (Bystry, *et al.*, 2001). The increased concentration of these multiple inflammatory mediators may contribute to the disease severity via increased cell recruitment, which is observed in mucocutaneous leishmaniasis (Vargas-Inchaustegui, *et al.*, 2010). Another factor that is correlated to disease severity is the presence of the double-stranded *Leishmania* RNA virus 1 (LRV-1). LRV1 acts to trigger a potent inflammatory anti-viral response, which increases lesional swelling and prolongs parasite survival (Ives, *et al.*, 2011). The presence of LRV1 has been shown to be associated with an increased risk of treatment failure in patients infected with *L. braziliensis* from Peru and Bolivia. However, no significant association with intrinsic SbV resistance among parasites has been made, suggesting that treatment failure arises from LRV1-mediated effects on the host metabolism and/or parasite survival (Adaui, *et al*. 2016). In addition, the LRV1 status in *L. guyanensis* infection has been shown to be highly correlated and prognostic of pentamidine treatment failure in patients from French Guiana (Bourreau, *et al*. 2016).

Figure 1.9: Multiple ulcers and lesions developed on mucosal regions (mouth and nose) in patients suffering from muco-cutaneous leishmaniasis. (a) adult suffering from muco-cutaneous leishmaniasis. Retrieved on 9th Oct, 2017, from photo gallery displaying muco-cutaneous pathology available at web.stanford.edu/class/humbio103/ParaSites2006/Leishmaniasis/Mucocutaneous.htm. (b) child suffering from muco-cutaneous leishamaniasis. Reproduced with permission from (Elfaituri, *et al.*, 2015) Mucocutaneous leishmaniasis in an 11-year-old girl with ataxia telangectasia case report, *Libyan Journal of Medicine*, 10(1), copyright (2015) published by coaction publishers.

1.3. Vectors and reservoirs

1.3.1. Taxonomy and biology of the vector

For leishmaniasis, the transmission vectors are sand flies, which belong to the order Diptera, suborder Nematocera, family Psychodidae and subfamily Phlebotominae (Killick-Kendrick, 1990). Out of the 800-known species of sand flies, 78 are reported as verified vectors of *Leishmania*, divided in two subgenera, *Phlebotomus* in the Old World and *Lutzomyia* in the New World (Figure 1.10) (Akhoundi, *et al.*, 2016). Morphologically, the sand fly is 2-3 mm long and can be black or white in colour and is usually noiseless (Figure 1.11) (Killick-Kendrick, 1990). In the Mediterranean region, sand flies are mostly active in warm summer seasons (Galvez, *et al.*, 2010). Due to their small size they can easily pass through screens usually used to prevent mosquito bites (Von Stebut, 2015). As with other parasitic diseases such as malaria, only the female can serve as a potential vector to transmit the disease by taking a blood meal from the host (Neuber, 2008). It has been reported that sand flies are attracted to hosts because of carbon dioxide production and human odour, but few published studies

address behaviour of phlebotomine females (Pinto, *et al.*, 2001; Pardo, *et al.*, 2017). Infection can also occur through needle sharing, infected blood transfusion (Cardo, 2006) or transplacentally (Figueiro-Filho, *et al.*, 2004).

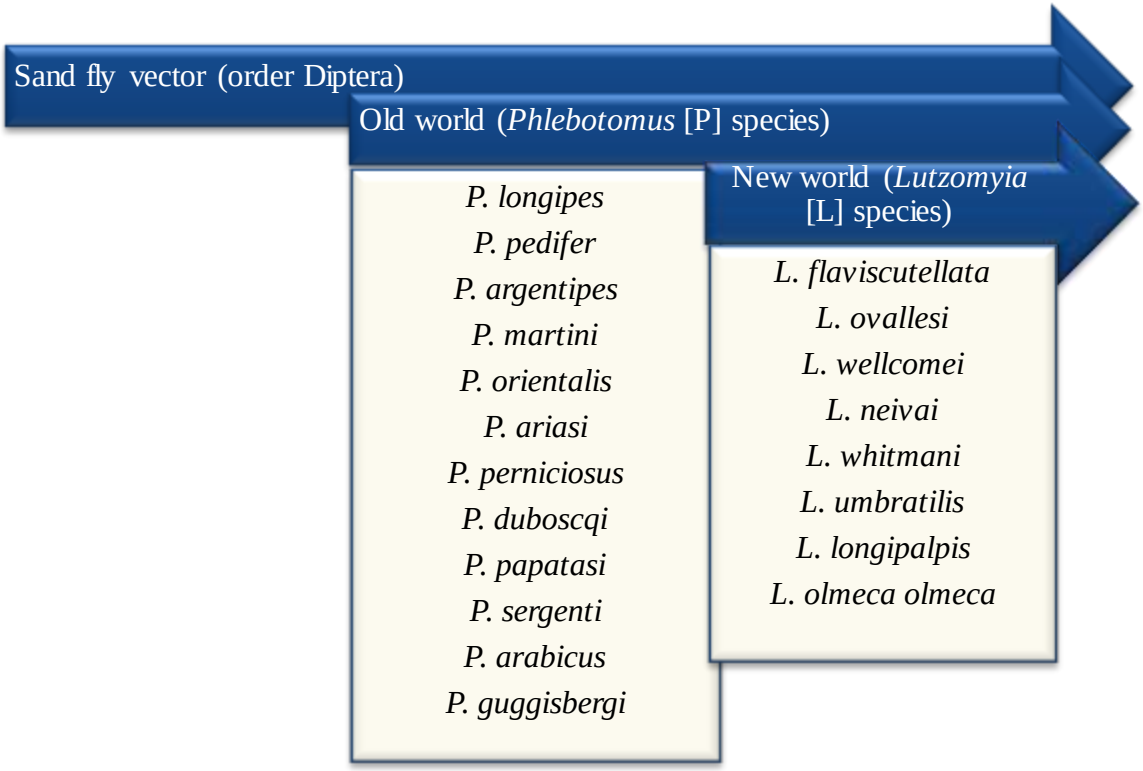

Figure 1.10: Known species of the order Diptera, subgenera *Phlebotomus*/*Lutzomia* found in the Old and New Worlds.

Figure 1.11: Sand fly taking a blood meal from the human host. Retrieved on Oct 9th, 2017 available at: www.who.int/campaigns/world-health-day/2014/photos/leishmaniasis/en/.

1.3.2. Interaction between *Leishmania* and its vector

The development of *Leishmania* within the vector, and consequently the parasite-vector interaction, is a complex process, and begins when a sand fly female feeds on an infected mammal host (Kamhawi, 2006). Females use their mouthparts to tear tissues and blood vessels, forming wells of blood in which they feed (Dostálová and Volf, 2012). During this process, infected macrophages are ingested; the macrophages break down and release the amastigotes. Due to changes in the gut of the phlebotomine, such as lower temperatures and increased pH, amastigotes become promastigotes that pass through different phases as they migrate from the midgut to the anterior regions (Dostálová and Volf, 2012; Liu and Uzonna, 2012). Each of these phases is characterized by morphological and functional changes designed to guarantee its nutritional requirements, growth, ability to divide, expression of surface molecules, as well as the survival of the parasite in the digestive tract of the vector (Figure 1.12) (Dostalova and Volf, 2012).

In order to comply with copyright this figure has been removed.

Figure 1.12: The time dependent changes taking place for various morphological forms of promastigotes in the midgut of the sand fly. Reproduced from "Phlebotomine sand flies and *Leishmania* parasites: friends or foes?" in *Trends in Parasitology* 22 (9), 439–445, copyright (2006) published by Elsevier.

To complete its development in sand flies, the parasite must be able to overcome some barriers (Podinovskaia and Descoteaux, 2015). These include, digestive enzymes in the

intestine that can promote the death of the parasites; the peritrophic matrix (MP), which can behave as a physical barrier allowing the escape of the parasite out of the midgut; excretion of digested blood, which may result in removal of parasites from the midgut (*Leishmania* subgenus); immune system reactions; anatomy and physiology of the anterior gut, which may prevent the fixation of *Leishmania* in the midgut epithelium, anterior migration and regurgitation of metacyclic promastigotes during blood feeding in host tissue (Sacks and Kamhawi, 2001; Dostalova and Volf, 2012; Rogers, 2012).

Based on experimental studies, identifying the ability of the vector to support the development of either a wide variety or a specific species of *Leishmania*, sand flies have been classified as permissive or specific, respectively (Volf and Myskova, 2007). To determine whether a given sand fly host is permissive or specific, it is important to understand disease transmission and the natural co-evolution of sand flies and *Leishmania* (Dobson, *et al.*, 2010). The interspecific and intraspecific variability of parasite lipophosphoglycan (LPG) may explain species specific vector competence (Dobson, *et al.*, 2010; Volf, *et al.*, 2014). For example, galactose residue ramifications of *L. major* LPG allow its attachment to the natural vector *P. papatasi*, whereas *L. donovani* cannot attach to it due to its non-branched LPG (Pimenta, *et al.*, 1994). *L. major* and *L. donovani* are unable to colonize the intestine medium of *P. sergenti* because of the excessive residues of glucose and arabinose in their LPG, whereas this vector serves as a natural vector for *L. tropica* (Kamhawi, *et al.*, 2000).

The development of LPG-independent *Leishmania* was observed in four permissive vectors for *L. major*: *P. arabicus*, *P. argentipes*, *P. perniciosus* and *L. longipalpis*. LPG-free parasites survived and developed infections comparable to wild type in these sand fly species (Myskova, *et al.*, 2007; Svárovská, *et al.*, 2010). Myskova and coworkers explained LPG is necessary in specific vectors, whereas, in permissive vectors, the parasite binds through an LPG-independent mechanism (Myskova, *et al.*, 2007).

1.3.3. Reservoirs

In addition to humans, domestic dogs, sloths, opossums and rodents are reservoirs for *Leishmania* (Pigott, *et al.*, 2014). Wolves, foxes, reptiles and amphibians among others, have also been reported to be potential reservoirs for *Leishmania* parasites (Neuber,

2008) whereas, reptiles and amphibians are reserviors for human non-infective forms of *Leishmania* parasites. In some epidemiological regions such as the Mediterranean region, leishmaniasis is a zoonotic disease (transmitted from living animals to humans), and in such cases, the migration of humans into the natural habitat of the animals could result in an increased risk of infection (Maia and Campino, 2011). However, in other regions such as Indian subcontinent transmission is anthroponotic (transmitted from human to human) (Reithinger, *et al.*, 2010). Human beings are the principal reservoir host for visceral leishmaniasis caused by *L. donovani* and cutaneous leishmaniasis caused by *L. tropica* (Hailu, *et al.*, 2016). Dogs are considered the most important reservoirs in visceral leishmaniasis caused by *L. infantum* (Maia and Cardoso, 2015). Generally, each *Leishmania* species falls into one or the other categories (zoonotic or anthroponotic). Even though, there are exceptions, for example, *L. tropica* which causes cutaneous infection is usually anthroponotic, but in some foci it derives not from humans but from other animals. For several cutaneous leishmaniasis species that are typically zoonotic, humans may constitute an occasional source of infection (WHO, 2016).

1.3.4. Vector and reservoirs control

The *Leishmania* parasite has evolved during the course of time to sustain its pathogenecity and trasmission in between the vectors and reservoirs (hosts) (Gonzalez, *et al.*, 2015). The epidemiology will depend on several factors, such as: parasite and vector species, environmental characteristics of transmission regions and human behavior (WHO, 2016). Logically the first approach to counter leishmaniasis should be vector control by reducing human contact with infected sand flies, and reservoir control, by reducing the number of infected animals, where the disease in commonly zoonotic (Dantas-Torres and Otranto, 2016).

The most widely used intervention to control vectors is insecticide spraying of houses, but this needs to be repeated regularly, which decreases its long-term sustainability (Cameron, *et al.*, 2016). Insecticides can also be sprayed onto the internal walls of houses, or impregnated into bednets, curtains, bedsheets or clothing (Davies, *et al.*, 2003; Wilson, *et al.*, 2014). In general, phlebotomine sandflies are highly sensitive to insecticides and a range of insecticides can be used: dichlorodiphenyltrichloroethane

(DDT), malathion, deltamethrin, cyfluthrin, alpha-cypermethrin, and lambda-cyhalothrin (Coleman, *et al.*, 2015). DDT, a persistent organic pollutant, which present bioaccumulation properties, high toxicity, and ubiquitous exposure of humans and wildlife, was the first insecticide used on a large scale for control of sand flies (Alexander and Maroli, 2003; van den Berg, 2009). In many countries like India, the Soviet Union, Brazil and China campaigns were initiated where DDT was sprayed in large amounts causing noticeable reductions in sand fly populations (Alexander and Maroli, 2003). A successful example is the control program in Bihar, India, between 1958 and 1970, over this period, no visceral leishmaniasis cases were reported in Bihar, but the disease resurfaced as soon as the program finished (Alexander and Maroli, 2003). Currently, there is a widespread resistance to DDT, mainly in India (Coleman, *et al.*, 2015).

The treatment of infected individuals is a key aspect for the control of the disease in anthropopathic transmission. In the case of zoonotic leishmaniasis, the methods used to control the reservoirs depend on which animal act as reservoir (Souza, *et al.*, 2014). Dogs which play a role as important leishmaniasis reservoirs in urban areas, respond well to antimony based treatment, but the treatment requires consecutive administrations, which serve as a compliance issue especially with the owners, leading to treatment failure (Gradoni, 2015). Another approach is to impregnate dog collars with insecticides to reduce the incidence of bites and prevent the dogs getting infected (Reithinger, *et al.*, 2004; Gradoni, 2015). Culling of dogs suffering from leishmaniasis was also widely used, but there is no available evidence that allows an estimate of the efficacy of diseased dog culling (Quinnell and Courtenay, 2009). For animal reservoirs, such as rodents, poisonous baits have been used as an option (Roberts, 2005).

In a review by González *et al.* the published reports on vector and reservoir control interventions for cutaneous and visceral leishmaniasis (Gonzalez, *et al.*, 2015) were reviewed. Apparently, there is a correlation between reducing phlebotomine sand fly numbers by insecticide spread and reducing cutaneous leishmaniasis incidence. However, there is insufficient evidence to indicate that the the better approach to use of insecticides (spray the internal walls of houses or impregnated bednets, curtains, bedsheets or clothing) is of significant long term impact, or that these measures are

effective or not in reducing visceral leishmaniasis incidence (Hailu, *et al.*, 2016). Concerning reservoir control, there is a need for future trials exploring: impregnated dog collars or lotions, poisonous baits for rodents eating seeds, removal of plants for rodents which feed on them, vaccines for canine leishmaniasis, destruction of burrows and trapping (Stockdale and Newton, 2013). Thus, elucidating whether these approaches play a role in decreasing leishmaniasis incidence (Gonzalez, *et al.*, 2015).

1.4. Treatment strategies used for leishmaniasis

Although leishmaniasis has a number of treatment options, anti-leishmanial therapy has been problematic, largely due to the complexity of the disease in its various forms (Tiuman, *et al.*, 2011; Singh and Kumar, 2017). The available therapies (Table 1.1) for the various forms of leishmaniasis are far from ideal primarily due to their extensive toxicity, lack of efficacy, parenteral route of administration affecting compliance, high costs, emerging drug resistance and lack of access in regional areas (de Menezes, *et al.*, 2015; Biswas, *et al.*, 2017). Some of the substances that have shown activity also vary in efficacy depending upon the species, symptoms and geographical regions of the *Leishmania* parasite (Tiuman, *et al.*, 2011; Adak and Datta, 2015). In many situations, the decision to proceed with treatment is based on the severity of the disease and risk to benefit ratio (No, 2016). Old World cutaneous leishmaniasis, mainly caused by *L. major*, tends to heal spontaneously, but the New World forms frequently require systemic treatment (Masmoudi, *et al.*, 2013; Copeland and Aronson, 2015). Overall, current treatment options are limited and are regarded as unsatisfactory irrespective of which form of leishmaniasis is being discussed (Zulfiqar, *et al.*, 2017).

Table 1.1: Current anti-leishmanial drugs and their main characteristics. Reproduced from (Zulfiqar, *et al.*, 2017), copyright (2017) with permission from Elsevier.

Drugs	Dosage, Regimen	Route of administration	Efficacy	Resistance	Toxicity	Advantages	Limitations	Disease type	Cost	Reference
Sodium stibogluconate and meglumine antimoniate	20 mg/kg/day for 30 days	Intravenous, Intramuscular or Intralymphatic	Varies between 35-95% based on area	Common more than 65% in Bihar, India	Severe cardiotoxicity, nephrotoxicity, pancreatitis and hepatotoxicity	Availability	• Confirmed resistance in Bihar, India • Compliance issues (lengthy treatment and painful administration)	VL (Except Bihar, India), CL	*US$ 82.36 per vial 100 ml	(Haldar, *et al.*, 2011; Rajasekaran and Chen, 2015)
Amphotericin B deoxycholate	1 mg/kg/day for 30 days	Intravenous	> 90%	Laboratory strains	Severe nephrotoxicity, thrombophlebitis and hypokalaemia	Primary resistance not documented	• Heat instability • Hospitalization for slow intravenous infusion	VL, CL	*US$ 7.5 per 50-mg vial	(Freitas-Junior, *et al.*, 2012; de Menezes, *et al.*, 2015)
Liposomal Amphotericin	3-5 mg/kg/day for 20 days	Intravenous	> 96%	Not documented	Mild nephrotoxicity, chills and fever during infusion	Low toxicity, resistance not documented	• Heat instability • High cost	VL	*US$ 18 per 50-mg vial	(Freitas-Junior, *et al.*, 2012; Berman, 2015; de Menezes, *et al.*, 2015)
Amphotericin B lipid emulsion	15 mg/kg single bolus injection	Intravenous	> 86%	Not documented	Infusion related pyrexia and chills	Low toxicity, resistance not documented	• Less efficacious than liposomal amphotericin	VL	-	(Sundar, *et al.*, 2014; de Menezes, *et al.*, 2015)
Miltefosine	2-2.5 mg/kg/day for 28 days	Oral	> 94%	Laboratory strains	Hepatotoxicity, nephrotoxicity and teratogenicity	Oral treatment	• Long half-life encourages emerging resistance • Cannot be administered to pregnant patients	VL	*US$ 47.98 – 58.20 for 56 (50-mg) capsules	(Sundar, *et al.*, 2012; de Menezes, *et al.*, 2015; Rajasekaran and Chen, 2015)
Paromomycin	15 mg/kg/day for 21 days	Intramuscular Topical	> 94% in Asia and 46-85% in Africa	Laboratory strains	Ototoxicity, nephrotoxicity and hepatotoxicity	Low cost	• Efficacy varies between different strains of *Leishmania* • Potential for resistance	CL, MCL	*US$ 15	(Sundar, *et al.*, 2007; Jhingran, *et al.*, 2009; Freitas-Junior, *et al.*, 2012)
Pentamidine	3 mg/kg/day for 4 days	Intramuscular	Varies between 36-96% based on area	Not documented	Severe hyperglycaemia, Mayocarditis hypotension and tachycardia	Short dosage regimen	• Efficacy varies based of geographical location of the disease	VL, CL	-	(Rajasekaran and Chen, 2015)

1.4.1. Pentavalent antimonials (SbV)

Since the 1940s pentavalent antimonials, namely sodium stibogluconate (SSG) (Figure 1.13A) and meglumine antimoniate (Figure 1.13B) have been used as the main therapy for all forms of *Leishmania* excluding Bihar, India where the parasites have acquired resistance against antimonials (Kevric, *et al.*, 2015). Pentavalent antimonials remain the treatment of choice in South America, Africa, Nepal, Bangladesh, and India (except North Bihar) (Haldar, *et al.*, 2011). For this reason, antimonials have been replaced by liposomal amphotericin B to treat visceral leishmaniasis in North Bihar, India (Balasegaram, *et al.*, 2012).

1.4.1.1. Mechanism of action

A variety of mechanisms of actions (MOAs) have been proposed for antimonials.

It has been suggested that pentavalent antimony (SbV), which behaves as a prodrug, is biologically reduced to the active form of the drug, trivalent antimony (SbIII). Various mechanisms have been proposed for this conversion from SbV to SbIII; these are as follows:

As the conditions inside the phagolysosome are acidic, it has been postulated that the SbV reduction can be either non-enzymatic via glutathione (GSH), trypanothione, glycylcysteine or enzymatic by the action of thiol-dependent reductase (TDR1) (Denton, *et al.*, 2004). The SbV reduction via the enzymatic and non-enzymatic process is still controversial. SbV reduction causes inhibition of trypanothione reductase (Baiocco, *et al.*, 2013). Trypanothione reductase is a flavoprotein oxidoreductase central to the unique thiol-redox system which is essential for parasite survival.

Another enzyme, arsenate reductase (ACR2), has been reported to increase the sensitivity of *Leishmania* to SbV by reducing it to the active form of the drug, the SbIII (Zhou, *et al.*, 2004; Sundar and Goyal, 2007). SbV has also been demonstrated to affect the cytokine levels of the host and kill the parasite in an indirect manner (Pathak and Yi, 2001).

Mandal *et al* demonstrated that the *Leishmania* species, which causes cutaneous leishmaniasis are more sensitive to trivalent antimony when compared to other species which cause visceral leishmaniasis (Mandal, *et al.*, 2015). Mandal and colleagues identified the link between antimonite accumulation and *Leishmania* aquaglyceroporin (AQP1), which help the parasite resist the osmotic changes that it may encounter during its life cycle. It has been found that the expression levels of a channel protein *Leishmania* aquaglyceroporin (AQP1) mRNA is directly proportional to the accumulation potential of antimonite in the parasite (Mandal, *et al.*, 2015).

1.4.1.2. Structure

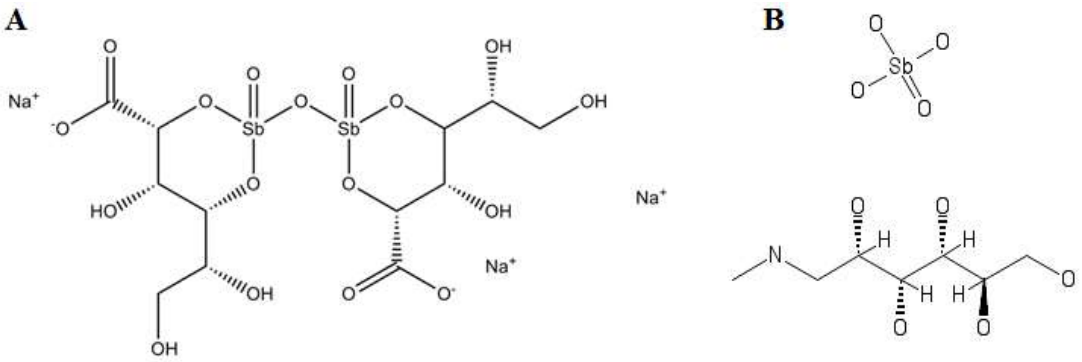

Figure 1.13: (A) Sodium stibogluconate and (B) Meglumine antimoniate.

1.4.1.3. Adverse effects

Common adverse effects reported for antimonials include reversible T-wave changes on electrocardiogram (ECG), which is a characteristic of myocardial ischemia, cardiotoxicity (Matoussi, *et al.*, 2007), nephrotoxicity (Zaghloul and Al-Jasser, 2004), gastrointestinal symptoms (stomach pain, diarrhea, vomiting, and stomach ulcers), fatigue, malaise, musculoskeletal pain, pancreatitis, leukopenia and thrombocytopenia, which are observed throughout the length of the therapy (Shahian and Alborzi, 2009).

1.4.1.4. Drug resistance

Pentavalent antimonials have been in use for treating cases of visceral and cutaneous leishmaniasis since the 1940s, with no or little evidence of resistance reported until the 1990s, when acquired resistance emerged as a clinical threat. However, low level responsiveness to antimonials in India was reported as early as the 1980s (Thakur, *et al.*, 1998).

Over 95% of the patients who were previously untreated responded to antimonial treatment effectively as the first line of treatment, with the exception of patients in the state of Bihar, India, where only 35% of the patients were reported to respond to the treatment (Sundar, *et al.*, 2000), (Sundar, 2001). Since 2005, SSG has not been officially recommended based on the high rates of treatment failures. A study was conducted by Perry *et al* in which 110 patients diagnosed with visceral leishmaniasis were treated with SSG were analysed. It was found that 41% of the patients responded to the treatment (Perry, *et al.*, 2015). A comparative study was conducted in Nepal, a neighbouring country in the north of Bihar state in India. Data shows a 90.5% cure rate with the use of SbV as a monotherapy with 9.5% treatment failures (Rijal, *et al.*, 2010). It has been proposed that the emergence of resistance is possibly due to wide spread use of the drug in these regions, as these drugs are available over the counter without prescription (Croft, *et al.*, 2006). SSG treatment failures have been linked to the arsenic contaminated ground water, which is used for drinking purpose. The continued exposure has led to the development of antimony resistant parasites (Perry, *et al.*, 2015).

1.4.2. Amphotericin B deoxycholate

Amphotericin B deoxycholate (Figure 1.14) was previouslyconsidered a second-line therapy in cases that do not respond to antimonials as it was demonstrated to be very effective against VL (>90% cure rate) (Sundar and Rai, 2005). However, due to safety concerns amphotericin B deoxycholate has been replaced by liposomal amphotericin B.

1.4.2.1. Mechanism of action

Numerous mechanisms of action have been proposed for amphotericin B but the exact mechanism is still not fully understood requiring further clarification and validation. Studies have shown that amphotericin B forms complexes with the 24 substituted sterols (Ergosterol) within the biological membrane of the parasite and produces pores within the membrane, which leads to cell death because of ion imbalance (Roberts, *et al.*, 2003). One of the reasons for toxicity observed with amphotericin B is because of the binding of amphotericin B to the cholesterol on the biological membrane of the mammalian cell hence causing potential adverse effects. In addition, it has been proposed that amphotericin B causes cholesterol complexation which hinders the binding of *L. donovani* metacyclic promastigotes to the host cells (Paila, *et al.*, 2010) there by inhibiting their entry into the host cell.

1.4.2.2. Structure

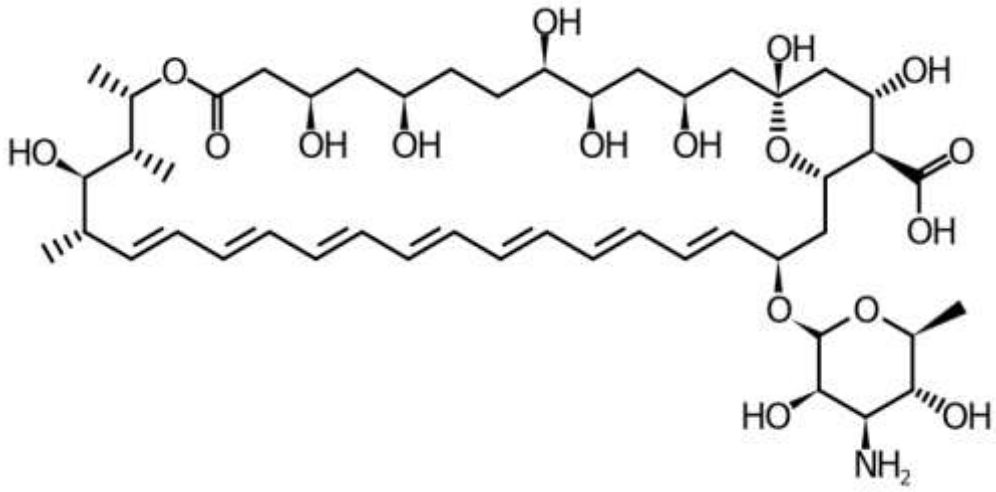

Figure 1.14: Amphotericin B.

1.4.2.3. Adverse effects

Serious nephrotoxicity is associated with amphotericin B deoxycholate in 49 % to 69% of patients treated with the drug (Noel, 1999; Wingard, *et al.*, 1999). In addition, it may cause anaemia, thrombophlebitis, severe hypokalaemia and renal dysfunction leading to

death (Corral, *et al.*, 2014). Complete blood count and metabolic panel should therefore be periodically assessed in patients undergoing therapy.

1.4.2.4. Drug resistance

Resistance is starting to emerge after a decade of using the drug. It is essential to understand the underlying mechanisms involved with this emerging resistance to amphotericin B. A clinical isolate of *L. donovani* was identified in Bihar, India in which there was an absence of ergosterol, as well as a variation in the expression profiles of the two transcripts of the C-24-Δ-sterol methyltransferase and S-adenosyl-l-methionine was found. The ergosterol was replaced by cholesta-5,7,24-trien-3β-ol thereby causing decreased amphotericin B affinity and uptake (Purkait, *et al.*, 2012). The role of Multi-Drug Resistance Gene (MDR1) has also been investigated as a threefold increase in expression was observed in the resistant strain (Purkait, *et al.*, 2012). The MDR1 is responsible for the drug efflux mechanism and this gene is an integral part of the ABC transporters of promastigotes (Mohapatra, 2014).

1.4.2.5. Lipid formulations of amphotericin B

Resurgence of lipid formulations of amphotericin B have been designed to diminishing toxicity, thereby permitting larger individual doses and a shorter total treatment period, including liposomal amphotericin B (Sundar, *et al.*, 2003), amphotericin B lipid complex, amphotericin B colloidal dispersion and amphotericin B lipid emulsion (Savoia, 2015). The amphotericin B deoxycholate has been replaced by liposomal amphotericin B, which functions to mask the toxic effects of amphotericin B on susceptible tissues. These formulations when injected are carried by the reticuloendothelial cells thus leading to targeted drug delivery to the parasite and increased activity (Sundar and Chakravarty, 2015).

1.4.2.5.1. Liposomal amphotericin B

The safety profile of liposomal amphotericin B has been approved by World Health Organization (WHO) and Food and Drug Administration Authority (FDA) for the treatment of visceral leishmaniasis in Indian Subcontinent, South America and the

Mediterranean region (Sinha and Bhattacharya, 2014). This drug is mostly prescribed to returning travellers for species-directed therapy of leishmaniasis and also used as a standard treatment in many countries (Hodiamont, *et al.*, 2014). Systemic evaluation of liposomal amphotericin has led to a very high dose of 10 mg/kg administered in a very short time period of 1 day, which in a large study conducted in India showed 96% efficacy (Berman, 2015). Liposomal amphotericin B is registered in India as AmBisome® (DND*i*, 2015).

However, the major constraint with the liposomal amphotericin is the administration route (parenteral), high cost and thermal stability as it requires cold storage (Freitas-Junior, *et al.*, 2012).

1.4.2.5.2. Amphotericin B lipid emulsion

Amphotericin B lipid emulsion is registered in India and available in ample quantities (Sundar, *et al.*, 2009). A multi-centric study was performed in India to assess the safety and efficacy of liposomal amphotericin B and a single infusion of preformed amphotercin B lipid emulsion in visceral leishmaniasis. Out of the 500 patients enrolled in the study, definitive cure was achieved in 85.9% with amphotericin B lipid emulsion and 98.4% with liposomal amphotericin B. It was observed that liposomal amphotericin B was more effective and better tolerated than preformed amphotericin B lipid emulsion due to longer half-life and membrane permeability (Sundar, *et al.*, 2014).

1.4.3. Miltefosine

Miltefosine (Figure 1.15) is the first anti-leishmanial drug with an oral route of administration (Dorlo, *et al.*, 2014). This drug was identified and evaluated independently in the early 1980s as a potential anticancer drug in Germany and as an antileishmanial drug in the UK (Simon L Croft and Engel, 2006). Due to the dose-limiting gastrointestinal side effects observed, it was discontinued as a treatment for cancer (Sindermann and Engel, 2006). Miltefosine demonstrated increased efficacy at a lower dose against the *Leishmania* parasite and is now being used as an anti-leishmanial agent to cure visceral leishmaniasis in India. Due to its quick onset of action the drug induces rapid cure for majority of patients who become asymptomatic (Sundar, *et al.*,

2013). CL cure rate upon miltefosine treatment varies among *Leishmania* species and also between the same species from different endemic areas (Soto, *et al.*, 2004; Soto, *et al.*, 2008).

1.4.3.1. Mechanism of action

The primary mode of action of the drug is not known, however, various mechanisms have been suggested, such as ether remodelling (Sundar, *et al.*, 2012). Ether-lipids constitute a major portion of the *Leishmania* lipid content mainly found in the glycoproteins and glycosylphosphatidylinositol-anchored glycolipids, which constitute the surface of the parasites (Lux, *et al.*, 2000). Ether remodelling causes a disturbance of glycoproteins and glycosylphosphatidylinositol-anchored glycolipids, which leads to the structural deformity and destabilization of the parasite surface symmetry causing parasite death. Inhibition of cytochrome c oxidase (Luque-Ortega and Rivas, 2007) has also been postulated to have a role in parasite death.

1.4.3.2. Structure

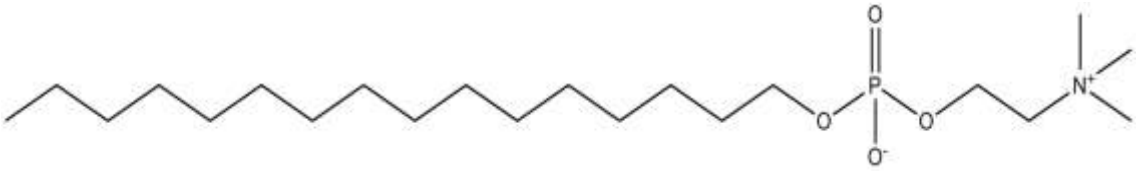

Figure 1.15: Miltefosine

1.4.3.3. Adverse effects

Miltefosine has been found to be less toxic when compared to antimonials and amphotericin B (Morais-Teixeira, *et al.*, 2011). Miltefosine is usually associated with gastrointestinal side-effects and in rare cases, hepatic and renal toxicities (Sundar, *et al.*, 2012). However, the major drawback of this particular drug is that it is teratogenic by virtue of its nature, so should not be given to pregnant women as it may cause deformities in the foetus (Sundar and Olliaro, 2007).

1.4.3.4. Drug resistance

Resistant strains of *L. donovani* promastigotes have been generated for miltefosine in *in vitro* experiments using up to 40 µM of drug, which remained resistant even after withdrawal of drug pressure at 2, 4 and 12 weeks (Seifert, *et al.*, 2003; Croft and Olliaro, 2011) One of the proposed mechanisms of resistance involves the inactivation of genes (LdMT and LdRos3) responsible for drug uptake (Seifert, *et al.*, 2003). In a study conducted to determine the resistance pattern in India against miltefosine it was noticed that 4-point mutations exist leading to variable drug response in miltefosine. However, no significant difference was observed in the genomic sequence of LdMT and LdRos3 thereby indicating that other mechanisms also exist except point mutations (Bhandari, *et al.*, 2012).

1.4.4. Paromomycin

This drug is an aminoglycoside antibiotic, which is off patent and termed as an orphan drug by the European Medicines Agency (EMEA) and the Food and Drug Administration Authority (Alvar, *et al.*, 2006). In August 2006, paromomycin (Figure 1.16) was recommended by the World Health Organization and was approved by the Indian government to treat patients with visceral leishmaniasis (Sundar, *et al.*, 2007). This drug is used for the treatment of both visceral leishmaniasis and cutaneous leishmaniasis in parenteral and topic formulations, respectively (Sinha, *et al.*, 2011).

1.4.4.1. Mechanism of action

The mechanism of action of paromomycin involves the inhibition of the mitochondrial membrane potential, which leads to respiratory dysfunction and inhibition of protein synthesis machinery thus altering lipid metabolism and membrane fluidity (Jhingran, *et al.*, 2009).

1.4.4.2. Structure

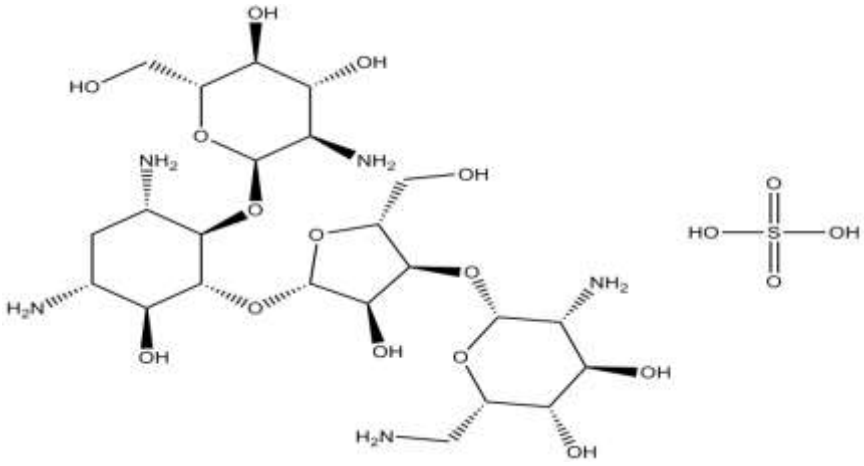

Figure 1.16: Paromomycin

1.4.4.3. Adverse effects

The main side effect associated with paromomycin is the toxicity of the auditory nerve and the vestibular system of the ear resulting in temporary deafness (Savoia, 2015). Moreover, paromomycin causes elevation in the level of liver enzymes (hepatic transaminases and aspartate aminotransferase) leading to drug-induced liver injury resulting from disruption of transport proteins (Sundar, *et al.*, 2007).

1.4.5. Other treatment options

1.4.5.1. Pentamidine

Pentamidine isethionate was used as a second line treatment in India, where antimony resistance is an issue in visceral leishmaniasis patients. However, high toxicity combined with poor efficacy and emerging resistance (Sundar, 2001) led to the discontinuation of this drug in India (Ouellette, *et al.*, 2004). It is effective for treatment of CL caused by *L. panamensis* or *L. guyanensis* in Brazil, Colombia, French Guiana and Suriname, but it is less efficacious than antimonials against disease caused by *L. braziliensis* (WHO, 2010). Its primary mechanism is unknown but it has been proposed that the drug accumulates in the mitochondria using the polyamine transporters and arginine and inhibits mitochondrial topoisomerase II (Mishra, *et al.*, 2007).

1.4.5.2. Sitamaquine

Sitamaquine (4-methyl-6-methoxy-8- aminoquinoline), last reported to be in phase 3 clinical trials (Sundar and Chakravarty, 2015), is effective against both the Old and New World visceral leishmaniasis with a success rate of 67-92% (Wasunna, *et al.*, 2005). Like miltefosine, sitamaquine is administered orally with a dose of 1.7-2mg/kg/day for 28 days (Jha, *et al.*, 2005).

1.4.6. New Treatments

The new lead compounds and potential new treatments based on the Drugs for Neglected Disease Initiative (DND*i*) portfolio are described in Table 1.2. DND*i* is a collaborative, non-profit drug research and development organization that is developing new treatments for neglected diseases.

1.4.6.1. VL-2098

A new compound, VL-2098 was discovered by the DND*i* (Gupta, *et al.*, 2015). In an *in vitro* amastigote macrophage model, the IC_{50} value of VL-2098 against the Indian antimony resistant strain, *L. donovani* DD8 was found to be 0.025 μM and is 0.7 – 2.6 μM against *L. donovani* ET67. In particular, the compound VL-2098 depicted good anti-leishmanial activity in acute mouse model (greater than 99% parasite inhibition at a dose of 50 mg/kg for 5 days) and chronic hamster models (85% inhibition) (Mukkavilli, *et al.*, 2014). After the initial pharmacokinetic and pharmacodynamics profiling of the compound in Hamsters, VL-2098 was tested in different species of animals. It was observed that the compound causes testicular toxicity in mice models and therefore a decision was made not to take the candidate drug further (DND*i*, 2016). Another compound DNDI-0690, from the same class which exhibited prominent activity in the *in vitro* assays, has been progressed to the translational phase in the DND*i* portfolio as a possible future treatment (DND*i*, 2017).

1.4.6.2. Anfoleish

Severe adverse effects are observed with the administration of amphotericin B though intravenous route thereby to overcome this issue, a cream was formulated for topical administration using 3% amphotericin B to treat cutaneous leishmaniasis lesions (Ben-Shimol, *et al.*, 2012). This formulation (Anfoleish®) is highly efficacious against *L. panamesis and L. braziliensis* and was selected by DND*i* for clinical trials in Latin America. Unfortunately, the results did not support the continuation of the clinical development of Anfoleish in its current formulation (DND*i*, 2015). The last update from DND*i* suggests that Anfoleish is in translational phase, alternative formulations are currently under consideration (DND*i*, 2015).

1.4.6.3. Fexinidazole sulphone

Fexinidazole is a drug from the nitro-imidazole class currently in the Phase II as an oral treatment for human African trypanosomiasis. The chemotherapeutic potential of this drug has been evaluated against the life cycle stages of *L. donovani*. Fexinidazole has an EC_{50} of 5.6 ± 0.2 µM and 2.8 ± 0.1 µM against the promastigote and axenic amastigote form of the parasite respectively (Wyllie, *et al.*, 2012). Against the intracellular amastigote form this drug showed an EC_{50} value of >50 µM. Fexinidazole sulphone has been synthesised using fexinidazole, which functions as a prodrug and will rapidly form active metabolites. These metabolites are 10-old potent than fexinidazole for the intracellular amastigotes with an EC_{50} value of 5.3 ± 0.1 (Wyllie, *et al.*, 2012). Last reported a phase II proof of concept trial was conducted to determine the efficacy of fexinidazole in visceral leishmaniasis patients in Sudan, the study was discontinued in 2014 as it failed to show conclusive efficacy in the majority of patients (Sundar and Singh, 2016). A patent has been applied for using fexinidaxole to treat canine leishmaniasis (Pollmeier and Blair, 2017).

1.4.6.4. CpG-D35

In order to find a potentially efficacious treatment for cutaneous leishmaniasis, the development and optimization of CpG-D35 was undertaken in collaboration with the U.S. Food and Drug Administration (FDA). DND*i* is combining the use of antimonials

with CpG-D35, a novel innate immune modulator that activates the immune cells embedded in the skin and therefore boosts parasite clearance. CpG-D35 is currently in the translational phase in the drug discovery pipeline for the treatment of cutaneous leishmaniasis (DND*i*, 2017).

1.4.6.5. Aminopyrazoles

DND*i* in collaboration with Takeda and the GHIT fund are working on an ongoing lead optimization program for new leads from the aminopyrazole class exhibiting anti-leishmanial activity against visceral and cutaneous leishmaniasis causing species (DND*i*, 2017). The most active compound from that class has an IC_{50} value of 1.3 µM for *L. donovani* intracellular amastigotes (Mowbray, *et al.*, 2015).

1.4.6.6. DNDI-5421 & DNDI-5610 oxaboroles

Oxaboroles, initially identified as showing promising activity against HAT have been progressed into anti-leishmanial drug discovery pipeline after exhibiting activity against intracellular amastigotes of *Leishmania* parasite. Two compounds from this class DND*i*-5421 & DND*i*-5610 are in research phase and one compound DND*i*-6148 is in the translational phase of the DND*i* portfolio (DND*i*, 2017).

1.4.7. Combination therapy

Continued development of resistance to anti-leishmanial drugs suggests that the current use of monotherapies require review. The rationale behind the combination therapy approach is to reduce the risk of parasite resistance, increase efficacy resulting from synergistic effects, lower dose requirements, and shorten the duration of therapy eventually leading to reduced toxic effects of the drugs (Sundar and Chakravarty, 2013; Sundar and Singh, 2016; Singh and Kumar, 2017).

Another factor in combined therapy is the half-life of drugs. Ideally the best approach is to use a very potent drug with a short half-life in combination with second lesser potent drug having an extended half-life to clear the remaining parasites (Singh, *et al.*, 2016) However, other factors like tissue distribution, volume of distribution and macrophage

drug uptake also play a crucial role especially in the case of *Leishmania* intracellular amastigotes, where they are localized in the organs of the reticuloendothelial system.

1.4.7.1. Sodium stibogluconate and paromomycin

The use of sodium stibogluconate (SSG) with paromomycin as a current standard treatment has been implemented in East Africa by World Health Organization (WHO) after a successful multi-country randomized control trial in four East African countries (Musa, *et al.*, 2012). A combination of sodium stibogluconate (20 mg/kg/day) plus paromomycin (15 mg/kg/day) was compared to individual drugs for a period of 17 days. A cure rate of 93% was achieved for 774 primary cases and of the 35 relapse cases reported, 77% were successfully treated with the combination.

1.4.7.2. Miltefosine and liposomal amphotericin B

Sequential treatments with miltefosine and liposomal amphotericin B (single dose) were highly effective in Bihar state, India for visceral leishmaniasis (Sundar, *et al.*, 2008). The overall cure rate for 46 subjects with a regimen (5 mg/kg of L-AmB followed by miltefosine for 10 days) was on average 98% whereas liposomal amphotericin B (5 mg/kg administered once) was only 91% effective when given alone with in 45 subjects (Sundar, *et al.*, 2008). This study suggests that the difference between the cure rate is not statistically significant, hence using a using a combination therapy of miltefosine and liposomal amphotericin B (L-AmB) does not have a profound effect on efficacy.

1.4.7.3. Liposomal amphotericin B, miltefosine and Paromomycin.

A phase III study was conducted in India using amphotericin B, miltefosine and paromomycin in combination. Three combinations were assessed, (single injection of 5 mg/kg liposomal amphotericin B + 50 mg miltefosine for 7 days), (5 mg/kg liposomal amphotericin B + 11 mg/kg intramuscular paromomycin for 10 days) and (11 mg/kg paromomycin and 50 mg miltefosine for 10 days). All combinations resulted in approximately 97% efficacy (Sundar, *et al.*, 2011). Presently a single dose of liposomal amphotericin B or the single injection of 5 mg/kg liposomal amphotericin B + 50 mg

miltefosine for 7 days are the preferred treatment options in the Indian subcontinent (Sundar and Chakravarty, 2015).

Table 1.2: New lead compounds for visceral and cutaneous leishmaniasis. Reproduced from "Leishmaniasis drug discovery: recent progress and challenges in assay development" *Drug Discovery Today*. 22(10), 1516-1531 (Zulfiqar, *et al*., 2017), copyright (2017) with permission from Elsevier.

Compounds/ Drug leads	Disease State	Assay used to identify the compounds	Developmental Phase	Reference
Nitroimidazole (VL2098)	VL	Reporter gene intracellular amastigote assay	Discontinued[a]	(Mukkavilli, *et al*., 2014; Gupta, *et al*., 2015)
Nitroimidazooxazine (DNDI-0690)	VL, CL	-	Translation Phase (Pre-clinical)	DND*i* (2016) Leishmaniasis Portfolio[b]
Oxaboroles (DNDI-5421 and DNDI-5610)	VL, CL	Colorimetry and direct counting of intracellular amastigotes using Giemsa stain.	Research Phase (Lead Optimization)	DND*i* (2016) Leishmaniasis Portfolio[b]
Oxaboroles (DNDI-6148)	VL	Colorimetry and direct counting of intracellular amastigotes using Giemsa stain.	Translation Phase (Pre-clinical)	DND*i* (2016) Leishmaniasis Portfolio[b]
2-substituted quinolines	VL	Reporter gene intracellular amastigote assay	-	(Gopinath, *et al*., 2014)
Aminothiazoles	VL	Reporter gene intracellular amastigote assay	-	(Bhuniya, *et al*., 2015)
Aminopyrazoles	VL	Colorimetry and direct counting of intracellular amastigotes using Giemsa stain.	Research Phase (Lead Optimization)	(Mowbray, *et al*., 2015)
CGH VL Series 1	VL	-	Research Phase (Lead Optimization)	DND*i* (2016) Leishmaniasis Portfolio[b]
Fexinidazole	VL	Colorimetry and direct counting of intracellular	Discontinued	(Wyllie, *et al*., 2012)
CpG D35	CL	-	Translation Phase (Pre-clinical)	WHO (2016) Class D CpG ODN (D35)[c]
Anfoleish	CL	-	Discontinued	(Ben-Shimol, *et al*., 2012)

[a]After the initial pharmacokinetic and pharmacodynamics profiling of the compound in Hamsters it was tested in different species of animals. It was observed that the compound causes testicular toxicity and therefore a decision was carried out not to take the candidate further. DNDi (2016) Target Product Profile for visceral leishmaniasis. Available at: http://www.dndi.org/diseases-projects/leishmaniasis/tpp-vl/.

[b]DNDi (2016) Leishmaniasis Portfolio. Available at: http://www.dndi.org/diseases-projects/leishmaniasis/leish-portfolio/.

[c]WHO (2016) Class D CpG ODN (D35). Available at: www.who.int/phi/implementation/USFDA_Osaka_documents.pdf.

1.5. Drug discovery and development process

Drug discovery has evolved into an interdisciplinary scientific field, which functions to integrate diverse disciplines like biology, chemistry, mathematical modelling and computer sciences in a bid to provide new drugs (Vogel and Vogel, 2013). Any chemical entity that is identified as a hit with a potential therapeutic value has to go through a series of steps to establish its efficacy and safety before it is marketed and is made available to patients (Hughes, *et al.*, 2011; Katsuno, *et al.*, 2015). This multi-stage process is referred to as the drug development pipeline (Figure 1.17).

It is important to note that various steps of the drug discovery pipeline may overlap and multiple steps can be undertaken simultaneously based on whether the molecular target has been identified or not. Bioinformatics tools are used to identify potential molecular targets of compounds which need to be validated experimentally. The discovery phase of the pipeline often begins with the identification of a hit molecule using HTS *in vitro* assays. For leishmaniasis, these assays are designed to depict a specific life cycle stage or a particular pathway. Lead compound selection and chemical optimisation to improve various physico-chemical parameters, such as solubility and metabolic stability, as well as biological activity and selectivity requires more extensive biological evaluation and thus more complex assays. *In vitro* and *in vivo* DMPK evaluation of molecules is assessed during lead optimization to evaluate the pharmacokinetic and pharmacodynamic properties of the compound and *in vivo* efficacy is also undertaken.

1.5.1. Drug discovery process for neglected tropical disease

Drug discovery for leishmaniasis has traditionally been carried out using both unbiased and biased phenotypic screening, plus target-based approaches (Katsuno, *et al.*, 2015). Historically this has generally been the domain of the academic community.However, with the establishment of not for profit organizations, such as DND*i* and Medicines for Malaria Venture (MMV), more focused efforts, incorporating both academic and industry partners, have evolved.

1.5.1.1. Unbiased and biased phenotypic screening

Phenotypic or whole cell/organism screening is an effective tool to select compounds, which impact on the viability of the parasite. Phenotypic screening was the approach utilised for the discovery and development of the majority of Food and Drug Administration (FDA) approved new molecular entities identified between 1998 and 2008 (Swinney and Anthony, 2011). In this approach, a molecular target or a pathway is not defined; the target per se is the organism itself (Vincent, *et al.*, 2015). A primary reason for selecting this approach for *Leishmania* drug discovery is that clearly defined druggable parasitic targets have been difficult to identify and validate. A benefit in the utilisation of phenotypic approaches is the advantage of demonstrating a direct impact on the parasite, determination of potential off target host cell toxicities and provision of insights into compound cell permeability and stability within the unique host parasite micro-environment (Mullard, 2015). Multiple proteins or pathways may be affected by the compounds, which may not be identified through targeted screens. However, the deconvolution to determine the specific molecular target or mechanism of action of the compound is an additional challenge created by unbiased phenotypic screening. This can be addressed with biased phenotypic screening, where an assay is established for a specific target and the impact of the compounds on this target can be assessed either directly or indirectly (Bogyo and Rudd, 2013; Jung and Kwon, 2015). Another consideration when undertaking drug discovery is the continual maintenance of biological cultures in sufficient quantities to perform assays for high-throughput and high-content analysis, particularly with respect to specific life cycle stages, species or strain of the organism and clinical relevance (Schirle and Jenkins, 2016).

1.5.1.2. Target based screening

The target-based drug discovery involves screening compounds against a defined target of interest, most commonly this involves a protein associated with a specific pathway (Seethala and Zhang, 2016). This target must be identified and validated as of functional relevance and druggable. Once identified, active compounds are further optimized for cellular activity, enzyme/pathway activity and selectivity (Gilbert, 2013; de Menezes, *et al.*, 2015). This target can be further validated using complementary assays (Chatelain and Ioset, 2011; Seethala and Zhang, 2016). Target based screening

has several disadvantages, particularly in the case of anti-leishmanial drug discovery. For example, the active compound must be capable of entering the macrophage parasitophorous vacuole where the intracellular amastigotes reside, in order to be effective. Therefore, the potential hit molecules require the essential chemical properties which facilitate transport across host cell membranes and must remain stable within the acidic environment of the parasitophorous vacuole. Some compounds may be metabolized in these acidic conditions converting them into pharmacologically active molecules whilst others are inactivated. Additionally, the compound should not act as a substrate of the xenobiotic-metabolizing enzymes for the host cell. If the active compound acts as a substrate for xenobiotic-metabolizing enzymes it will be degraded before reaching its molecular target. Though significant progress has been made in the identification and validation of new targets, a drug specifically directed to one validated target has not yet been developed for leishmaniasis (Field, *et al.*, 2017).

Due to the limited number of validated targets and issues related to the confirmation of on-target effects depicted using the active compounds, drug discovery efforts for leishmaniasis have shifted from target based to unbiased and biased phenotypic screening (Don and Ioset, 2014; de Menezes, *et al.*, 2015).

1.5.2. DND*i* target profile for leishmaniasis

A target candidate profile (TCP) and a target product profile (TPP) (Table 1.3) has been established by DND*i* (Don and Ioset, 2014). The guidelines established from DND*i* for compound progression within the drug discovery pipeline have been determined as the minimal requirements for the development of a safe, oral, effective anti-leishmanial drug, enabling short course treatment schedule with a bid to replace the existing current treatments available.

According to the target candidate profile (TCP) established by DND*i* (Don and Ioset, 2014) for classification of a compound as an active hit against visceral leishmaniasis, the molecule should have an activity against the intracellular amastigote form of *L. donovani* or *L. infantum* with an IC_{50} value less than 10 µM. The selectivity of the compound should be 10-fold more active when compared to a mammalian cell line. It should not have any structural alerts which might have an effect in metabolism, stability

or reactivity of the compound. The compound should not have any toxicity *in silico* and *in vivo* models. It should have chemical tractability in which it can be synthesized by as acceptable synthetic pathway with less than 8 steps. It is imperative to assess the stereo-chemistry of the compound so that its structure activity is already established.

Table 1.3: Target product profile of new chemical entities for visceral and cutaneous leishmaniasis. Reproduced from "Leishmaniasis drug discovery: recent progress and challenges in assay development" *Drug Discovery Today*. 22(10), 1516-1531 (Zulfiqar, *et al*., 2017), copyright (2017) with permission from Elsevier.

	Visceral leishmaniasis		**Cutaneous leishmaniasis**	
	Optimal Target Profile	**Minimal Target Profile**	**Optimal Target Profile**	**Minimal Target Profile**
Target	VL and PKDL	VL	CL	CL
Species	All species	*L. donovani*	All species	*L. tropica or L. braziliensis*
Distribution	All areas	Either India or Africa	All areas	All areas
Target Population	Immunocompetent and immunosuppressed	Immunocompetent	-	-
Clinical Efficacy	> 95%	> 90%	>95%	60% for *L. tropica* 70% for *L. braziliensis*
Resistance	-	Active against resistant strains	-	-
Safety and Tolerability	Should not require monitoring	1 monitoring visit in mid/end – point	Should not require monitoring	Primary Health Care (minimal contact). No major safety concerns.
Contraindications	None	Pregnancy/lactation	None	Can be assessed at primary health care level level.
Interactions	None – Compatible for combination therapy	None for malaria, TB, and HIV therapies	None – Compatible for combination therapy	-
Formulation	Oral /intramuscular depot	Oral /intramuscular depot	Topical / oral	Non-parenteral or few doses if parenteral
Treatment Regimen	1/day for 10 days po/ 3 shots over 10 days	bid for <10 days po; or <3 shots over 10 days	Topical: 14 days Oral: < 7 days	Topical: 28 days Oral: Oral: bid for 28 days
Stability	3 yrs in zone 4	Stable under conditions that can be reasonably achieved in the target region (> 2 yr)	No cold chain, at least 3 years at 37ºC	2 years at 4-8ºC
Cost	< $10 / course	< $80 / course	US$5	US$50

In order to comply with copyright this figure has been removed.

Figure 1.17: Drug discovery pipeline. Reproduced from "Antitrypanosomatid drug discovery: an ongoing challenge and a continuing need" *Nat Rev Microbiol*. 2017 April ; 15(4): 217–231 (Field, *et al*., 2017),copyright (2017) Macmillan Publishers Limited, part of Springer Nature.

1.5.3. Currently available screening assays

The need to discover and develop new compounds, which demonstrate activity against *Leishmania* parasites, is crucial. The primary motivation is the need for drugs with improved toxicity, efficacy and administration profiles (Bhargava and Singh, 2012; Field, *et al.*, 2017). In the last two decades, numerous assays (Table 1.4) have been developed for use in screening programs using different life cycle stages of the *Leishmania* parasite, which are relevant to the disease states within the human host. The intracellular amastigote form of the parasite is the clinically relevant stage and active compounds against this stage are often then progressed to *in vivo* testing (after medicinal chemistry analysis and initial pharmacokinetic and pharmacodynamics assessments). The promastigote and the amastigote stages are not only morphologically different but also vary in respect to the biochemical components hence often the activity of compounds against them may be different (Naderer and McConville, 2011).

During the course of the development of the promastigote in the gut of the sand fly, it transforms into the metacyclic form, which is regarded as the infective stage in the human host. The majority of assays designed against the promastigote stage use early or mid-log growth promastigotes not metacyclic promastigotes, which is a non-dividing life cycle stage. Moreover, obtaining pure cultures of metacyclic parasites is difficult (Spath and Beverley, 2001).

Comparisons of compound efficacy performed on both life cycle stages revealed that promastigotes are more sensitive to the majority of active compounds when compared to amastigotes (De Muylder, *et al.*, 2011; Annang, *et al.*, 2015). This sensitivity is potentially associated with the immediate and direct interaction between compound and promastigotes, whereas several membranes must be traversed and the micro-environment housing the intracellular amastigotes is biochemically quite distinct. Another significant advantage of such an axenic amastigote or promastigote assay is the potential to identify a subset of compounds distinct from those identified with the intracellular amastigote assay. Localization of intracellular parasites within the parasitophorous vacuole may add an additional hurdle for small molecules, as they have to cross several membranes and exert their action at a neutral or acidic pH. Compounds which are active on the extracellular parasite may be modified during drug development

to improve solubility and stability within the intracellular environment. Thus, assays targeting promastigotes and/or axenic amastigotes provide an option for identifying alternative hit molecules However, the *in vitro* assays which have been designed for intracellular amastigotes correlated more closely to *in vivo* outcomes compared to *in vitro* promastigote assays (De Muylder, *et al.*, 2011; Sangshetti, *et al.*, 2015; Field, *et al.*, 2017). It is yet to be determined if the intracellular amastigote assay can imitate the same microenvironment present in the infected patient, however it is considered the closest approximation to the clinically prevalent form of the disease (Rajasekaran and Chen, 2015).

Leishmania promastigotes and amastigotes survive and proliferate in very different environments, thus, significant metabolic differences exist between them. Amastigotes of several *Leishmania* species were found to exhibit reduced glucose uptake, as compared to rapidly dividing promastigotes, while simultaneously increasing the uptake of amino and fatty acids (Saunders *et al*, 2014). Studies of metabolomics have been reported with an aim to understand the strategies used by the parasite to optimize their metabolism in accordance with the environment in order to utilize the available resources (Saunders *et al*, 2014; Subramanian and Sarkar, 2017). *Leishmania* metabolism operates such that the parasite is ableto select an appropriate alternative to compensate for limited external substrates, providing a wide range of options for the parasite to achieve optimal survival. A restriction and redistribution of resources to produce the necessary essential metabolites is achieved by a dynamic motif of non-essential amino acids existing within the network. In addition to this, regulation of this metabolic re-routing is attained via subcellular compartments reinforcing the physiological coupling of specific reactions (Subramanian and Sarkar, 2017). This phenomenon explains the stage-specific differences to drugs observed between promastigotes and intracellular amastigotes.

Table 1.4: Anti-leishmanial screening formats for promastigotes, axenic amastigotes and intracellular amastigotes forms of the parasite. Reproduced from (Zulfiqar, *et al.*, 2017), copyright (2017) with permission from Elsevier.

Assay Type		Parasite form	Advantages	Disadvantages	Analytical	References
Direct counting		Promastigotes	• Simplicity • Cost effectiveness	• Limited precision • Cumbersome / labour intensive • Poor scalability	Variable coefficient of variance and Z' values. Sensitivity and reproducibility issues. Limited sample number	(Chan-Bacab, *et al.*, 2003; Khan, *et al.*, 2003)
		Axenic amastigotes				(Callahan, *et al.*, 1997)
		Intracellular amastigotes				(Gaspar, *et al.*, 1992)
Colorimetry	Acid phosphatase activity	Promastigotes	• Simplicity • Cost effectiveness • Robust data generation Scalable for HTS	• Non-representative of human disease model • Poor confirmation rate for intracellular amastigote assay • Questionable similarity of axenic amastigotes compared to intracellular amastigotes • Limits of detection dependant on plate reader • Indirect measurement of activity • Population measurement	Consistent coefficient of variance value and Z' ranging from 0.7-1	(Bodley, *et al.*, 1995)
	Alamar Blue (Resazurin)	Promastigotes				(Mikus and Steverding, 2000)
		Axenic amastigotes				(De Rycker, *et al.*, 2013)
	MTT assay	Promastigotes				(Berg, *et al.*, 1994; Maarouf, *et al.*, 1997)
		Axenic amastigotes				(Sereno and Lemesre, 1997)
	BacTiter-Glo	Axenic amastigotes				(Nuhs, *et al.*, 2015)
Flow cytometry		Promastigotes	• Automated output and analysis • Accurate determination of promastigote viability based on expression of identifying markers • Single cell populations identifiable	• Expensive equipment • High running costs • Cell samples require suspension format	Consistent coefficient of variance and Z' ranging from 0.6-0.8.	(Delgado, *et al.*, 2001; Kamau, *et al.*, 2001)
		Intracellular amastigote				(Abdullah, *et al.*, 1999)
Bioluminescent and fluorescent transgenic parasites	GFP (fluorescent)	Promastigote, Axenic amastigote	• Amenable to HTS • Cost effective • Reproducible	• Varying signal based on expression, as GFP signal cannot be amplified in a controlled manner • Transgenic parasite requirement – strain limitation • Potential loss of physiological relevance with transgenic	Consistent coefficient of variance (value) and Z' ranging from 0.7-1	(Chan, *et al.*, 2003; Singh, *et al.*, 2009; Calvo-Alvarez, *et al.*, 2012; Zhu, *et al.*, 2012; Rocha, *et al.*, 2013)
	Luciferase	Promastigote, Axenic amastigote				
	mCherry (fluorescent)	Promastigote				
	GFP/RFP (fluorescent)	Promastigote				

			parasites		
Radionucleotide uptake	Promastigotes Axenic amastigotes	• Direct measures of proliferation possible	• Use of radioactive substances • Requires specialised radiation detection equipment	Consistent coefficient of variance(value) and Z' ranging from 0.7-1	(Mauel and Ransijn, 1997) (Armson, *et al.*, 1999)
High content imaging	Intracellular amastigote assay	• Quantitative and amenable to HTS • Mimics the pathophysiological model of the disease • Information rich strategy with direct visualization of intracellular parasites • Multiplexing of different parameters / measurements possible • Sampling and analysis is objective • Avoid compound artefact interference	• High equipment and running costs • Technical expertise required for complex data analysis	Consistent coefficient of variance(value) but Z' values less stringent 0.4-0.7	(Siqueira-Neto, *et al.*, 2010; Siqueira-Neto, *et al.*, 2012; De Rycker, *et al.*, 2013; Dagley, *et al.*, 2015; Tegazzini, *et al.*, 2016)
Ex vivo	Intracellular amastigote	• Mimics the natural microenvironments with respect to the crossing of macrophages membranes by the discovered compounds • Detect the level of toxicity surrounding the primary macrophages	• Expensive nature of the experiment using the mice animal model • Limited throughput Complex co-cultures.	Consistent coefficient of variance(value) but Z' values less stringent (0.4-0.7)	(Osorio, *et al.*, 2011; Aulner, *et al.*, 2013)

The following screening assays have been utilised in either HTS or lower throughput screening programs to identify active compounds against the *Leishmania* parasite:

1.5.3.1. Classical methods

1.5.3.1.1. Direct counting of promastigotes and intracellular amastigotes

Traditional analysis to assess the effect of compounds on parasite viability involved manual counting and quantification by an individual or groups of microscopy users. This method has been used to assess the activity of compounds against all forms of the parasite; intracellular amastigotes, axenic amastigotes and promastigotes (Callahan, *et al.*, 1996). This method was extremely slow and prone to user bias, with subjective interpretation and is no longer routinely used in *Leishmania* drug discovery.

Direct counting of intracellular amastigotes is still being used in hematology laboratories for diagnosis of leishmaniasis (Figure 1.18). The parasites are directly visualized within the macrophage present in the peripheral blood or aspirates from marrow, lymph nodes, spleen and skin lesions using a specific stain, such as Giemsa and Diff quik.

In order to comply with copyright this figure has been removed.

Figure 1.18: Infected macrophages infected with intracellular *Leishmania* parasites using Giemsa staining. Reproduced from Visceral leishmaniasis among liver transplant recipients: an overview. *Liver Transplantation*, 14(12), 1816-1819 (Campos-Varela, *et al*., 2008), copyrights (2008) published by Wiley Online Library.

1.5.3.1.2. Absorbance and fluorescence

Following are a number of methods that have been developed, which utilise absorbance and fluorescence measurements in order to assess the activity of compounds against promastigotes and axenic amastigotes, however this approach has not been used for assays involving the intracellular amastigote form. Screening against the promastigote stage and axenic amastigotes, although more suitable for automation, has previously been shown to have limited success in the identification of active compounds against the intracellular form and has led to numerous false positive hits.

1.5.3.1.2.1. Acid phosphatase activity assay

The assessment of parasite growth in the presence of drugs or compounds has been evaluated via measuring acid phosphatase activity (Bodley, *et al.*, 1995). The acid phosphatases function as hydrolytic enzymes that appear to play a role in the resistance of the parasite to its host as well as in its pathogenicity (Croft, *et al.*, 2006).

Compounds are added to promastigote cultures, which are in the mid-log phase. Following incubation, P-nitrophenyl phosphate (PNPP), a non-specific, non-proteinaceous substrate is added to measure the activity of acid phosphatase (Hardie, 1999). The phosphatases catalyze the hydrolysis of PNPP to P-Nitrophenol, a chromogenic product (Figure 1.19). At the end of the reaction, the optical density is measured at a wavelength of 405 nm. The simplicity and cost effectiveness of the assay makes it suitable for medium-large scale screening. One disadvantage of this method is the low phosphatase activity obtained with avirulent clones of the parasites in comparison to the virulent clones. As both virulent and avirulent clones are present in cell cultures, the signal obtained will not accurately reflect the number of parasites present.

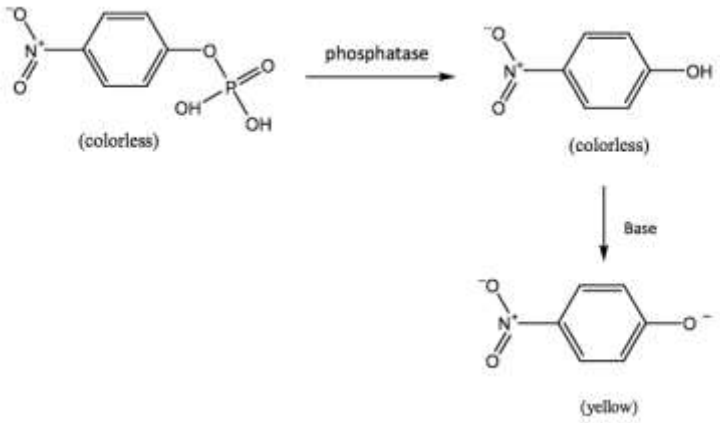

Figure 1.19: Conversion of PNPP to a P-Nitrophenol chromogenic product. Retrieved on 9th Oct, 2017, available at http://bitesizebio.com/7214/ask-a-chemist-how-colorimetric-assays-work/.

1.5.3.1.2.2. Alamar Blue (Resazurin)

AlamarBlue® is an oxidative reductive indicator, used to estimate the number of metabolically active promastigotes remaining after incubation with compounds or drugs. The oxidized form of the active component of AlamarBlue®, resazurin, has a dark blue colour which has little intrinsic fluorescence. Within metabolically active cells the dye is reduced and converted into a highly fluorescent form (red colour) (Figure 1.20) which reflects cell number and can be estimated by reading the absorbance (Ex570nm/Em600nm) or fluorescence (Ex530-560 nm/ Em590 nm) (Nakayama, *et al.*, 1997). Resazurin has also been used successfully in drug sensitivity assays with culture-adapted bloodstream forms of *Trypanosoma brucei rhodesiense*, *Trypanosoma brucei gambiense* (Raz, *et al.*, 1997) and *Trypanosoma brucei brucei* (Sykes and Avery, 2009).

Commonly, promastigotes and axenic amastigotes are grown in culture and treated with the drugs for desired lengths of time e.g. 24 hours, 48 hours or 72 hours. AlamarBlue® is then added and determination is made using fluorescence spectrophotometer at an excitation of 560 nm and an emission of 590 nm. Alternatively, the absorbance of AlamarBlue® can be read on a UV-Vis spectrophotometer at 570 nm.

The advantage of this assay is that it is a simple cost effective approach, enabling the effects of a drug to be measured without complex reagent additions, cell lysis and extraction or counting individual parasites.

One disadvantage of this assay is the limit of detection (LOD) of resazurin which can result in high false positive rates due to the identification of slow acting and cytostatic compounds in addition to the cytocidal compounds. Due to the maximum limit of detection of resazurin, the starting cell density of the parasites has to be kept low to maintain the signal within the linear range of most fluorescence\absorbance detectors. The low starting concentration of parasites leads to growth slowing and cytostatic compounds have a tendency to give the same signal as the truly cytocidal. In an attempt to enhance the sensitivity of these assays, a recent axenic assay was designed (Nuhs, *et al.*, 2015), in which another indicator, BacTiter-Glo™, was used. This provides increased sensitivity for lower detection levels. As a result, the starting density of the cells can be increased by 80-fold to the levels historically used for axenic assays, which improves the assay such that only the cytocidal compounds are identified.

A limitation of metabolic based whole well assays is that it is not evident, based on the output, whether the effect observed is across the whole population or a sub population of parasites. For example, a 50% reduction in activity could reflect 50% death or a reduction in overall metabolism across the entire population. Whilst there are limitations but this assay has potential

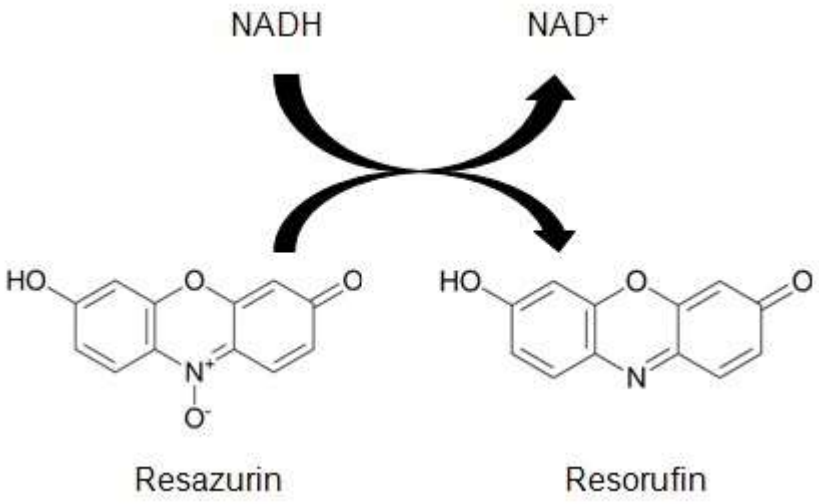

Figure 1.20: Reduction of resazurin to a resorufin fluorescent product. Retrieved on 9th Oct, 2017 from Riss TL, Moravec RA, Niles AL, *et al*. Cell Viability Assays.

1.5.3.1.2.3. 3-(4, 5-Dimethylthiazol-2-yl)-2, 5-Diphenyltetrazolium Bromide (MTT) assay

In this assay the metabolic activity of promastigotes and axenic amastigote forms of the parasite is measured following compound exposure, and is determined by using 3-[4.5-dimethylthiazol-2-yl]-2.5-diphenyl- tetrazolium bromide (MTT). MTT is reduced and converted into formazan which is fluorescent (Figure 1.21) (Maarouf, *et al.*, 1997). After incubation of parasite cultures with compounds or drugs, MTT is added for a given time period. The reaction is then stopped using either sodium dodecyl sulphate or isopropanol. Optical density of the reaction is measured at a wavelength of 570 nm. Disadvantages of this technology include the interaction of some drugs with the tetrazolium salt e.g. meglumine antimonite and the damaging effects of the denaturants on the parasites during the washing steps.

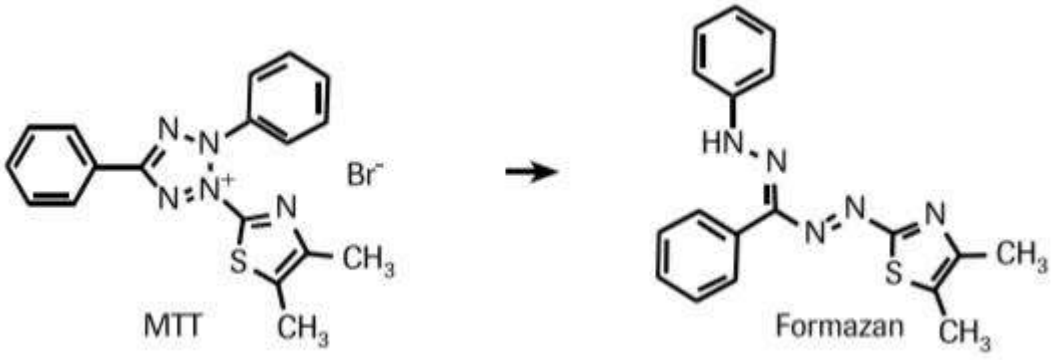

Figure 1.21: Conversion of MTT to Formazan via mitochondrial reductase. Retrieved on 9th Oct, 2017 available at http://www.sigmaaldrich.com/technical-documents/articles/biofiles/cell-viability-and-proliferation.html.

1.5.3.1.3. Flow cytometry

Flow cytometry has been used to determine the efficacy of compounds against *L. infantum* promastigotes. Parasites were exposed to various concentrations of the reference drugs and their action quantified by two flow cytometric approaches: (i) quantitative assessment to calculate the cell division using 5-,6-carboxyfluorescein diacetate succinimidyl ester (CFSE) which binds to lysine residues and (ii)

measurement of cell viability by dual-staining with the membrane-permeable nuclear stains, SBRY-14 and propidium iodide (Kamau, *et al.*, 2001).

Abdullah *et al* conducted an experiment to compare the different fluorescent dyes comparing metacyclic promastigotes and U-937 monocytic cells infected with *Leishmania* parasites (U-937) (Abdullah, *et al.*, 1999). Metacyclic promastigotes were labelled with specific markers including SYTO 17, PKH2-GL and BCECF-Am, and parasite density and viability determined using haemo-cytometry. The results indicated that none of the dyes affected the metacyclic promastigotes as viability was preserved. Infectivity of U-937 cells with metacycylic promastigotes was evaluated using Acridine orange (AO), which is a nucleic acid-selective fluorescent cationic dye and directly compared with Giemsa staining. No differences in activity were observed with any of the reference compounds evaluated.

An infrared fluorescent *L. infantum* strain overexpressing the infrared fluorescent protein (*iRFP*) reporter gene was generated and used to perform phenotypic screening of a small molecule collection of 298 compounds by using *ex vivo* splenocytes from the infected BALB/c mice (Calvo-Álvarez, *et al.*, 2015). Indenoisoquinoline was identified as the most active compound exhibiting an IC_{50} value of 0.011 ± 0.001 µM with a selectivity index of 30 (Calvo-Álvarez, *et al.*, 2015).

The advantage of this technique is the automation and associated accurate determination (Delgado, *et al.*, 2001). Disadvantages include the need for specialised equipment thus access, high running costs of flow cytometry-based assays and limited throughput capability as needs mouse splenocytes for compound screening.

1.5.3.1.4. Radionucleotide uptake assay

To assess parasite viability, a ^{3}H thymidine uptake assay was established for *L. enriettii* and *L. major* promastigotes (Mauel and Ransijn, 1997). New strands of chromosomal DNA incorporate ^{3}H thymidine during mitotic cell division (Figure 1.22). The assay has been used for both life cycle stages e.g. metacyclic promastigotes and axenic amastigotes (Armson, *et al.*, 1999), illustrating, drug induced inhibition A liquid scintillator counter was used for determining the number of parasites based on the radiometric output. An advantage of this type of radiometric incorporation assay is the

direct measurement of proliferation. One of the concerns with this method, is the use of radioactive substances which can be detrimental to user's health and environment, as well as requiring specialized equipment.

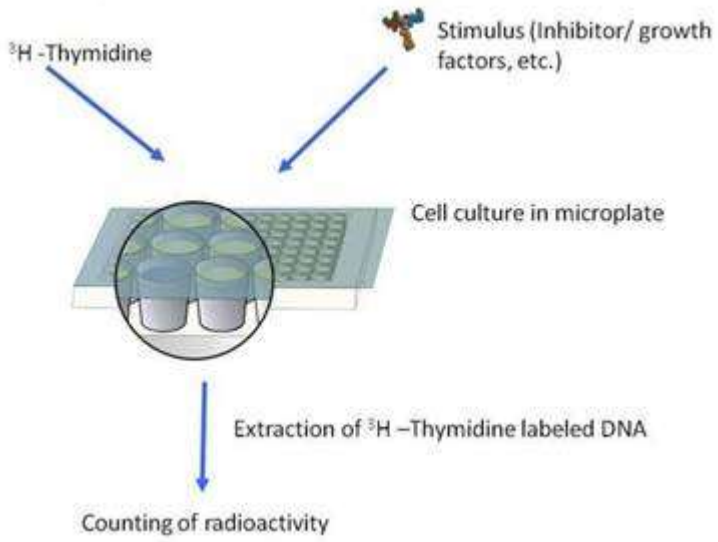

Figure 1.22: Schematic representation of ^{3}H thymidine uptake assay. Retrieved on 9th Oct, 2017, http://www.perkinelmer.com/Resources/TechnicalResources/ApplicationSupportKnowledgebase/radiometric/thymidine.html.

1.5.3.2. Modern methods

Methods that have been frequently used to assess compound efficacy in the last decade and being employed by DND*i* and collaborators for compounds screening.

1.5.3.2.1. Reporter gene assays

Reporter gene assays rely on a reporter gene with a readily measurable phenotype, which can be distinguished on a background of endogenous proteins. During the past decade, scientific literature for pathogens expressing bioluminescence and fluorescent proteins has grown exponentially. Moreover, the methodology has been used as a powerful tool in *in vitro* HTS assays. Furthermore, deep genomics analysis in combination with fluorescent strains has led to the discovery of novel strains of *Leishmania* in addition helped to study the genetic exchange between them. For anti-

leishmanial drug discovery, several reporter genes assays have been used including the β galactosidase, β lactamase and firefly luciferase assays, frequently combinations of reporter genes are also used, *Leishmania* parasites have also been tagged with fluorescent proteins, such as mCherry, tdTomato and DsRed (Beattie and Kaye, 2011; Calvo-Álvarez, *et al.*, 2012; Vacchina and Morales, 2014).

1.5.3.2.1.1. Green fluorescent protein (GFP)

In a study by Chan *et al, L. amazonensis* was genetically modified to express green fluorescent protein (GFP) and was used to infect murine macrophages. A fluorescent assay was designed in a 96 well format to assess the activity of compounds on the genetically modified transgenic *L. amazonensis* parasites (Chan, *et al.*, 2003). Since then improvements have been made in the GFP system for *in vitro* and *in vivo* screening of anti-leishmanial compounds (Sereno, *et al.*, 2007; Muñoz, *et al.*, 2009; Pulido, *et al.*, 2012). To detect the GFP signal a fluorescent microplate reader is required with appropriate filter sets.

An advantage of this technique is the reliability of a prominent signal from the GFP molecule making it easy to detect, as well as the low cost. Studies investigating cell division, gene expression, protein localization and dynamics, chromosome replication and organization, protein-protein interactions and intracellular transport pathways can also be undertaken using GFP-tagged parasites. The disadvantage associated with this technique is the varying signal based on expression, as GFP signal cannot be amplified in a controlled manner. The impact using a transgenic parasite may have on cellular functions (Freitas-Junior, *et al* 2012), thus on the data obtained, may also be difficult to interpret.

1.5.3.2.1.2. β galactosidase reporter assay (BGA)

Leishmania promastigotes expressing β-galactosidase were selected by Okuno *et al* forcompound screening (Okuno, *et al.*, 2003). To visualize expression of *lacZ* in both promastigotes and intracellular amastigotes, 5-bromo-4-chloro-3-indolyl- β-D-galactopyranoside (CPRG) was used. Data obtained using CPRG correlated well with the numbers of Lz/lacZ amastigotes in macrophages determined microscopically, hence

proving this to be a useful assay for screening compounds against the amastigote form of the parasite. The major drawback with using β galactosidase is its large size (116 kDa monomer) and endogenous expression in mammalian cells, including macrophages.

1.5.3.2.1.3. β lactamase reporter assay (BLA)

β lactamase reporter assay (BLA) uses a catalytic system developed to circumvent the short comings of the β galactosidase reporter system. In a study conducted by Zhu *et al*, *L. donovani* promastigotes were genetically modified to express the β lactamase reporter gene. Approximately 200,000 compounds were screened using this approach, and 70 new compounds were discovered having an EC_{50} of less than 1μM (Zhu, *et al.*, 2012). In terms of its robustness, sensitivity and ease of use, the BLA reporter system significantly outshines all the other reporter genes technologies. A major drawback includes the identification of false positive compounds in a primary screen, which modulate β lactamase expression by interfering with the signaling pathway invoked by receptor activation.

1.5.3.2.1.4. Luciferase based assay

Assays have been established and validated with classical anti-leishmanial agents for various species of *Leishmania* parasites expressing luciferase reported gene (Roy, *et al.*, 2000). This system was adapted to evaluate the activity of synthetic and marine extract compounds in a 96 well microtiter plate format for *Leishmania donovani* cell lines expressing firefly luciferase reporter gene (Ashutosh, *et al.*, 2005). Activity of compounds for the intracellular amastigote form has also been assessed via infecting J774.1 cells (mouse macrophage cells) with metacyclic promastigotes expressing firefly luciferase (Ashutosh, *et al.*, 2005). The main advantages of this approach include high sensitivity, with substrates continually being improved, and the absence of background noise in host cells. Disadvantages include requirement of specific substrates with poor cellular uptake efficiency. Other drawback includes, unfeasibility in repeated measurement of the same sample because of short half-life after the fixation of plate to record the sample.

1.5.3.2.1.5. Use of transgenic *Leishmania* for *in-vivo* real-time imaging:

Fluorescent or bioluminicient-engineered parasites represent an exciting tool for exploring *in vivo* host-parasite interactions. Establishment of an *in-vivo* imaging model paves the way to further evaluate frequency, efficacy, and treatment duration of novel therapies at pre-clinical stages. In addition, they provide a bioethical aspect as fewer animals are used in the study, resulting in less animal-to-animal variation and statistical significant results (Lang, *et al.*, 2005). Quantifying in-*vivo* bioluminescence is method of choice for evaluation of *Leishmania* parasite load in internal organs. The limitation of this technique is the low resolution which only provides a 2D image (Dube, *et al.*, 2009). In addition, an efficient uptake is essential for the specific light-emitting substrate required for bio-luminescent imaging to reach the parasite in the parasitophorous vacuole. Hence fluorescent proteins have been only used for cutaneous leishmaniasis models because visceral form requires high tissue penetration. The first cutaneous leishmaniasis murine model was developed with luc-transfected *L. amazonensis* strain (Lang, *et al.*, 2005). In a latter study, parasites were isolated from a cutaneous lesion of a BALB/c mice 10 days after infecting them with luc-transfected *L. mexicana* strain (Thalhofer, *et al.*, 2010).

1.5.3.2.2. High content imaging

Multi-parametric, single cell information of biological events can be obtained using high content imaging (HCI) and analysis (HCA), which employ the use of mathematical algorithms to produce biologically relevant data from images (Sirenko, *et al.*, 2015). Fluorescence microscopy is one of the most powerful tools available to study biological processes, and combining this technology with automated image acquisition and analysis can provide a huge resource of quantitative cellular information (Kubitscheck, 2017). The imaging and analysis tools have been, and continue to be, developed to provide automated and higher throughput screening of a range of biological events (Figure 1.23), such as cellular morphology, protein expression and cellular interactions following drug exposure (Zanella, *et al.*, 2010). HCI employs sophisticated algorithms to automatically and rapidly analyse differences in biological parameters upon drug

exposure (Zanella, *et al.*, 2010). The data acquired through automated processes in HCI are more robust since the risk of human bias is minimal, thereby making the whole process more reproducible and time efficient (Bickle, 2010).

A number of HCI assays for the intracellular amastigote form of the parasite have been established (Siqueira-Neto, *et al.*, 2012; De Rycker, *et al.*, 2013; Dagley, *et al.*, 2015). These assays can be discriminated based on the differentiation of host cells, infectivity with either the metacyclic promastigotes or axenic amastigotes, incubation times and the fluorophores used for detection of the intracellular amastigotes.

The majority of these assays utilize the THP-1 human monocytic cell line derived from acute monocytic leukemia patients activated with Phorbol 12-myristate 13-acetate (PMA) to produce cells with macrophage-like properties. Other cell lines, such as J774.1 and RAW 264.7 (murine macrophages) cells have also been used as host cells but have not been reported as routinely used in high-throughput HCI assays for *Leishmania* because they are morphologically not good for imaging. These cell lines are adherent in nature and do not require differentiation. Primary macrophages and *ex vivo* amastigotes have been used previously for hit-to-lead to identify potential anti-leishmanial compounds (Seifert, *et al.*, 2010; Fernandez, *et al.*, 2012).

De Rycker *et al* (De Rycker, *et al.*, 2013) infected PMA differentiated THP-1 cells with axenic amastigotes in a 384-well assay plate, whereas Siqueira-Neto *et al* (Siqueira-Neto, *et al.*, 2012) initially differentiated the THP-1 cells using PMA in a large volume in a cell culture flask, then subsequently trypsinized and added them to 384-well assays plates with metacyclic promastigotes. In a separate assay, Dagley *et al* (Dagley, *et al.*, 2015) used PMA to differentiate the THP-1 cells in 384-well plates after which metacyclic promastigotes pre-stained with a fluorescent dye, CellTrackerTM Orange CMRA were added. After 72 or 96 hours post addition of drugs, cells were fixed and stained with nuclear and cytoplasmic dyes. De Rycker *et al* used DAPI to stain the nucleus and CellMask™ deep red to stain the cytoplasm. Siqueira-Neto *et al* used the nucleic dye Draq5 whereas Dagley *et al* used cytoplasmic dye CellTracker Green CMFDA along with DAPI to accurately quantify the number of parasites per macrophage. Images were subsequently acquired on high content imaging systems, such as GE INCell-1000™, Cellomics ArrayScan-VTI™ and PerkinElmer Opera™ confocal microscope.

De Rycker *et al* have shown that the intracellular amastigote assay is more suited as a drug screening platform when compared to the currently employed axenic amastigote drug screening assays. A library of 16,000 diverse compounds was screened with the historic axenic and intracellular amastigote assays described above, out of which 378 compounds were identified as active in the axenic amastigote assay with >70% activity at 3 µM (2.4% hit-rate) and 83 compounds showed >70% activity at a concentration of 50 µM in the intracellular amastigote assay (22% of the active hits). The results indicated a false positive rate with high magnitude for the axenic assay implying that the intracellular amastigote assay is more reliable.

A recent HCI assay for intracellular *L. donovani* amastigotes was developed by Tegazzini *et al*, which replaced standard foetal bovine serum with horse serum in order to eliminate the extracellular parasites from the assay, as these can influence the data generated. Incorporation of Edu was used to identify the proliferation of *L. donovani* intracellular amastigotes within the THP-1 host cells (Tegazzini, *et al.*, 2016).

High content screening (HCS) is information rich and has more specificity and sensitivity when compared to the indirect fluorometric or colorimetric assays. In HCI assays, there exists the possibility to differentiate between pathogen killing and any sub-cellular response or any damage to the host, thereby giving an indication about the possible mechanism of action of the compound or general cytotoxicity. From a HTS perspective, throughput for some HCI assays is limited due to the necessity to image a 384-well plate with numerous fields per well over a period of hours.

Image analysis software associated with automated microscopy enable custom designed algorithms to be developed for image analysis. These algorithms can be modified and further optimised based on the user needs. Simultaneous image acquisition and analysis provides a significant advantage and expedites data evaluation and decision making. Disadvantages of HCI include the initial expenditure for specialised high content screening equipment, in addition to ongoing maintenance and running costs, added to the need to have a level of technical expertise and a proper data storage and analysis system.

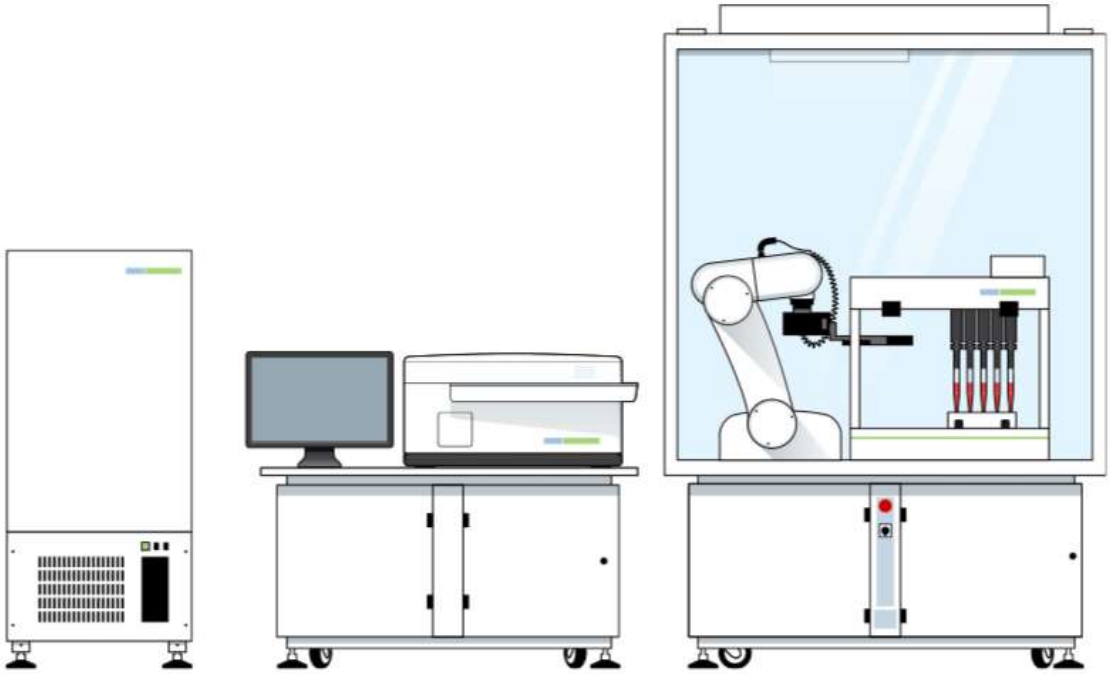

Figure 1.23: High-content imaging platform. From left to right is a Tri-gas CO_2 Incubators set at 37ºC with 5% CO_2, an Opera™ confocal microscope with image analysis software and an automated liquid handler and dispenser with a robotic arm in a biosafety cabinet.

1.5.3.2.3. High throughput screening

High-throughput screening (HTS) is often the first method of choice for examining large numbers of compounds to identify modulators and effectors against selected targets, whether molecular or whole organism (Annang, *et al.*, 2015).

For screening and identification of new molecules active against *Leishmania* in higher throughput formats, several different assays have been developed using either promastigotes or amastigotes stages of the parasite. Assessing the effects of compounds on cell viability using free-living parasites is the mostsimple and time efficient approach. Such assays frequently employ promastigotes; however, these assays may provide poor predictive indications of compound activity from the disease-causing life stage of the parasite.

Axenic amastigotes, which are adapted to grow outside host cells, present an alternative approach with the advantage of better mimicking the disease-causing life stage, in

comparison to promastigotes. However, axenic amastigotes have also been reported to display different protein expression profiles and drug sensitivities from amastigotes residing *in vivo* in host cells (De Rycker, *et al.*, 2013).

A HCS/HTS for L. donovani was performed by colleagues at the Institute Pasteur Korea (IPK) screening 26,500 structurally diverse chemical compounds (Siqueira-Neto, *et al.*, 2010) subsequently HTS of 700,000 compounds by the Genomic Institute of the Novartis Research Foundation (GNF) was also undertaken (Bustamante, *et al.*, 2011). In 2011, a HCS method using a clinically relevant form of the parasite was adapted to a 96 well plate format to screen a few hundred compounds (De Muylder, *et al.*, 2011).

High-throughput phenotypic screening was more recently employed by GlaxoSmithKline to screen 1.8 million compounds against *T. brucei*, *T. cruzi* and *L. donovani* (Pena, *et al.*, 2015). Identified hits were clustered based on desirable physiochemical properties. Bioinformatics tools were used to identify the hypothetical biological target and the potential hit to lead compounds were clustered to make anti-kinetoplastid chemical boxes against the respective diseases containing approximately 200 compounds each.

Outcomes from these HTS campaigns will be included in the discussion in chapter 4.

1.5.3.2.4. *Ex vivo* screening assays

Ex vivo models provide a pathophysiological environment that is relevant to the spleen and can be used to identify pharmacologically active compounds against the visceral form of leishmaniasis (Osorio, *et al.*, 2011). The ex-vivo splenic explant culture was developed by injecting metacyclic promastigotes transfected with a luciferase (luc) reporter gene via the intracardial route into female inbred Chester Beatty hamsters and BALB/C mice. Out of the 4035 compounds screened, 239 were active in the primary screen, of which 84 compounds were further identified as potential lead compounds.

L. amazonensis LV79 genetically modified to constitutively express DsRed 2 protein were injected in the hind foot of Swiss nu/ nu mice, resulting in a lesion. The lesion was excised, amastigotes purified and added to adherent bone marrow cells (6 days old) plated in 384-well plates. Following overnight incubation, compounds were added and cultures incubated for 72 hours. Cells were stained with Hoechst and LysoTracker

DND-26 and images acquired on an Opera™ QEHS (Aulner, *et al.*, 2013). Of sixty compounds tested, eight compounds showed anti-leishmanial activity against the *Leishmania* parasites at less than 10 µM, with little or no host cell toxicity. The advantage of this assay is the fact that it mimics the natural *in vivo* microenvironments with respect to the crossing of macrophages membranes by the discovered compounds and can detect the level of toxicity surrounding the primary macrophages. It is the closest screening to a real infection; thus, it can be a second screening stage for optimized hits or lead compounds before to the preclinical studies. Additionally, the environment where the exposure to the drug takes place includes cells of the immune response that can play a role in the efficiency of the drug. The main disadvantage of this approach is the expensive nature of the experiment using the mice animal model (Swiss nu/nu and BALB/C), and reproducibility concerns and limited throughput of the assay.

1.6. Conclusion

Classical microscopic methods of screening for anti-leishmanial compounds are cumbersome, laborious and time-consuming with limited throughput. Flow cytometric analysis using monoclonal antibodies and fluorescent dyes has been used for drug discovery but is faced with limitations such as decreased sensitivity, expensive antibodies and minimal exposure times with the compounds thus reducing efficacy. Screening using reporter genes requires drug selection for maintaining the episomal expression and, in certain situations where the episomal plasmid constitutes the reporter gene, the relative output of the reporter will depend on the copy number of the transfected plasmid, rather than the compound efficacy. Another limitation of the reporter gene expression assays (e.g., GFP reporter gene 15) is that this assay cannot differentiate between dead and living intracellular amastigotes. Luc-based reporter gene assays have the ability to differentiate cell viability; however, they are often too expensive to be used in HTS owing to the cost of substrates and lysis buffers. *Ex vivo* models are not suitable for translation HTS, because the primary macrophages obtained from animals are a non-homogenous population of cells, impacting reproducibility. Homogenous populations can be acquired using monocytic-cell-derived cell lines, for example THP-1 cells. These cells provide a nondividing monolayer and can be differentiated into macrophage-like cells.

To overcome these limitations, the current anti-leishmanial drug discovery efforts have shifted to high-content screening using imaging technology to obtain multiparametric information-rich data. HCI has contributed significantly to the recent advances in *Leishmania* drug discovery, enabling the screening of large collections of compounds in complex phenotypic assays. Although expensive and often technically challenging, HCI currently provides the most biologically relevant assay for identifying molecules with clinical potential. HCI of the intracellular amastigote is thus likely to remain the gold standard for *Leishmania* drug discovery in the coming decade.

1.7. Aims and objectives

1. **Develop sensitive and reproducible assays to estimate the effect of compounds:**

   - Develop a promastigote viability assay for the identification and characterization of novel molecules against *L. donovani* DD8.
   - Develop complementary THP-1 cytotoxicty assays mimicking the promastigote and intracellular amastigote assay conditions.
   - Evaluate assay sensitivity using the reference compounds amphotericin B and miltefosine.
   - Evaluate assay reproducibility of these assays by statistical parameters.

2. **Determine the activity of compounds from a scaffold library against *L. donovani* DD8 promastigotes and intracellular amastigotes:**

   - Screen 5560 compounds synthetic scaffold library using promastigote and intracellular amastigote assays to identify hit molecules.
   - Reconfirm compound activity and perform cytotoxic profiling of both using THP-1 and HEK-293 cytotoxicity assays.

3. **Determine the activity of natural product derived compounds against *L. donovani* DD8 promastigotes and intracellular amastigotes:**

- Screen 472 natural product compounds using the promastigote and intracellular amastigote assays.
- Reconfirm compound actives and determine cytotoxic profile of the active hits using the THP-1 and HEK-293 cytotoxicity assays.

4. Prioritisation of hits based on structure activity relationship and medicinal chemistry tools:

- Identification and biological evaluation of analogues of the active compounds using established assays for *L. donovani* DD8 parasites.

5. Target identification and mechanism of action studies:

- Characterization of hit compounds **BZ1** and **BZ1-I** to determine target or mechanism of action.
- To employ *in vitro* assays to ascertain the mode of action of the compound/s including time to kill assays, host cell preincubation studies etc.
- Establish whether cyclopental quinolin-9-amines are apoptotic inducers or not.
- Determine the effects of cyclopental quinolin-9-amines on *L. donovani* DD8 mitochondrial transmembrane potential.
- Measure the stability of **BZ1** and **BZ1-I** in a physiological model based on changes in pH.
- Generation of resistant paarsites against **BZ1** and **BZ1-I** compounds and stability of resistant cell line after removal of drug pressure.

6. Comparison of compound efficacy between different species and strains from the Old and New World visceral leishmaniasis. Comparison of anti-trypanosomal and anti-malarial activity within different species and strains of *T. brucei*, *T. cruzi* and *P. falciparum*.

7. Downstream processing in drug discovery

- *In vitro* Drug Metabolism and Pharmacokinetic studies on identified compounds

- Establish a cytotoxicity panel for HepG2, Raw264.7, J774.1, HEK-293 and THP-1 cell lines.

Chapter 2: **Materials and Methods**

This section contains the materials and methods for routine protocols performed throughout this research project and referenced throughout this thesis.

2.1. Materials/ Biologicals

2.1.1. Reagents

- RPMI (1X) Roswell Park Memorial Institute Medium 1640 GlutaMAX™ (Gibco®- Life Technologies, Australia).
- DMEM (1X) Dulbecco's Modified Eagle Medium (Gibco®- Life Technologies, Australia).
- Medium 199 (1X) (Gibco®- Life Technologies, Australia).
- Heat inactivated fetal bovine serum (HIFBS) (Hyclone™ ThermoFisher, Australia).
- PBS (0.01 M) Phosphate Buffer Saline (Sigma-Aldrich, Australia) (NaCl 0.138 M; KCl 0.0027 M); pH 7.4, at 25°C.
- Adenosine (Purity ≥99%) (CAS Number 58-61-7) (Sigma-Aldrich, Australia).
- Folic Acid (Purity ≥97%) (CAS Number 59-30-3) (Sigma-Aldrich, Australia).
- L-glutamine 200 mM (Gibco®- Life Technologies, Australia).
- BME vitamin mix 100X (Sigma-Aldrich, Australia).
- DMSO Dimethyl sulfoxide (Purity ≥99.7%) (CAS Number 67-68-5) Hybri-Max™, BioReagent (Sigma-Aldrich, Australia).

- Penicillin-Streptomycin solution (10,000 U/mL) (Gibco®- Life Technologies, Australia).
- Mercaptoethanol ≥99.0% (CAS Number 60-24-2) (Sigma-Aldrich, Australia).
- PMA Phorbol 12-myristate 13-acetate (Purity ≥99%) (CAS Number 16561-29-8) (Sigma-Aldrich, Australia).
- Amphotericin B (CAS No 1397-89-3) (Purity ≥95%) was obtained from Caymen® Chemicals. Stored at -20ºC as dry powder. Stock solution of 1 mM was prepared in 100% Dimethyl sulfoxide (DMSO) immediately before use.
- Miltefosine (CAS No 58066-85-6) (Purity ≥98%) was obtained from Caymen® Chemicals. Stored at -20ºC as dry powder. Stock solution of 10 mM was made up in sterilised MilliQ® water immediately prior to use.
- Resazurin (CAS No 62758-13-8) was obtained from Caymen® Chemicals. Stored at -20ºC as 60 mM stocks were made in autoclaved MilliQ® water. Five mL aliquots stored at -20ºC for up to six months; stocks were thawed at room temperature before use.
- Puromycin (CAS No 58-58-2) (Purity ≥98%) was obtained from Sigma-Aldrich, Australia. Stored at -20ºC as dry powder. Stock solution of 10 mM was made in sterilised MilliQ® water immediately before use.
- VL-2098 and DNDI-1044 were provided by DND*i*. Stored at room temperature. Stock solution of 10 mM was made in 100% DMSO immediately before use.
- Phorbol 12-myristate 13-acetate (PMA) 1 mg was obtained from Sigma-Aldrich, Australia. A stock solution was made by dissolving 1mg/mL and stored at -80ºC, stock solution was diluted 1:20 in 100% DMSO and then the working solution diluted 1:2000 to give a final concentration of 25 ng/mL.
- MitoTracker™ Red CM-H2Xros (catalog number M7513) obtained from ThermoFisher, Australia.

- m-chlorocarbonylcyanide phenylhydrazone (CAS Number 555-60-2) was obtained from Sigma-Aldrich, Australia. Stored at -20ºC as dry powder. Stock solution of 37.5 mM was prepared in 100% Dimethyl sulfoxide (DMSO) immediately before use.

- Valinomycin (CAS Number 2001-95-8) was obtained from Sigma-Aldrich, Australia. Stored at -20ºC as dry powder. Stock solution of 37.5 mM was prepared in 100% Dimethyl sulfoxide (DMSO) immediately before use.

2.1.2. Maintenance of mammalian cell lines

• THP-1 (human monocytic leukemia) cells obtained from the American Type Culture Collection (ATCC®), USA (THP-1 TIB-202™) were maintained in RPMI 1640 medium GlutaMAX™ supplemented with 0.05 mM Mercaptoethanol and 10% (v/v) HIFBS at 37ºC in a humidified atmosphere of 95% air and 5% CO_2. The cells were passaged every 48 hours to maintain cell density between $2.5x10^5$ and $8x10^5$ cells/mL. The THP-1 culture was discarded after they reached passaged 20.

• HEK (human embryonic kidney) 293 cells obtained from the ATCC®, USA (HEK-293 CRL-1573™) were maintained in DMEM supplemented with 10% (v/v) HIFBS at 37ºC in a humidified atmosphere of 95% air and 5% CO2. The cells were passaged as they reach 80% confluence.

2.1.3. Parasites

Leishmania donovani MHOM/IN/80/DD8 promastigotes obtained from the ATCC®, USA (Laveran and Mesnil) Ross (ATCC® 50212™) were cultivated at 27ºC at normal atmospheric conditions in M199 medium supplemented with 100 µM Adenosine, 23 mM Folic Acid, 2 mM L-glutamine and 1% (v/v) BME vitamin mix and 10% (v/v) HIFBS. The pH of the media was adjusted to 6.8 with 1 M Hydrochloric Acid (HCl) before filter sterilized with cellulose acetate membrane filter, pore size 0.22 µm (Corning® bottle-top vacuum filter system). Penicillin-Streptomycin solution (50,000 U/mL) was added to the filtered media prior to use. *L. donovani* DD8 parasites for use in the promastigote assay were maintained in mid-log phase growth by sub-culturing

every 96 hours. In order to obtain metacyclic promastigotes for use in the intracellular amastigote assay, *L. donovani* DD8 promastigotes were subcultured every 7 days. All *L. donovani* DD8 promastigote cultures were seeded at a concentration of $1x10^5$ parasites/mL in a 75 cm^2 culture flask. The *L. donovani* DD8 parasite cultures were discarded when they reach passage 20.

2.2. Cell counting techniques

2.2.1. Counting mammalian cells

THP-1, HEK-293, HepG2, J774.1 and RAW-264.7 were counted on a haemocytometer using 0.4% Trypan Blue dye.

2.2.2. Formaldehyde fixation

Motile forms of *L. donovani* DD8 from liquid cultures were diluted in 4% formaldehyde and counted on a haemocytometer. The formaldehyde solution was prepared by the addition of 100% formaldehyde in to saline-sodium-citrate buffer (SCC), comprised of 3M NaCl, and 300 mM sodium citrate $Na_3C_6H_5O_7$ (sodium citrate) at pH 7. Cells were allowed to settle on to the haemocytometer surface for 5 to 10 minutes before counting.

2.3. Assay protocols

2.3.1. *L. donovani* DD8 promastigote viability assay

An initial parasite density of $1x10^5$ parasites /mL was inoculated into a 75 cm^2 flask (in a total of 30 mL of M199 medium + 10% (v/v) HIFBS) and incubated at 27ºC. After 96 hours, the parasites reached the mid-log phase and were seeded in the 384-well Greiner™ black/clear bottom plates at a concentration of $5x10^5$ parasites/mL in a volume of 55 µL using an Agilent BRAVO™ automated liquid handling platform. The stocks were diluted 1:25 in M199 media without HIFBS using a dilution plate. The compounds were dispensed in 5 µL using a Agilent BRAVO™ and plates incubated for an additional 68 hours at 27ºC at normal atmospheric conditions. Resazurin was then added to give

(0.142 mM final assay concentration) to the plates in a volume of 10 µL/well using a Multidrop™ 384 Reagent Dispenser (Thermo Scientific®, Newington, NH) and incubated at 27ºC at normal atmospheric conditions. The plates were read after 4 hours using an EnVision™ Multilabel plate reader (PerkinElmer®) using fluorometry settings with excitation of 530 nm and emission 590 nm. The IC_{50} value for each compound was calculated by normalizing the data based on 1µM amphotericin B (100% inhibition of parasites) serving as positive control and 0% inhibition = 0.4% DMSO as negative control against log of concentration in PRISM™ 6 software (GraphPad Software Inc., San Diego, CA) (denoted IC_{50} by PRISM™). Each concentration was screened in duplicate. The assay protocol is illustrated in Figure 2.1.

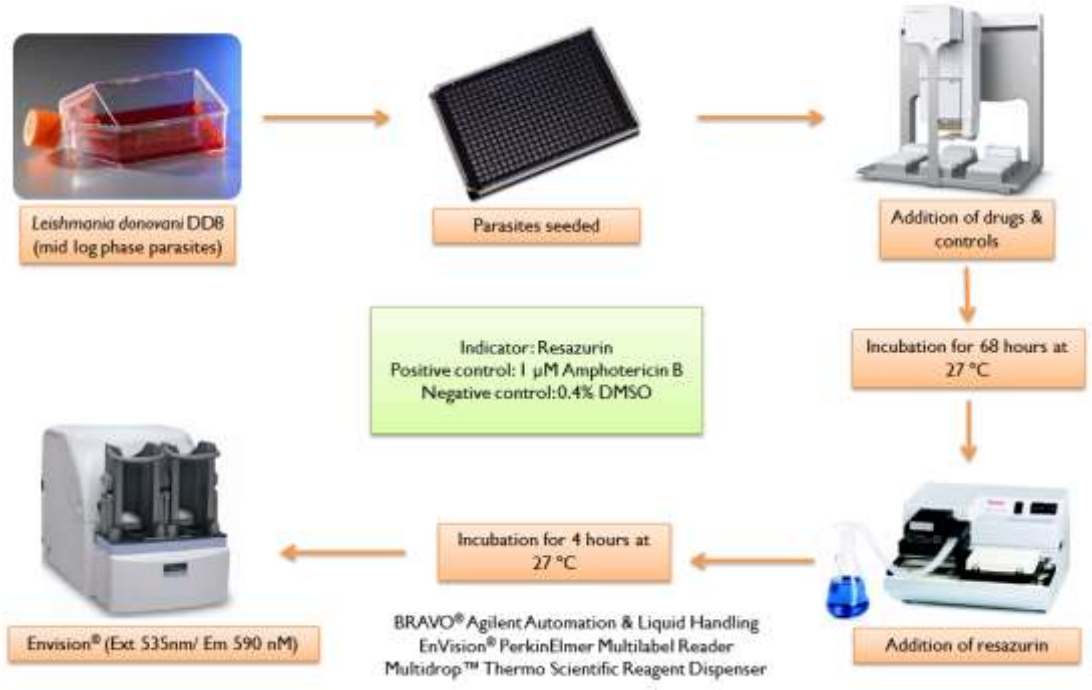

Figure 2.1: Schematics for promastigote viability assay.

2.3.2. *L. donovani* DD8 intracellular amastigote assay

A 9-day high content, high-throughput imaging assay was used to identify compounds active against *L. donovani* DD8 intracellular amastigotes as described previosuly (Figure 2.2) (Duffy, *et al.*, 2017).

THP-1 cells were prepared at $2.5x10^5$ cells/mL for addition to 384-well CellCarrier™ assay plates in a 150 mL sterile clear polystyrene bottle (Corning®). The cells were suspended in RMPI medium + 10% HIFBS (v/v). PMA was added to induce cell differentiation into macrophage like cells in a concentration of 25 ng/mL. 1 mg/mL of PMA stock solution was diluted 1:20 in DMSO and then the working solution diluted 1:2000 in the cell suspension to give a final concentration of 25 ng/mL. 50 µL of cell suspensions at a density of $2.5x10^5$ cells/mL were added to 384-well CellCarrier™ assay plates (PerkinElmer®, USA) using a BRAVO™, which was also used for all subsequent additions unless otherwise stated. The plates were incubated for 45 minutes at room temperature followed by 24 hours at 37°C/ 5% CO_2. After 24 hours the plates were washed 3 times with PBS. After washing 40 µL RMPI + 10% HIFBS (v/v) was added to assay plates. The assay plates were incubated for 48 hours at 37°C/ 5%CO_2.

L. donovani DD8 promastigotes were then added to the assay plates. Parasites with a long/thin body and long tail were counted as metacyclics. Culture of *L. donovani* DD8 promastigotes seeded 168 hours before with $1x10^5$ cells/mL in standard medium in a 75 cm^2 cell culture flask were centrifuged at 3000 revolutions per minute (RPM) for 8 minutes, the supernatant was removed and the pellet resuspended in RPMI medium + 10% HIFBS (v/v). The multiplicity of infection was established as 1:5 (host cells: parasites). Ten (10) µL of the above diluted parasite sample was added to assay plates, incubated for 2 hours at room temperature followed by 24 hours incubation at 37°C / 5% CO_2. Assay plates were then washed to remove any non-internalized parasites.

Within a biosafety cabinet, plates were flicked to remove media, 50 µL of PBS added and flicked again to remove the PBS and non-internalized parasites. Forty-five µL RMPI medium + 10% HIFBS (v/v) was added to the plates incubated for 72 hours at 37°C / 5% CO_2. A reference compound plate was prepared containing amphotericin B, miltefosine and VL-2098. Stock concentrations were made for amphotericin B (1 mM) in 100% DMSO, miltefosine (10 mM) in autoclaved MilliQ™ water and VL2098 in 100% DMSO.

The reference compound plate was diluted 1:25 in RMPI with no HIFBS and 5 µL of this dilution dispensed into the assay plates. The plate to ascertain Z' values was prepared containing 0.4% DMSO and 1 µM amphotericin B (100% Inhibition). The Z' plate was diluted 1:25 in RMPI with no HIFBS and 5 µL of this dilution was dispensed

to assay plates using a BRAVO™. All plates incubated for 72 hours at 37°C/5% CO_2. The assay plates were fixed with 4% paraformaldehyde (PFA) with the addition of 20 µL of 4% PFA and incubated for 15 minutes. Plates were washed twice with 50 µL of PBS/well. Fifty (50) µL of dye mix containing Sybr Green (Life Technologies, Australia) (1:10,000), Cell Mask Deep Red (Life Technologies, Australia) (1:30,000) and 0.1% Tween added to assay plates and incubated for 30 minutes. Plates were washed three times with PBS and wrapped in aluminum foil to protect it from light exposure until imaging on Opera® High Content Screening System (PerkinElmer®, USA).

2.3.2.1. Re-optimized of intracellular amastigote assay

A variation in the assay protocol for the intracellular amastigote assay (2.3.2.) was undertaken to improve and maintain infectivity throughout the duration of the assay,and increase the assay window. The re-optimization steps were as follows

1. Washing off PMA and extracellular parasites three times with 100 µL/well PBS using the Aqua Max™ DW4 plate washer (Molecular Devices®).

2. Re-addition of PMA at a final concentration of 25 ng/mL after removal of the extracellular parasites and extending the compound exposure from 72 hours to 96 hours.

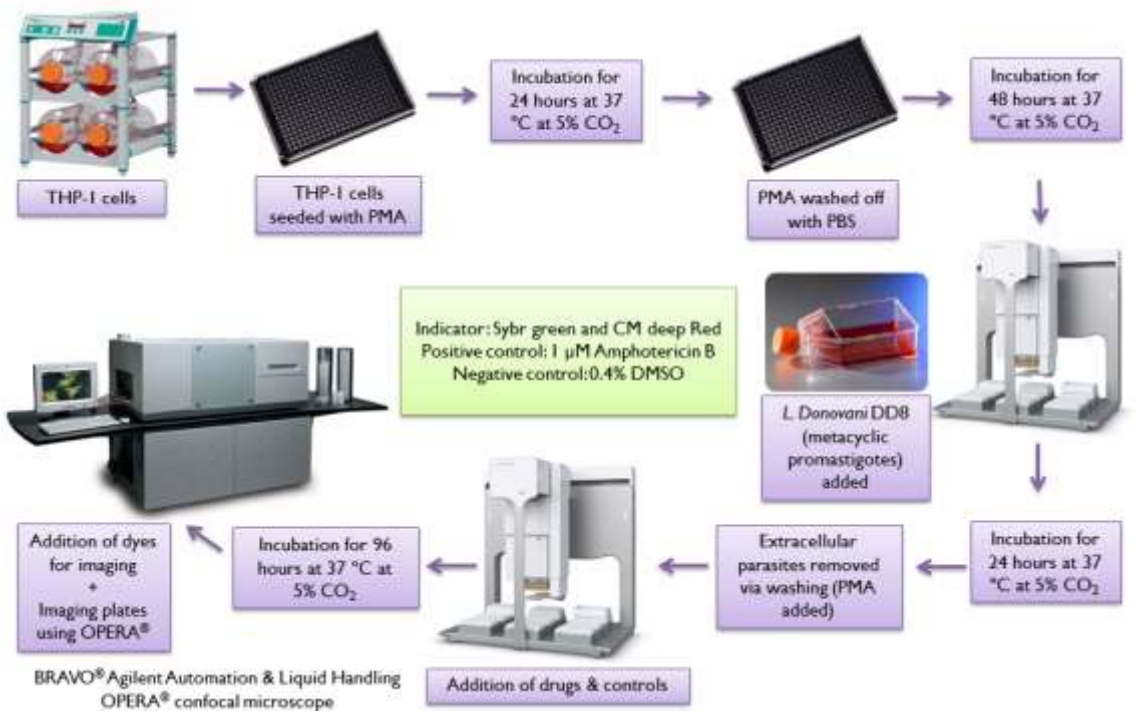

Figure 2.2: Schematics for intracellular amastigote assay.

2.3.2.2. Image acquisition

Two channel images were acquired in a fully automated and unbiased manner using a spinning disk confocal microscope Opera® High Content Screening system (PerkinElmer®, USA) using a 20X water objective. The 488 nm (blue channel) and 640 nm (red channel) lasers were used.

2.3.2.3. Image analysis

The images were analysed using Acapella™ High Content Imaging and Analysis Software (Figure 2.3). An algorithm was developed to individualize and identify the macrophages by setting an intensity threshold to discriminate the foreground (macrophage area) from the background (extracellular space). CellMask™ deep red stains the cytoplasm of the macrophage containing the amastigotes there by discriminating the fore ground with the dark black ground. The macrophage nuclei and the amastigotes nuclei (both stained with the Sybr green differentiated based on the size) were identified and counted as foreground. The extracellular parasites are excluded

from the calculations. Host cell infection was calculated based a spot detection protocol of the stained parasite nuclei. The percentage infectivity was determined by the number of infected cells divided by the total number of cells in the field after normalization of the data based on the internal controls

The images were uploaded to the Columbus™ Image Data Storage and Analysis System (PerkinElmer®, USA). The image analysis was performed by batches in Columbus™ using custom designed image analysis scripts developed beforehand with the Acapella™ image analysis software.

- Raw image (Figure 2.3A): Represent the original image acquired by Operetta. Parameters such as exposure time, excitation (light intensity) and focal plane height were precisely determined, for the purpose of generating high quality images for subsequent analyses. With the use of fluorophores such as Sybr Green and CellMask Deep Red we were able to mark both the nuclei of the host cell and parasite and cytosolic region were removed, respectively.

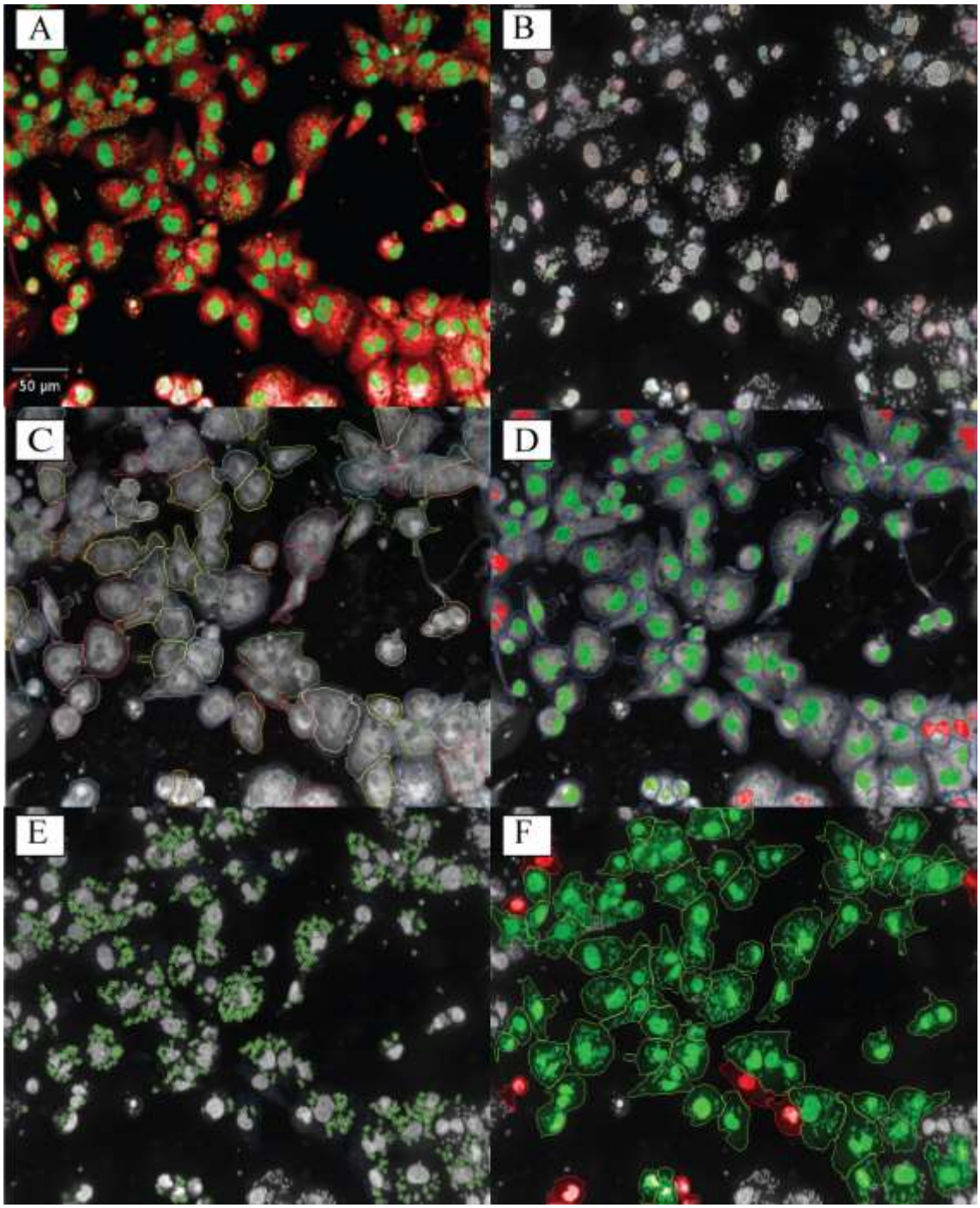

Figure 2.3: Image analysis for intracellular amastigote assay using Acapella® software. (A) Screen shot depicting input image with green colour as Sybr green (host cell and parasitic nucleus) and red colour as CellMask™ Deep Red (host cytoplasm) **(B)** Find nuclei function marking the nucleus of the host cell **(C)** Find cytoplasm function marking the cytoplasmic border of the host cells **(D)** Image analysis with select population function marking the host nucleus with in the border **(E)** Spots showing intracellular parasites **(F)** Input image with green as infected cells and red as non-infected cells. The cells at the borders are excluded as half or part of them is visible in the field.

- Find nuclei (Figure 2.3B): Responsible for the detection and quantification of the nuclei of the host cells in the image. Detection is based on the difference in intensity of the fluorescence signal from the nucleus area compared to the other regions of the image. With the objective of establishing the best detection method, four scripts were tested available in the software, adjusting the analysis settings (parameters) and viewing the detection. When detection errors were noted, another rendering method was selected. After choosing the optimal method, we perform a fine adjustment in the configuration sublevels to optimize detection, based on size characteristics, cell spacing, minimum signal intensity and contrast thresholds;

- Find cytoplasm (Figure 2.3C): It operates in the selection and demarcation of the cytoplasmic area in the image. The cytoplasm of the cell is detected as the marginal region to the cellular nucleus that has a signal of intensity higher than the background. A method was opted which provided more precise segmentation of the cytoplasm. The refinement was applied in this processing step to set the intensity detection threshold.

- Select population (Figure 2.3D): Creates a subpopulation from the existing populace. The first population selection was applied to remove the present cells from the edge of the image.

- Find spots (Figure 2.3E): Responsible for the detection, selection and counting of individual parasites within the host cells. Spots are detected as a small circular region with a reduced area whose high signal intensity stands out from the bottom signal, within the boundaries of the previously defined cytoplasm region. The spots represent the signal of DNA marked from the parasite from the nucleus and the kinetoplast indistinguishable under this magnification. In this step, after appropriate adjustment, we were able to precisely detect individual parasites in the image, without identifying an excessive number of false positives (commonly generated by natural differences of contrast in the cytoplasm or presence of debris. In subsequent processing levels, we determine the properties of the spots for detection: size, minimal contrast, minimum distance intensity between two points to be considered different individuals.

- Select population II (Figure 2.3F): Selects infected individuals from the cellular populations in the image field. The use of the "Filter by Properties" method has been adapted to consider as infected cells that have number of spots ≥ 3 was identified as an infected cell.

- Defines results: This signifies the last stage of image processing. The user has the ability to select a vast series of outputs, such as the descriptive information of the analysis steps as well as the quantitative data generated from mathematical formulas. We have established the following quantitative outputs: number of host cells, number of infected cells and average number of spots per infected cell.

2.3.2.4. Macrophage (Induced THP-1) cytotoxicity assay

A resazurin based cytotoxicity assay was developed using the host cells (THP-1), from the intracellular amastigote assay (Figure 2.4). The assay conditions mimic that of the intracellular amastigote assay described in section 2.3.2 with respect to cell seeding density, assay format, differentiation into macrophages with PMA incubation times, compound exposure times and washing steps.

The THP-1 cells were suspended at a concentration of $2.5x10^5$ cells/mL in RMPI medium + 10% (v/v) HIFBS in a 150 mL sterile clear polystyrene bottle (Corning®). One mg/mL of PMA stock solution was diluted 1:20 in DMSO and then the working solution diluted 1:2000 in cell suspension to give a final concentration of 25 ng/mL. 50 µL of cell suspensions at a density of $2.5x10^5$ cells/mL were added to Greiner™ black/clear bottomed 384-well plates using a BRAVO™, which was also used for all subsequent additions unless otherwise stated After 24 hours incubation at 37ºC/ 5%CO_2 the plates were washed 3X with PBS and incubated for an additional 48 hours at 37ºC/5% CO_2 in accordance with the intracellular amastigote assay conditions. The reference compounds, amphotericin B, miltefosine were prepared in 100% DMSO, whereas puromycin was prepared in MilliQ water. The reference compounds were serially diluted in 100% DMSO to give 14 concentrations (40 µm – 0.002 µM). An intermediate dilution of the reference plate was prepared in water, PBS or RMPI medium and 5 µL of these dilutions subsequently dispensed into the THP-1 assay

plates. The plates were incubated for 64 hours at 37ºC/ 5% CO_2. Cell viability was assessed using resazurin at a concentration of 1.5 mM (0.3 mM final assay concentration) in a volume of 10 µL using a Multidrop™ 384 Reagent Dispenser for an incubation period of 8 hours. The plates were read on an EnVision™ Multilabel plate reader using fluorometry settings with excitation of 530 nm and emission 590 nm.

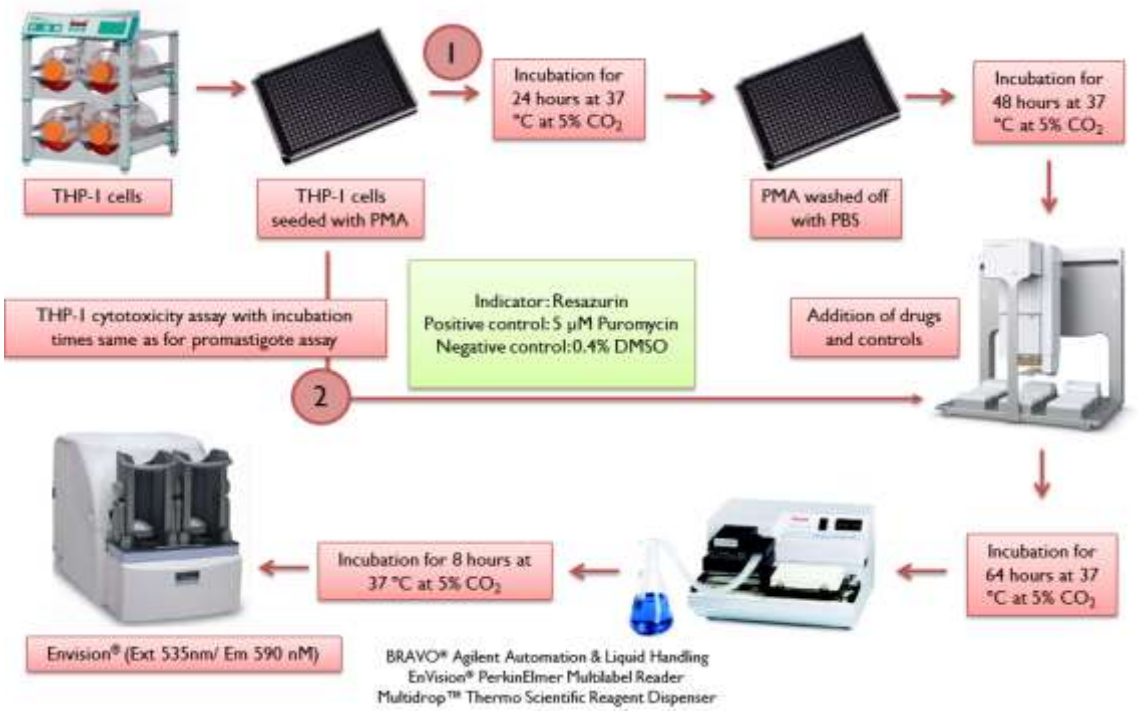

Figure 2.4: Schematics for THP-1 cytotoxicity assay.

2.3.2.5. HEK-293 resazurin viability assay

The method of Sykes *et al* was used for the HEK-293 cytotoxicity profiling (Sykes, *et al.*, 2012). Briefly, the protocol is as follows:

HEK-293 cells at $7.27x10^4$ cells/mL in DMEM + 10% HIFBS (v/v), were added in 55 µL to Greiner™ black 384-well plates using a Multidrop™ liquid handling system. The compounds at 20 mM in 100% DMSO were diluted in DMEM without HIFBS in a ratio 1:24 and 5 µL of the compounds were added to give a final concentration of 0.4% DMSO and desired compound final concentration (34.72 µM - 0.0017 µM). The plates were incubated for 48 hours at 37ºC with 5% CO_2. Resazurin was diluted in

DMEM+10% HIFBS to give a concentration of 0.49mM. 10uL of this dilution was added to assay plates, and plates were further incubated for 5 hours at 37ºC/ 5% CO_2, then left at room temperature for 19 hours. The plates were read on an EnVision™ Multilabel plate reader using fluorometry settings with excitation of 530 nm and emission 590 nm. A DMSO concentration of 0.4% was used as a negative control and 5 µM (final assay concentration) of puromycin was used as a positive control.

2.3.3. Data normalization and quality control of assay

The raw data points generated from the EnVision™ plate reader and Acapella™ image analysis software were exported to an Excel (Microsoft® office) spreadsheet. Normalization was performed on the calculated activity based on the number of infected cells with 0.4% DMSO as negative control and reference compounds as positive control in the assay. Normalization is an important step to directly compare the complex data between separate experiments and correct for intra- and inter-plate variability. The average infectivity from the positive and negative controls was normalized to 0% and 100% infection. The number of infected cells from each compound activity was made proportional within the range. The formula for normalizing the data is as follows:

Normalization= 100 – (100 x Sample – Average of minimum signal) / (Average of maximum signal – Average of minimum signal).

2.3.4. Assay reproducibility

The promastigote viability assay and the intracellular amastigote assay were conducted in triplicate on the same day (Intra-day) in multiple 384-well plates and also performed on different days (Inter-day) using the same culture conditions, resazurin concentration, volumes, incubation times and reference drugs.

A number of parameters were assessed during development and validation of the assays and subsequent screening, including Z-factor (Zhang, *et al.*, 1999), signal to background and signal to noise ratios. Evaluation of unexpected plate patterns, such as edge effects, was also taken into consideration when assessing assay integrity. To minimize potential plate edge effects, border wells were excluded from the test set and instead contained only column 2-22 and row B to O in the 384-well plates.

The parameters to assess assay reproducibility are as follows:

% CV (Coefficient of Variance) is the ratio of the standard deviation to the mean for the control wells (Positive control= 1 µM amphotericin B and Negative control= 0.4% DMSO).

Formula: %CV= SD (Standard deviation)/ Average x 100

Z' (Z factor) is the ratio of the separation band to the signal dynamic range of the assay.

Formula: Z': 1- 3SD of wells with negative control + 3SD of wells with positive control/ mean of negative control-mean of positive control

Signal Window (Signal/ Background) is the ratio between the signal mean (negative control with 100% growth [0.4% DMSO]) to the background mean (positive control with 0% growth [1 µM amphotericin B]). The signal to background does not provide any information regarding the data variability in an assay.

Formula: S/B= mean signal/ mean background

S/N (Signal/ Noise) is the ratio between the signals (negative control with 100% growth [0.4% DMSO]) minus background (positive control with 0% growth [1 µM amphotericin B]) to the background (positive control with 0% growth [1 µM amphotericin B]). The signal to noise gives an indication regarding the degree of confidence in a signal that it is different from the associated background noise.

Formula: S/N= mean signal – mean background/ standard deviation of background

Chapter 3: **Assay Development**

3.1. Introduction

In the initial stages of anti-leishmanial drug discovery, *in vitro* assays are designed, optimized and validated to identify active hits. These assays should be biologically relevant, automated, robust, reproducible, highly sensitive and user friendly with respect to the experimental procedures and data analysis. Additionally, a format enabling high throughput is preferred so that large compound libraries can be tested. Significant advances have been achieved since 2010 with the development of the first high throughput - high content imaging assay for anti-leishmanial drug discovery using intracellular amastigotes (Siqueira-Neto, *et al.*, 2010).Various assays for anti-leishmanial drug discovery have been reported which are based on colorimetric techniques, bioluminescent and fluorescent transgenic parasites using promastigote and axenic amastigote forms of the parasites to identify potential hit molecules, reviewed in (Zulfiqar, *et al.*, 2017). A comparison of these techniques with HCI has been provided in chapter 1 (section 1.5.3).

Promastigote assays have been used mainly because of the relative simplicity with which these assays can be performed, when compared to the axenic or intracellular amastigotes assays. However, using only promastigotes presents substantial limitations, as this extracellular form of the parasite exists in different forms in the insect vector but only exists as metacyclic form in the human host (Gupta, 2011). Compounds identified using promastigote assays do not translate into molecules that necessarily hit the intracellular amastigotes stage, which is relevant to the physiological model of the disease we are aiming to treat. The work published by Muylder *et al*, indicates high levels of stage specific compounds, with 59 hits selected in the promastigote models, only 26 were detected in the intracellular amastigote assay (De Muylder, *et al.*, 2011). This data corroborates with the results found by Siqueira-Neto *et al*, which show that the compound set found in the primary screening of promastigote assay, only about 4% were confirmed in the in the intracellular amastigote assay (Siqueira-Neto, *et al.*, 2012).

The predictive value to identify promising anti-leishmanial compounds for development using promastigote assays is highly debatable when compared to susceptibility in

intracellular amastigote assays (Hendrickx, *et al.*, 2015). However, despite of all the limitations associated with promastigote assays they are still used for frontline screening in conjunction with intracellular amastigotes assays for further characterization of compounds. Hence, they can be termed as not essential but beneficial for anti-leishmanial drug discovery. On the other hand, using HCI assays for intracellular amastigote for mechanistic studies alone is not possible for some areas of investigation. Example include the determination of cytostatic or cytocidal effect of the compound on the intracellular parasites as the replication rate of parasites is too low (De Rycker, *et al.*, 2013).

Axenic amastigotes, which are biologically relevant to the intracellular amastigotes based on morphology have also been used to develop assays for identifying anti-leishmanial compounds. Two decades ago, it was believed that, in contrast to the compounds identified through the promastigote assays, there exists a greater similarity in the compounds identified between the axenic amastigotes and intracellular amastigote assays (Callahan, *et al.*, 1997). However, several studies subsequently showed that the axenic amastigote forms still differ from the intracellular amastigotes, in terms of expression of proteins and susceptibility to drugs (Holzer, *et al.*, 2006; Pescher, *et al.*, 2011). This was confirmed in a study conducted by De Rycker *et al*, where it was reported that only 22% of the compounds active in the axenic amastigote assay were also active in the intracellular amastigote assay (De Rycker, *et al.*, 2013). However, as different approaches have been undertaken to identify new anti-leishmanial molecules this also impacts on the outcome, thus it is not possible to directly compare the data in the literature obtained using different techniques used.

Moreover, promastigotes and axenic amastigotes assays do not provide information about the cytotoxicity and selectivity of the compounds against the host cells. Both these assays illustrate an effect of the compound directly on the parasites and fail to provide any indication of the ability of the compounds to cross multiple membranes of the host and parasite, which is required to be effective *in vivo*; and the chemical stability of the compounds in the acidic pH environment of the parasitopharous vacuole is not demonstrated (Durieu, *et al.*, 2016). In addition, unlike intracellular amastigote assays, both of these assays are unable to provide any information regarding pro-drugs or compounds that have an immuno-therapeutic or immuno-modulatory effect on the

infected host cell (Gupta, 2011). Nuhs and colleagues have modified the existing axenic amastigote model by increasing starting density of cells and lowering the limit of detection to identify compounds that are cytotoxic to parasites from that of cytostatic compounds (Nuhs, *et al.*, 2015). This new approach has provided a better translational rate for the intracellular models. By selecting molecules exclusively with cytotoxic action against parasites, out of all the hits (97 compounds) for intracellular amastigotes, 43.2% (42 compounds) were confirmed in the novel axenic amastigote assay (Nuhs, *et al.*, 2015).

HCI assays have revolutionized the drug discovery efforts for leishmaniasis. These imaging assays are highly sensitive, mimicking more accurately the pathophysiological model of the disease, providing multiplexing of different parameters/measurements (infectivity ratio, cellular morphology, protein expression etc.) and reducing interference from artifacts. Despite the advances achieved by establishing image-based strategies, these platforms have some limitations including expensive infrastructure, including automated microscopes and data storage system. They require trained people with higher operational cost when compared to other techniques such as bioluminescent and fluorescent assays.

In our efforts to identify and characterize novel compounds for anti-leishmanial drug discovery, we have used a screening cascade inclusive of a promastigote viability assay; an intracellular amastigote assay and a host cell cytotoxicity assays. In this chapter, the assay development, optimization and validation parameters will be discussed for the promastigote viability assay and the complementary THP-1 cytotoxicity assays for both the promastigote assay and the intracellular amastigote assay accommodating their different incubation times. The intracellular amastigote assay, developed and optimized by Drs Jones and Shelper in the Discovery Biology team, was transferred and established as a routine assay for this project. The sensitivity and reproducibility of these assays determined using reference drugs were evaluated and will be discussed in this chapter.

3.2. Materials and Methods

Assay optimization conditions were as follows:

3.2.1. Maximum cell density and doubling time of *L. donovani* DD8:

3.2.1.1. Flask culturing:

To determine the maximum density of *L. donovani* DD8 promastigotes that could be maintained in a 75 cm^2 culture flask, $1x10^4$, $1x10^5$, $5x10^5$ and $1x10^6$ promastigotes/mL were seeded into a 75 cm^2 flask (Greiner Bio One, Frickenhausen, Germany) containing 30 mL of M199 + 10% (v/v) HIFBS and incubated at 27ºC. A 10 µL sample of the culture was taken at 24 hour intervals over 7 days to determine the number of promastigotes present in the culture at each time point. The culture samples were diluted 1:20 or 1:50 in 4% formaldehyde and the number of promastigotes determined by visually counting on a haemocytometer. Duplicate counts were performed for each culture sample with a difference of no more than 10 parasites per quadrant on the haemocytometer.

The doubling time of the promastigote cultures was calculated using the equation:

$$t^d = (t^2 - t^1) \times \log(2)/\log\ (q^2/q^1)$$

Where t^d = doubling time, q^1 is the initial count, t^1 is the time of the initial count, q^2 is the next count and t^2 is the time for the next count.

3.2.1.2. 384-well plate

L. donovani DD8 promastigotes were maintained in a 75 cm^2 culture flask and the culture was resuspended into the following densities $1x10^4$, $1x10^5$, $5x10^5$ and $1x10^6$ promastigotes/mL in M199 + 10% HIFBS. The resuspended culture was dispensed in volumes of 55, 45, and 35 µL at day 0 into the 384-well plates and incubated at 27ºC. A 10 µL sample of the culture from the 384-well plates was taken at 24 hour intervals over a 7-day period. Samples for three wells were taken for each concentration and for each

volume and the experiment was completed as independent biological replicates of N=2. Cell counts were determined as above (section 3.2.1.1) using different wells each time. A growth curve was plotted to estimate the maximum number of cells attainable in 384-well plates before cell death occurred.

3.2.2. Optimizing resazurin concentration

Different volumes (10, 15 and 20 µL) of resazurin stock (0.49 mM) giving a final concentration of 0.714, 0.357, 0.142, 0.071, 0.035, 0.014 and 0.007 mM were added to the optimized volume 55 µL of mid log phase promastigotes in the 384-well plate (Table 3.1). These mid log phase promastigotes were acquired after initially seeding the promastigotes in M199 + 10% HIFBS at a starting density of $1x10^5$ cells/mL and incubating for 96 hours at 27°C at normal atmospheric conditions. The samples were incubated for various time intervals ranging from 2-12 hours at 27°C at normal atmospheric conditions before measuring the signal on an EnVision™ (PerkinElmer®, USA) Multilabel plate reader using fluorometry settings with excitation of 530 nm and emission 590 nm.

Table 3.1: Calculations for resazurin final assay concentration based on dilution factors for final assay volumes. Resazurin concentration was added in 10, 15 and 20 µL to 55 µL of parasite culture.

Final assay concentration	Resazurin concentration for a volume of 10 µL	Resazurin concentration for a volume of 15 µL	Resazurin concentration for a volume of 20 µL
0.714 mM	5 mM	3.57 mM	2.856 mM
0.357 mM	2.5 mM	1.785 mM	1.428 mM
0.142 mM	1.0 mM	0.714 mM	0.571 mM
0.071 mM	0.5 mM	0.357 mM	0.285 mM
0.035 mM	0.25 mM	0.178 mM	0.142 mM
0.014 mM	0.1 mM	0.071 mM	0.056 mM
0.007 mM	0.05 mM	0.035 mM	0.028 mM

3.2.3. Optimizing the DMSO concentration

Final DMSO concentrations ranging from 0.021% to 8.33% were tested in the 384-well promastigote viability assay. Stock 100% DMSO was taken and diluted to 1:2 on a 10 point scale in M199 without HIFBS. After seeding the parasites at a concentration of $5x10^5$ cells/mL in a volume of 55 µL/well, 5 µL of the DMSO dilutions were added to the assay mixture. After 68 hours, resazurin was added in a concentration of 0.142 mM in a volume of 10 µL and further incubated for 4 hours. The plate was incubated for 4 hours at 27°C at normal atmospheric conditions and the signal was measured on EnVision™ (PerkinElmer®, USA) Multilabel plate reader using fluorometry settings with excitation of 530 nm and emission 590 nm.

3.2.4. Optimizing dilution media

In order to ascertain the best media for diluting compounds the reference drugs, amphotericin B and miltefosine were used. Stock concentrations were made for amphotericin B (10 mM) in 100% DMSO and for miltefosine (10 mM) in autoclaved MilliQ™ water, since miltefosine presents low solubility in DMSO. The stocks were diluted 1:25 in (Water, PBS and M199 media without HIFBS) using a dilution plate. After seeding the parasites at a concentration of $5x10^5$ cells/mL in a volume of 55 µL/well, 5 µL of the above-mentioned dilutions were added to the assay mixture using a BRAVO™. The plate was incubated for 68 hours at 27°C and then 10 µL of 0.142 mM resazurin as final assay concentration was added. The plate was incubated for 4 hours at 27°C and the signal was measured on EnVision™ Multilabel plate reader using fluorimetry settings with excitation of 530 nm and emission 590 nm.

3.2.5. Reference drugs 50% inhibitory concentration (IC_{50})

Reference drugs used for estimation of drug sensitivity of the promastigote resazurin assay included amphotericin B and miltefosine. Stock concentrations were made for amphotericin B (10 mM) in 100% DMSO and for miltefosine (10 mM) in autoclaved MilliQ™ water. A 384 well Axygen® diamond bottom master plate was established with 14-point concentrations of amphotericin B and miltefosine ranging from 33.3 µM to 0.0166 µM in an increment of 1:2, 1:4 and then 1:10 for the rest of the points. The

drugs in the master plate were diluted 1:25 in M199 media without HIFBS. Fifty-five microliters of mid log phase promastigotes were plated into a sterile 384-well plate clear bottom using the BRAVO™ and 5 µL of the above-mentioned dilutions were added to the assay mixture. The plate was incubated for 68 hours at 27°C under normal atmospheric conditions and then 10 µL of 0.142 mM resazurin as final assay concentration was added. The plate was incubated for 4 hours at 27°C under normal atmospheric conditions and the signal was measured on EnVision™ Multilabel plate reader using fluorometry settings with excitation of 530 nm and emission 590 nm.

The IC_{50} value of each reference drug was calculated by normalizing the data based on 0% inhibition = 0.4% DMSO (estimated via DMSO sensitivity experiment) and 100% inhibition = 1 µM amphotericin B (concentration at which 100% inhibition of parasites occurs, determined using a 14-point concentration response curve) against log of concentration in PRISM 4™ software (GraphPad Software Inc., San Diego, CA, USA) (denoted IC_{50} by PRISM).

3.2.6. Assay reproducibility

The assay was conducted in triplicate on the same day (Intra-day) in multiple 384-well plates and also performed on different days (Inter-day) using the same culture conditions, resazurin concentration, volumes, incubation times and reference drugs. A total of N=2 experiments with different cell passage numbers [early passage (P4) and late passage (P18)] were compared to determine assay reproducibility.

A number of parameters were assessed during development and validation of the assays and subsequent screening, including Z' factor (Zhang, *et al.*, 1999), signal to background (S:B) and signal to noise (S:N) ratios. Evaluation of unexpected plate patterns, such as edge effects, was also taken into consideration when assessing assay integrity. To minimize potential plate edge effects, border wells were excluded from the test set and instead contained only column 2-22 and row B to O in the 384-well plates.

3.3. Results

3.3.1. Promastigote viability assay

3.3.1.1. Maximum cell density and doubling time of *Leishmania donovani* DD8

3.3.1.1.1. Flask culturing

The maximum number of parasites that could be grown in a 75 cm^2 flask was estimated to be $4.09x10^7$ and $4.29x10^7$ promastigotes/mL, obtained with starting densities of $1x10^4$ and $1x10^5$ promastigotes/mL incubated for 144 hours, respectively (Table 3.2). A total of $4.34x10^7$ promastigotes/mL were obtained for a starting density of $5x10^5$ promastigotes/mL and $4.26x10^7$ promastigotes/mL were obtained with the starting density of $1x10^6$ promastigotes/mL incubated for 96 hours (Figure 3.1). The doubling time calculated for the logarithmic phase of growth was assessed as 12.7 hours. The comparison of parasite growth curves with different starting seeding concentrations is described in Table 4. Based on the observed data, to keep the parasite in the mid-log phase, cultures were seeded at an initial density of $1x10^5$ promastigotes/mL. They were subcultured every 96 hours.

Table 3.2: Maximum cell density achieved by different concentrations of *Leishmania donovani* DD8 cultures in a 75cm^2 flask over seven days. The inoculum density at day 0 was $1x10^4$ cells/mL, $1x10^5$ cells/mL, $5x10^5$ cells/mL and $1x10^6$ cells/mL.

Starting density (parasites/mL)	Maximum cell density achieved (Parasites/mL)	Time to achieve maximum cell density (Hours)
$1x10^4$	$4.09x10^7$	144
$1x10^5$	$4.29x10^7$	144
$5x10^5$	$4.34x10^7$	96
$1x10^6$	$4.26x10^7$	96

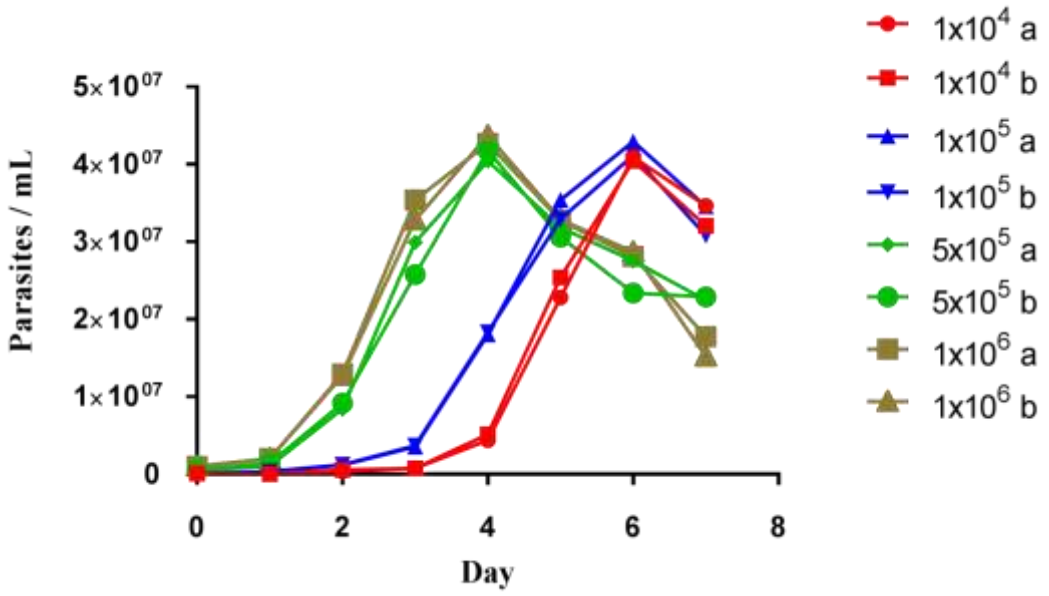

Figure 3.1: Growth curve of *Leishmania donovani* DD8 in a 75cm^2 flask over seven days. The inoculum density at day 0 was 1x10^4 cells/mL, 1x10^5 cells/mL, 5x10^5 cells/mL and 1x10^6 cells/mL. Each point was determined from duplicate points, for N=2.

3.3.1.1.2. 384-well plate

To determine the most suitable inoculum volume to obtain the optimal concentration of promastigotes that can be plated in the well of a 384-well plate, *L. donovani* DD8 were seeded at concentrations of 1x10^4, 1x10^5, 5x10^5 and 1x10^6 promastigotes/mL (Figure 3.2). It was observed that the optimum concentration of promastigotes that could be plated in a 384-well was 5x10^5 promastigotes/mL/well with an inoculum volume of 55 µL. At this concentration the maximum cell density was achieved at day 4 with a concentration of 4.3x10^7 promastigotes/mL (Figure 3.2c). As the assay was scheduled to be a 3 day assay, it was imperative that the parasites did not reach the stationary phase. From the growth curve obtained for an initial seeding density of 5x10^5 promastigotes/mL, it was observed that the parasites reached the stationary phase at day 4.

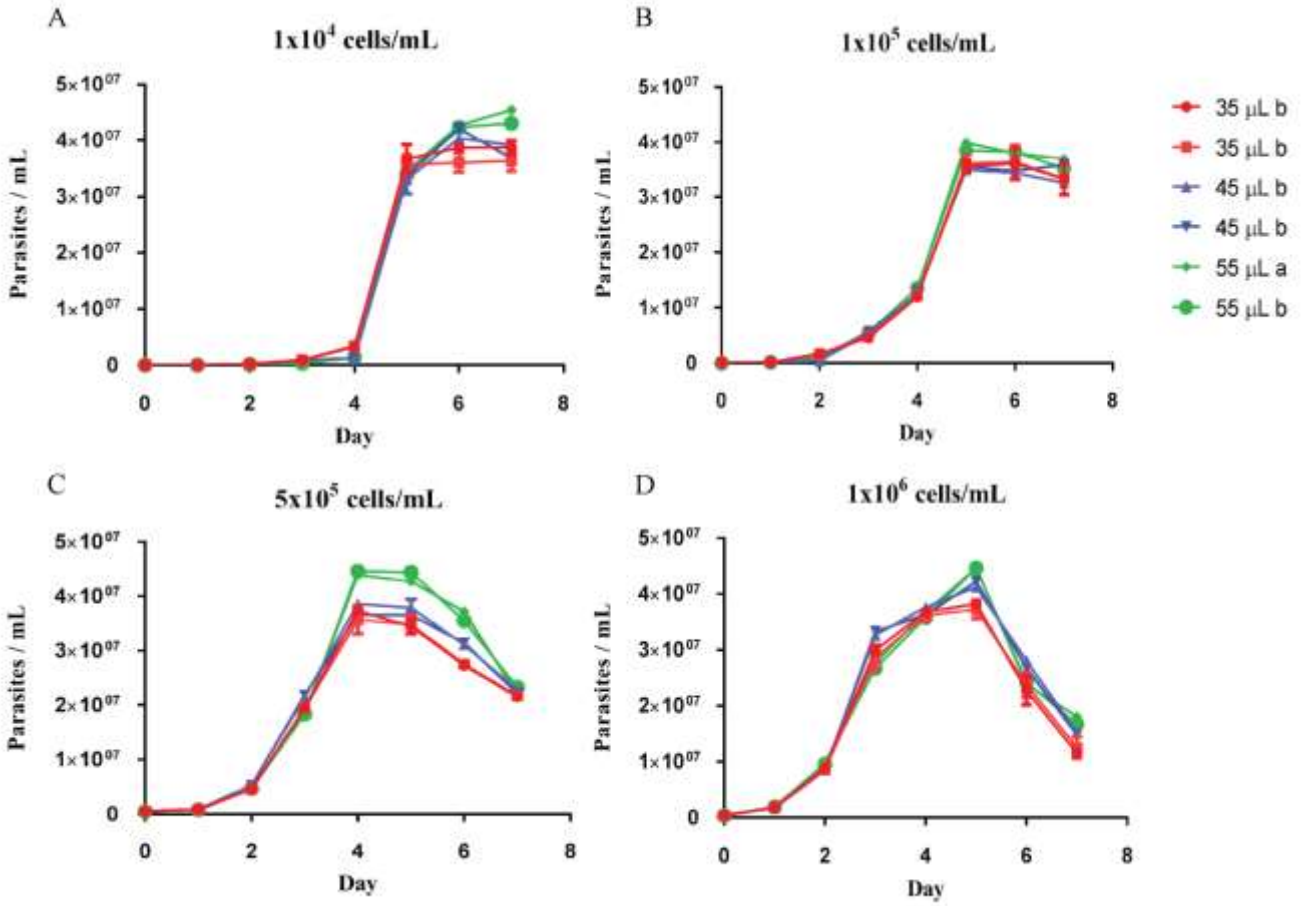

Figure 3.2: Growth curve of *Leishmania donovani* DD8 promatigotes in a 384-well plate over seven days. (A) Inoculum density at day 0 was at $1x10^4$ cells/mL **(B)** Inoculum density at day 0 was at $1x10^5$ cells/mL **(C)** Inoculum density at day 0 was at $5x10^5$ cells/mL **(D)** Inoculum density at day 0 was at $1x10^6$ cells/mL. Red represent 35 µL inoculum, blue represent 45 µL inoculum and green represent 55 µL inoculum. Each point was estimated from 3 pooled wells from a 384-well plate, for N=2.

3.3.1.2. Determining optimal resazurin concentration and linearity

To determine whether a linear correlation existed between the indicator (resazurin) and the cell concentration, resazurin was added to different concentrations of *L. donovani* DD8 and signal intensity measured after 72 hours.

It was observed that there existed a linear correlation with the parasite concentration and the signal intensity with an R^2 value of 0.987 (Figure 3.3). A linear signal of fluorescence to parasite means resazurin could be used as an effective indicator to determine the effects of compounds on parasite viability and proliferation.

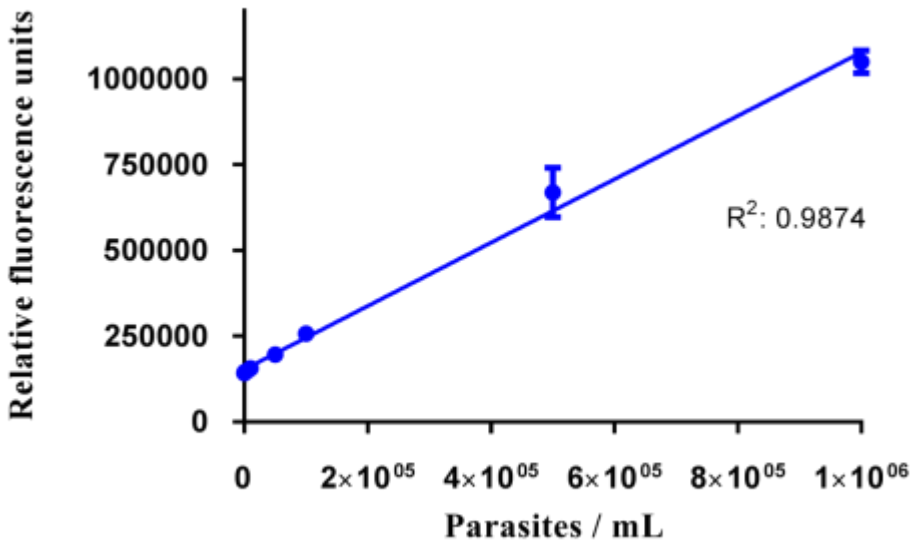

Figure 3.3: Linearity of detection for parasite number. Inoculation of *Leishmania donovani* DD8 promastigotes added directly from flask and parasites inoculated with 10 µL of resazurin (0.714 mM final assay concentration). R2= 0.987. Replicates were averaged over three wells for each cell density, for N=2.

The concentration of resazurin was plotted against the relative florescence intensity (RFU) to determine the concentration at which the maximum signal intensity was achieved. Figure 3.4 shows that the maximum signal was achieved at a concentration of

0.142 mM. Each point was estimated from triplicate points per experiment for two independent experiments.

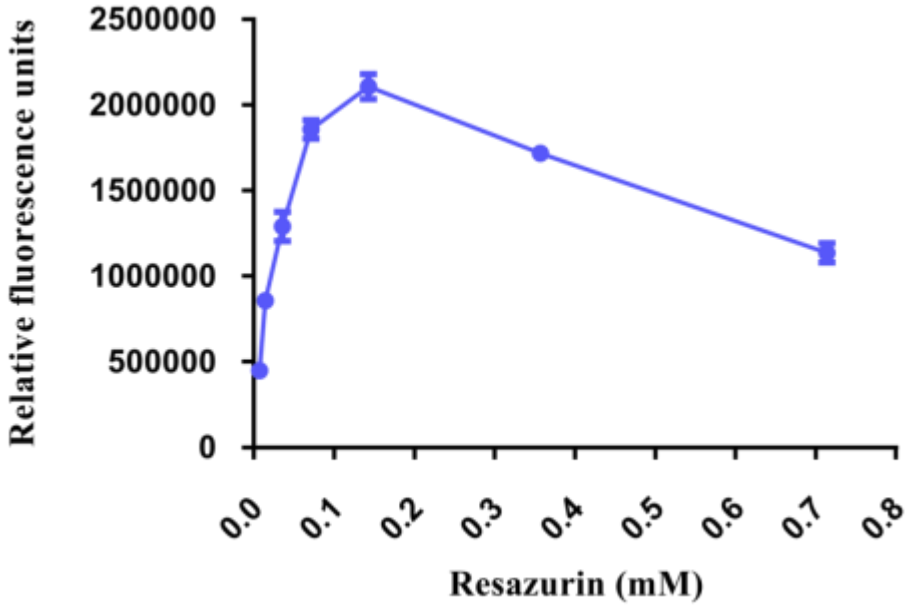

Figure 3.4: Resazurin concentrations (0.714, 0.357, 0.142, 0.071, 0.035, 0.014 and 0.007 mM) vs relative fluorescence units (RFU). The starting promastigote density was $5x10^5$ parasites/mL and the incubation period after resazurin addition was 4 hours. Each point was calculated from duplicate points, for N=2.

Two concentrations of resazurin (0.142 and 0.071 mM as final assay concentrations) were selected to determine which gave the best signal at the specified volumes of 10, 15 and 20 µL. It was observed that a concentration of 0.142 mM resazurin (final assay concentration) gave the best signal when compared to 0.071 mM at all three volumes tested (Figure 3.5). Furthermore, comparison between the three volumes was conducted to determine the optimal volume for the assay at a concentration of 0.142 mM resazurin. No statistical difference was observed between the three sets of volumes, using a two-way ANOVA (P value: 0.742), in relation to signal intensity, therefore 10 µL was used for subsequent experiments.

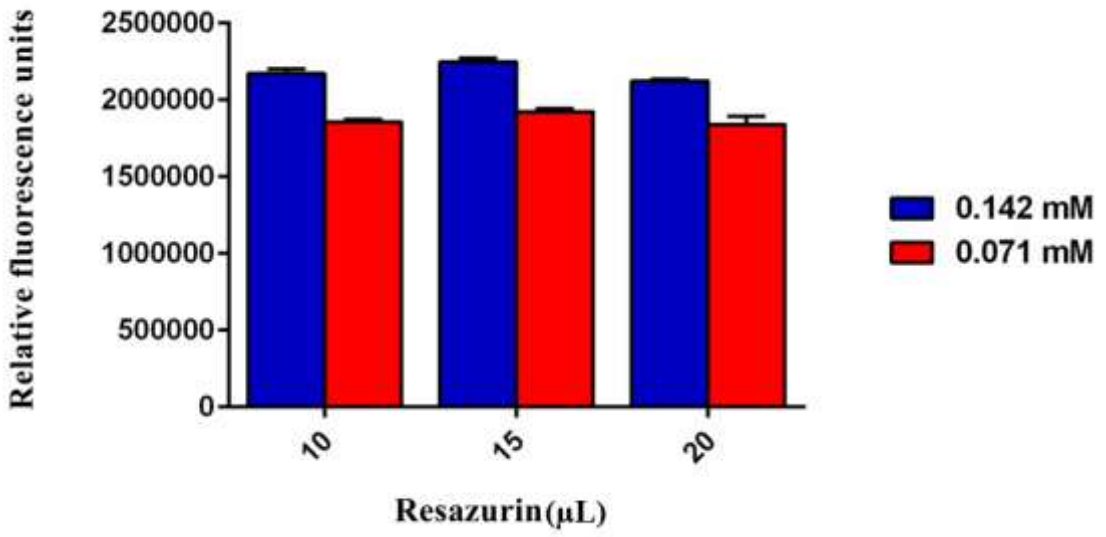

Figure 3.5: Comparison of reasazurin concentrations (0.142 mM and 0.071 mM) based on different volumes in relation to relative florescence units (RFU). Each point was estimated from duplicate points, for N=2.

The optimum time period for incubation after resazurin addition was assessed to be 4 hours. As illustrated in Figure 3.6, a linear correlation exists between the resazurin and the cell concentration until 4 hours, after that time point the curve starts to flatten out, indicating that the maximum signal window has been reached, thus additional incubation beyond this point is of no additional benefit.

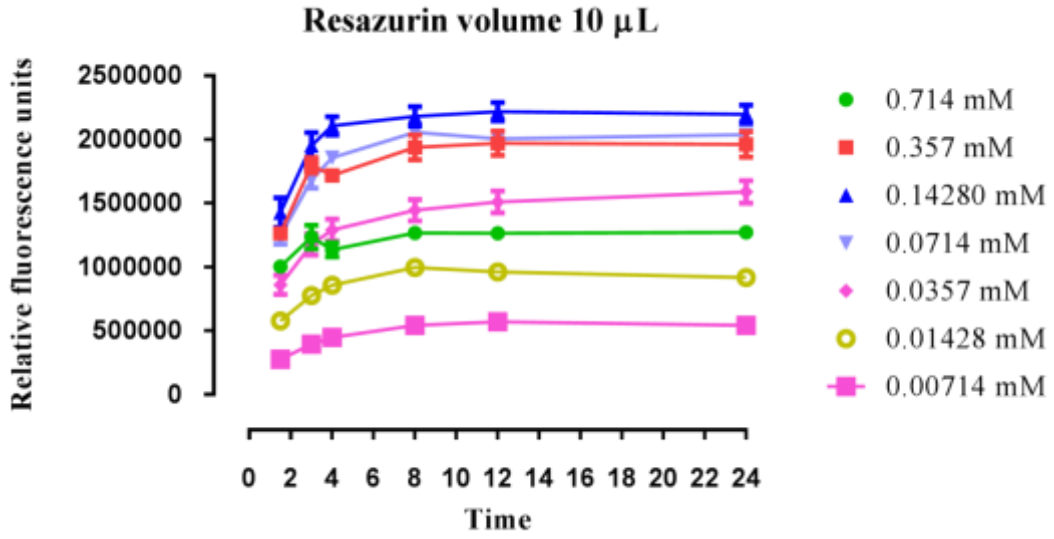

Figure 3.6: Comparison of resazurin concentrations with signal intensity and multiple time points. The signal at each resazurin concentration was averaged from triplicate samples, for N=2.

3.3.1.3. Optimization of assay DMSO concentration

Final DMSO concentrations ranging from 0.021% to 8.33% were tested in the 384-well promastigote viability assay. The results show that a final concentration of 0.417% DMSO was well tolerated by the promastigotes in the resazurin assay and demonstrated no significant decrease in signal using two-way ANOVA (P value: 0.2751) (Figure 3.7). DMSO added to the assay up to a maximum concentration of 2% was tolerated before any detrimental effects on parasite growth were observed.

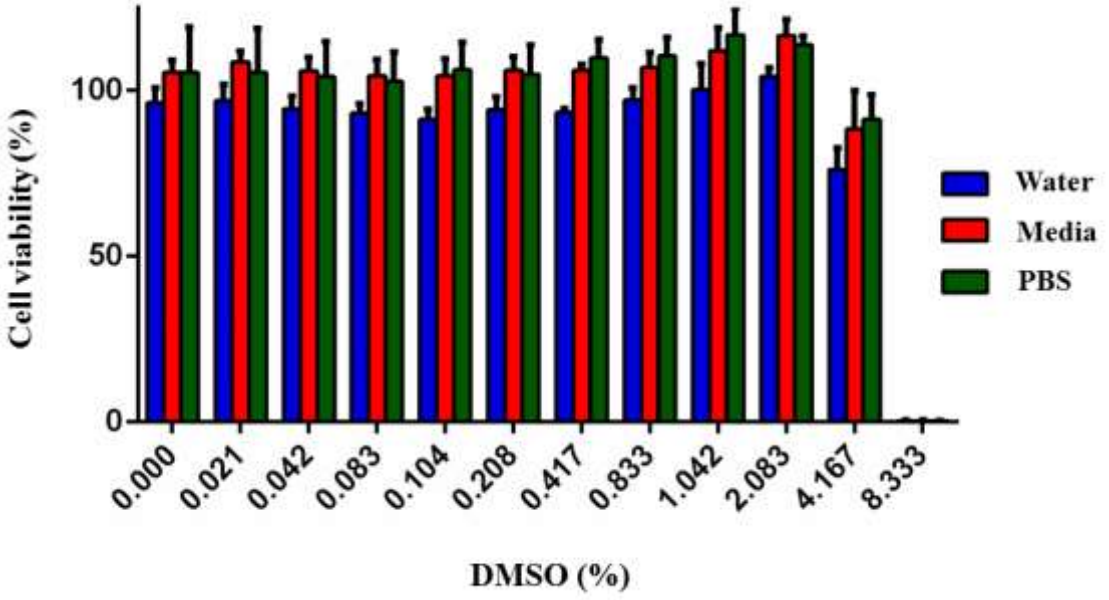

Figure 3.7: The impact of of Dimethylsulfoxide (DMSO) on parasite viability in a 384-well assay format. The signal different DMSO concentrations were averaged from triplicate samples, for N=2.

3.3.1.4. Determining optimal dilution media for the assay

No significant differences were observed between the inhibitory concentrations for amphotericin B (P value: 0.989) and for miltefosine (P value: 0.927) for all three mediums used for dilution (Water, PBS, and Media without HIFBS) (Figure 3.8), according to a one-way ANOVA (Figure 3.8c).

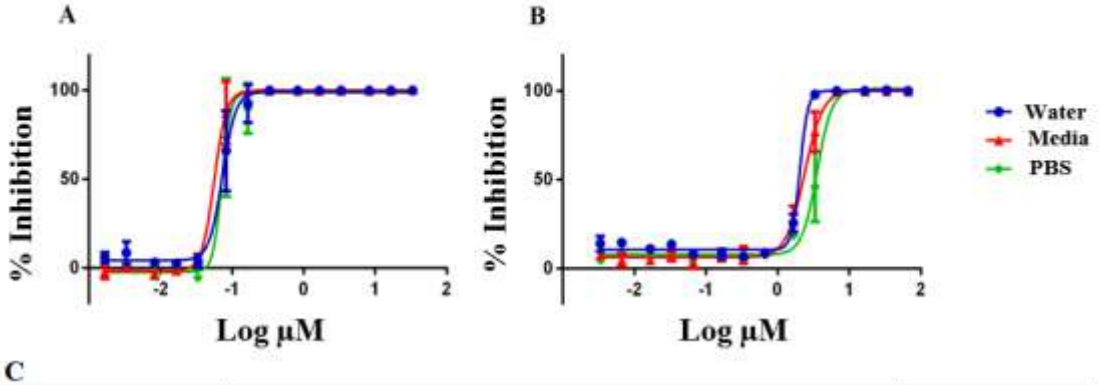

C

Drug	IC_{50} (µM) [Mean ± SD]			One Way ANOVA (P values)
	Water	Media	PBS	
Amphotericin B	0.073 ± 0.018	0.056 ± 0.024	0.071 ± 0.015	0.989
Miltefosine	2.047 ± 0.32	2.378 ± 0.28	3.552 ± 0.42	0.927

Figure 3.8: Optimal dilution media. (A) amphotericin B and (B) miltefosine 50% inhibitory concentration curves and (C) IC_{50} values determined using the promastigote viability assay. Dilutions of compound were made in water, media without HIFBS and PBS. Each dilution was made in duplicate, for N=2.

3.3.1.5. Intra-day and Inter-day reproducibility of the promastigote viability assay

The average IC_{50} values obtained for amphotericin B and miltefosine in the promastigote assay were calculated to be 0.043 ± 0.015 and 2.088 ± 0.561 units to be included for four replicates, respectively (Figure 3.9). No significant differences between the inhibitory concentrations were found using one-way analysis of variance (ANOVA) (Figure 3.9c) for amphotericin B (P value: 0.982) or for miltefosine (P value: 0.990) when comparing data between the intra-day and inter-day assays. This highlights the reproducibility of the assay.

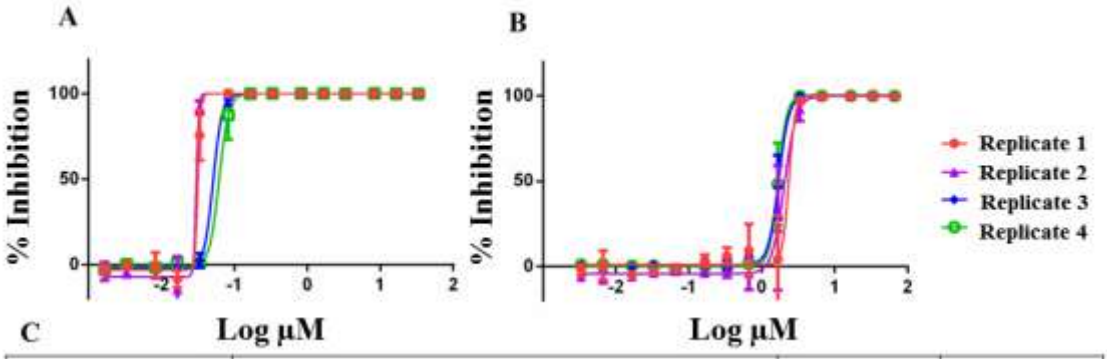

C

Drug	IC_{50} (µM)					One Way ANOVA (P values)
	R1 [Intra]	R2 [Intra]	R3 [Inter]	R4 [Inter]	Mean ± SD	
Amphotericin B	0.031	0.030	0.051	0.061	0.043 ± 0.015	0.982
Miltefosine	2.884	2.083	1.706	1.679	2.088 ± 0.561	0.990

Figure 3.9: Intra-day and Inter-day reproducibility. (A) amphotericin B and (B) miltefosine 50% inhibitory concentration curves and (C) IC_{50} values determined using the promastigote viability assay. Dilutions of compound were made in M199 media without HIFBS. Four experiments were conducted as R1 and R2 within the same day (Intra-day) and R3 and R4 separate days (Inter-day). Each experiment was conducted with duplicate, for N=2.

3.3.1.6. Assessing assay reproducibility in early and late passages of *L. donovani* DD8 promastigotes

Early and late passages of *L. donovani* cultures were compared to determine whether the assay performance was influenced using parasites from different passages (Figure 3.10).

It was observed that there were no statistical differences in the activities of amphotericin B (P value: 0.584) and miltefosine (P value: 0.672) obtained using either the early or late passage of proamastigote parasites, which is evident from t-test analysis and the IC_{50} values obtained (Figure 3.10c).

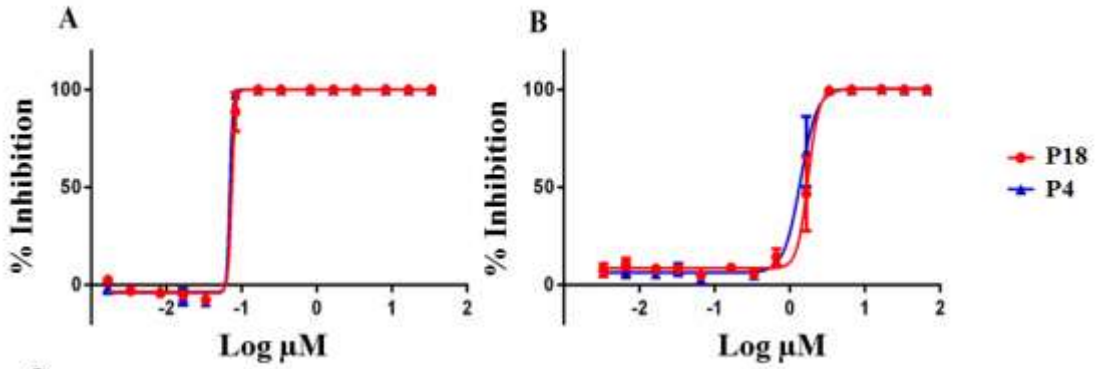

C

Drug	IC_{50} (µM) [Mean ± SD]		t-test (P values)
	P18	P4	
Amphotericin B	0.073 ± 0.002	0.069 ± 0.003	0.584
Miltefosine	1.754 ± 0.255	1.393 ± 0.28	0.672

Figure 3.10: Assessing reproducibility of early and late passages of *L. donovani* DD8 promastigotes. (A) amphotericin B and (B) miltefosine 50% inhibitory concentration curves and (C) IC_{50} values determined using the promastigote viability assay. The assay was performed with different numbers of parasite passages (early passage 4 and late passage 18). Each evaluation was made in duplicate, for N=2.

The quality control and reproducibility of the assay were determined using statistical parameters including Z' values, % coefficient of variance and signal widow (Table 3.3) The results indicate that the Z' for the promastigote assay was 0.872 ± 0.048 (Figure 3.11). This value suggests the assay was extremely robust and suitable for use in HTS. The % coefficient of variance for all the replicates was below 10% showing the accuracy of the assay. The signal window between the positive and negative controls was more than 15 times, hence showing an excellent dynamic range of assay signal (Table 3.3).

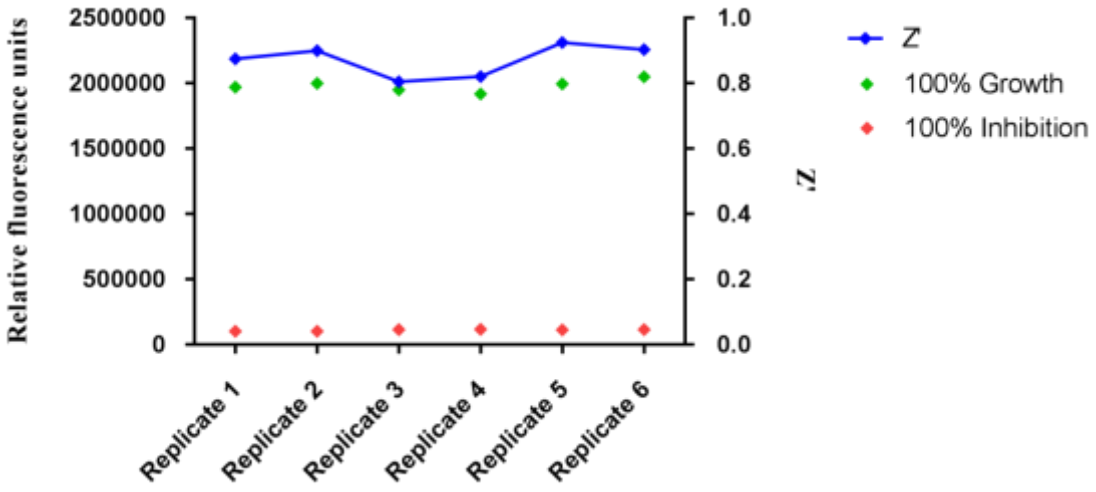

Figure 3.11: Assay reproducibility for multiple replicates in promastigote viability assay. Red dots represent 100% inhibition obtained using the positive control 1 µM amphotericin B, green dots represent 0% inhibition with negative control 0.4% DMSO and blue dots represent Z' values for each plate. Each data point was calculated from duplicate plates, for N=2.

Table 3.3: Statistical parameters for multiple replicates in the promastigote viability assay.

Statistical Parameters	Rep 1	Rep 2	Rep 3	Rep 4	Rep5	Rep 6
% CV (0% Inhibition)	3.74 %	2.98 %	5.95 %	5.46 %	2.24 %	2.94 %
% CV (100% Inhibition)	3.45 %	3.10 %	2.42 %	2.03 %	1.57 %	1.56 %
Signal Window	19-fold	19-fold	17-fold	16-fold	17-fold	17- fold

3.3.2. Intracellular amastigote assay

3.3.2.1. Determination of reference compound 50% inhibitory concentration (IC_{50}):

The IC_{50} values of the reference drugs (amphotericin B, miltefosine) and the preclinical candidate, VL-2098, were determined for the intracellular amastigote assay as described in chapter 2 (section 2.3.2). The results indicated an IC_{50} value for amphotericin B was calculated to be 0.089 µM (Figure 3.12), VL-2098 as 0.708 µM (Figure 3.12) and miltefosine as 1.973 µM (Figure 3.12). 0.4% DMSO was used as a negative control with 100% viability of the amastigotes in the host cells. Amphotericin B 1 µM (Figure 3.13) was used as positive control with 0% viability of amastigotes in the host cells (Figure 3.13).

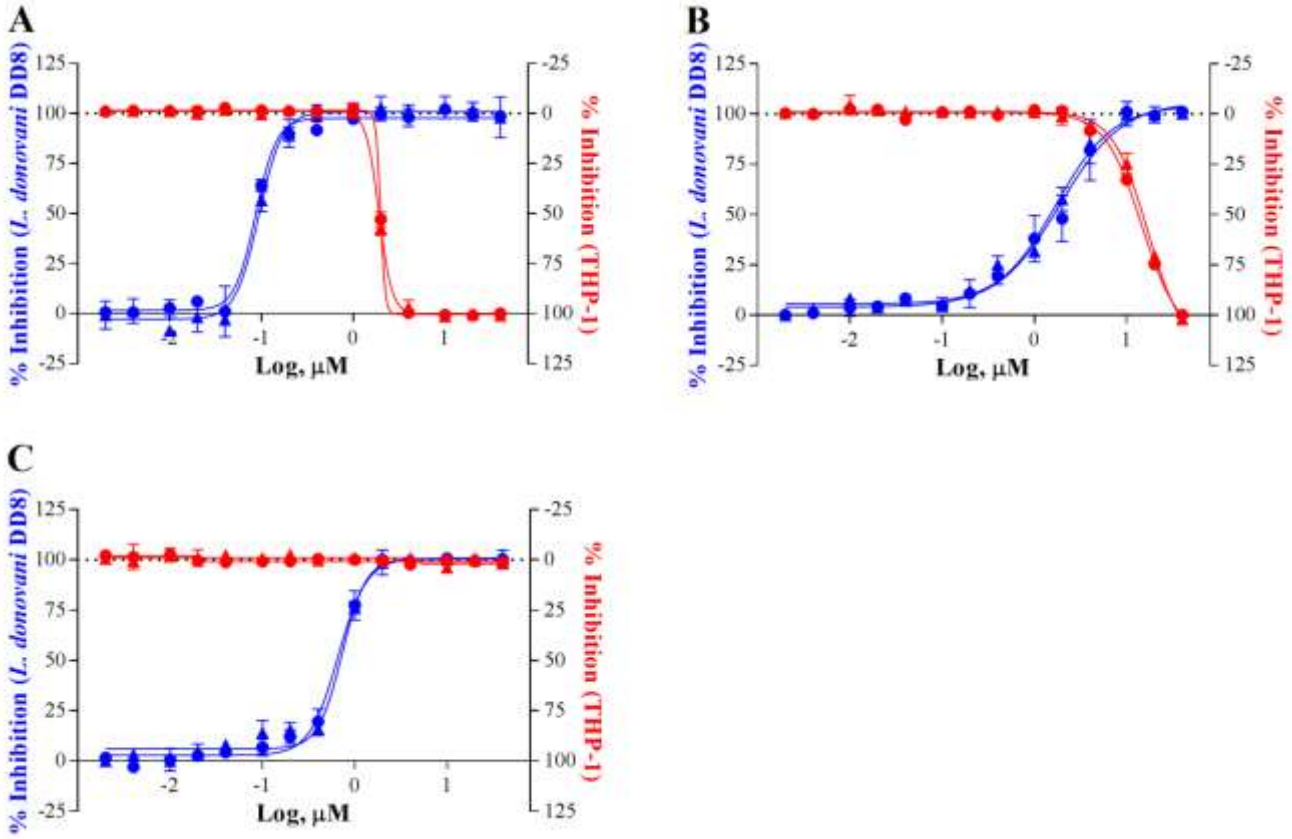

Figure 3.12: Reference compound 50% inhibitory concentration for *L. donovani* DD8 intracellular amastigote assay. (A) amphotericin B, (B) miltefosine, (C) VL-2098 inhibitory concentrations obtained using intracellular amastigote assay. The percentage inhibition was determined from quadruplicate assay data points after normalization of the data with 1 µM amphotericin B (100% death, final assay) as positive control and 0.4% DMSO (0% inhibition) as negative control. Each evaluation was made in triplicate, for N=2.

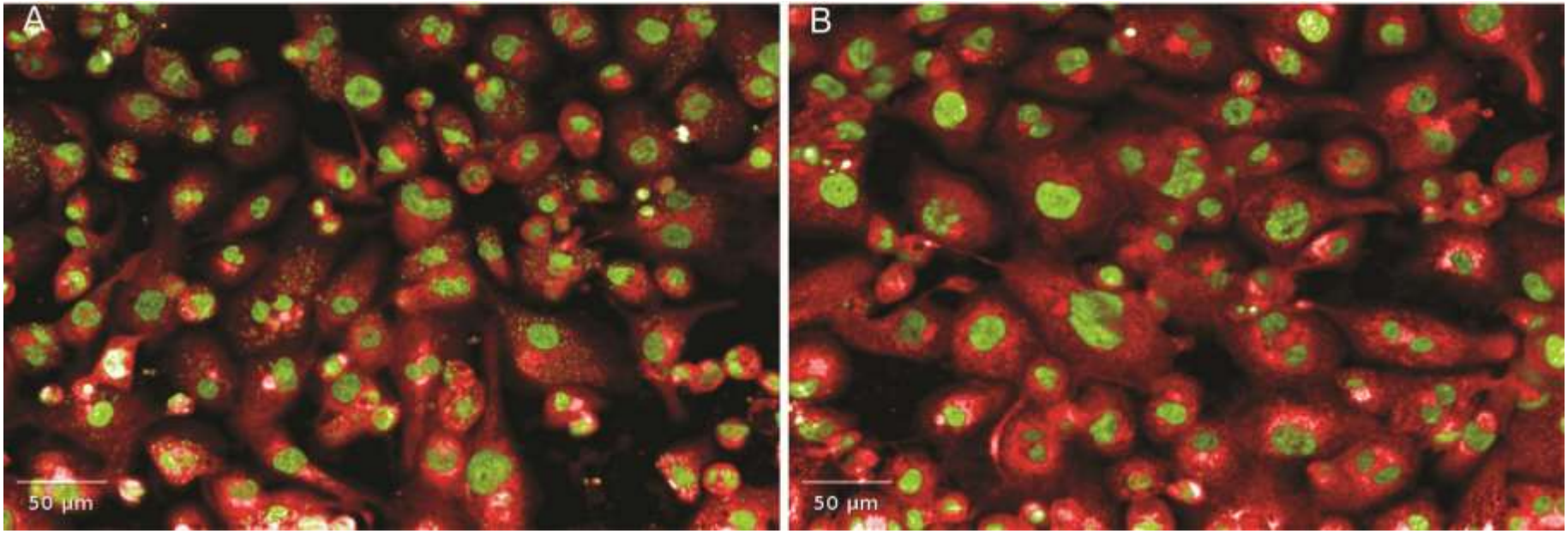

Figure 3.13: THP-1 cells, 2.5x105 cells/mL infected with *Leishmania donovani* DD8 metacyclic promastigotes, imaged on the Opera™ using the 20X objective magnification following staining with SYBR® Green and CellMask™ Deep Red. (A) Amastigotes were observed within the host cells with 0.4% DMSO (B); Treatment with 1 µM amphotericin B, no amastigotes can be observed within the host cells.

3.3.3. THP-1 (host cell) resazurin cytotoxicity assays

3.3.3.1. Resazurin as a suitable indicator

It was observed that the curve for the graph plotted for different THP-1 cell concentrations to that of relative fluorescence units (RFU) (Figure 3.14) started to flatten after a concentration of 2.5 x 10^5 cells /mL was exceeded, showing that the signal intensity achieved the maximum limit. After this point there was no longer a linear relationship between cell number and fluorescent value, thus it was no longer a suitable indicator to assess the number of cells based on metabolism.

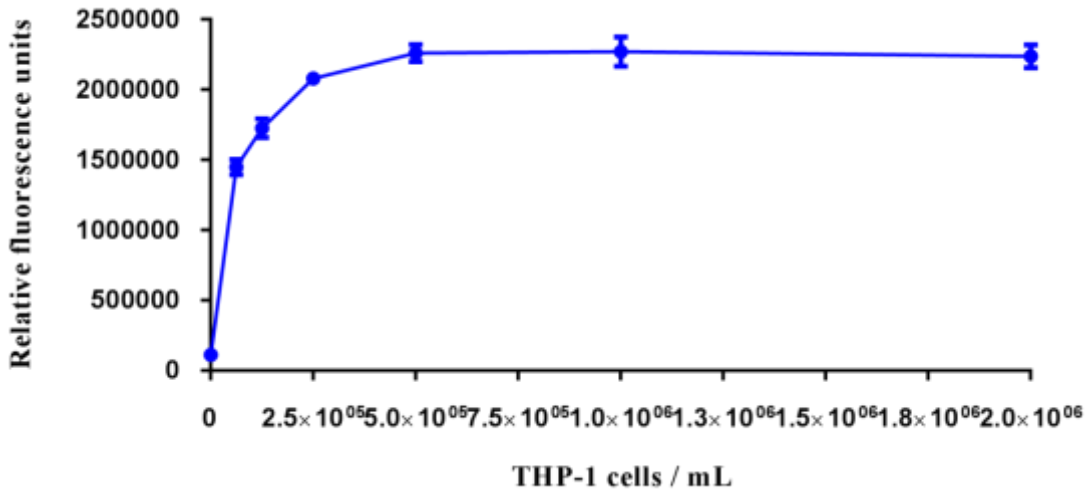

Figure 3.14: Maximum limit of signal intensity reached based on relative fluorescence units (RFU). with different THP-1 cell concentrations ($6.25x10^4$, $1.25x10^5$, $2.5x10^5$, $5x10^5$, $1x10^6$ and $2x10^6$) The signal at each resazurin concentration was averaged from triplicate samples, for N=2.

3.3.3.2. Determining optimal resazurin concentration and linearity

To determine the optimal resazurin concentration, volume and incubation time for the THP-1 cytotoxicity assay, a range of concentrations (0.02, 0.05, 0.098, 0.15, 0.2, 0.3 and 0.4 mM) were assessed (Figure 3.15). Different volumes of resazurin (10, 15 and 20 µL) were also compared for these concentrations. The 384-well plates were incubated and readings were taken after 2, 4, 8, 12 and 24 hours.

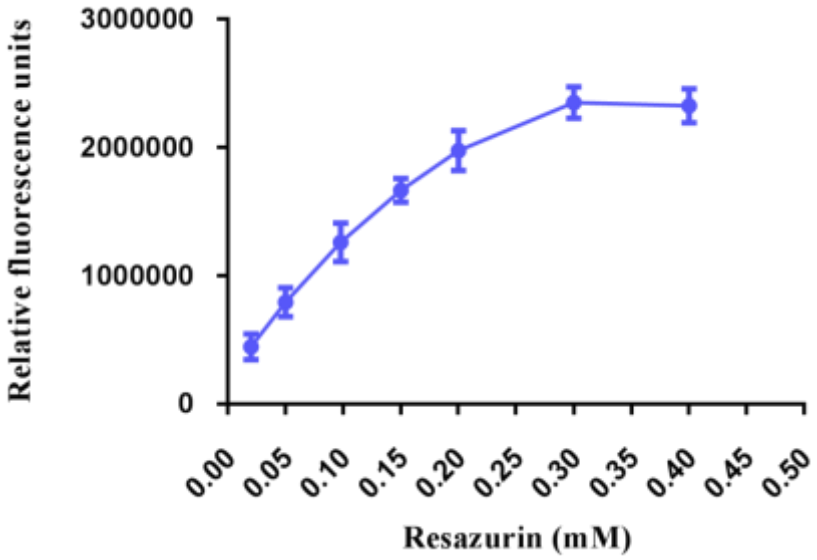

Figure 3.15: Evaluation of 10 µL resazurin concentrations (0.02, 0.05, 0.098, 0.15, 0.2, 0.3 and 0.4 mM) vs relative fluorescence units. The starting cell density was $2.5x10^5$ cells/mL and incubation period after resazurin addition was 8 hours. Each concentration was assessed based on triplicate, for N=2.

The optimum time period was assessed to be 8 hours. As shown in Figure 3.16, for all the concentrations tested the signal intensity no longer increases after 8 hours indicating that the maximum signal window had been reached. Thus, additional incubation beyond this point was of no additional benefit. This indicated that the optimal time period for incubation after resazurin addition was 8 hours.

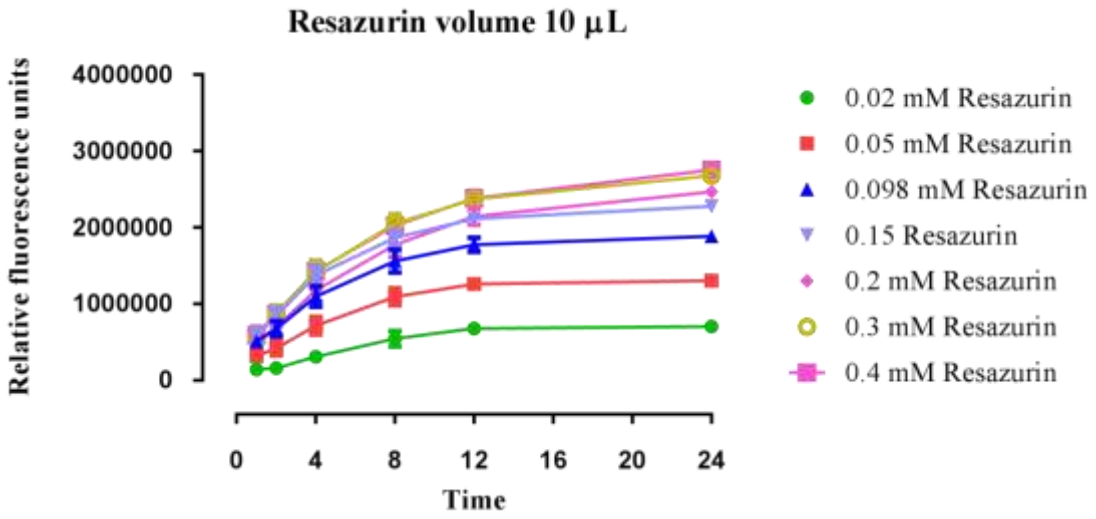

Figure 3.16: Comparison of resazurin concentrations with signal intensity and multiple time points. The signal at each resazurin concentration was averaged from duplicate samples, for N=2.

3.3.3.3. Determining DMSO Sensitivity

Final DMSO concentrations ranging from 0.0125% to 10% (v/v) were tested in the 384-well THP-1 resazurin cytotoxicity assay. The results shown by the cells in Figure 3.17 suggest that a final concentration of 0.5 % (v/v) DMSO was well tolerated in the resazurin THP-1 resazurin cytotoxicity assay and demonstrated no significant decrease (Two-way ANOVA, P value: 0.9010) in signal regardless of diluent used. Increasing the concentration of DMSO to greater than 1.0 % (v/v) significantly reduced the number of cells.

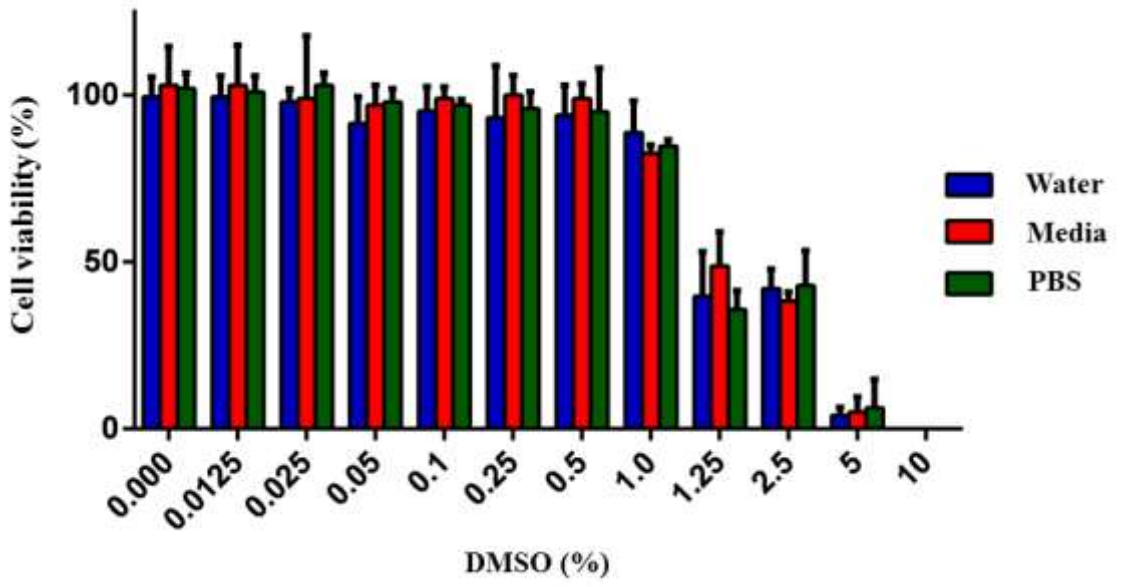

Figure 3.17: Impact of Dimethylsulfoxide (DMSO) concentration on cell viability of cells in a 384-well assay format. The signal at each DMSO concentration was averaged from triplicate samples, for N=2.

3.3.3.4. Optimal dilution medium and reference compound

The reference compound, the antibiotic Puromycin, was used for determining the optimal dilution media for the THP-1 cytotoxicity assay (Figure 3.18). The protocol used was described in chapter 2.

No significant differences were observed between the inhibitory concentrations for Puromycin (P value: 0.999), according to one-way ANOVA analysis (Figure 3.18B), when diluted in all three mediums (Water, PBS, and RPMI without HIFBS) (Figure 3.18). Therefore, RPMI without HIFBS was selected as the optimal dilution media for the assay. Water and PBS could be used as alternatives to RPMI media without HIFBS but it was observed that using RPMI media without HIFBS gave more consistent results mostly because of maintaining the buffering capacity of the assay.

A

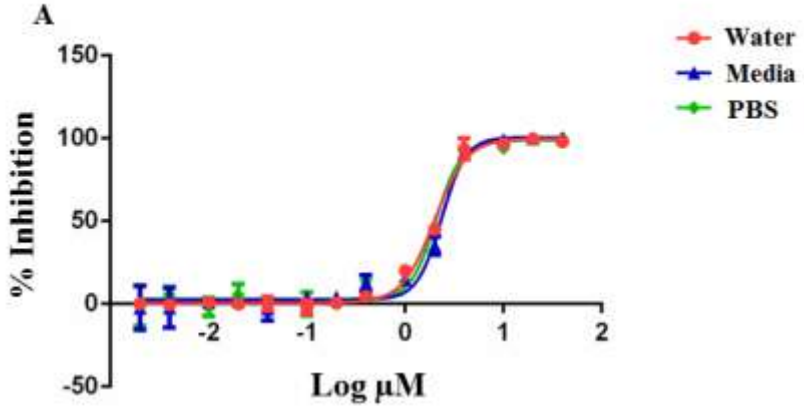

B

Drug	IC_{50} (µM) [Mean ± SD]			One Way ANOVA (P values)
	Water	Media	PBS	
Puromycin	2.495 ± 0.631	2.913 ± 0.823	2.956 ± 0.735	0.999

Figure 3.18: Optimal dilution media and reference compounds inhibitory concentration (50%) for THP-1 cytotoxicity assay. (A) The concentration response graph plotted and (B) IC_{50} values calculated for puromycin was determined for the THP-1 cytotoxicity assay. Dilutions of puromycin were made in water, media without HIFBS and PBS for comparison. Each dilution was prepared in duplicate, for N=2 experiments.

3.3.3.5. Intra- and Inter-day reproducibility of the THP-1 cytotoxicity assay

The *Z'* for the THP-1 cytotoxicity assay was 0.847 ± 0.019 (Figure 3.19). The % coefficient of variance for all of the replicates was below 10%, showing the accuracy of the assay. The signal window obtained between the positive and negative controls was more than 15 times, hence showing an excellent dynamic range of assay signal (Table 3.4). All of the values obtained for the above-mentioned parameters suggest that the assay was extremely robust and thus suitable as a HTS assay.

There was no statistical difference between the Intra-day and Inter-day IC_{50} values obtained for Puromycin (2.036 ± 0.255 µM) (Figure 3.20) with P value of 0.998 (Figure 3.20B).

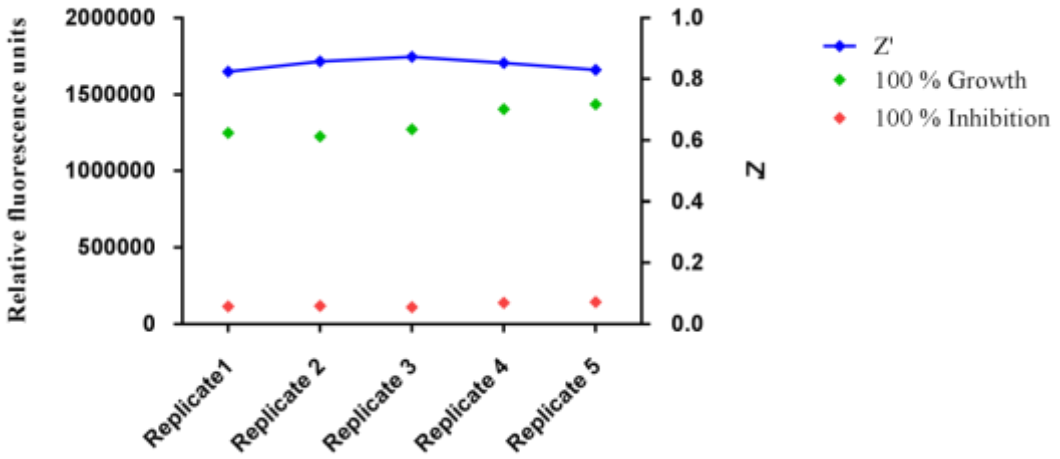

Figure 3.19: Reproducibility of the THP-1 cytotoxicity assay. Red dots represent 100% inhibition with positive control 5 µM puromycin, green dots represent 0% inhibition with negative control 0.4% DMSO and blue dots represent Z' values for each plate. Each data point was calculated from duplicate plates, for N=2.

Table 3.4: Statistical parameters for multiple replicates in THP-1 cytotoxicity assay.

Statistical Parameters	Rep 1	Rep 2	Rep 3	Rep 4
% CV (0% Inhibition)	4.40 %	5.02 %	5.48 %	5.31 %
% CV (100% Inhibition)	3.52 %	4.85 %	3.34 %	4.53 %
Signal Window	17 fold	17 fold	16.5 fold	17 fold

A

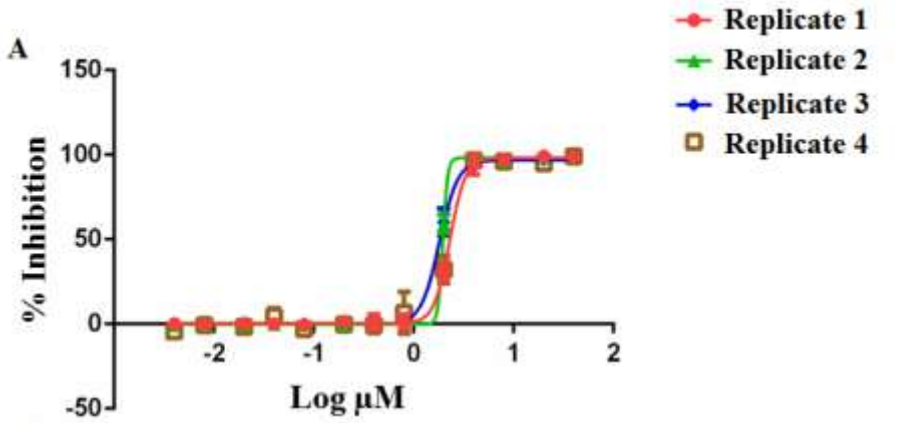

B

Drug	IC_{50} (µM) [Mean ± SD]					One Way ANOVA (P values)
	R1 [Intra]	R2 [Intra]	R3 [Inter]	R4 [Inter]	Average ± SD	
Puromycin	2.288	1.954	1.806	2.141	2.036 ± 0.255	0.998

Figure 3.20: Intra- and Inter-day reproducibility of the THP-1 cytotoxicity assay. (A) The concentration response graph plotted and (B) IC_{50} values calculated for puromycin was determined for the THP-1 cytotoxicity assay. Each concentration is in duplicate, for N=2 experiments.

3.4. Discussion

A promastigote viability assay for *L. donovani* DD8 and a complementary cytotoxicity assay using the THP-1 host cells have been established. The assays were robust and reproducible, using standard statistical parameters such as *Z'* and coefficient of variance to assess assay quality and suitability for use in HTS drug discovery. The sensitivity with which the assays could determine activity was measured using the clinical drugs amphotericin B and miltefosine. The data obtained correlated well with previously reported values for similar assay formats in the literature (Siqueira-Neto, *et al.*, 2010; De Muylder, *et al.*, 2011).

Leishmania donovani MHOM/IN/80/DD8 is a WHO reference strain, isolated from the bone marrow of a nine year old Indian male in 1980 from the state of Bihar, India (WHO, 1990). This species was found to be the causative agent of visceral leishmaniasis (Xu, *et al.*, 1984). This strain was selected for this project as a representative strain for developing a biologically relevant assay for identifying novel anti-leishmanial drugs against visceral leishmaniasis, the lethal form of the disease.

A screening cascade, which included a promastigote viability assay and an intracellular amastigote assay, was developed to discover new compounds with potential against *Leishmania* parasites. Indubitably, the intracellular amastigote assay is the golden standard for *in vitro Leishmania* drug discovery research. However, other models (promastigote and axenic amastigote) are still being used for primary screening campaigns involving large libraries (Pena, *et al.*, 2015). An example in this aspect is the recent screening of 3 million compounds against *Leishmania donovani* axenic amastigotes to identify promising anti-leishmanial compounds (Khare, *et al.*, 2016). An azabenzoxazole compound, GNF5343, was identified as a hit in the *L. donovani* model. The optimization of GNF5343, focused on improving bioavailability and potency on inhibition of *L. donovani* growth within macrophages, led to the discovery of GNF6702, which has an even better efficacy *in vivo* mouse models. Therefore, it is possible to identify new compounds from other model assays, which can be associated with intracellular amastigotes assays for further characterization of compounds.

In order to develop an assay to discover new compounds against *Leishmania* parasites, it is imperative to optimize parameters such as optimal parasite concentration, resazurin and DMSO concentrations, optimal dilution media, reference drugs /compounds and the validity of the assay with respect to reproducibility.

An important factor for the assay was the selection of a parasite concentration to ensure reproducibility each time the assay was performed. It was essential to ascertain the concentration of parasite that could be cultured in a flask and the 384-well assay format in order to reduce reagent usage and increase throughput, making the assay more cost effective (Hertzberg and Pope, 2000). The quantification of parasites in the flask was to ensure they were in mid-log phase when plated into the 384-well plates. The maximum number of parasites that could be cultured in the $75cm^2$ flask was found to be $4.3x10^7$ parasites/mL with a starting density of $1x10^5$ parasites/mL (Figure 3.1). The maximum

number of parasites cultured in a 384-well plate was found to be $4.3x10^7$ parasites/ mL with a starting density of $5x10^5$ parasites/mL (Figure 3.2). The growth pattern of the parasites varied from species and strain of the parasite; hence the growth pattern of *L. donovani* DD8 strain was evaluated and compared with the previously reported data for the same species and strain. The doubling time for *L. donovani* DD8 parasite was estimated to be 12.7 hours; previously a doubling time of 11.4 hours and 12 hours had been reported for *L. donovani* DD8 (Kar, *et al.*, 1990; Barak, *et al.*, 2005)

The optimum inoculum density was estimated to be $1x10^5$ parasites/mL. With this starting density the parasites reached the concentration of $4.3x10^7$ parasites/mL (Figure 3.2c) after 4 days, after which they entered the stationary phase. The majority of previously reported assays designed for the promastigotes stage use early or mid-log promastigotes and not the metacyclic promastigote form, which appear in the late log phase and stationary phase. Metacyclic promastigotes are non-dividing and obtaining pure cultures of them is difficult. Due to this reason, the parasites used in this assay were from the mid-log phase. The concentration for seeding the parasites was calculated to be $5x10^5$ parasites/mL in a volume of 55 µL (27,500 parasites/well) based on maximum parasites obtained. Similar concentrations 20,000 parasites/well were used for other species such as *L. major (*MHOM/IL/81/FRIEDLIN) *and L. donovani (*MHOM/ET/67/HU3) (Siqueira-Neto, *et al.*, 2010). A similar study has used the *L. donovani* (MHOM/SD/62/IS-cl2D) promastigotes from an exponentially growing culture at 10^6/mL (De Muylder, *et al.*, 2011). Determination of a linear relationship is an important consideration in assay development, particularly for HTS, to ensure that the assay is within the limits of the detection method (Hsieh and Liu, 2008).

It was estimated that a linear correlation exists between the resazurin concentration and the parasite load (Figure 3.3). A linear signal of fluorescence to parasite suggests that resazurin could be used as an effective indicator to determine the effects of compounds on parasite viability and proliferation. It is an active component of the commercially available Alamar Blue™ (O'Brien, *et al.*, 2000). It was determined that a final assay concentration of 0.142 mM gave a better signal when compared to the other concentrations tested (Figure 3.4). Resazurin concentrations ranging from 0.044 to 0.45 µM have been reported previously to assess drug cytotoxicity against *Leishmania* (Mikus and Steverding, 2000; Siqueira-Neto, *et al.*, 2010; Corral, *et al.*,

2013; Prajapati, *et al.*, 2013). Determining the DMSO tolerability of the assay is critical for HTS, as compounds libraries are principally diluted in 100% DMSO. Through evaluating a range of DMSO concentrations, it was assessed that there was no effect on cell viability until an assay DMSO concentration of 2.0% was reached (Figure 3.7). Exceeding this concentration, resulted in the cell viability starting to decline; therefore, a DMSO concentration of 0.4% was selected as a negative control (100% growth). Final assay concentrations up to 1% DMSO have been used in previous experiments with no obvious effects on the parasite viability (De Muylder, *et al.*, 2011).

It was observed that the different diluent options for diluting the drugs / compounds (water, phosphate buffer saline and M199I without HIFBS) did not have a significant effect on compound activity when comparing the IC_{50} values of established reference compounds under the different test conditions (Figure 3.8). Therefore, M199 without HIFBS was selected as the optimal dilution media for the assay. Water and PBS could be used as alternatives to M199 media without HIFBS, however it was observed that using M199 media without HIFBS gave slightly more consistent results. It was predicted that this was most likely because of the ability to maintain the buffering capacity of the assay.

As a positive control, different reference drugs and compounds were evaluated. These included amphotericin B, miltefosine, VL-2098 and puromycin. Amphotericin B was selected as the positive control at a final assay concentration of 1 µM, as this concentration kills 100% of the parasites. This drug showed consistent activity against the parasites when IC_{50} values were measured over a course of multiple experiments: IC_{50} of 0.043 ± 0.015 µM. The effect of the drugs was strain specific with *L. donovani* MHOM/SD/1968/IS having an IC_{50} value of 0.135 ± 0.047 µM (van den Bogaart, *et al.*, 2014) and with *L. donovani* (MHOM/SD/62/IS-cl2D) promastigotes gave an IC_{50} value for amphotericin B of 1.61 µM (De Muylder, *et al.*, 2011). The IC_{50} value for miltefosine was found to be 2.088 ± 0.561 µM (Table 3.4) which was consistent with the literature for other strains (Siqueira-Neto, *et al.*, 2010). A new lead compound, VL-2098, generously provided by DND*i*, was also assessed in the assay. This pre-clinical drug candidate served as a highly potent reference molecule (Mukkavilli, *et al.*, 2014; Gupta, *et al.*, 2015). Development of the compound has been discontinued due to *in vivo* testicular toxicity associated with it. However, for this project it served as a good *in*

vitro control molecule (DND*i*, 2015). The IC_{50} value for VL-2098 obtained in the promastigote assay was ascertained to be 0.121 ± 0.001 µM.

Reproducibility of an assay is extremely vital for HTS. As numerous plates are processed over multiple days in a HTS campaign, the variability from batch to batch, as well as internal plate variation, may affect the overall performance of the assay and thus interpretation of the results obtained. Assay reproducibility for the promastigote viability assay was assessed using different parameters such as intra/ inter day reproducibility and the use of different passage numbers for the parasites (Figure 3.9). Statistical parameters were evaluated which include Z' factor (Zhang, *et al.*, 1999), signal to background and signal to noise ratio. These parameters were compared for screening validation and hit selection in the primary screening for this assay. Although the clinically relevant form of the parasite is the intracellular amastigote, the promastigote viability assay serves as a preliminary assay.

A novel assay established by Dr's Jones & Shelper (Duffy, *et al.*, 2017) served as a clinically relevant high content, high throughput imaging assay to identify compounds active against *L.donovani* DD8 intracellular amastigotes. This assay was used for the primary screening and retest of hits. Reference compound activity was optimized for the amastigote assay using amphotericin B (average IC_{50} value of 0.089 ± 0.020 µM) (Figure 3.12A). The effect of the drug in the intracellular amastigote assay was strain specific; *L. donovani* MHOM/ET/67/HU3 has a reported IC_{50} value of 1.3 µM (Siqueira-Neto, *et al.*, 2010) and *L. donovani* (MHOM/SD/62/IS-cl2D) the IC_{50} value of amphotericin B is 1.12 µM (De Muylder, *et al.*, 2011). Not only is the effect of amphotericin B strain specific, it also has species specificity with an IC_{50} value of 0.506 µM in *L. mexicana* (MNYC/BZ/62/M379) (Dagley, *et al.*, 2015). The IC_{50} value for miltefosine was found to be 1.967 ± 0.569 µM (Figure 3.12B) in the amastigote assay, which was consistent with the literature, namely 3.1 ± 2.3 µM (Siqueira-Neto, *et al.*, 2012); and the IC_{50} value for VL-2098 was 0.865 ± 0.545 µM (Figure 3.12C) which was not consistent to previous reports for the this compound (0.025 µM) (Mukkavilli, *et al.*, 2014). Whilst differences in activity may be due to the different assay formats used, it has come to light that the value reported for VL-2098 was indeed incorrect and was actually closer to the values obtained within this study. Bhuniya *et al.*, 2015used a chemiluminescence assay with a genetically modified *L. donovani DD8* LUCI

expressing the firefly luciferase reporter gene, in conjunction with the mouse macrophage cell line J-774A.1 as the host cells (Bhuniya *et al.*, 2015). A change in host cell type, host cell concentrations, genetically modified parasites, parasite infectivity ratios, assay format and detection system can account for differences in reported IC_{50} values.

A THP-1 cytotoxicity assay was also established, which served as a complementary assay to assess the cytotoxicity of the compounds. This assay was designed to match the incubation periods for PMA washing and compound exposure for both the intracellular amastigote and promastigote assay. The acute monocytic cell line, THP-1, was transformed into macrophage-like cells using phorbol myristate acetate (PMA) (Tsuchiya, *et al.*, 1982). The mechanism of action of PMA to induce differentiation involves modulation of expression of various cell cycle regulators, which in turn are initiated by cellular generation of reactive oxygen species (ROS). It has been proposed that PMA-induces the upregulation of p21 via the protein kinase C (PKC)-mediated ROS-dependent signalling mechanism, which involves MAP kinase activation (Traore, *et al.*, 2005). As these cells act as the host cells in the amastigote assay it was necessary to determine the cytotoxicity of the compounds on these cells. This assay was designed to ascertain potential cytotoxicity during the different incubation periods for both the promastigote and intracellular amastigote assays. Other conditions, such as cell densities, resazurin, DMSO, reference compounds concentrations and volumes were kept constant for both the assays. The positive control (100% inhibition) for the assays was 5 µM Puromycin and the negative control (no inhibition) was 0.4% DMSO. In addition to the THP-1 cytotoxicty assay, a HEK-293 cytotoxicty assay was also used to assess the cytotoxicity of the compounds on human embryonic kidney cells. Human Embryonic Kidney 293 cells have been considered as a representative for mammalian cells and have been used extensively as an *in vitro* cell model to assess compound nephrotoxicity (Knasmuller, *et al.*, 2004; Hynes, *et al.*, 2006; Park, *et al.*, 2007).

A highly sensitive and reproducible promastigote viability assay was developed and optimized in a 384-well format for high throughput phenotypic screening of *Leishmania donovani* DD8 parasites. The promastigote viability and intracellular amastigote assays were validated using reference clinical drugs currently used for the treatment of the disease. Complementary THP-1 cytotoxicity assays were also established that mimic

both the promastigote and the intracellular amastigote assay formats enabling comparable cytotoxicological profiling of the compounds.

Chapter 4: *In vitro* profiling of compound collections

4.1. Introduction

A screening programme to identify potential anti-leishmanial compounds was established. Primary screening was undertaken using the promastigote viability and intracellular amastigote imaging assays, both optimised for 384-well plate format. Active compounds (hits) were subjected to further testing using a concentration response curve to ascertain the IC_{50} values of the compounds against both promastigote and intracellular amastigotes. In addition, three independent cytotoxicity assays were also performed (HEK-293 cytotoxicity assay, THP-1 cytotoxicity assay mimicking the amastigote assay conditions and the THP-1 cytotoxicity assay mimicking the promastigote assay conditions).

The compound libraries screened were comprised of both synthetic and natural product derived molecules. The synthetic scaffold library contained 5560 compounds which were representative of a larger diverse library housed within Compounds Australia®, a compound management facility based in Griffith University, Australia. The scaffold library currently constitutes of >33,000 pure compounds, acquired from various commercial vendors as shown in Table 4.1.

This library provides novel chemotypes with lead like scaffolds and having approximately 30 compounds per scaffold (1200 scaffold in total). This collection was clustered in this configuration with the help of Queensland Facility of Advanced Bioinformatics (QFAB). The chemical fingerprint for this compound collection has been generated using the inhouse software developed by Compounds Australia. The 5560 compounds collection was handpicked as a representative set of the total 1200 scaffolds within the library. All compounds selected follow the Lipinski rule of five, with respect to lead-like properties and for diversity of chemotype.

Table 4.1: Commercial sources of compounds obtained from Compounds Australia®.

Vendor	Number of scaffolds	Compounds available
Enamine	507	13,999
ChemDiv	712	20,000
Total	1219	33,999

The second library that was screened to identify anti-leishmanial compounds was the Davis open access natural product-based (DOANP) library, which currently consists of 472 distinct compounds (Figure 4.1), the majority (53%) of which are natural products that have been obtained from Australian natural sources, such as endophytic fungi (Davis, 2005), plants (Levrier, *et al.*, 2013), macrofungi (Choomuenwai, *et al.*, 2012), and marine invertebrates (Barnes, *et al.*, 2010). Approximately 28% of this library contains semi-synthetic natural product analogues (Barnes, *et al.*, 2016), while a smaller percentage (19%) are known commercial drugs or synthetic compounds inspired by natural products.

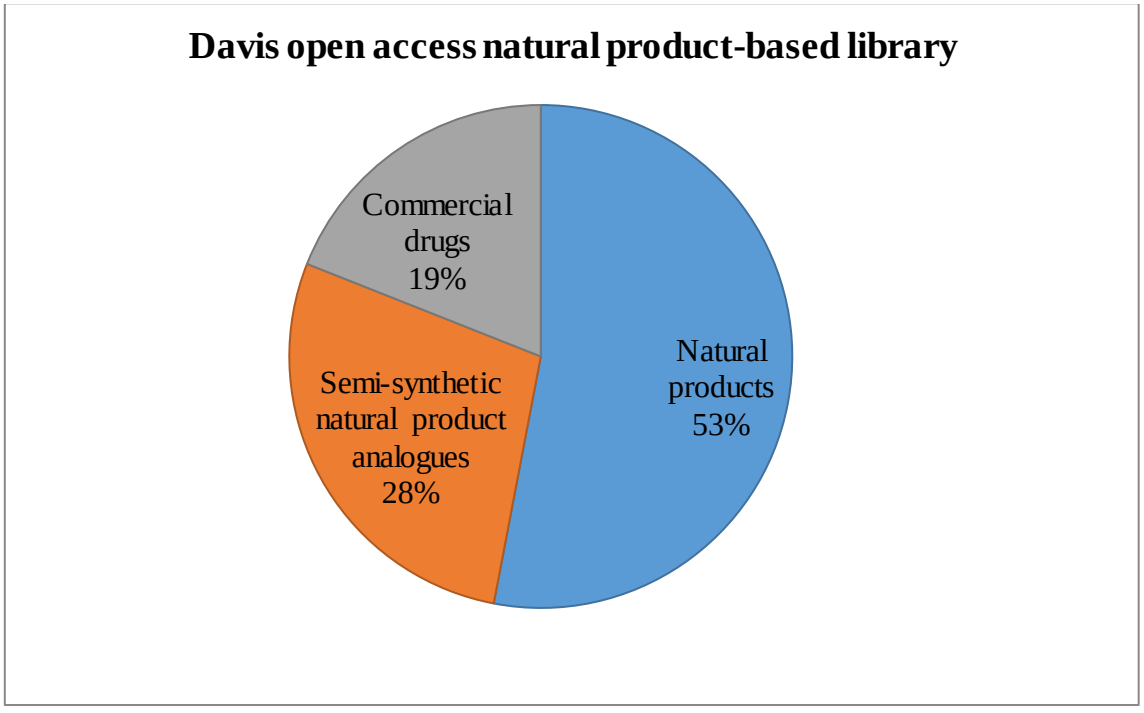

Figure 4.1: Classification of 472 compounds from the Davis open access natural product-based (DOANP) library.

Natural products have been widely used as a source of compounds suitable for the development of drugs, and at least 60% of the drugs marketed currently were either directly or indirectly from a natural origin (Newman and Cragg, 2016). Examples include artemisinin, an anti-malarial; morphine, an analgesic; penicillin, an anti-microbial; lovastatin, used in treatment of high cholesterol, and paclitaxel, an anti-tumour agent (Harvey, 2008; Harvey, *et al.*, 2015). With respect to the specific treatment of leishmaniasis t, amphotericin B is extracted from the filamentous bacteria called *Streptomyces nodusus* and paromomycin is extracted from *Streptomyces rimosus* variety paromomycinus (Oryan, 2015). Natural products have traditionally been used to treat parasitic diseases, primarily through ethnopharmacology approaches (Silva, *et al.*, 2011). More recent efforts to elucidate the structural and biological properties of the chemical entities within complex anti-parasitic natural product extracts have identified molecules with significant potential for treating neglected tropical diseases (NTDs). Recently, the anti-protozoal activity of the isolated alkamide dodeca-2E,4E-dien acid 4-hydroxy-2-phenylethylamide from *Anacyclus pyrethrum* roots was reported for *L. donovani*, *T. b. rhodesiense*, *T. cruzi* and the NF54 strain of *Plasmodium falciparum* exhibiting an IC_{50} value of 4.19 ± 1.64, 2.26 ± 0.18, 1.88 and 3.18 ± 0.20 µM, respectively (Althaus, *et al.*, 2017). In the field of drug development for *Leishmania*, various extracts and isolated compounds from plants have been exploited, as reviewed by Singh and co-workers (Singh, *et al.*, 2014).

The DOANP library was also screened to determine whether it contained compounds with activity against other kinetoplastids, specifically *T. b. brucei* bloodstream form strain 427 (a surrogate species for human African trypanosomiasis (HAT): bloodstream trypomastigotes) *and T. cruzi* (Chagas disease: intracellular amastigotes). Kinetoplastid pathogens share much of their cellular and molecular biology even though they cause clinically distinctive diseases and are trasmitted by different insect vectors (Stuart, *et al.*, 2008). The parasites in these studies share common molecular targets, including trypanothione reductase, pteridine reductase and cysteine protease enzymes, which have been proposed for target-based screening (Jones and Avery, 2015; Bermudez, *et al.*, 2016; Field, *et al.*, 2017). Inhibitors have been designed in the past for these enzymes as anti-leishmanials (Corona, *et al.*, 2012; Baiocco, *et al.*, 2013; Schroder, *et al.*, 2013) and anti-trypanosomals (Cavalli, *et al.*, 2009; Mpamhanga, *et al.*, 2009; Breuning, *et al.*, 2010). Fexinidazole is the most

advanced oral candidate under development for Chagas disease and HAT, currently in the Phase II and Phase III clicical trials, respectively (DND*i*, 2017). This lead compound has also shown potent activity against *L. donovani in vitro* and *in vivo* in a visceral leishmaniasis mouse model, illustrating the significant value of screening against multiple kinetoplastids (Wyllie, *et al.*, 2012).

4.2. Materials and Methods

4.2.1. Synthetic scaffold library

4.2.1.1. Library specifications, reference compound and assay plate preparation

For the initial screen, 5560 compounds from a diverse chemical library were provided by Compounds Australia® in master plates in single point 5 mM concentrations in 100% DMSO. These compounds were diluted in RPMI without HIFBS and screened at 10 and 20 µM (0.4% DMSO) for the promastigote viability and the intracellular amastigote assays, respectively. The data was normalized with in-plate controls based on 100% inhibition of parasites with 1 µM amphotericin B, 0% parasite inhibition in the presence of 0.4% DMSO, and percentage inhibition of each test molecule calculated for each concentration. The plate maps showing in-plate and external controls are illustrated in Figure 4.2. Retest of the active hits was performed using the following concentration range, 20 – 0.2 µM (0.4% DMSO vehicle) based on a 7-point concentration response scale for the intracellular amastigote, promastigote viability, HEK-293 cytotoxicity, and THP-1 cytotoxicity assays that mimic the amastigote and the promastigote assay conditions. Amphotericin B, miltefosine, VL-2098 and puromycin were used as reference drugs and compounds.

A

	1	2	3	4	5	6	7	8	9	10	11	12	13	14	15	16	17	18	19	20	21	22	23	24
A																								
B		DMSO	DMSO	DMSO	DMSO	DMSO	DMSO	DMSO	DMSO	DMSO	DMSO	DMSO	AMP	AMP	AMP	AMP	AMP	AMP	AMP	AMP	AMP	AMP	AMP	
C		DMSO	DMSO	DMSO	DMSO	DMSO	DMSO	DMSO	DMSO	DMSO	DMSO	DMSO	AMP	AMP	AMP	AMP	AMP	AMP	AMP	AMP	AMP	AMP	AMP	
D		DMSO	DMSO	DMSO	DMSO	DMSO	DMSO	DMSO	DMSO	DMSO	DMSO	DMSO	AMP	AMP	AMP	AMP	AMP	AMP	AMP	AMP	AMP	AMP	AMP	
E		DMSO	DMSO	DMSO	DMSO	DMSO	DMSO	DMSO	DMSO	DMSO	DMSO	DMSO	AMP	AMP	AMP	AMP	AMP	AMP	AMP	AMP	AMP	AMP	AMP	
F		DMSO	DMSO	DMSO	DMSO	DMSO	DMSO	DMSO	DMSO	DMSO	DMSO	DMSO	AMP	AMP	AMP	AMP	AMP	AMP	AMP	AMP	AMP	AMP	AMP	
G		DMSO	DMSO	DMSO	DMSO	DMSO	DMSO	DMSO	DMSO	DMSO	DMSO	DMSO	AMP	AMP	AMP	AMP	AMP	AMP	AMP	AMP	AMP	AMP	AMP	
H		DMSO	DMSO	DMSO	DMSO	DMSO	DMSO	DMSO	DMSO	DMSO	DMSO	DMSO	AMP	AMP	AMP	AMP	AMP	AMP	AMP	AMP	AMP	AMP	AMP	
I		DMSO	DMSO	DMSO	DMSO	DMSO	DMSO	DMSO	DMSO	DMSO	DMSO	DMSO	AMP	AMP	AMP	AMP	AMP	AMP	AMP	AMP	AMP	AMP	AMP	
J		DMSO	DMSO	DMSO	DMSO	DMSO	DMSO	DMSO	DMSO	DMSO	DMSO	DMSO	AMP	AMP	AMP	AMP	AMP	AMP	AMP	AMP	AMP	AMP	AMP	
K		DMSO	DMSO	DMSO	DMSO	DMSO	DMSO	DMSO	DMSO	DMSO	DMSO	DMSO	AMP	AMP	AMP	AMP	AMP	AMP	AMP	AMP	AMP	AMP	AMP	
L		DMSO	DMSO	DMSO	DMSO	DMSO	DMSO	DMSO	DMSO	DMSO	DMSO	DMSO	AMP	AMP	AMP	AMP	AMP	AMP	AMP	AMP	AMP	AMP	AMP	
M		DMSO	DMSO	DMSO	DMSO	DMSO	DMSO	DMSO	DMSO	DMSO	DMSO	DMSO	AMP	AMP	AMP	AMP	AMP	AMP	AMP	AMP	AMP	AMP	AMP	
N		DMSO	DMSO	DMSO	DMSO	DMSO	DMSO	DMSO	DMSO	DMSO	DMSO	DMSO	AMP	AMP	AMP	AMP	AMP	AMP	AMP	AMP	AMP	AMP	AMP	
O		DMSO	DMSO	DMSO	DMSO	DMSO	DMSO	DMSO	DMSO	DMSO	DMSO	DMSO	AMP	AMP	AMP	AMP	AMP	AMP	AMP	AMP	AMP	AMP	AMP	
P																								

B

	1	2	3	4	5	6	7	8	9	10	11	12	13	14	15	16	17	18	19	20	21	22	23	24
A																								
B		COMP	COMP	COMP	COMP	COMP	COMP	COMP	COMP	COMP	COMP	COMP	COMP	COMP	COMP	COMP	COMP	COMP	COMP	COMP	COMP	DMSO	AMP	
C		COMP	COMP	COMP	COMP	COMP	COMP	COMP	COMP	COMP	COMP	COMP	COMP	COMP	COMP	COMP	COMP	COMP	COMP	COMP	COMP	DMSO	AMP	
D		COMP	COMP	COMP	COMP	COMP	COMP	COMP	COMP	COMP	COMP	COMP	COMP	COMP	COMP	COMP	COMP	COMP	COMP	COMP	COMP	DMSO	AMP	
E		COMP	COMP	COMP	COMP	COMP	COMP	COMP	COMP	COMP	COMP	COMP	COMP	COMP	COMP	COMP	COMP	COMP	COMP	COMP	COMP	DMSO	AMP	
F		COMP	COMP	COMP	COMP	COMP	COMP	COMP	COMP	COMP	COMP	COMP	COMP	COMP	COMP	COMP	COMP	COMP	COMP	COMP	COMP	DMSO	AMP	
G		COMP	COMP	COMP	COMP	COMP	COMP	COMP	COMP	COMP	COMP	COMP	COMP	COMP	COMP	COMP	COMP	COMP	COMP	COMP	COMP	DMSO	AMP	
H		COMP	COMP	COMP	COMP	COMP	COMP	COMP	COMP	COMP	COMP	COMP	COMP	COMP	COMP	COMP	COMP	COMP	COMP	COMP	COMP	DMSO	AMP	
I		COMP	COMP	COMP	COMP	COMP	COMP	COMP	COMP	COMP	COMP	COMP	COMP	COMP	COMP	COMP	COMP	COMP	COMP	COMP	COMP	DMSO	AMP	
J		COMP	COMP	COMP	COMP	COMP	COMP	COMP	COMP	COMP	COMP	COMP	COMP	COMP	COMP	COMP	COMP	COMP	COMP	COMP	COMP	DMSO	AMP	
K		COMP	COMP	COMP	COMP	COMP	COMP	COMP	COMP	COMP	COMP	COMP	COMP	COMP	COMP	COMP	COMP	COMP	COMP	COMP	COMP	DMSO	AMP	
L		COMP	COMP	COMP	COMP	COMP	COMP	COMP	COMP	COMP	COMP	COMP	COMP	COMP	COMP	COMP	COMP	COMP	COMP	COMP	COMP	DMSO	AMP	
M		COMP	COMP	COMP	COMP	COMP	COMP	COMP	COMP	COMP	COMP	COMP	COMP	COMP	COMP	COMP	COMP	COMP	COMP	COMP	COMP	DMSO	AMP	
N		COMP	COMP	COMP	COMP	COMP	COMP	COMP	COMP	COMP	COMP	COMP	COMP	COMP	COMP	COMP	COMP	COMP	COMP	COMP	COMP	DMSO	AMP	
O		COMP	COMP	COMP	COMP	COMP	COMP	COMP	COMP	COMP	COMP	COMP	COMP	COMP	COMP	COMP	COMP	COMP	COMP	COMP	COMP	DMSO	AMP	
P																								

Figure 4.2: Plate map showing (A) whole plate independent controls and (B) internal plate controls Column 22 represent the negative control with 0.4% DMSO indicating 0% inhibition whereas column 23 represent the positive control with 1µM amphotericin B indicting 100% inhibition. The outer wells were just filled with media, ultimately reducing the edge effect observed during long incubations. Colour coding: (Blue) 1 µM amphotericin B and (Pink) 0.4% DMSO as final assay concentrations, the sample compounds to be tested as shown as (Green).

4.2.2. Davis open access natural product-based library

4.2.2.1. Library specifications and assay plate preparation

The DOANP library containing 472 compounds housed within Compounds Australia® was dispensed into microtitre plates as 5 mM DMSO solutions. The natural product isolation procedures or semi-synthetic studies for the majority of compounds in this unique library have been previously published (Davis, 2005; Barnes, *et al.*, 2010; Choomuenwai, *et al.*, 2012; Levrier, *et al.*, 2013). All compounds were >95% pure when submitted for storage within Compounds Australia®.

For the primary screen, compounds were prepared as a stock concentration of 5 mM in 100% DMSO and tested in duplicate point for two independent experiments (N=2) at final assay concentrations of 20 µM and 16.7 µM for the *L. donovani* intracellular amastigote and promastigote viability assays, respectively. Primary screening against *T. b. brucei* was undertaken at 5 µM and for *T. cruzi* a 10 µM final screening concentration was used as described in Appendix 4. Actives were defined as compounds which exhibited >70% activity at 20 µM and 16.7 µM for *L. donovani* DD8 intracellular amastigote and promastigote assays, respectively. In addition, compounds exhibiting >50% activity at 5 µM for *T. b. brucei* and showing ≥50% activity at a concentration of 10 µM for *T. cruzi* intracellular amastigote were classified as active compounds. These compounds were subsequently retested in a 14-point concentration format to determine the IC_{50} values against the parasites, and against the host cells for *L. donovani* and *T. cruzi*, THP-1 and 3T3 cells respectively. In addition, the cytotoxicity of the compounds was also evaluated against HEK-293 cells to determine their selectivity for the parasite. To determine IC_{50} values, 14 point concentration response curves with top concentrations of 20 µM and 16.7 µM were used for the *L. donovani* DD8 intracellular amastigote and promastigote viability assays, respectively. A top concentration of 20 µM was used for *T. b. brucei* and 18.3 µM for *T. cruzi* in the 14 point concentration repsonse curves.

4.3. Results

4.3.1. Synthetic scaffold library

4.3.1.1. Primary screening

4.3.1.1.1. Promastigote viability assay

Of the 5560 compounds tested, there were 29 compounds which exhibited >60% activity at 10 µM (Hit rate: 0.52%). The activity cut off for active hit compounds was defined as inhibition ≥60 % at 10 µM. Figure 4.3 is a scatterplot of the screening data with the active hits were defined by the blue dots above the cut off line (black line). Normal distribution was plotted for all of the compounds based on percentage activity (Figure 4.4).

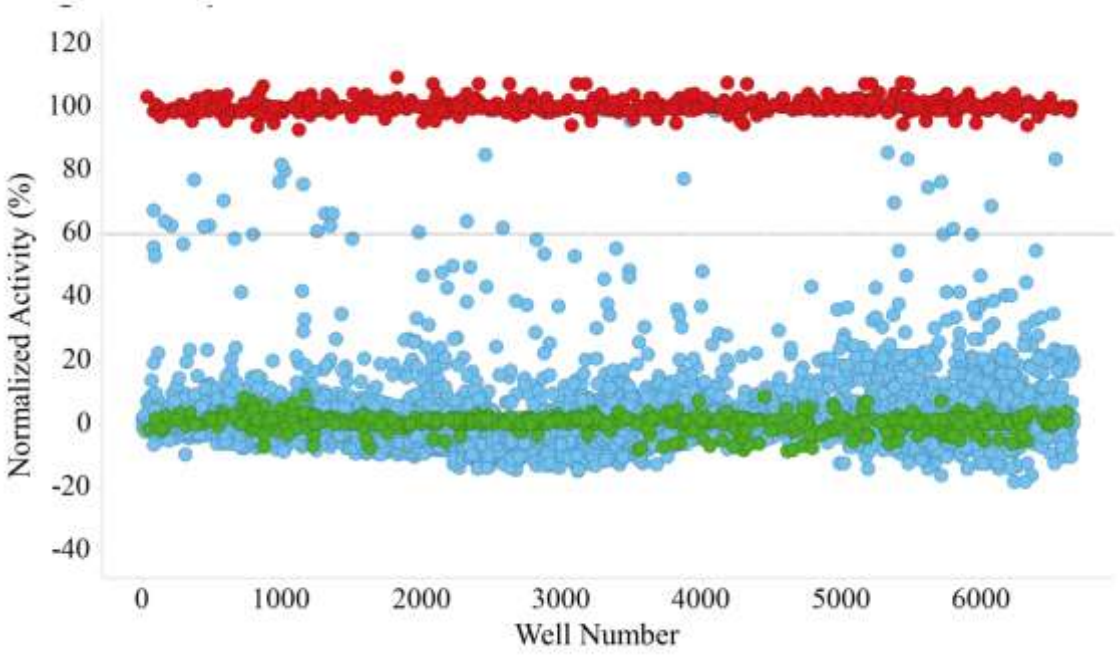

Figure 4.3: Scatter plot for primary screening using *L. donovani* DD8 promastigote viability assay. Red dots represent 100% inhibition with positive control 1 µM amphotericin B (100% inhibition), green dots represent 0% inhibition with negative control 0.4% DMSO and blue dots represent compound samples.

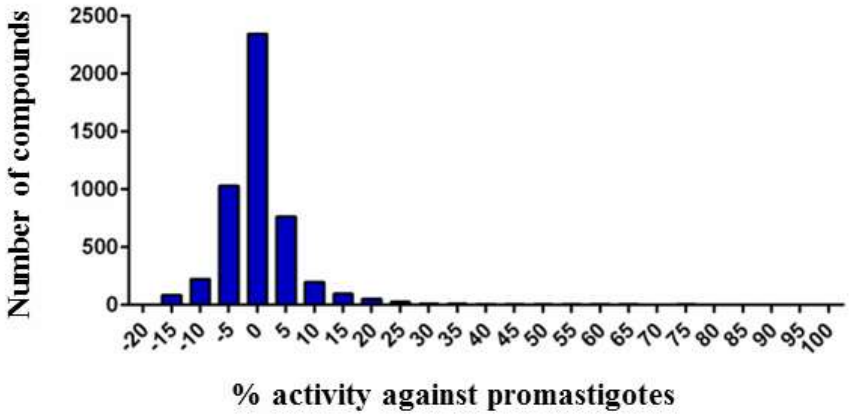

Figure 4.4: Activity distribution of primary screening data obtained using the *L. donovani* DD8 promastigote viability assay. The data was normalized using positive control 1 µM amphotericin B and negative control 0.4% DMSO.

The *Z*' of the primary screen for the *L. donovani DD8* promastigote viability assay was 0.929 ± 0.034 (Figure 4.5), calculated using the positive (1 µM amphotericin B) and negative (0.4% DMSO) using internal plate controls in each batch of plates. The % coefficients of variance for the positive and negative controls were 1.37 ± 0.50 and 2.10 ± 1.06, respectively. The dynamic range of assay signal (signal window) was 17.64 ± 0.61 fold.

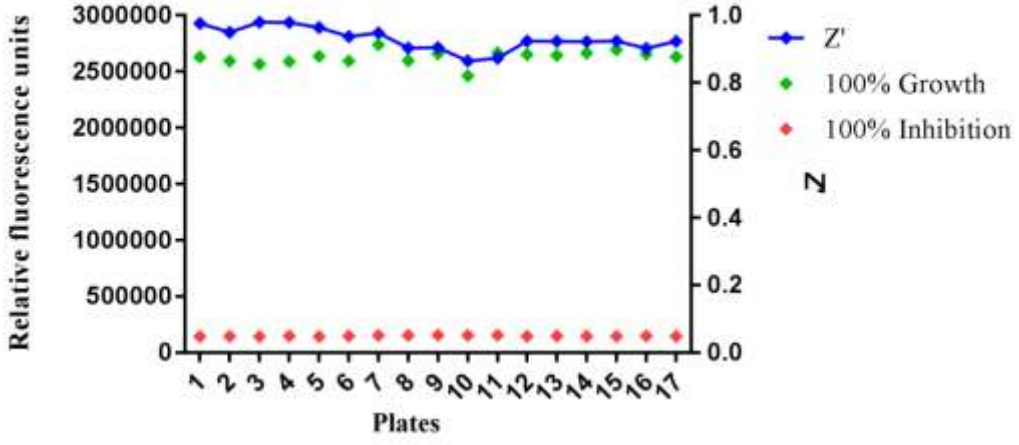

Figure 4.5: Controls for the primary screening using *L. donovani* DD8 promastigote viability assay. Red dots represent 100% inhibition obtained using 1 µM amphotericin B (100% inhibition), green dots represent 0% inhibition which is the negative control determined using 0.4% DMSO; and blue dots represent Z' values for each plate.

4.3.1.1.2. Intracellular amastigote assay

Of the 5560 compounds tested in the intracellular amastigote assay, 90 compounds exhibited >50% activity at 20 µM, representing a hit rate of 1.61%. The cut off for percentage inhibition was set at 50%, with compounds having activity greater than 50% regarded as active hits. There were minimal plate effects observed within the screening plates and the normalized activity of compounds is demonstrated in Figure 4.6. A normal distribution of activity was demonstrated, as shown in Figure 4.7.

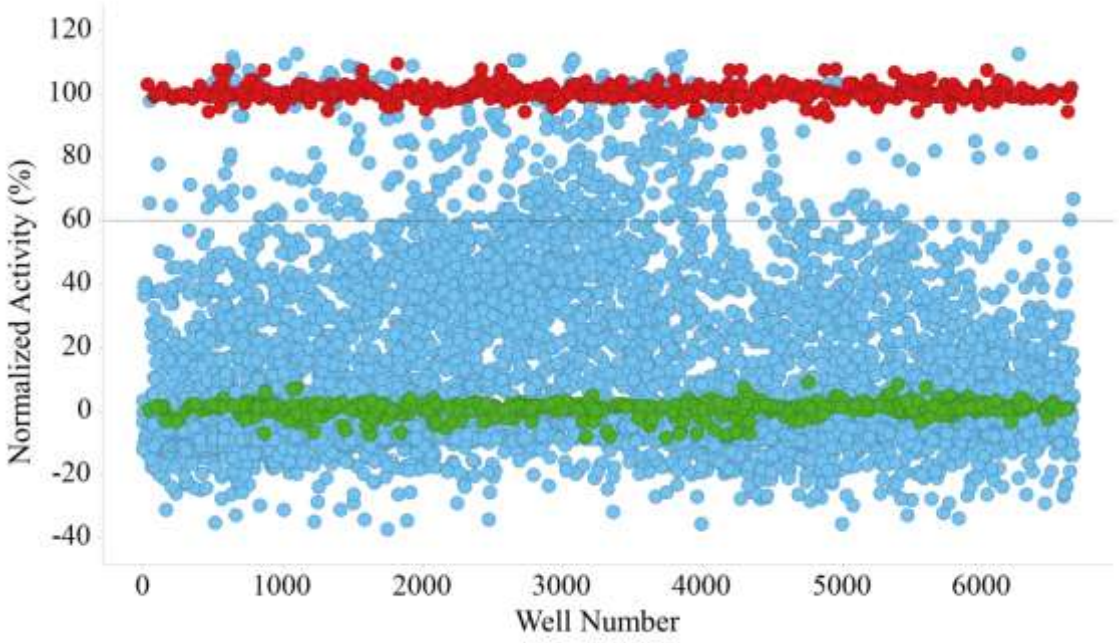

Figure 4.6: Scatter plot for primary screening using *L. donovani* DD8 intracellular amastigote assay. Red dots represent 100% inhibition (1 µM amphotericin), green dots represent 0% inhibition (0.4% DMSO) and blue dots represent the activities of the compound samples.

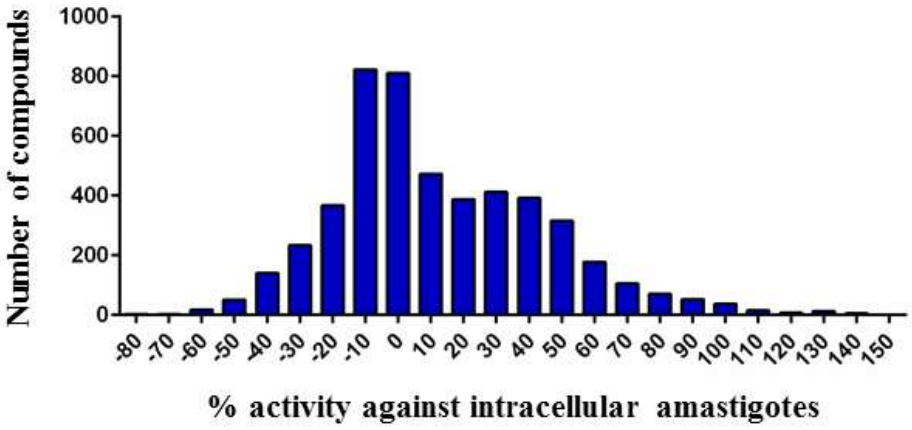

Figure 4.7: Activity distribution for primary screening using *L. donovani* DD8 intracellular amastigote assay. The data was normalized using positive control 1 µM amphotericin B and negative control 0.4% DMSO.

4.3.1.2. Retest

4.3.1.2.1. Promastigote viability assay

Primary screening utilizing the *L. donovani DD8* promastigote viability assay identified 29 compounds with >60% inhibitory activity at 10 µM. These 29 compounds were retested in the same assay in 7 concentrations (20 - 0.2 µM) resulting in 22 compounds confirming with >60% inhibitory activity at 10 µM, thus, a 75.85 % reconfirmation rate. Only 10 compounds were able to have an accurate IC_{50} value determined against promastigotes (Table 4.2), as a stable plateau of activity could not be established for the remaining 12 compounds. IC_{50} values against the THP-1 cells or the HEK-293 cells were unable to be determined for these compounds as cytotoxicity had not reached 50% at 20 µM, which was the top concentration tested due to limited solution stocks of the samples under investigation. Thus, in order to obtain IC_{50} values against HEK293 and THP-1 cells for these compounds, higher concentration were required to be tested.

The selectivity index for each compound was calculated as the ratio between cytotoxicity or inhibitory activity against mammalian cells (IC_{50}) and the inhibitory activity (IC_{50}) against *L. donovani* promastigotes. As compound activity against the mammalian cells did not reach 50%, values obtained at the highest tested concentration (20 µM) are used and activity is

considered greater than this. Table 4.2 shows the selectivity indices of the compounds with respect to their activity against either HEK-293 cells or the host cells used in the related amastigote assay, THP-1 cells.

.

Table 4.2: IC_{50} values of compounds obtained after retesting in the *L. donovani* DD8 promastigote viability assay.

	Compound ID	IC_{50} values	Selectivity index (HEK-293 cells)	Selectivity Index (THP-1 cells)
1	SN00769486	4.25 ± 0.15 µM	>5	>5
2	SN00770707	4.31 ± 0.41 µM	>5	>5
3	SN00771508	7.20 ± 1.24 µM	>3	>3
4	SN00780556	4.3 ± 0.87 µM	>5	>5
5	SN00788696	2.70 ± 0.64 µM	>7	>7
6	SN00790062	5.66 ± 0.45 µM	>3	>3
7	SN00799594	2.55 ± 0.75 µM	>7	>7
8	SN00773312	4.00 ± 0.37 µM	>5	>5
9	SN00784192	7.65 ± 1.84 µM	>3	>3
10	SN00785594	1.86 ± 0.33 µM	>10	>10

4.3.1.2.2. Intracellular amastigote assay

Ninety compounds were identified as having >50% activity at 20 µM from primary screening of samples in the *L. donovani* DD8 intracellular amastigote assay. Of these, a total of 40 compounds confirmed activity >50% at 20 µM upon retesting with multiple concentrations (20 - 0.2 µM). Of the 40 compounds retested, one compound, N-(4-Ethoxyphenyl)-2,3-

dihydro-1H-cyclopenta[b]quinolin-9-amine referred to herein as **BZ1**, had an IC_{50} value of 0.592 µM. The SI of compound **BZ1** at 20 µM was >33 for both HEK-293 and THP-1 cells, which was the top concentration tested due to limited solution stocks of the samples under investigation. Fresh stocks of **BZ1** were purchased in a powder form from commercial vendors and higher concentrations (40 - 0.002 µM) were tested to obtain a more accurate the selectivity index.

4.3.1.2.3. Assays reproducibility

The *Z'* was used as an indicator to assess the reproducibility of the assays. The results indicated that the *Z'* for the retest for the promastigote viability assay was 0.92 ± 0.023 (Figure 4.8A) and for the THP-1 cytotoxicity assay mimicking the amastigote assay conditions was 0.77 ± 0.090 (Figure 4.8) for the THP-1 cytotoxicity assay mimicking the promastigote assay conditions was 0.78 ± 0.097 (Figure 4.8C). For the HEK-293 cytotoxicity assay the *Z'* was 0.852 ± 0.076 (Figure 4.8D) and for the intracellular amastigote assay a *Z'* of 0.24 ± 0.11 was obtained.

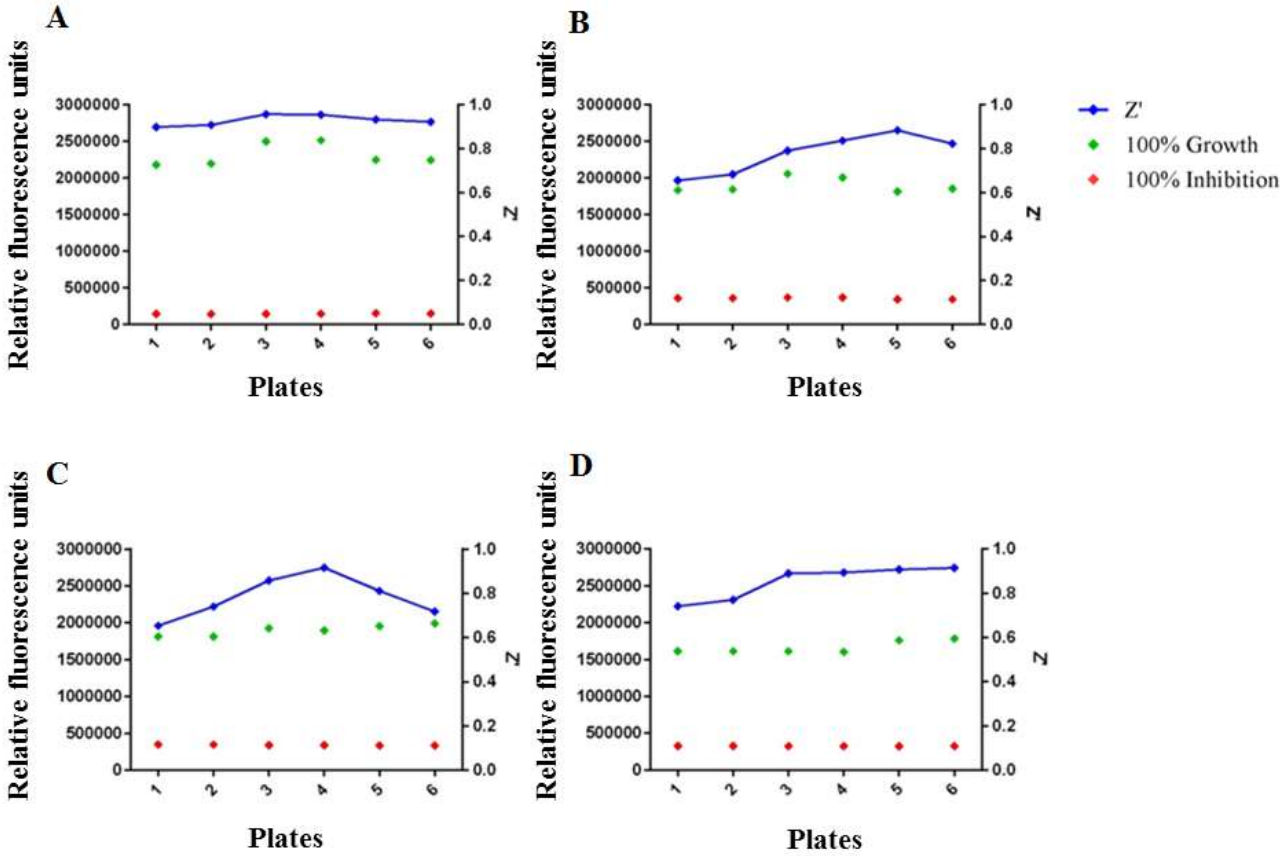

Figure 4.8: Assay reproducibility when screening the synthetic scaffold library. Controls for the the retest (A) using promastigote viability assay, (B) THP-1 cytotoxicity assay with same incubation periods as intracellular amastigote assay (C) THP-1 cytotoxicity assay with same incubation periods as promastigote assay (D) HEK-293 cytotoxicity assay. The green dots represent 0% inhibition obtained using the negative control (0.4% DMSO) and the blue dots represent the Z' values for each plate. The red dots are the 100% inhibition levels obtained with the positive controls in each of the assays which include 1 µM amphotericin B (A) and 5 µM puromycin (B), (C) and (D).

4.3.1.2.4. Active hits

Of the 104 compounds tested on both the *L. donovani DD8* promastigote and intracellular amastigote assays, 22 compounds returned activity at >60% activity against the promastigotes when tested at 10 µM (Figure 4.9), and 40 compounds exhibited >50% activity against the amastigote at a screening concentration of 20 µM (Figure 4.9), of which 26 compounds were found to also be active at 10 µM against the intracellular amastigotes. Four compounds demonstrated >50% activity against both the promastigote and the amastigote forms of the parasite when tested at 20 µM. Of these 4 compounds, compound N-(4-Ethoxyphenyl)-2,3-dihydro-1H-cyclopenta[b]quinolin-9-amine, referred to herein as **BZ1**, was selected as the most promising hit for further biological profiling.

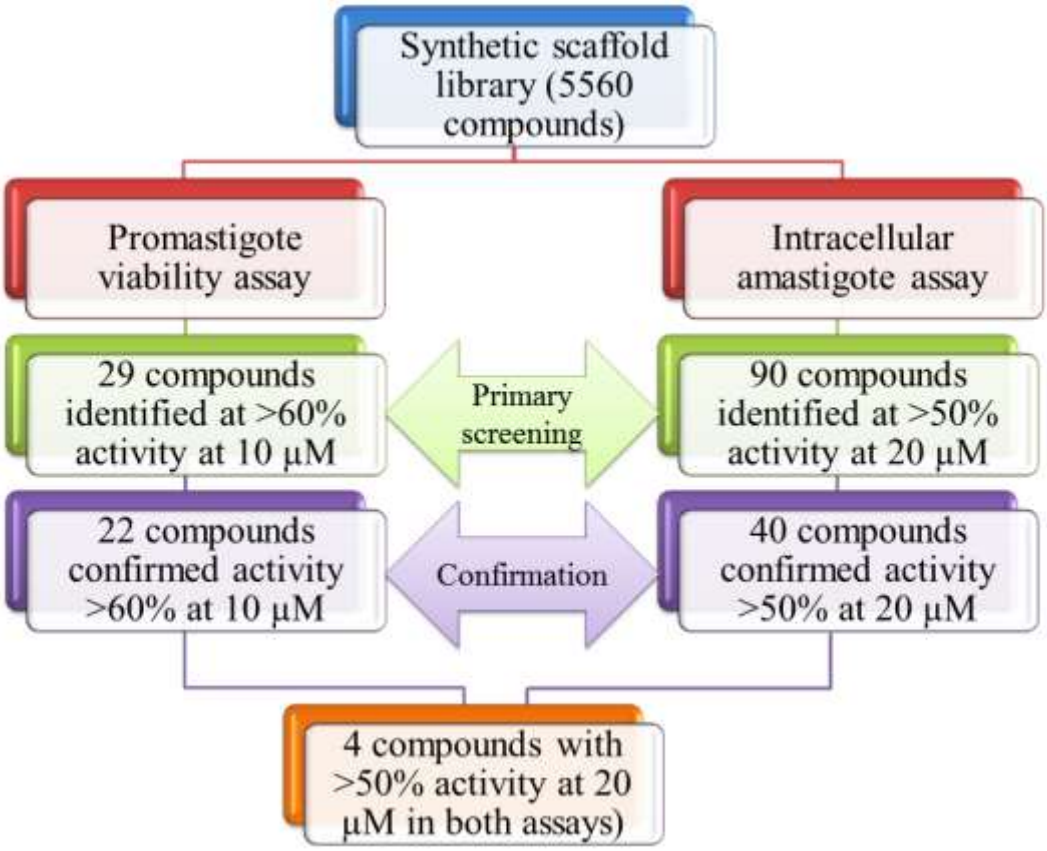

Figure 4.9: Schematics for synthetic scaffold library primary screening and confirmation in the *L. donovani* DD8 promastigotes and intracellular amastigotes.

4.3.1.3. Selection of active compounds

The high throughput screening approach employed against the 5560 compound scaffold library resulted in the discovery of a new anti-leishmanial compound, N-(4-Ethoxyphenyl)-2,3-dihydro-1H-cyclopenta[b]quinolin-9-amine referred to herein as BZ1 (Figure 4.10). This compound was shown to have an IC_{50} value of 0.592 ± 0.139 µM against the intracellular form of the parasite and an IC_{50} value of 2.374 ± 0.859 µM against the extracellular form (Figure 4.11).

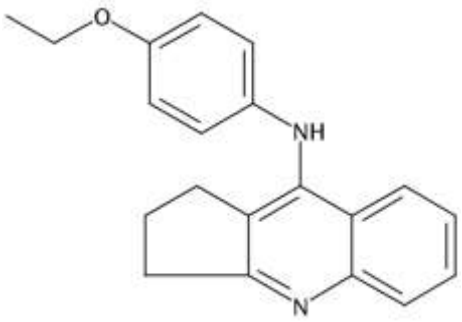

Figure 4.10: Structure of compound "N-(4-Ethoxyphenyl)-2,3-dihydro-1H-cyclopenta[b]quinolin-9-amine" referred as BZ1.

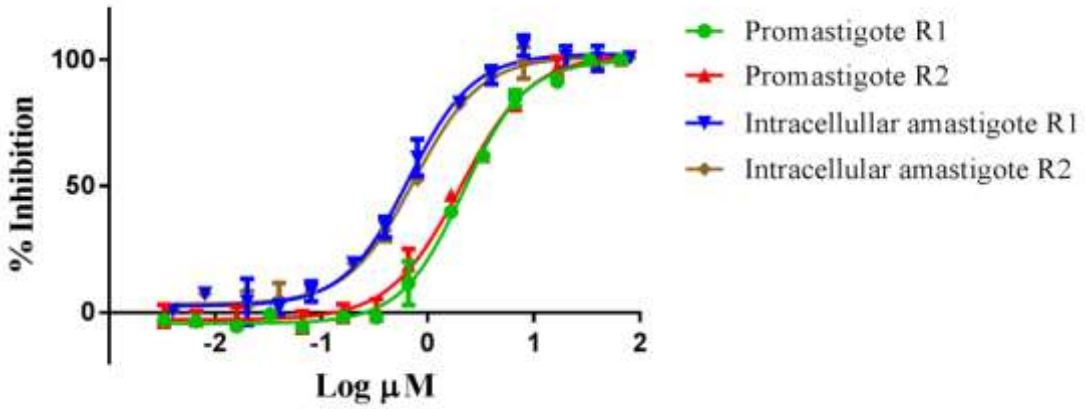

Figure 4.11: Concentration response curve compound BZ1 for *L. donovani* DD8 intracellular amastigote and promastigote viability assay. Each evaluation was performed in triplicate, for N=2.

As mentioned earlier, **BZ1** was purchased from a commercial vendor enabling a comparison between the original solution stock obtained from Compounds Australia

and the new solid stock, with respect to their anti-leishmanial activity against both parasite forms. No statistically difference was observed between the activity obtained for the original solution stock and new solution prepared from new solid of compound BZ1 (Table 4.3).

Table 4.3: Comparison of the 50% inhibitory concentrations for new and old batches of BZ1. Each evaluation was performed in triplicate, for N=2.

Assay	IC_{50} (µM) [Mean ± SD]		t-test (P values)
	BZ1 (Original solution stock)	BZ1 (New stock from solid)	
Promastigote viability assay	2.37 ± 0.85	2.15 ± 0.35	0.71
Intracellular amastigote assay	0.59 ± 0.13	0.79 ± 0.03	0.75

4.3.1.4. Structure activity relationships and identification of potential analogues for "N-(4-Ethoxyphenyl)-2,3-dihydro-1H-cyclopenta[b]quinolin-9-amine".

The hit compounds were compared structurally to the complete compound collection of >33,000 pure compounds using the Compounds Australia® structural portal (CASPER™) to ascertain the available analogues. A series of substructure searches, performed in Scifinder® (CAS, American Chemical Society), ChemSpider® (Royal Society of Chemistry) and ChEMBL® (European Bioinformatics Institute) were defined and refined to retrieve analogues most relevant to SAR interpretation. In collaboration with Dr. Brad Sleebs (The Walter and Eliza Hall Institute of Medical Research,

Melbourne, Australia) potential analogues were identified. Compounds were selected which displayed no structural alerts (metabolism/stability/ reactivity) associated with them. The selected compounds were chosen based on the following criteria: no more than 5 H-bond donors (total number of N–H and O–H bonds), not more than 10 H bond acceptors (all N or O atoms), a molecular mass < 500 and octanol-water partition coefficient (log P) < 5. Thirty compounds were selected (referred to as **BZ1-A - BZ1-d**), the structures of which have been shown in Figure 4.12. The activity of the analogues was assessed in both the promastigote viability and intracellular amastigote assays (Table 4.4).

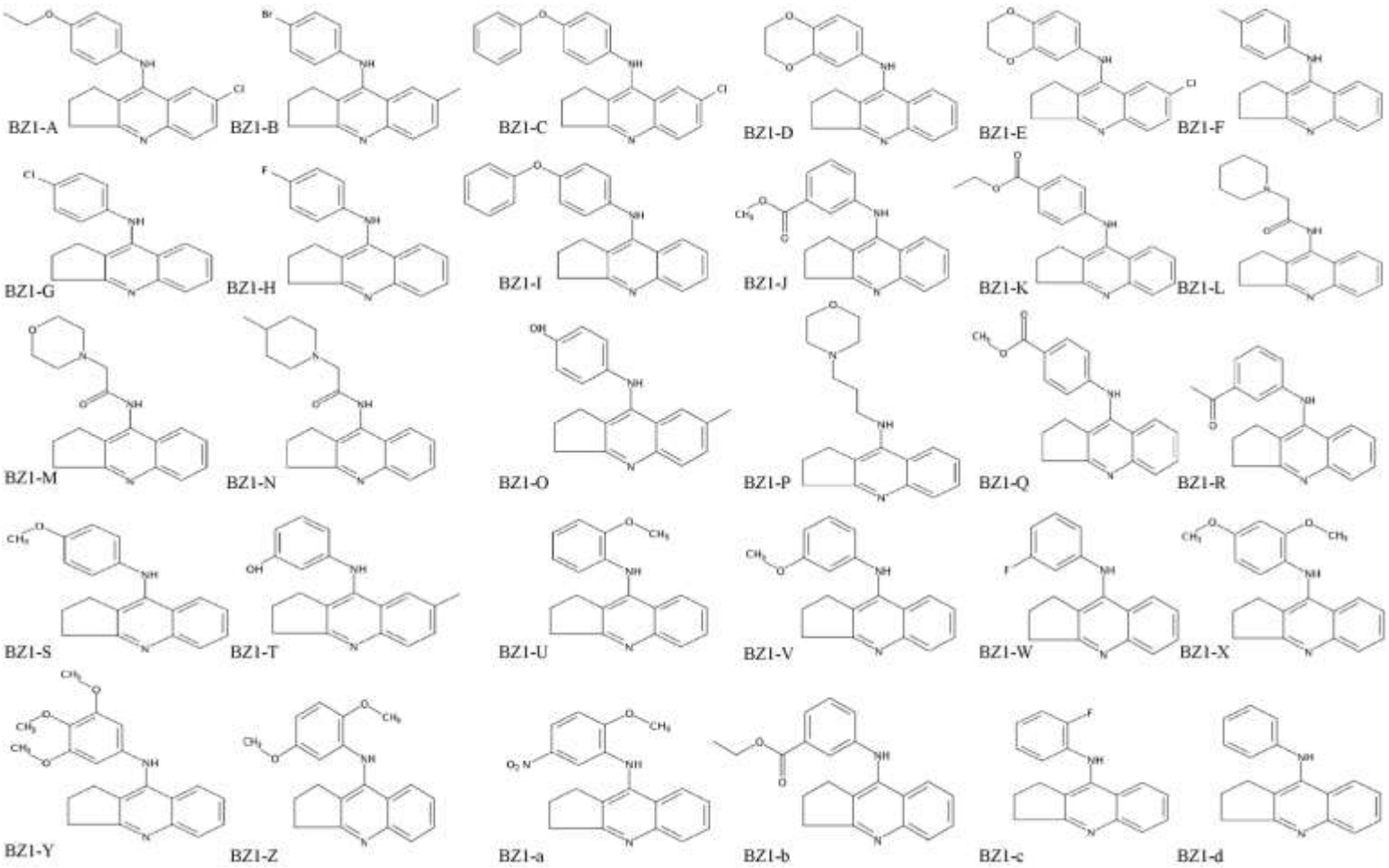

Figure 4.12: Potential analogues (BZ1-A – BZ1-d) for the compound "N-(4-Ethoxyphenyl)-2,3-dihydro-1H-cyclopenta[b]quinolin-9-amine" (BZ1).

Table 4.4: *In vitro* anti-leishmanial activities of analogues.

Compounds	Molecular Weight	LogP	HBA	HBD	PSA	Rot Bonds	Promastigote viability assay	Intracellular amastigote assay
BZ1	304	4.7	3	1	35	4	2.15 ± 0.14 (9.27)[a] (9.17)[b]	0.592 ± 0.04 (33.78)[a] (33.55)[b]
BZ1-A	338	4.6	3	1	34	4	4.84 ± 0.31 (4.13)[a] (1.64)[b]	3.98 ± 0.24 (5.02)[a] (2.01)[b]
BZ1-B	353	4.3	2	1	25	2	1.37 ± 0.07 (14.59)[a] (11.64)[b]	4.64 ± 0.17 (4.31) [a] (3.44)[b]
BZ1-C	386	5.5	3	1	34	4	10.18 ± 0.33 (1.96)[a] (0.98)[b]	6.82 ± 1.11 (2.93)[a] (1.46)[b]
BZ1-D	318	4.4	4	1	43	2	1.82 ± 0.17 (10.69)[a] (5.49)[b]	4.78 ± 0.74 (4.18)[a] (2.09)[b]
BZ1-E	352	5.1	4	1	43	2	0.70 ± 0.03 (28.57)[a] (14.28)[b]	9.47 ± 1.14 (2.11)[a] (1.05)[b]
BZ1-F	274	4.4	2	1	25	2	5.49 ± 1.21 (3.64)[a] (3.60)[b]	4.58 ± 0.98 (4.36)[a] (4.32)[b]
BZ1-G	294	5.1	2	1	25	2	6.56 ± 0.37 (3.04)[a] (1.52)[b]	11.48 ± 1.34 (1.74)[a] (0.87)[b]
BZ1-H	278	4.6	2	1	25	2	6.58 ± 1.01 (3.03)[a] (2.43)[b]	4.50 ± 0.64 (1.74)[a] (0.87)[b]
BZ1-I	352	5.2	2	1	35	4	0.60 ± 0.04 (33.11)[a] (16.55)[b]	0.57 ± 0.52 (34.84)[a] (17.42)[b]
BZ1-J	318	4.3	4	1	51	4	4.71 ± 0.24 (4.24)[a] (4.20)[b]	7.54 ± 0.19 (2.65)[a] (2.62)[b]
BZ1-K	332	4.7	4	1	51	5	6.87 ± 0.33 (2.91)[a] (2.88)[b]	9.57 ± 0.79 (2.08)[a] (2.06)[b]
BZ1-L	309	3.2	4	1	45	4	63% inhibition at 16.7 µM	Inactive at 20 µM
BZ1-M	311	2	5	1	54	4	Inactive at 16.7 µM	Inactive at 20 µM
BZ1-N	323	3.4	4	1	45	4	71% inhibition at 16.7 µM	Inactive at 20 µM
BZ1-O	290	4.6	3	2	45	2	3.41 ± 0.08 (5.86)[a] (5.80)[b]	6.87 ± 0.10 (2.91)[a] (2.88)[b]
BZ1-P	311	2.9	4	1	37	5	Inactive at 16.7 µM	Inactive at 20 µM
BZ1-Q	318	4.3	4	1	51	4	5.41 ± 0.35	9.87 ± 0.45

							(3.69)[a] (3.65)[b]	(2.02)[a] (2.00)[b]
BZ1-R	302	4.7	3	1	42	3	3.52 ± 0.68 (5.68)[a] (5.62)[b]	8.54 ± 0.47 (2.34)[a] (2.31)[b]
BZ1-S	290	4.5	3	1	34	3	3.34 ± 1.10 (>5.98)[a] (>2.99)[b]	4.87 ± 0.52 (>4.10)[a] (>2.05)[b]
BZ1-T	290	4.6	3	2	45	2	70% inhibition at 16.7 µM	Inactive at 20 µM
BZ1-U	290	4.5	3	1	34	3	4.12 ± 0.29 (>2.42)[a] (>2.37)[b]	Inactive at 20 µM
BZ1-V	290	4.5	3	1	34	3	4.12 ± 0.64 (>4.85)[a] (>4.80)[b]	7.41 ± 0.37 (>2.70)[a] (>2.67)[b]
BZ1-W	278	4.7	2	1	24	2	7.41± 0.71 (1.34)[a] (1.32)[b]	5.46 ± 0.67 (1.83)[a] (1.79)[b]
BZ1-X	320	4.6	4	1	43	4	3.15 ± 0.37 (>6.34)[a] (>6.28)[b]	Inactive at 20 µM
BZ1-Y	350	4.6	5	1	52	5	2.14 ± 0.21 (>9.34)[a] (>9.25)[b]	8.41 ± 0.26 (>2.37)[a] (>2.35)[b]
BZ1-Z	320	4.6	4	1	43	4	4.37 ± 0.44 (>4.57)[a] (>4.53)[b]	Inactive at 20 µM
BZ1-a	335	5	6	1	80	4	8.71 ± 1.81 (1.14)[a] (1.12)[b]	Inactive at 20 µM
BZ1-b	332	4.7	4	1	51	5	3.87 ± 0.05 (5.16)[a] (5.11)[b]	8.77 ± 0.94 (2.28)[a] (2.25)[b]
BZ1-c	278	4.7	2	1	24	2	7.51 ± 0.24 (2.66)[a] (2.63)[b]	80% inhibition at 20 µM
BZ1-d	260	4.5	2	1	24	2	4.16 ± 0.97 (>4.80)[a] (>4.75)[b]	6.54 ± 0.35 (>3.05)[a] (>3.02)[b]

All results from two independent experiments (N=2).

↲a Selectivity index (SI) compared to THP-1 cells.

↲b Selectivity index (SI) compared to HEK-293 cells

4.3.1.5. Selection from analogues

Out of the 30 analogues tested for *L. donovani* promastigote and amastigote activity, one compound, **BZ1-I,** displayed better activity than the original hit compound, **BZ1**, resulting in an IC_{50} value of 0.51 ± 0.27 µM against the intracellular form of the parasite (amastigotes) and an IC_{50} value of 0.62 ± 0.24 µM against the extracellular form (promastigotes) (Figure 4.13).

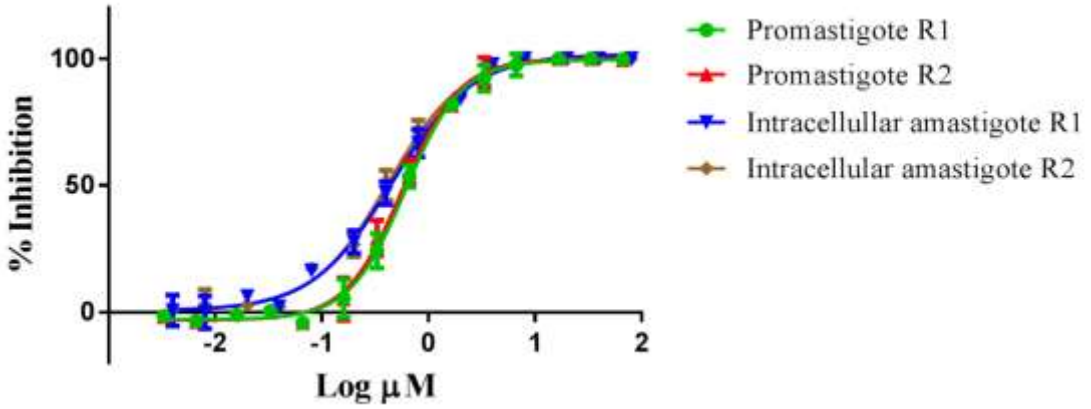

Figure 4.13: Concentration response curve for compound BZ1-I for intracellular amastigote and promastigote viability assays. Each evaluation was performed in triplicate, for N=2.

New solids stocks were purchased for **BZ1-I** and re-evaluated in both assays. No statistical difference was observed between the activities of the original DMSO stocks and the newly prepared stocks from the solid stocks of compound **BZ1-1** (Table 4.5).

Table 4.5: Comparison of the 50% inhibitory concentrations for new and old batches of BZ1. Each evaluation was performed in triplicate, for N=2.

Assay	IC_{50} (µM) [Mean ± SD]		t-test (P values)
	BZ1-1 (Original solution stock)	BZ1-1 (New stock from solid)	
Promastigote viability assay	0.62 ± 0.24	0.58 ± 0.71	0.73
Intracellular amastigote assay	0.51 ± 0.27	0.58 ± 0.85	0.79

Based on the *in vitro* activity (Figure 4.14) against the *L. donovani DD8* promastigotes and intracellular amastigotes, in addition to the selectivity for the parasite in relation to the host cell, a decision was taken to pursue compound **BZ1** and **BZ1-I** for further profiling and to determine their mode of action through mechanism of action studies.

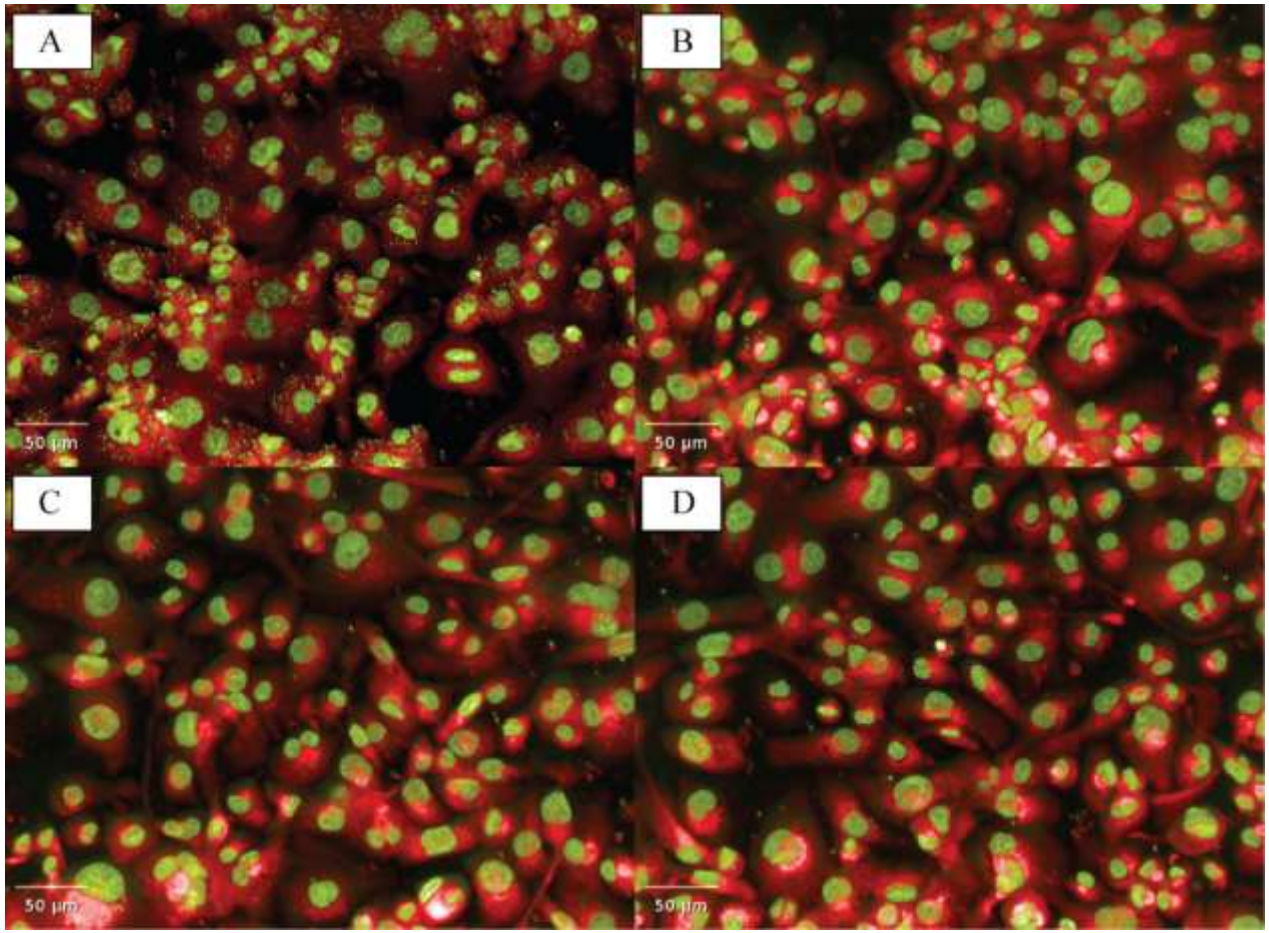

Figure 4.14: THP-1 cells, 2.5x105 cells/mL infected with *L. donovani* DD8 metacyclic promastigotes, imaged on the Opera™ using the 20X objective magnification following staining with SYBR® Green and CellMask™ Deep Red. (A) Amastigotes were observed within the host cells with 0.4% DMSO (vehicle), (B) Treatment with 1 µM amphotericin B, no intracellular amastigotes can be observed within the host cells (C) Treatment with 2 µM compound BZ1, no intracellular amastigotes can be observed within the host cell, (D) Treatment with 2 µM compound BZ1-I, no intracellular amastigotes can be observed within the host cell.

4.3.2. Davis Open Access Natural Product-based library

4.3.2.1. Primary screening

4.3.2.1.1. Promastigote viability assay

Twenty-nine compounds from the 472 compounds belonging to the Davis Open Access Natural Product (DOANP) library tested against the promastigote stage of *L. donovani* exhibited >70% activity at 16.7 µM, with a hit rate of 6.14%. The cut off criteria for active hit compounds was defined as inhibition ≥70 % at 16.7 µM. The selection criteria for the cut-off value was determined as three standard deviations of the mean.

Figure 4.15 shows the scatter plot generated from the primary screening of 472 compounds using the promastigote viability assay. The active hits are represented by the blue dots above the cut off line (black line) which is 70% inhibition (Figure 4.15). Normal distribution was plotted for all the compounds based on percentage activity (Figure 4.16).

The Z' of the primary screen for the promastigote viability assay was 0.886 ± 0.028 (Figure 4.17), calculated from the positive/negative controls used in each batch of 2 plates. The % coefficient of variance (% CV) for the positive (1 µM amphotericin) and negative (0.4% DMSO) controls were 3.28 ± 0.90 and 3.02 ± 0.59, respectively. The dynamic range of assay signal (signal window) was 14.26 ± 2.35-fold.

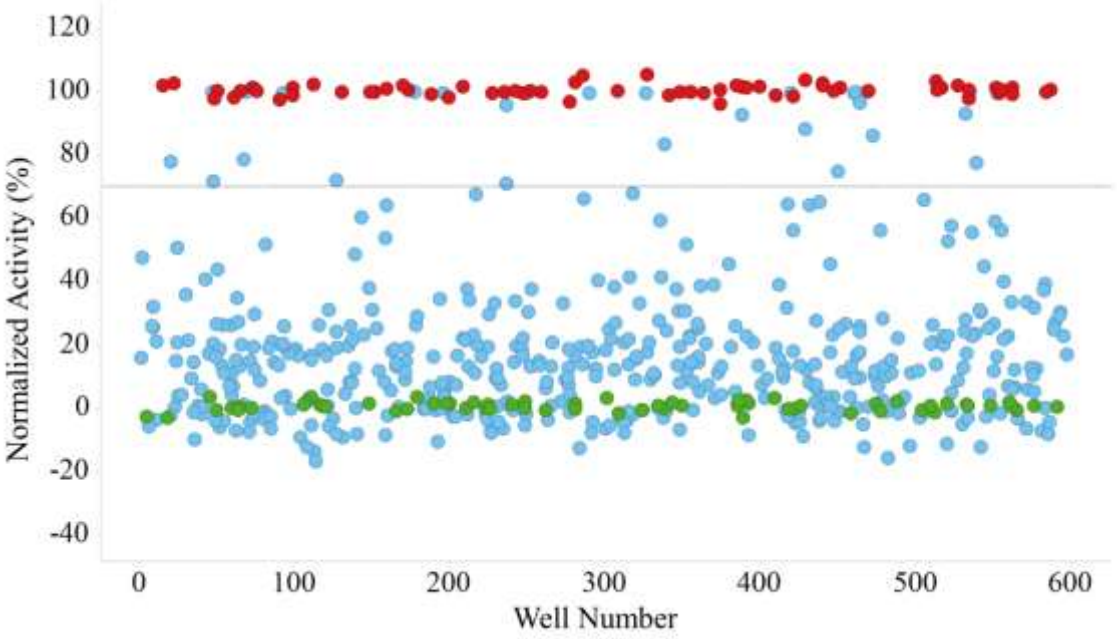

Figure 4.15: Scatter plot of the primary screening data obtained for the DOANP library 472 compounds determined using the L. donovani DD8 promastigote viability assay. Each evaluation was performed in triplicate, for N=2 independent experiments. Red dots represent 100% inhibition with the positive control, 1 µM amphotericin B, green dots represent 0% inhibition with negative control 0.4% DMSO and blue dots represent compound samples.

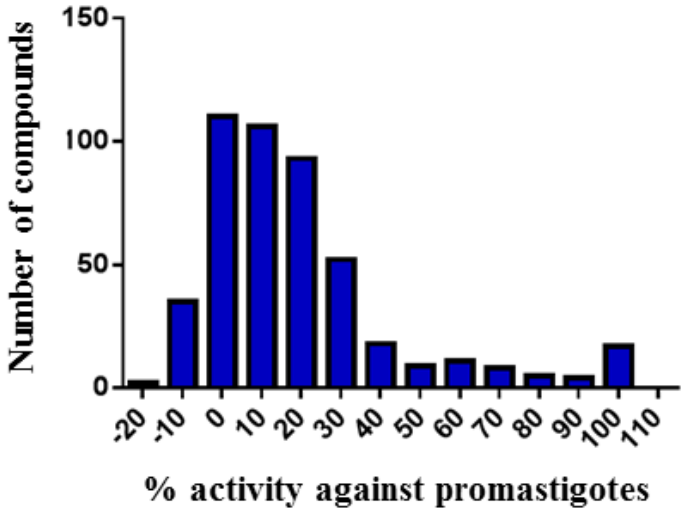

Figure 4.16: Normal distribution for primary data obtained for 472 compounds using the *L. donovani* DD8 promastigote viability assay. Each evaluation was performed in triplicate, for N=2.

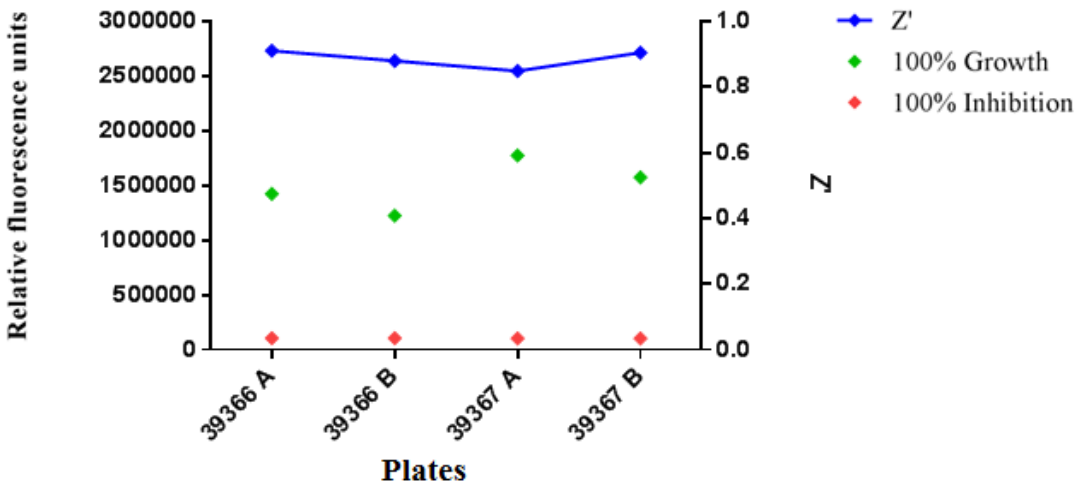

Figure 4.17: Reproducibility of the primary screening of the 472 compounds using promastigote viability assay. Red dots represent 100% inhibition with positive control 1 µM amphotericin B (100% inhibition), green dots represent 0% inhibition with negative control 0.4% DMSO and blue dots represent Z' values for each plate. Each evaluation was performed in triplicate, for N=2.

4.3.2.1.2. Intracellular amastigote assay

Of the 472 compounds in the diverse natural product derived compound library tested using the intracellular amastigote assay, 12 compounds exhibited >70% activity at 20 µM. The cut off for active hit compounds was defined as inhibition ≥70 % at 20 µM, determined as three standard deviations of the mean. Out of these 12 compounds, 7 were found to be cytotoxic to the THP-1 cells, exhibiting activity against the host cells from 20 µM. Thus, selectivity indices > 1 were unobtainable.

The primary screening data was analyzed to ascertain the overall reproducibility and quality of the assay performance. A scatter plot of the data for the primary screening of the 472 compounds undertaken with the intracellular amastigote assay is shown in Figure 4.18. The active hits are represented by the blue dots above the activity cut off line (black line) which is 70% as represented in figure 4.18. Normal distribution of data obtained for primary screening of 472 compounds using the *L. donovani* DD8 intracellular amastigote assay was plotted for all the compounds based on percentage activity (Figure 4.19).

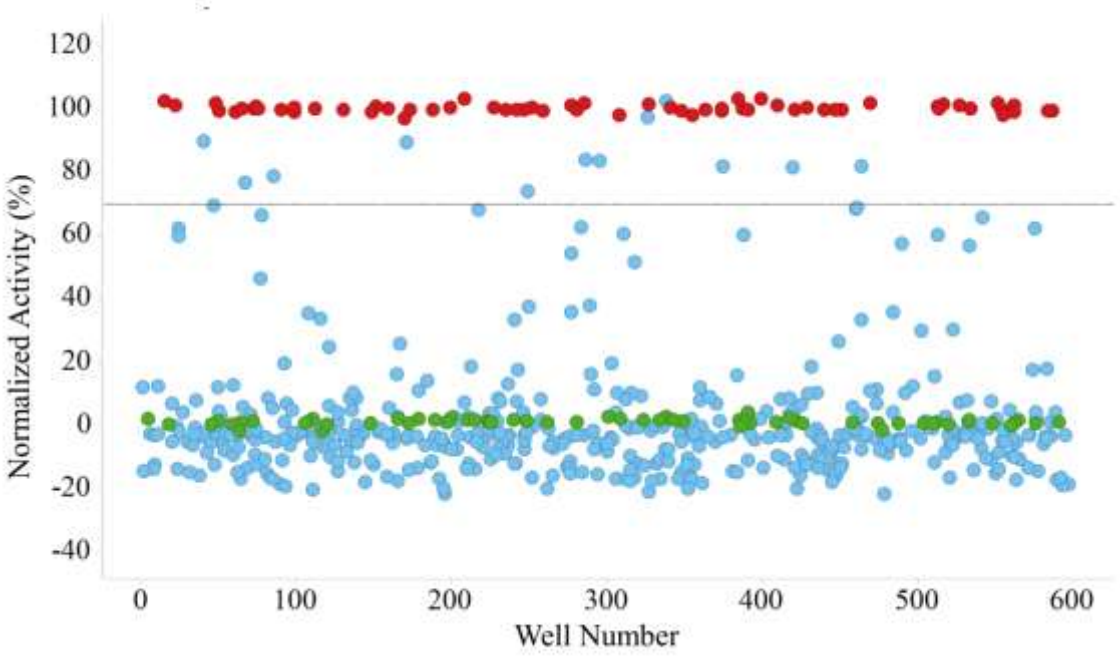

Figure 4.18: Scatter plot of the primary screening data obtained for 472 compounds using the *L. donovani* DD8 intracellular amastigote assay. Each evaluation was performed in triplicate, for N=2 independent experiments. Red dots represent 100% inhibition with the positive control, 1 µM amphotericin B, green dots represent 0% inhibition with negative control 0.4% DMSO and blue dots represent compound samples.

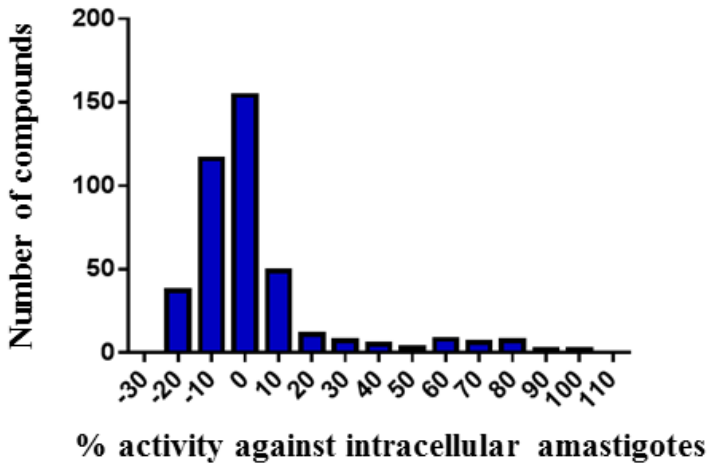

Figure 4.19: Normal distribution of data obtained for primary screening of 472 compounds using the *L. donovani* DD8 intracellular amastigote assay. Each evaluation was performed in triplicate, for N=2.

The Z' of the primary screen for the intracellular amastigote assay was 0.713 ± 0.0326 (Figure 4.20), calculated from the positive and negative controls used in each batch of 2 compound plates. The dynamic range of the assay signal (signal window) was 26.298 ± 13.007-fold.

A cross comparison was conducted to identify common hits between both the promastigote and intracellular amastigote assays for *L. donovani* DD8 parasite (Figure 4.21). It was observed that 5 compounds demonstrated > 70% inhibition at the screening concentrations, specifically 16.7 µM for the promastigote viability assay and 20 µM for the intracellular amastigote image-based assay (Figure 4.22).

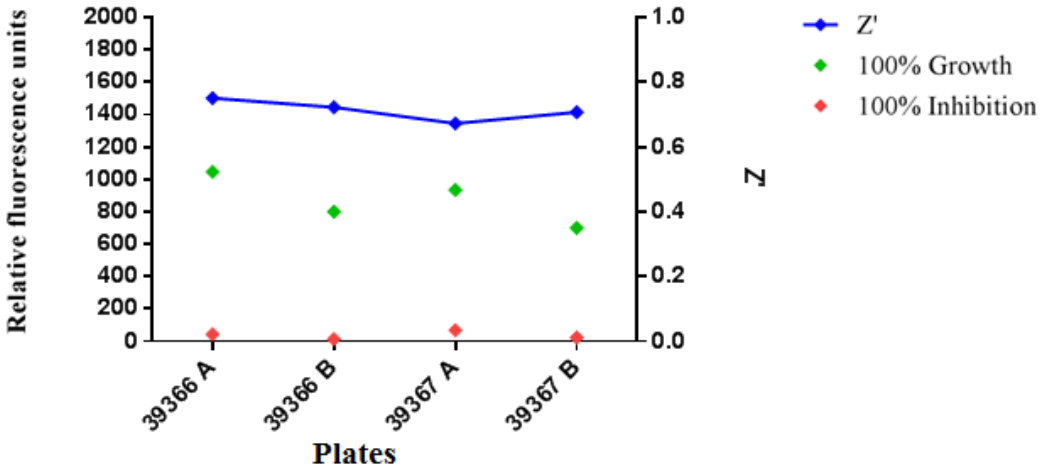

Figure 4.20: Reproducibility of the primary screening of the 472 compounds using the intracellular amastigote assay. Red dots represent 100% inhibition with positive control 1 µM amphotericin B (100% inhibition), green dots represent 0% inhibition with negative control 0.4% DMSO and blue dots represent Z' values for each plate. Each evaluation was performed in triplicate, for N=2.

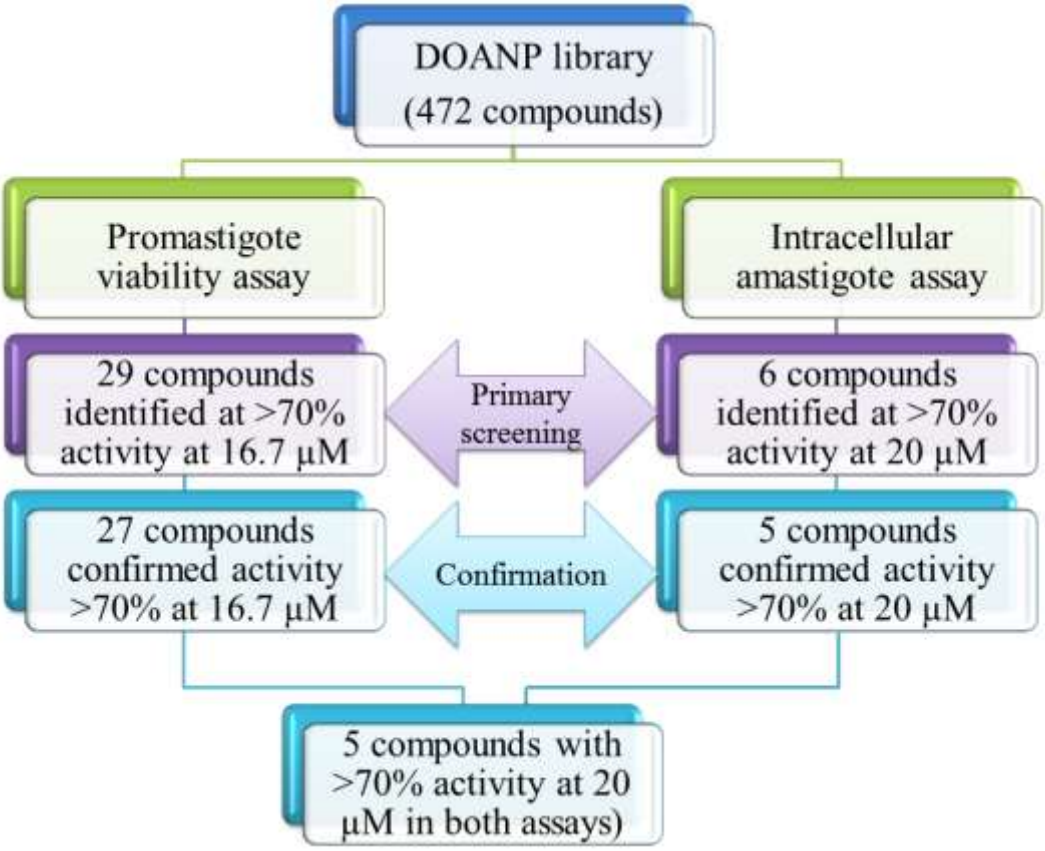

Figure 4.21: Schematics for DOANP library primary screening and confirmation of actives identified against *L. donovani* DD8 promastigotes and intracellular amastigotes.

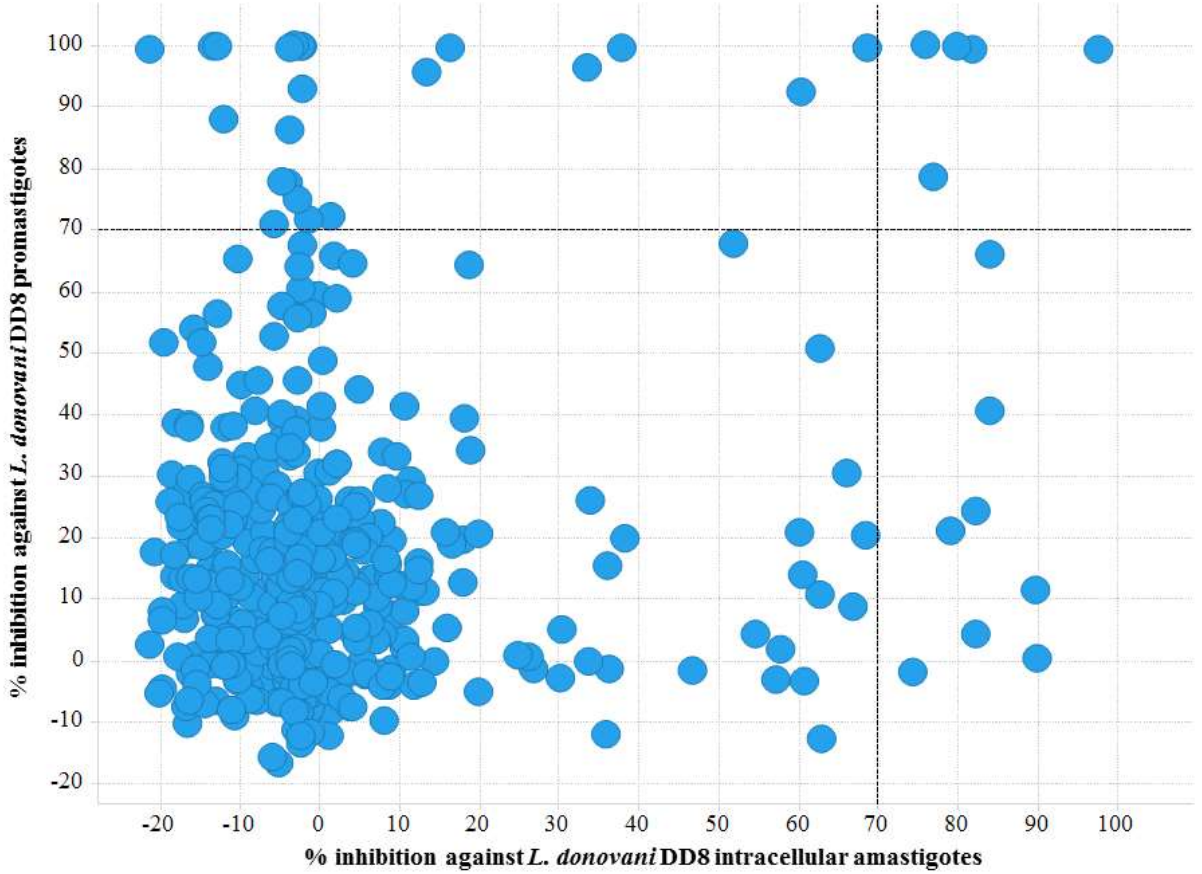

Figure 4.22: Scatter plot of active hits from primary screening against the 472 compounds against *L. donovani* DD8 promastigotes and *L. donovani* DD8 intracellular amastigotes. Right top quadrant exhibiting compounds found to be > 70% active on both *L. donovani* DD8 promastigotes and *L. donovani* DD8 intracellular amastigotes. Each evaluation was performed in triplicate, for N=2 independent experiments.

4.3.2.1.3. *T. b. brucei* screening

A *T. b. brucei* resazurin based viability assay (Sykes and Avery, 2009) was used to screen the Davis open access natural product-based library. Twenty-eight compounds were identified with an activity cut-off of >50% at the screening concentration of 5 µM. This outcome indicated a hit rate of 5.93% (Figure 4.23).

4.3.2.1.4. *T. cruzi* intracellular amastigote screening

The DOANP library was screened using a *T. cruzi* intracellular amastigote image-based assay (Sykes and Avery, 2015). Fifteen compounds were selected that met the proposed cut off criteria of ≥50% activity at a concentration of 10 µM. This translated to a hit rate of 3.17% (Figure 4.23).

4.3.2.2. Retest

To readily differentiate the retested compounds from the DOANP library they have been referred to as **NP** compounds, rather than their individual chemical names, and the structures of these compounds illustrated in Figure 4.24.

4.3.2.2.1. Promastigote viability assay

From the 29 compounds that were identified as >70% active at 16.7 µM from primary screening of samples in the promastigote viability assay, a total of 27 compounds returned activity at >70% at 16.7 µM when retested in multiple concentrations. Retesting of the compounds from primary screening resulted in a 93.1 % reconfirmation rate. Compound (**NP1**) (Figure 4.24) exhibited sub-micromolar activity against the *L. donovani* promastigotes with an IC_{50} value of 0.73 ± 0.16 µM (Table 4.6).

4.3.2.2.2. Intracellular amastigote assay

From the 5 compounds that were identified from primary screening of the DOANP library using >70% activity against the intracellular amastigotes at 20 µM as the cut for hit molecules, all compounds returned activity at >70% at 20 µM when retested in multiple concentrations, thus a 100 % reconfirmation rate. Compound (**NP1**) (Figure 4.24) was the most active with an IC_{50} value of 4.410 ± 0.247 µM (Table 4.6).

Table 4.6: *In vitro* anti-kinetoplastid activities of compounds identified through screening of DAONP library against *L. donovani* DD8 Promastigotes and intracellular amastigotes, *T. b. brucei* strain 427 and *T. cruzi* Tulahuen strain parasites.

Compounds	Antileishmanial activity		Antitrypanosomal activity		Comments
	L. donovani DD8 Promastigotes	*L. donovani* DD8 Intracellular amastigotes	*T. b. brucei* strain 427	*T. cruzi* Tulahuen strain	
	IC_{50} (mean ± SD) (µM)	IC_{50} (mean ± SD) (µM)	IC_{50} (mean ± SD) (µM)	IC_{50} (mean ± SD) (µM)	
Lissoclinotoxin E (NP1)	0.725 ± 0.162 (>11.72)[a] (6.88)[b]	4.410 ± 0.247 (>2.26)[a] (1.132)[b]	0.571 ± 0.201 (>17.68)[a]	3.922 ± 0.381 (>2.52)[a](>4.67)[c]	Active on all three parasites with 5< IC_{50}. Exhibits high selectivity for *T. b. brucei* in relation to HEK-293 cells.
Spermatinamine (NP12)	11.870 ± 0.565 (0.332)[a] (0.419)[b]	6.150 ± 0.056 (0.642)[a] (0.808)[b]	1.003 ± 0.261 (5.89)[a]	Not active	Active on *L. donovani* DD8 and *T. b. brucei*. Moderate selectivity for *T. b. brucei* in relation to HEK-293 cells.
Thiaplakortone A (NP3)	Not active	Not active	3.940 ± 0.780 (0.70)[a]	4.2625 ± 0.6515 (0.535)[a] (1.06)[c]	Active on *T. b. brucei* and *T. cruzi* with no selectivity.
Gambogic acid (NP4)	100% inhibition at 16.7 µM	Not active	0.274 ± 0.043 (7.11)[a]	1.873 ± 0.070 (1.501)[a] (1.005)[c]	Active on *T .b. brucei* and T. cruzi. Moderately selective for *T. b. brucei* in relation to HEK 293 cells.
Mycophenolic acid (NP5)	Not active	Not active	0.510 ± 0.102 (1.01)[a]	1.591 ± 0.039 (0.372)[a] (0.132)[c]	Active on *T. b. brucei* and *T. cruzi* with no selectivity.
Narciclasine (NP6)	100% inhibition at 16.7 µM	Not active	0.031 ± 0.010 (1.09)[a]	0.207 ± 0.019 (0.214)[a] (3.28)[c]	Active on *T. b. brucei* and *T. cruzi*. Low selectivity for *T. cruzi* in 3T3 cells.
Thiaplakortone analogue (NP7)	Not active	Not active	0.680 ± 0.017 (4.19)[a]	3.551 ± 0.384 (1.466)[a] (1.335)[c]	Active on *T. b. brucei* and *T. cruzi*. Moderately selective for *T. b. brucei* in relation to HEK-293 cells.
Mefloquine HCl (NP8)	100% inhibition at 16.7 µM	Not active	0.622 ± 0.063 (7.97)[a]	3.962 ± 0.589 (>5.06)[a] (>1.705)[c]	Moderate selectivity for *T. cruzi* and *T. b. brucei* in relation to HEK 293 cells.
3,4-dihydro-2H-naphtho[2,3-b][1,4]thiazine-5,10-dione 1,1-dioxide (NP9)	100% inhibition at 16.7 µM	Not active	Not active	3.819 ± 0.606 (1.11)[a] (1.244)[c]	Only active on *T. cruzi* with no selectivity.
Emetine dihydrochloride	100% inhibition at 16.7 µM	Not active	0.050 ± 0.011 (1.61)[a]	0.097 ± 0.001 (0.927)[a] (6.04)[c]	Active on *T. b. brucei* and *T. cruzi* with selectivity for *T. cruzi* in 3T3 cells.

(NP10)					
Lissoclinotoxin F (NP11)	5.515 ± 0.304 (>3.62)[a] (>1.814)[b]	8.311 ± 0.678 (>2.40)[a] (>1.203)[b]	Not active	Not active	Active on both forms of *L. donovani* DD8 parasite. Low selectivity both forms of *L. donovani* DD8 parasite.
ethyl 4-((diethylamino)methyl)-5-hydroxy-1-(4-methoxyphenyl)-2-methyl-1H-indole-3-carboxylate (NP12)	100% inhibition at 16.7 µM	11.090 ± 0.311 (>2.97)[a] (>1.502)[b]	Not active	Not active	Low selectivity for *L. donovani* DD8 intracellular amastigotes.
Chalcone analogue (NP13)	100% inhibition at 16.7 µM	5.65 ± 0.261 (11.87)[a] (3.59)[b]	Not active	Not active	Active on *L. donovani* DD8 intracellular amastigotes. Highly selective for *L. donovani* DD8 intracellular amastigotes in relation to HEK 293 cells.
Psammaplysin F (NP14)	Not active	Not active	Not active	5.637 ± 0.764 (>3.51)[a] (>1.904)[c]	Moderate Selectivity for *T. cruzi* in relation toagainst HEK-293 cells,
Chelerythrine chloride (NP15)	Not active	Not active	0.23 ± 0.04 (>18.71)[a]	Not active	Only selective on *T. b. brucei*. Highly selective for *T. b. brucei* in relation to HEK-293 cells.

All results from two independent experiments (N=2).

↲a Selectivity index (SI) compared to HEK-293 cells.

↲b Selectivity index (SI) compared to THP-1 cells.

↲c Selectivity index (SI) compared to 3T3 cells

4.3.2.2.3. *T. b. brucei* screening

Whilst all of the compounds identified as actives in the primary screening for *T. b. brucei* strain 427 subsequently confirmed activity during retest at the primary screening concentration (5 μM), accurate IC_{50} values could only be acquired for 21 out of the 28 compounds. These compounds exhibited IC_{50} values between 0.05 and 4.84 μM against *T. b. brucei*, with two compounds showing good selectivity (~18 fold) against HEK-293 cells (Table 4.6).

4.3.2.2.4. *T. cruzi* intracellular amastigote screening

Screening against the kinetoplastid, *T. cruzi* Tulahuen strain, resulted in 15 compounds with anti-parasitic activity ≥50% activity at a concentration of 10 μM, being identified. Thirteen of these compounds returned activity at the original screening concentration, giving a confirmation rate of 86.6% (Table 4.6). In addition to determining the IC_{50} values against *T. cruzi* and the 3T3 host cells, compounds were also tested in a HEK-293 assay to determine the activity against a dividing human cell line as 3T3 cells are contact inhibited during the course of the amastigote assay.

4.3.2.2.5. Common activity against kinetoplastids

The activity of compounds against multiple kinetoplastid parasites is described in table 4.6. Compounds lissoclinotoxin E (**NP1**) and spermatinamine (**NP2**) demonstrated activity against both *L. donovani* DD8 forms and *T. b. brucei* strain 427. Seventeen compounds active against *L. donovani* DD8 promastigotes were also shown to be active against *T. b. brucei* strain 427. Eight compounds were shown to have activity against both *T. b. brucei* strain 427 and *T. cruzi* Tulahuen strain (Figure 4.23A). Compound (**NP1**) was the only compound active for all three parasites with IC_{50} value of <5 μM, however only showed moderate selectivity for *T. b. brucei* strain 427 (Figure 4.23B).

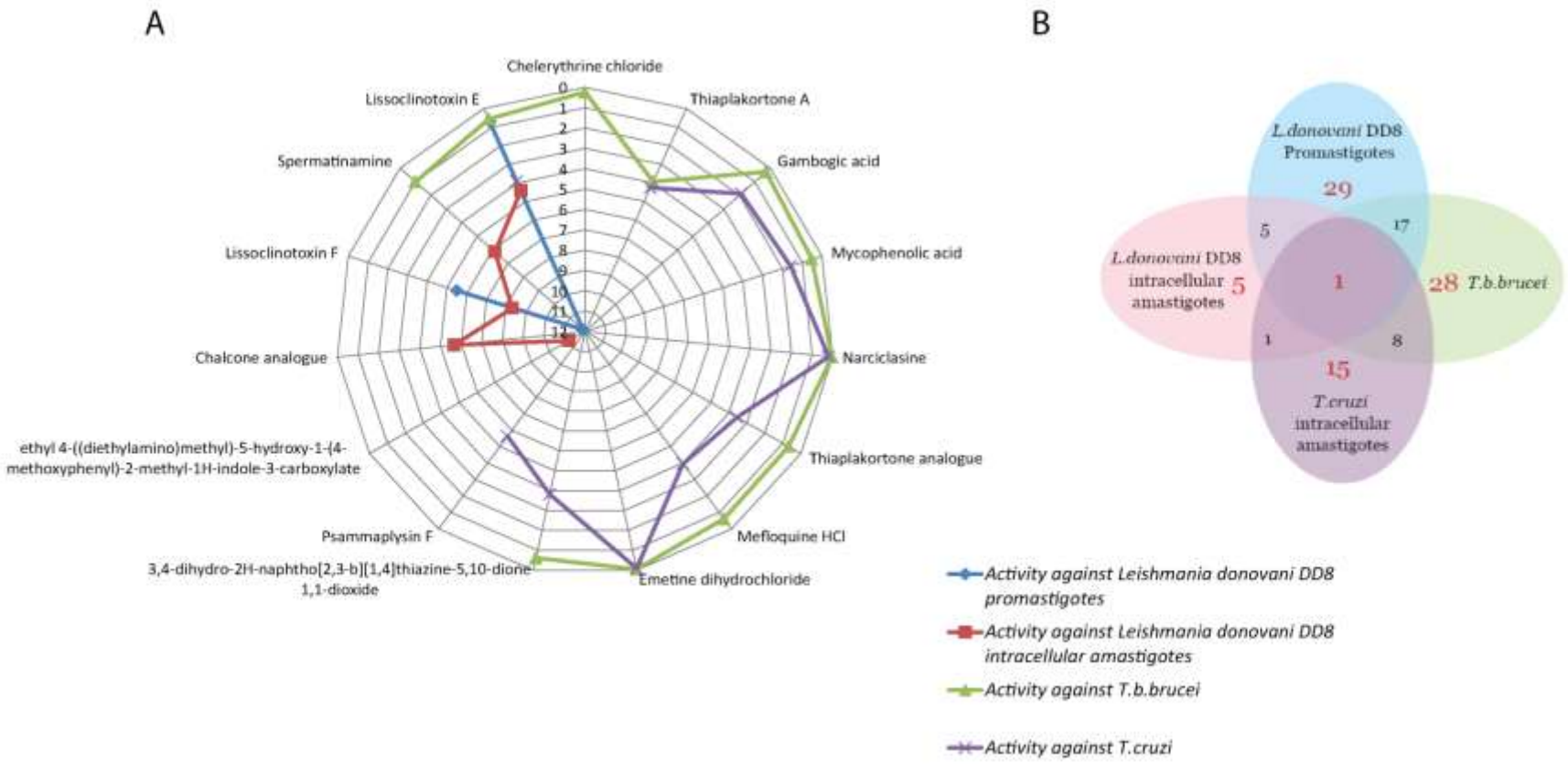

Figure 4.23: (A) Spider plot exhibiting the IC_{50} values of compounds for *L. donovani* DD8 promastigotes, *L. donovani* DD8 intracellular amastigotes, *T. b. brucei* strain 427 and *T. cruzi* Tulahuen strain. (B) Venn diagram for overlapping active hits identified against *L. donovani* DD8 promastigotes, *L. donovani* DD8 intracellular amastigotes, *T. b. brucei* strain 427 and *T. cruzi* Tulahuen strain.

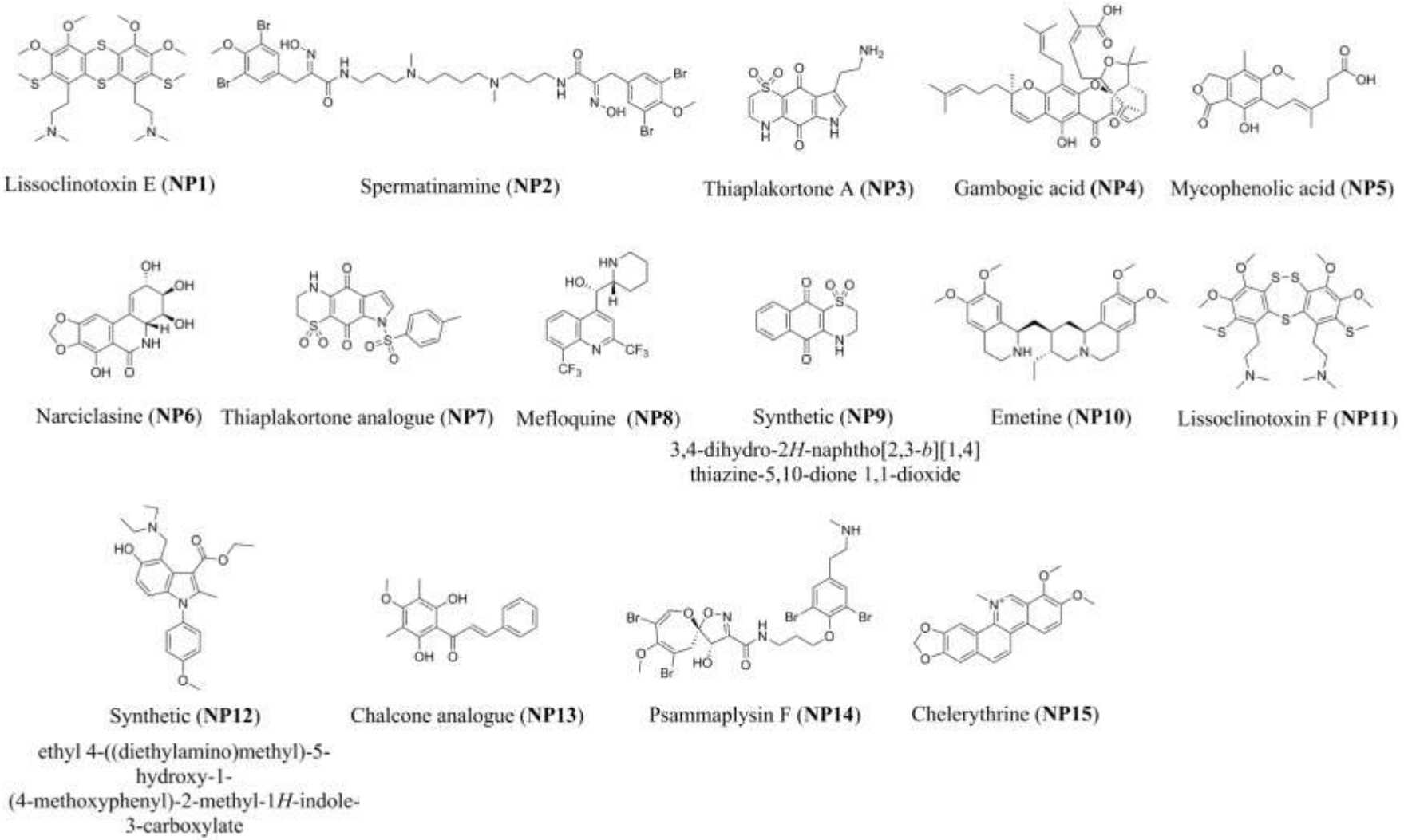

Figure 4.24: Structures of NP compounds 1-15.

4.3.2.3. Reference drugs/compounds:

Reference drugs and compounds, most of which are currently used in clinical settings for the different kinetoplastid diseases, were used to validate the screening process. The mechanism of action of these drugs/compounds, where known, has been described in Table 4.7. The IC_{50} values and SI of the reference drugs/compounds was calculated as described in Table 4.7. The reference drugs/compounds used for *L. donovani* DD8 promastigote viability and intracellular amastigote assay were amphotericin B, miltefosine, compound VL-2098 and compound DND*i* 1044 (Figure 4.25 and Figure 4.26). The reference drugs used for the *T. b. brucei* resazurin assay were pentamidine, diminazene and puromycin. The reference drugs used for *T. cruzi* intracellular amastigote assay were benznidazole and nifurtimox.

Table 4.7: IC_{50} values and mechanism of action of reference drugs and compounds against *L. donovani* DD8, *T. b. brucei* and *T. cruzi*.

Compound	*L. donovani* DD8 promastigotes	*L. donovani* DD8 intracellular amastigotes	*T. b. brucei* strain 427	*T. cruzi* Tulahuen strain	Mechanism of action
	IC_{50} (mean ± SD) (µM) (S.I HEK-293)b S.I THP-1)	IC_{50} (mean ± SD) (µM) S.I HEK-293) S.I THP-1)	IC_{50} (mean ± SD) (µM) S.I HEK-293)	IC_{50} (mean ± SD) (µM) S.I HEK-293)	
Amphotericin B	0.122 ± 0.010 (68.27)[a] (16.39)[b]	0.208 ± 0.023 (41.65)[a] (9.61)[b]	Not tested	Not tested	Binds to ergosterol, the principal sterol in fungal cell membranes and *Leishmania* cells (Roberts, *et al.*, 2003).
Miltefosine	3.481 ± 0.267 (9.57)[a] (5.74)[b]	2.543 ± 0.570 (13.12)[a] (7.27)[b]	Not tested	Not tested	Interacts with lipids (phospholipids and sterols), including membrane lipids, inhibition of cytochrome C oxidase (mitochondrial function), and apoptosis (Luque-Ortega and Rivas, 2007; Freitas-Junior, *et al.*, 2012).
DNDi VL-2098	0.117 ± 0.003 (>341.88)[a] (>341.88)[b]	0.771 ± 0.092 (>51.88)[a] (>51.88)[b]	Not tested	Not tested	
DNDi 1044	0.707 ± 0.021 (14.14)[a](>56.57)[b]	0.430 ± 0.089 (23.25)[a](>92.59)[b]	Not tested	Not tested	
Pentamidine	Not tested	Not tested	0.002 ± 0.001 (>334.5)[a]	Not tested	Accumulates in trypanosomes; disrupts mitochondrial processes (Barrett, *et al.*, 2007).
Diminazene	Not tested	Not tested	0.040 ± 0.012 (>962.75)[a]	Not tested	Interferes with RNA editing and trans-splicing (Barrett, *et al.*, 2007).
Puromycin	Not tested	Not tested	0.038 ± 0.006 (12.96)[a]	1.650 ± 0.350 (0.150) [a]	Protein synthesis inhibitor via premature chain termination during translation in the ribosome (Barrett, *et al.*, 2007).
Benznidazole	Not tested	Not tested	Not tested	3.360 ± 1.524 (>44.84)[a]	Causes oxidation in the nucleotide pool which in turn causes the formation of breaks in double stranded DNA (Rajao, *et al.*, 2014).
Nifurtimox	Not tested	Not tested	Not tested	0.623 ± 0.103 (> 243.03)[a]	Unknown. Possibly appears to be due to oxidative stress – potentially from the formation of hydrogen peroxide (Boiani, *et al.*, 2010).

All results from two independent experiments (N=2). ↵a Selectivity index (SI) compared to HEK-293 cells. ↵b Selectivity index (SI) compared to THP-1 cells.

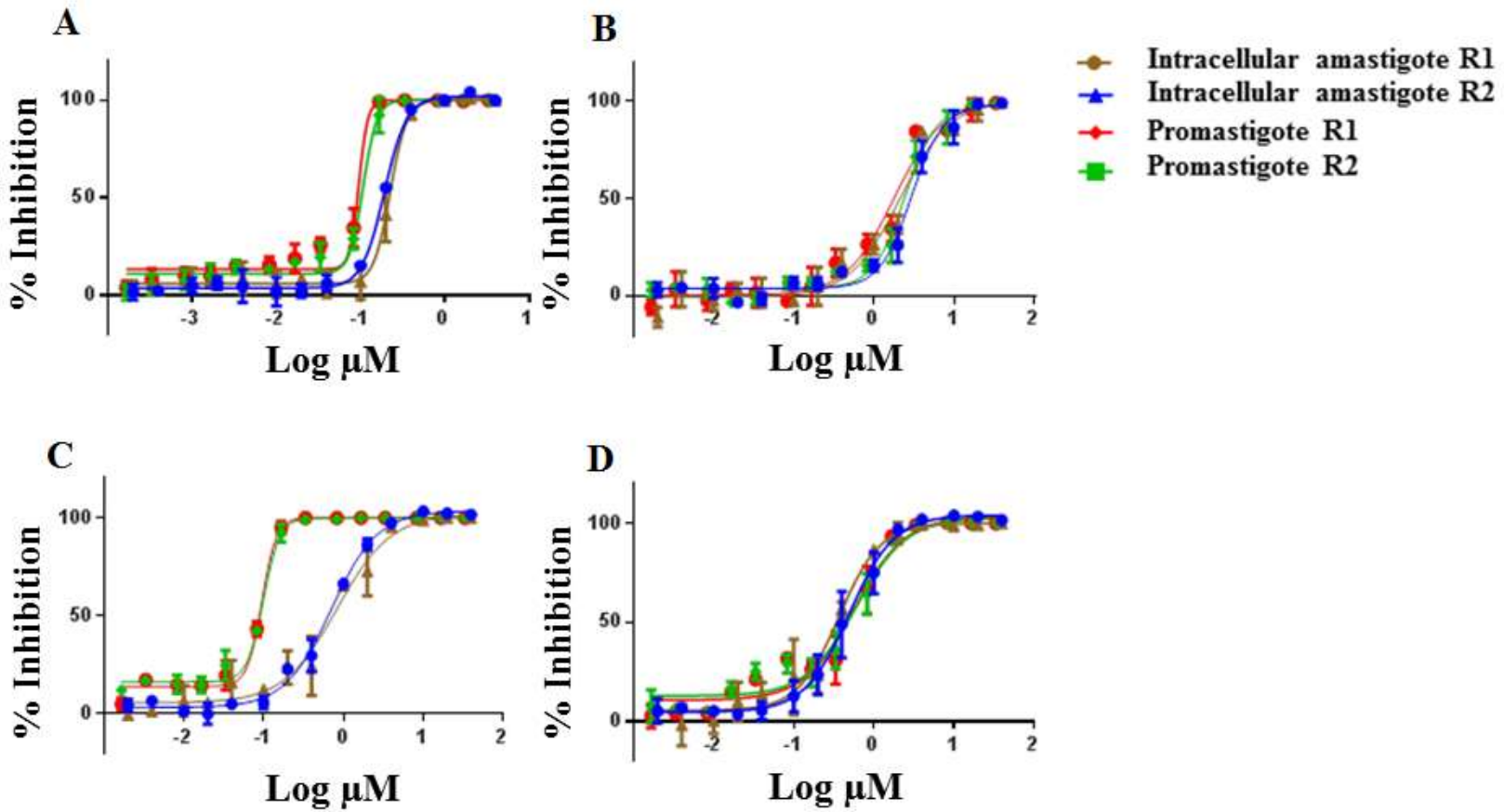

Figure 4.25: Concentration response curves obtained for the reference drugs and compounds. (A) amphotericin B, (B) DNDi VL-2098, (C) DNDi 1044 and (D) miltefosine tested in the *L. donovani* DD8 intracellular amastigote and promastigote viability assays. Each evaluation was performed in triplicate, for at least N=2 independent experiments.

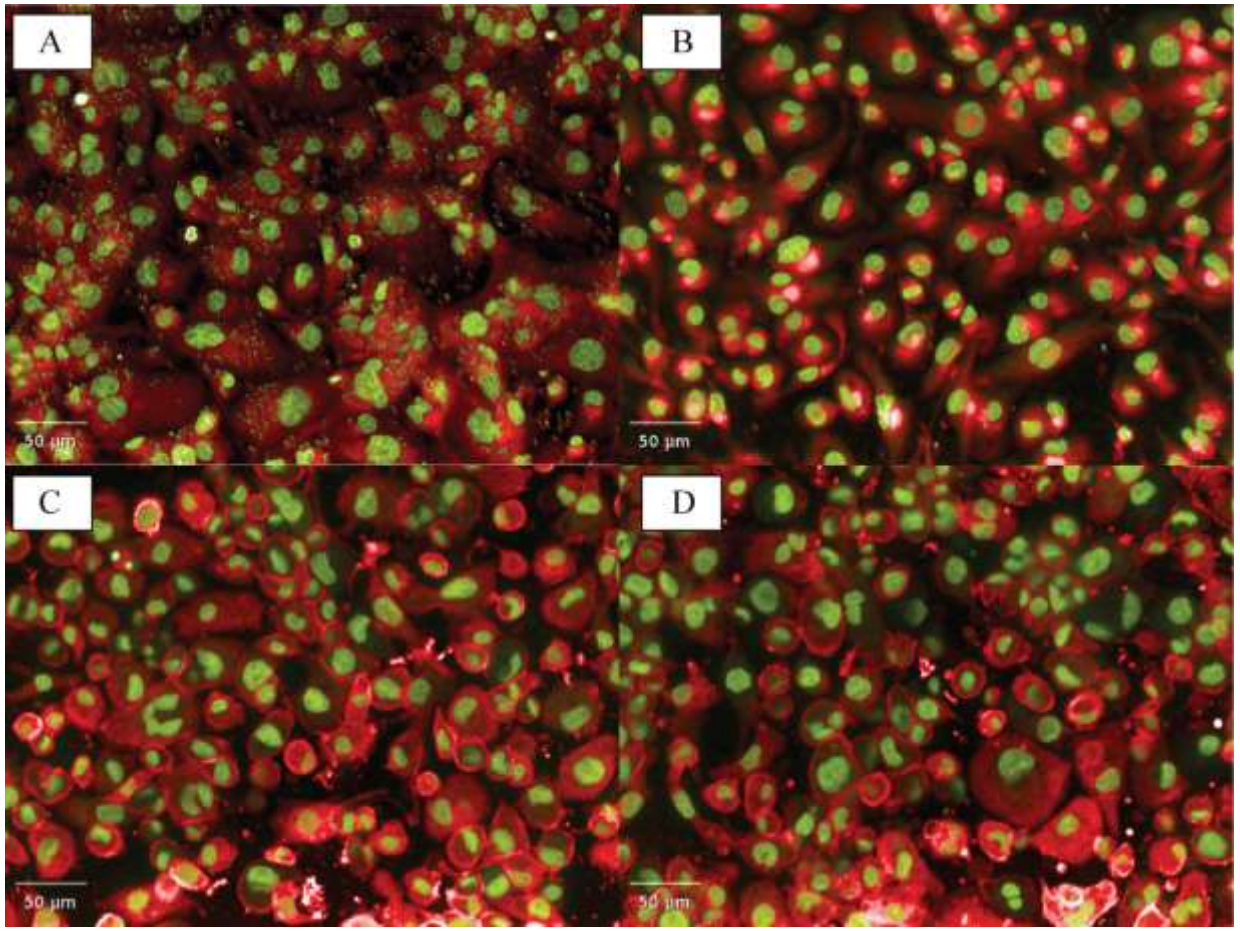

Figure 4.26: Reference compounds used in *L. donovani* DD8 intracellular amastigote assay imaged on the Opera™ using the 20X objective magnification following staining with SYBR® Green and CellMask™ Deep Red. (A) Amastigotes were observed within the host cells with 0.4% DMSO, (B) Treatment with 1 µM amphotericin B, no intracellular amastigotes can be observed within the host cells (C) Treatment with 2 µM compound VL2098, no intracellular amastigotes can be observed within the host cell, (D) Treatment with 2 µM compound DNDI-1044, no intracellular amastigotes can be observed within the host cell.

4.4. Discussion

The drug discovery pipeline for neglected trypanosomatid diseases remains sparse. In particular, drug discovery has had limited success in translating potential drug candidates into viable therapies for leishmaniasis.

A total of 5560 compounds from a diverse synthetic compound collection, which encompassed up to 4 analogues per chemotype, were selected for evaluation and screened against the two different parasite stages. In the primary screen, the concentration at which the compounds were screened for the intracellular amastigote assay was 20 µM and the concentration for the promastigote viability assay was 10 µM. These concentrations were high when compared to standard industry based screening concentrations for the following reasons: (1) in the intracellular amastigote assay the compound must cross multiple physical barriers to reach the amastigotes which reside within the parasitophorous vacuoles as illustrated in Figure 4.27; (2) previously reported screens against intracellular amastigotes (Siqueira-Neto, *et al.*, 2010; De Rycker, *et al.*, 2013) have shown there exists a high attrition rate for hits obtained from screening at low concentrations, therefore in order to obtain more hits, which can potentially be taken on to become leads, it was considered pertinent to screen at higher concentrations.

Of the 5560 compounds tested, there were 29 compounds which exhibited >60% activity at 10 µM against the promastigotes (Figure 4.9), demonstrating a hit rate of 0.52%. Siqueira-Neto *et al* screened 26,500 compounds against the promastigote stage obtaining a hit rate of ~ 2% when stipulating >70% activity at a concentration of 10µM (Siqueira-Neto, *et al.*, 2010). One potential explanation given for this high hit rate was that the compound library contained small collections of protease-focused and kinase-focused compounds (Siqueira-Neto, *et al.*, 2010). Specifically, out of a screen of 26,500 compounds conducted for the intracellular amastigote form of the parasite only two compounds (CH872 and CA272 based on 4-hydroxyquinoline and hydrazine scaffolds, respectively) were progressed further (Siqueira-Neto *et al.*, 2010). In 2011, De Muylder and colleagues screened 909 compounds in their promastigote high throughput assay and identified 59 compounds, thus a hit rate of 6.49% at >60% activity. The compounds were screened initially at 10 µM. In this assay, instead of

reduction of resazurin, the presence of cellular ATP was measured (De Muylder, *et al.*, 2011).

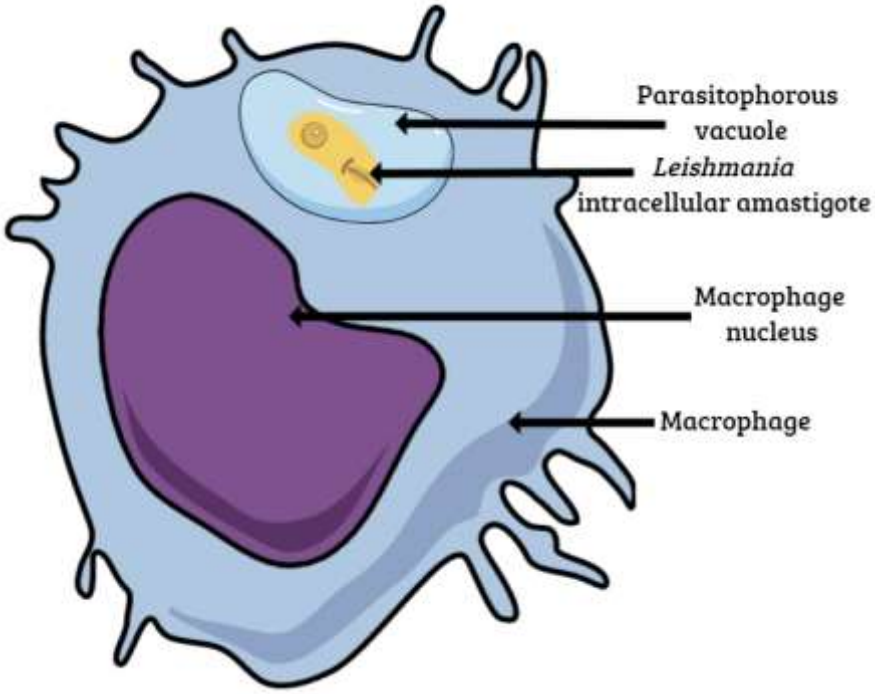

Figure 4.27: *Leishmania* intracellular amastigote residing within the parasitophorous vacuole within the macrophage cell.

For the intracellular amastigote assay, ninety compounds out of the 5560 compounds screened exhibited >50% activity at 20 µM, translating to a hit rate of 1.61% (Figure 4.9. De Muylder and co-workers identified 27 active compounds from screening at 10 µM and using >60% activity as the criteria for an active molecule, generating a hit rate of 2.97% for the intracellular amastigote assay. One of these compounds, naloxonazine, which was later identified as a mu-opioid receptor (MOR) antagonist, has been progressed through the drug discovery pipeline as a promising compound for host directed therapy (De Muylder, *et al.*, 2016). From the HTS performed by Siqueira-Neto *et al*, 2010, which utilized the intracellular amastigote assay to screen 26,500 compounds, 124 compounds were identified, thus a hit rate of 0.46% at a screening concentration of 10 µM (Siqueira-Neto *et al.*, 2010). From the HTS campaign using the intracellular amastigote assay performed by De Rycker *et al.*, 2013 to screen a 15,659 diverse compounds library, a hit rate of 0.51% was reported at 50 µM with a cut off of

>70% percentage activity (De Rycker, *et al.*, 2013). It was suggested that the use of higher compound concentrations (50 µM), increased the potential for compounds to cross multiple membranes (the cell membrane of the host cell and then cross the parasitophorous vacuole membrane) to reach the intracellular amastigotes. The limitation for using higher compounds concentrations to screen libraries is the toxicity associated with these higher concentrations, so it is difficult to identify compounds which are selective for the parasite but not toxic to the host cell. The variations in hit rates are not unusual and is greatly dependent on a number of factors including, but not limited to, the composition of the library and whether a focused or targeted library, different assay parameters such as differentiation of host cells, infectivity with either the metacyclic promastigotes or axenic amastigotes and the dyes used for detection of the intracellular amastigotes and the criteria for determining the activity level commensurate with an active compound.

We observed that the promastigote stage assay failed to identify all the compounds that showed activity in the intracellular amastigote assay. Only 4 compounds were active in both the promastigote and the intracellular amastigote assays undertaken as part of this study (Figure 4.9). Similar results have been shown in other screening campaigns when comparing promastigotes with intracellular amastigotes (De Muylder, *et al.*, 2011) or axenic amastigotes with intracellular amastigotes (De Rycker, *et al.*, 2013). There could be a number of reasons for this difference in activity on the parasite stage which include the difference in proteomics and transcriptomics of the promastigotes, axenic amastigotes and the intracellular amastigotes forms (Pescher, *et al.*, 2011). Other reasons may include the free-living nature of the promastigote and axenic amastigotes compared to the cellular localization of the intracellular amastigotes, as well as the difference in the rate of replication of all three forms of the parasite (Somanna, *et al.*, 2002; Debrabant, *et al.*, 2004; Wheeler, *et al.*, 2011).

From a broader perspective, hit rates are less important with respect to other factors such as the *in vitro* activity of the compound across the promastigote and intracellular amastigote stages, chemical properties of the compound, activity across different strains/ species and eventually *in vivo* translation. Promising molecules have been identified in the past displaying excellent *in vitro* activity but were discontinued because the activity could not be translated in *in vivo* models. Example includes a recently

published molecule DDD806905, identified as a potent inhibitor of *L. donovani* Methionyl-tRNA synthetase (MetRS) (a validated drug target in kinetoplastids) with a Ki of 18 nM which failed to translate *in vivo* (Torrie, *et al.*, 2017). On the other hand, there are molecules displaying promising *in vitro* and *in vivo* activity against the parasite but have been discontinued in the later stages because of toxicity associated in the *in vivo* models, which was not evident prior to that. An example in this context is VL-2098, initially identified from a library of 72 nitroimidazo-oxazole compounds, displaying excellent *in* vitro and *in vivo* activity (Mukkavilli, *et al.*, 2014; Gupta, *et al.*, 2015), but was discontinued because of toxicity associated in *in vivo* animal models (DND*i*, 2016).

Generally speaking, backup next generation lead compounds are generated by chemical modifications of compounds failing *in vivo* testing to significantly increase their selectivity for the parasite compared to the host cell. For VL-2098 a backup programme was initiated where a library of nitroimidazooxazine based compounds were screened at IPK (Institut Pasteur Korea) in a HTS-HCI intracellular amastigote assay. This resulted in the identification of 10 compounds from a subseries of 7-substituted nitroimidazooxazines and 8 compounds from the PA-824 analogue series with SI > 1000 for most of the compounds (DND*i*, 2017). The 7-substituted nitroimidazooxazines exhibited IC_{50} values ranging from 0.01-2.25 µM against *L. donovani* species amastigotes. The other 8 compounds from the PA-824 analogue series exhibited IC_{50} values ranging from 0.83-2.32 µM. The promising compounds from this series were further progressed into a lead optimization program. Of the 7-substituted nitroimidazooxazines, one compound demonstrated good activity in the *in vivo* hamster model, with 90% reduction in infection when administered at a dose of 25 mg/kg bid for 5 days. The compound DNDI-0690 from the same class has progressed to the translational phase in the DND*i* portfolio (DND*i*, 2017).

Our screening campaign to identify promising molecules from the 5560 synthetic scaffold library active against *L. donovani* DD8 resulted in the discovery of compound N-(4-Ethoxyphenyl)-2,3-dihydro-1H-cyclopenta[b]quinolin-9-amine, referred to as compound **BZ1** (Figure 4.10). This compound exhibited activity against the intracellular form (amastigote) of the *Leishmania donovani* DD8 parasite with an IC_{50} of 0.59 ± 0.13 µM. In addition, **BZ1** was active against the extracellular form

(promastigote) of *Leishmania donovani* DD8 (Old World- Indian strain) parasites with an IC_{50} of 2.37 ± 0.85 µM (Figure 4.11). This compound not only showed interesting *in vitro* activity but also displayed good selectivity (>33) for HEK-293 and THP-1 host cells. **BZ1** fulfilled the DND*i* criteria for the target candidate profile for promising molecules based on this *in vitro* activity (Don and Ioset, 2014). When compared with the reference drug amphotericin B, compound **BZ1** had a ~3-fold lower *in vitro* activity of 0.59 ± 0.13 µM compared to the activity of amphotericin (0.20 ± 0.02 µM) in the intracellular amastigote assay. Interestingly, compound **BZ1** had a greater selectivity index of >33 compared to the selectivity of amphotericin B which is 9.6 for the THP-1 host cells. This data demonstrated that compound **BZ1** had a better starting safety profile. In comparison to the other reference drug, miltfosine, compound **BZ1** displayed 5-fold greater activity than miltefosine (IC_{50}: 2.54 ± 0.57 µM). Compound **BZ1** also demonstrates a better selectivity profile than miltefosine, as the SI of miltefosine is 13.12 and 7.27 for HEK-293 and THP-1 cells, respectively. In comparison to the clinical candidate DNDI-1044 (IC_{50}: 0.430 ± 0.08), compound **BZ1** was slightly less active however, possessing an improved selectivity profile, as DNDI-1044 has a SI of 14.14 for *Leishmania* parasites over HEK-293 cells.

The next phase was to identify analogues of compound **BZ1** and test them in the assay to find compounds with better activity and selectivity. For this purpose, potential analogues were identified based on SAR studies undertaken in collaboration with Dr. Brad Sleebs (The Walter and Eliza Hall Institute of Medical Research, Melbourne), and subsequent substructure searches to retrieve those analogues. Thirty compounds were selected (**BZ1-A to BZ1-d**) (Figure 4.12) and tested in a 14-point concentration response (40 - 0.002 µM) curve format (Table 4.4). The analogues gave a range of activities resulting in IC_{50} values from 0.57 to 11.48 µM for the intracellular amastigote assay. The analogue **BZ1-I** was demonstrated to have the best activity with an IC_{50} value of 0.51 ± 0.27 µM against intracellular amastigotes and an IC_{50} value of 0.62 ± 0.24 µM against the promastigotes form of the parasites. The compound had a SI of 34.84 and 17.42 for the intracellular amastigote over the HEK-293 and THP-1 host cells (Figure 4.13). The *in vitro* activity of compound **BZ1-I** against intracellular amastigotes was similar to compound **BZ1** but the *in vitro*

activity of compound **BZ1-I** was 4-fold greater for the promastigotes which prioritized this as a promising molecule for further investigatation.

As far as we know both of these compounds, **BZ1** and **BZ1-I**, are novel compounds however *in vitro* anti-leishmanial activity has been reported for similar chemotypes from the class of Quinolines and 9-Anilinoacridines compounds (Dietze, *et al.*, 2001; Di Giorgio, *et al.*, 2007; Loiseau, *et al.*, 2011). The mechanism of action for anti-leishmanial activity of Quinolines and 9-Anilinoacridines compounds has been discussed in detail in chapter 5. Based on the *in vitro* data of the compound activity and selectivity, we decided to take both of these compounds, **BZ1** and **BZ1-I,** through for further mechanism of action studies.

Thus, the screening campaign incorporating the synthetic scaffold library of 5560 was successful providing a promising hit molecule and an interesting analogue from the series.

To identify molecules with alternative or more diverse chemotypes, a screening campaign using a small natural product library was conducted. Natural products have, and continue, to serve as an attractive alternative source of chemical starting points for drug discovery against kinetoplastid parasites (Jones, *et al.*, 2013; Annang, *et al.*, 2015). Australia has one of the world's highest levels of biodiversity (Scheuer, 2013) providing an exceptional resource for natural product drug discovery. It has been previously reported that identification and biological profiling of compounds originating from Australian plants (Yang, *et al.*, 2011), marine invertebrates (Davis, *et al.*, 2011; Feng, *et al.*, 2012; Davis, *et al.*, 2013) and fungi (Choomuenwai, *et al.*, 2015), possess anti-parasitic activity.

We decided to screen the DOANP library, which consists of 472 distinct compounds, the majority (53%) of which are natural products that have been obtained from Australian natural sources, such as endophytic fungi (Davis, 2005), plants (Levrier, *et al.*, 2013), macrofungi (Choomuenwai, *et al.*, 2012), and marine invertebrates (Barnes, *et al.*, 2010). Approximately 28% of this library contains semi-synthetic natural product analogues (Barnes, *et al.*, 2016), while a smaller percentage (19%) are known commercial drugs or synthetic compounds inspired by natural products.

In addition to the *L. donovani* DD8 promastigote viability and intracellular amastigote assays, this library was also screened for other kinetoplasttids, specifically *T. b. brucei* and *T. cruzi*. Kinetoplastid pathogens share much of their cellular and molecular biology even though they cause clinically distinctive diseases and are trasmitted by different insect vectors (Stuart, *et al.*, 2008). The parasites in these studies share common molecular targets including trypanothione reductase, pteridine reductase and cysteine protease enzymes, which have been proposed for target-based screening. Inhibitors have been designed in the past for these enzymes as anti-leishmanials (Corona, *et al.*, 2012; Baiocco, *et al.*, 2013; Schroder, *et al.*, 2013) and anti-trypanosomals (Cavalli, *et al.*, 2009; Mpamhanga, *et al.*, 2009; Breuning, *et al.*, 2010). Fexinidazole is the most advanced oral candidate under development for Chagas disease and HAT, currently in the Phase II and Phase III clicical trials, respectively (DND*i*, 2017). This lead compound has also shown potent activity against *L. donovani in vitro* and *in vivo* in a visceral leishmaniasis mouse model, illustrating the significant value of screening against multiple kinetoplastids (Wyllie, *et al.*, 2012).

To classify a compound as an active hit against *Leishmania*, *T. b. brucei* and / or *T. cruzi* we used the target candidate profile established by DND*i* (Don and Ioset, 2014). We have used their criteria in terms of efficacy *in vitro* with an IC_{50} value <10 µM as the classification of a potential anti-kinetoplastid hit molecule. For *L. donovani* DD8, less priority has been given to compounds that are only active against the promastigotes alone, in comparison to compounds active only on intracellular amastigotes, as intracellular amastigotes represent the pathophysiological relevant form of the disease (Siqueira-Neto, *et al.*, 2012).

Out of the 472 compounds screened for the *L. donovani* DD8 promastigote viability assay twenty-nine compounds fulfilling the hit criteria of > 70% inhibition at 16.7 µM; whereas only 5 compounds were identified from screening against the *L. donovani* DD8 intracellular amastigotes (Figure 4.23B). We predict that the differences observed in these hit rates are due to several factors such as the compounds ability to pass host cell membrane, phagolysosome membrane and eventually the parasite membrane, significant pH change from 6.8 for promastigotes to a pH of 4.8-5.4 in the intracellular amastigotes within the host cell (Peña, *et al.*, 2015). Reduced metabolism in the host cell can also be a contributing factor as intracellular amastigotes are slow replicating as compared to promastigotes (Peña, *et al.*, 2015). Around 28 molecules were identified

for *T. b. brucei* which is also an extracellular parasite like the *Leishmania* promastigotes (Figure 4.23B). Eight compounds, identified from screening the natural product collection, showed activity against both *T. b. brucei* (extracellular) and *T. cruzi* intracellular amastigotes (Table 4.6). As the biochemical similarity, as well as closer phylogeny between *T. b. brucei and T. cruzi,* is much higher than that for *Leishmania* (Marr and Muller, 1995), the number of mutual hits between them is much greater than between *T. b. brucei* and intracellular *Leishmania,* and *T. cruzi* and intracellular *Leishmania*. Several compound screening campaigns against on trypanosomes have identified good correlation for compound potency between *T. b. brucei* and *T. cruzi* parasites (Peña, *et al.*, 2015).

The hit molecules identified from this study were confirmed using a 14-point concentration response curve format for *L. donovani* DD8 promastigotes *L. donovani* DD8 intracellular amastigotes, *T. b. brucei* trypomastigotes and *T. cruzi* intracellar amastigotes to establish IC_{50} values enabling comparison (Table 4.6). The reconfirmed compounds showing common activity between one or more parasites were named as NP compounds to differentiate them from the BZ compounds identified from the synthetic scaffold library.

Using the SMILE string of active compounds, which was obtained using ChemSpider (http://www.chemspider.com/), previously reported biological activities of compounds were identified using SciFinder (http://www.cas.org/products/scifinder) and ChEMBL (https://www.ebi.ac.uk/chembl/).

Lissoclinotoxin E (**NP1**) was the only compound that was pan-active against all three parasites tested, with an IC_{50} value <5 µM. Lissoclinotoxin E was identified as one of two new dimeric alkaloids [the other is lissoclinotoxin F (**NP11**)] which were extracted from a Philippine didemnid ascidian (Davis, *et al.*, 2003). Lissoclinotoxin E exhibted an IC_{50} value of 0.57 ± 0.20 µM and 3.92 ± 0.38 µM for *T. b. brucei and T. cruzi,* respectively. The structure of **(NP1)** and **(NP11)** compounds are illustrated in Figure 4.28. The anti-leishmnial activities for compound (**NP1**) on promastigotes and intracellular amastigotes were 0.72 ± 0.16 and 4.41 ± 0.24 µM, respectively. Compound (**NP1**) exhibits high selectivity for *T. b. brucei* in relation to HEK-293 cells. The selectivity for HEK-293 and 3T3 cells needs to be confirmed at higher concentrations for the *L. donovani* DD8 and *T. cruzi*. The other dimeric alkaloid, Lissoclinotoxin F

(**NP11**), also showed activity for both forms of the *Leishmania* parasite (promastigote: 5.51 ± 0.30 and amastigote: 8.31 ± 0.67 µM), albeit lower. This is novel activity against kinetoplastid parasites reported for these compounds. Previously, both compounds have shown interesting activity against PTEN-deficient (PTEN2/2) cell lines indicating anti-tumor activity (Davis, *et al.*, 2003). This class of compounds has shown prominent activity against all three parasites and it could be of interest to further explore the anti-protozoal potential of this class. Analogues can be synthesized which may address any potential cytotoxicity issues.

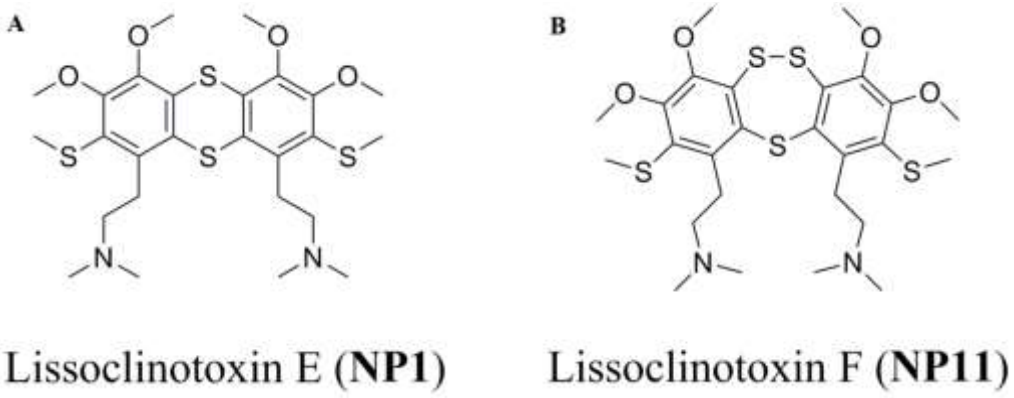

Figure 4.28: Structures of compound (A) (NP1) and (B) (NP11).

Spermatinamine (**NP 2**), isolated from the sponge *Pseudoceratina* sp. displayed activity against both forms of *L. donovani* DD8, as wel as *T. b. brucei.* This compound was shown to have IC_{50} values of 6.15 ± 0.056, 11.87 ± 0.565 and 1.00 ± 0.26 µM against *L. donovani* DD8 intracellular amastigotes, promastigotes and *T.b.brucei* parasites, respectively. Compound (**NP 2**) (Figure 4.29) exhibited moderate selectivity for *T. b. brucei* in relation to HEK 293 cells, with no selectivity for *L. donovani* DD8 intracellular amastigotes and promastigotes. Spermatinamine was originally discovered as a inhibitor of isoprenylcysteine carboxyl methyltransferase (ICMT) (Buchanan, *et al.*, 2007). ICMT is a potential target for cancer therapeutics as this enzyme catalyses the final step in post translational modification, where carboxyl methylation of oncogenic proteins takes place. Spematinamine has also been shown to have anti-bacterial activity against Gram-negative bacteria (Yin, *et al.*, 2011) as well as having anti-malarial activity (IC_{50}: 0.23 µM) against *Plasmodium falciparum* (3D7) parasites (Choomuenwai, *et al.*, 2013). Therefore, this may also be the target of this

compound in *T. b. brucei* parasites and warrants further investigation, as this parasite also shares a protein carboxyl methyltransferase (Buckner, *et al.*, 2002). This is the first time that the activity of these compounds has been reported against these parasites and it would be beneficial to identify more kinetoplastid-selective compounds from this class.

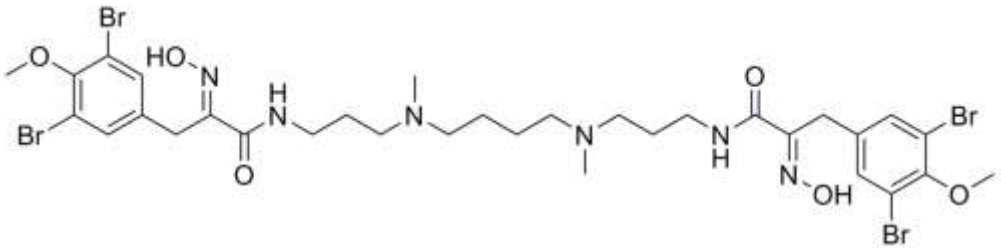

Spermatinamine (**NP2**)

Figure 4.29: Structure of compound (NP2).

On the basis of the information currently available, it seems fair to suggest that thiaplakortone A (**NP3**) and thiaplakortone analogue (**NP7**) have novel activity against both *T. b.brucei* and *T. cruzi* parasites. In addition, gambogic acid (**NP4**), mycophenolic acid (**NP5**), narciclasine (**NP6**), 3,4-dihydro-2H-naphtho[2,3-b][1,4]thiazine-5,10-dione 1,1-dioxide (**NP9**) and Psammaplysin F (**NP14**) have novel activity against *T. cruzi* parasites.

Thiaplakortone A (**NP3**) is a thiazine-derived alkaloid, initially isolated from an Australian marine sponge *Plakortis lita* (Davis, *et al.*, 2013). This compound was active against *T. b. brucei* and *T. cruzi* with IC_{50} values of 3.94 ± 0.71 and 4.26 ± 0.65 µM, respectively. Compound (**NP3**) exhibited no selectivity for *T. b. brucei* and *T. cruzi*. Interestingly, a truncated synthetic thiaplakortone analogue (**7**), 6-tosyl-2,3-dihydro-[1,4]thiazino[3,2-f]indole-5,9(1H,6H)-dione 4,4-dioxide, has also been shown to be active against *T. b. brucei* and *T. cruzi* (IC_{50} of 0.68 ± 0.01 and 3.55 ± 0.38 µM, respectively). Compound (**NP7**), which is an analogue of (**NP3**) exhibited better selectivity for *T. b. brucei* and *T. cruzi* than compound (**NP3**), indicating the possibility of other analogues to be explored to identify selective compounds. The structure of

compounds (**NP3)** and (**NP7)** are illustrated in Figure 4.30. Compound (**NP3**) was previously reported to have potent activity against both chloroquine sensitive (3D7) and multi-drug resistant (Dd2) *P. falciparum* parasites (IC_{50} of 51, and 6.6 nM, respectively) (Davis, *et al.*, 2013). Subsequently, activity against 3D7 and Dd2 strains of *Plasmodium falciparum* was reported with IC_{50} values of 546 ± 119 and 509 ± 30.9 nM (Schwartz, *et al.*, 2015). The significant difference in activity is likely related to the assay format used and lower sensitivity. *In vivo* testing of the thiaplakortone A in a murine mouse model of malaria infection did not completely suppress parasitemia with oral administration, possibly due to associated poor bioavailability (Schwartz, *et al.*, 2015).

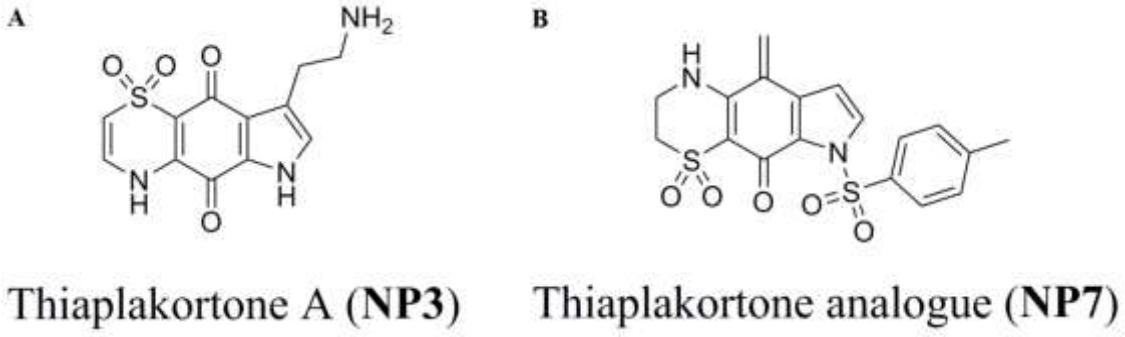

Figure 4.30: Structures of compound (A) (NP3) and (B) (NP7).

Gambogic acid (**NP4**) is a xanthonoid isolated from the gamboge resin of the *Garcinia hanburyi* tree (Zhang, *et al.*, 2004) which we have demonstrated to have anti-trypanosomal activity against *T. b. brucei* and *T. cruzi* (IC_{50} of 0.27 ± 0.04 and 1.87 ± 0.07 µM, respectively). Compound (**NP4**) (Figure 4.31) exhibits moderate selectivity for *T. b. brucei* in relation to HEK-293 cells. *T. b. brucei* activity for compound (**NP4**) has been previously reported (Mackey, *et al.*, 2006) indicating similar values to those we obtained for *T.b. brucei*. The activity on *T. cruzi* is indicative of host-cell damage as this compound has been shown to be cytotoxic, inducing apoptosis through caspase 3 activation and mitochondrial destabilization (Wu, *et al.*, 2002).

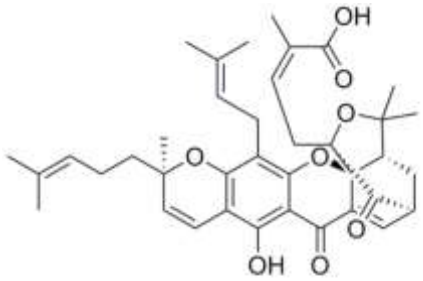

Gambogic acid (**NP4**)

Figure 4.31: Structure of compound (NP4).

Mycophenolic acid (**NP5**) (Figure 4.32) is classified as an inosine 5'-monophosphate dehydrogenase inhibitor and the anti-trypanosomal effects of this compound have been identified against *T. b. brucei* (Bessho, *et al.*, 2013) in addition to many other protozoan parasites (Sullivan, *et al.*, 2005; Cao, *et al.*, 2013). We observed activity for *T. b. brucei* (IC_{50} of 0.51 ± 0.10 µM) which correlates with the previously reported IC_{50} value (Suganuma, *et al.*, 2016). An IC_{50} of 1.59 ± 0.03 µM was demonstrated against *T. cruzi* and showed no selectivity, as had a considerable effect on the the host cells. To the best of our knowledge this compound has not been tested against *T.cruzi* previously.

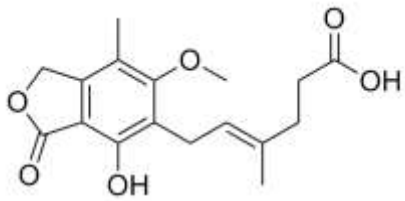

Mycophenolic acid (**NP5**)

Figure 4.32: Structure of compound (NP5).

The natural compound, narciclasine (**NP6**), was first isolated from daffodils, which belong to the *Amaryllidaceae* plant family (Ceriotti, 1967). This compound was active against *T. b. brucei* and *T. cruzi* (IC_{50} =0.03 ± 0.01 and 0.20 ± 0.01 µM, respectively)

and like gambogic acid, has been previously reported to have activity against *T. b. brucei* (Mackey, *et al.*, 2006) but not for *T. cruzi*. Compound (**NP6**) (Figure 4.33) has no selectivity for *T. b. brucei* or *T. cruzi* being equally cytotoxic against the mammalian host cells. The mechanism of action of this compound suggests that it inhibits protein synthesis by blocking peptide bond formation in *Saccharomyces cerevisiae* yeast (Carrasco, *et al.*, 1975). The compound has also been demonstrated to have anti-viral activity against yellow fever, Japanese encephalitis and dengue fever but due to off target toxicity it has not been tested in *in vivo* models (Gabrielsen, *et al.*, 1992). Whether a similar mechanism of action is the means by which this compound exerts the effects we observed has not been verified, however as the activity is non-specific, pursuing this compound further is of limited value.

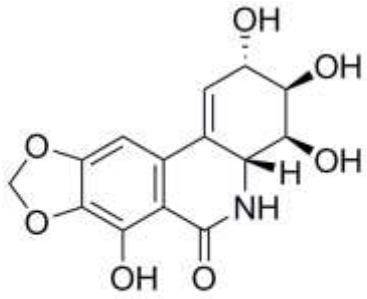

Narciclasine (**NP6**)

Figure 4.33: Structure of compound (NP6).

Compound (**NP9**) and (**NP14**) showed interesting activity for *T. cruzi* intracellular amastigotes with IC_{50} values of 3.82 ± 0.61 and 5.64 ± 0.76 µM, respectively. The structure of compound (**NP9)** and (**NP14)** are illustrated in Figure 4.34. Compound (**NP9**) is a synthetic compound, which exhibits no selectivity for *T. cruzi*. Compound (**NP14**), a bromotyrosine alkaloid was isolated from the marine sponge, *Hyatella* sp (Yang, *et al.*, 2010). Although IC_{50} values could not be determined for the host cells or HEK-293 cells for this compound, there was similar activity against the mammalian cell at the concentrations eliciting activity for *T. cruzi*. This compound has been shown to exhibit anti-malarial activity against *P. falciparum* strains (3D7 and Dd2) with IC_{50} values of 0.87 and 1.4 µM, respectively (Yang, *et al.*, 2010).

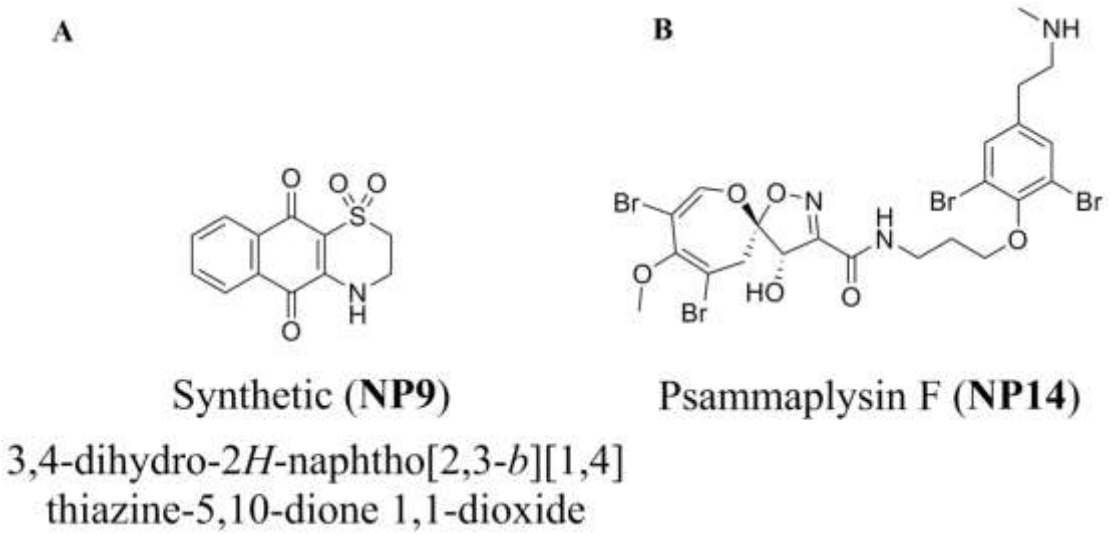

Figure 4.34: Structures of compound (A) (NP9) and (B) (NP14).

Compounds (**NP12**) (ethyl 4-((diethylamino)methyl)-5-hydroxy-1-(4-methoxyphenyl)-2-methyl-1H-indole-3-carboxylate) and (**NP13**) [(E)-1-(2,6-dihydroxy-4-methoxy-3,5-dimethylphenyl)-3-phenylprop-2-en-1-one] showed activity on both the intracellular and extracellular forms of *L. donovani* DD8. Compounds (**NP12**) and (**NP13**) displayed IC_{50} values of 11.09 ± 0.311 and 5.65 ± 0.26 µM against the *L. donovani* DD8 intracellular amastigotes. Both of these compounds showed no significant activity against either *T. b. brucei* or *T. cruzi*. The structure of compound (**NP12)** and (**NP13)** are illustrated in Figure 4.35. Compound (**NP13**) has shown high selectivity for *L. donovani* DD8 intracellular amastigotes in relation to HEK-293 cells. Compound (**NP13**) was previously reported to have activity against both *L. donovani* (MHOM/SD/62/1S-CL2D) axenic amastigotes and *T. b. brucei* variant 221 with IC_{50} values of 16.75 ± 4.35 and 21.11 ± 3.68 µM, respectively (Salem and Werbovetz, 2005). Compound (**NP13**) also caused a 96 ± 2% reduction in infection of *L. mexicana* intracellular amastigotes at 41.89 µM (Salem and Werbovetz, 2005). Previously, it has been reported that compound activity varies based on the geographical location of the species and strains (Croft, *et al.*, 2002). An example in this context is parmomycin, which has negligible activity against *L. donovani* DD8 when compared to other strains (Neal, *et al.*, 1995). This may explain the difference in activity observed for compound (**NP13**) for *Leishmania* species; however, differences in assays and compound handling may also be a factor and play a role. Compound (**NP13**) is a

promising hit as it fulfils the TCP criteria set by DND*i* for anti-leishmanial drug discovery. It will be interesting to further explore this compound by synthesizing analogues and assessing structure activity relationships.

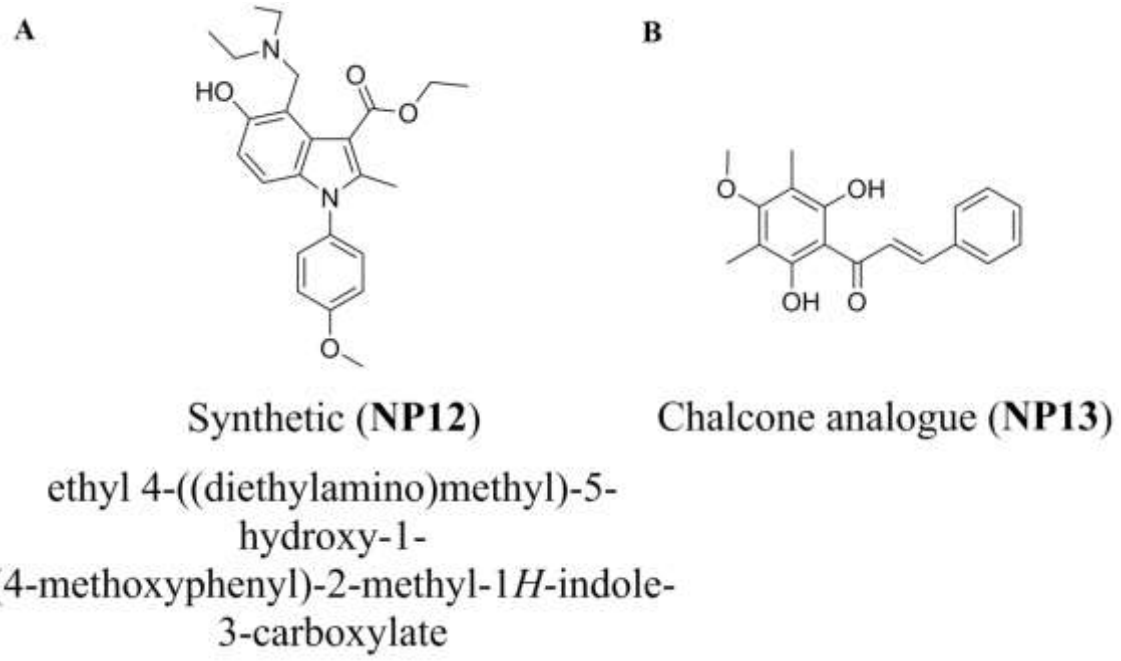

Figure 4.35: Structures of compound (A) (NP12) and (B) (NP13).

A small percentage (5%) of the library is comprised of commercial or synthetic compounds inspired by natural products. Mefloquine HCl (**NP8**), emetine dihydrochloride (**NP10**), chelerythrine chloride (**NP15**) which belong to this sub-group were shown to have activity against *Leishmania donovani* DD8, *T. b. brucei* and *T. cruzi* serving as internal controls. The structure of compound (**NP8**), **(NP10) and (NP15)** are illustrated in Figure 4.36. The 50% inhibitory concentration observed for mefloquine HCl (**NP8**) was 0.62 ± 0.06 and 3.96 ± 0.58 µM for *T. b. brucei* and *T. cruzi*, respectively, with moderate selectivity for *T. b. brucei*. Mefloquine has previously been shown to have activity against *T. b. brucei in vitro* and *in vivo* (Otigbuo and Onabanjo, 1992) and has a reported EC_{50} value of 6.1 µM against *T. cruzi*, with a SI of 2 to 3T3 host cells (Planer, *et al.*, 2014). Mefloquine and emetine have shown efficacy in the treatment of human cutaneous leishmaniasis (CL) (Landires *et al.*, 1995; Sinderson, I924). Herein we found that 3T3 activity was close to that of *T. cruzi* activity, although higher concentrations would be needed to confirm the selectivity. We have previously identified mefloquine as active against *T. cruzi* from screening of the ***MMV Pathogen Box*** collection of compounds (Duffy *et al*, 2017).

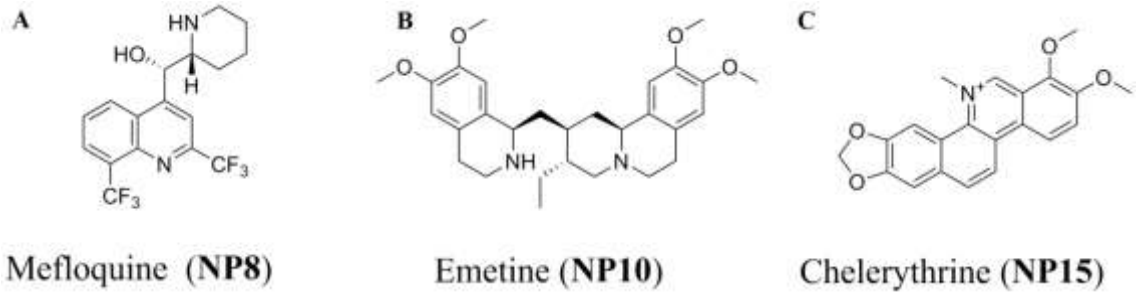

Figure 4.36: Structures of compound (A) (NP8), (B) (NP10) and (C) (NP15).

Emetine dihydrochloride (**NP10**) was found to have activity against both *T. b. brucei* and *T. cruzi* with IC_{50} values of 0.05 ± 0.01 and 0.09 ± 0.01 µM, respectively. This compound has shown no selectivity for HEK-293 cells (replicating cells with no contact inhibition) in relation to *T. b. brucei* and *T. cruzi.* Whereas selectivity was observed for 3T3 cells (replicating cells with contact inhibition) in *T. cruzi* indicating its cytotoxicity on replicating cell without contact inhibition. This compound was previously used as an anti-protozoal drug for the treatment of amoebic liver abscess and invasive intestinal amoebiasis (Lasserre, 1979). Its use was discontinued due to severe adverse effects associated with the drug which included cardiotoxic effects (Lemmens-Gruber, *et al.*, 1996), severe irritation of oral mucosa, nausea and vomiting (Matthews, *et al.*, 2013). Emetine dihydrochloride has been tested for *T. b. brucei* (Jones, *et al.*, 2010), in which the IC_{50} value was 7.9 µM, however it also displayed poor selectivity (3.8) toward MRC5 cells. No data is currently reported in the literature for activity of this compound against *T. cruzi.*

Chelerythrine chloride (**NP15**) exhibited an IC_{50} of 0.23 ± 0.04 µM against *T. b. brucei* with good selectivity of >18 fold for HEK-293 cells. Chelerythrine was previously discovered following testing as an oncology drug candidate (Chan, *et al.*, 2003). Trypanocidal activity has been previously been reported, with an IC_{50} of 1.3 µM against *T. b. brucei* (Rosenkranz and Wink, 2008).

Thus, from the natural product collection screened here, compounds (**NP1)** and (**NP2)**, have shown pan activity against the kinetoplastid parasite, but unfortunately both these compounds have also demonstrated extensive cytotoxicity, hence a decision was taken not to pursue them further for target identification studies at this time. Structural modifications have been proposed and these analogues will be synthesized in the near

future and tested for anti-protozoal activity. In contrast, (**NP13**) which fulfils the TCP criteria established by DND*i* will be investigated further.

The elimination of poor-quality compoundswhich include toxic compounds with physicochemical structural alerts, poor absorption, distribution, metabolism and excretion (ADME) properties and the presence of Pan Assay Interference Compounds (PAINS) in early stages is critical. PAINS are compound classes with a common substructural motif that frequently results in promiscuous activity in multiple assay formats for a variety of indications. A common issue with compounds classified as PAINS is that the substructure can interfere in biochemical reactions, such as metal chelation, redox cycling and protein reactivity (Baell and Willem, 2018). In this context, phenotypic screening is less susceptible to direct interference, but the issue of PAINS is still relevant as membrane perturbation is an additional promiscuity mechanism (Ingolfsson *et al*, 2014). Few natural products are defined as PAINS, but the most important issue to be considered is the context of the biological readout (Baell, 2016). The relatively few known PAINS-containing drugs were discovered in a traditional manner after observation of potent downstream efficacy, not through target-based screening (Baell and Willem, 2018). The possibility exists that many of the natural product compounds identified in these screens could turn out to be PAINS. Therefore, further characterization of these compounds is required.

Two compounds, **BZ1** and **BZ1-I,** identified from screening the synthetic scaffold library, were selected for further biological characterization based on their anti-leishmanial and selectivity profiles, discussed in chapter 5.

Chapter 5: Mode of action, mechanism of action and resistance studies

5.1. Introduction

In this chapter the mechanisms by which the 1H-cyclopenta[b]quinolin-9-amine compounds, **BZ1** and **BZ1-I** interact with *Leishmania donovani* DD8 parasites and produce their effect(s) was investigated. 1H-Cyclopenta[b]quinolin-9-amine compounds are related to quinoline derivatives and 9-anilinoacridines (Figure 5.1) which have previously been shown to have *in vitro* anti-leishmanial properties (Dietze, *et al.*, 2001; Di Giorgio, *et al.*, 2007; Loiseau, *et al.*, 2011).

In 1934, the first quinine-based drug, a 4-aminoquinoline called chloroquine was synthesized (Simonsen, *et al.*, 2009), which was later used for the treatment of malaria. Chloroquine and hydroxyl chloroquine have been shown to have activity against *L. amazonensis* intracellular amastigotes with IC_{50} values of 0.78 ± 0.08 µM and 0.67 ± 0.12 µM, respectively (Rocha, *et al.*, 2013). For malaria the mechanism of action of 4-aminoquinolones is suggested to be the inhibition of enzymes such as DNA polymerases, and proteases, as well as damage to the malaria parasite's vacuolar membrane via lipid peroxidation (Aft and Mueller, 1983; Slater, 1993). Chloroquine accumulates down the pH gradient from the outside of the digestive vacuole (pH = 7.4) to the inside of the digestive vacuole (pH 5.5) (Hayward, *et al.*, 2006). This is also the possible mechanism for the anti-leishmanial activity associated with chloroquine, as a similar pH gradient exists within *Leishmania* parasites within the host cell (Field, *et al.*, 2017). Within the acidic environment within *Plasmodium* parasites chloroquine accumulates because of structural modifications converting it into chloroquine^{2+} (Mushtaque and Shahjahan, 2015). Chloroquine^{2+} functions to form a dimeric hematin complex by inhibiting heme crystallization to hemazoin. The crystallization results in the rapid increase in Heme concentration within the acidic vacuole of plasmodium resulting in the death of the malaria causing parasite (Hempelmann, 2007).

Another aminoquinoline based anti-malarial drug, amodiaquine was tested for *in vitro* activity against *L. donovani* (MHOM/ET/67/HU3) and demonstrated an IC_{50} value of

1.4 µM. An IC_{50} value of 90 µM was determined on KB cells (cell line derived from an oral epidermal carcinoma), suggesting limited cytotoxicity (Guglielmo, *et al.*, 2009). Other derivatives of amodiaquine were also tested but were found to be cytotoxic to the host cells (Guglielmo, *et al.*, 2009). It has been reported that quinolines inhibit leishmanial GDP mannose-pyrophosphorylase (Lackovic, *et al.*, 2010). This enzyme is essential for parasite virulence and survival as it produces a range of mannose-rich glycoconjugates.

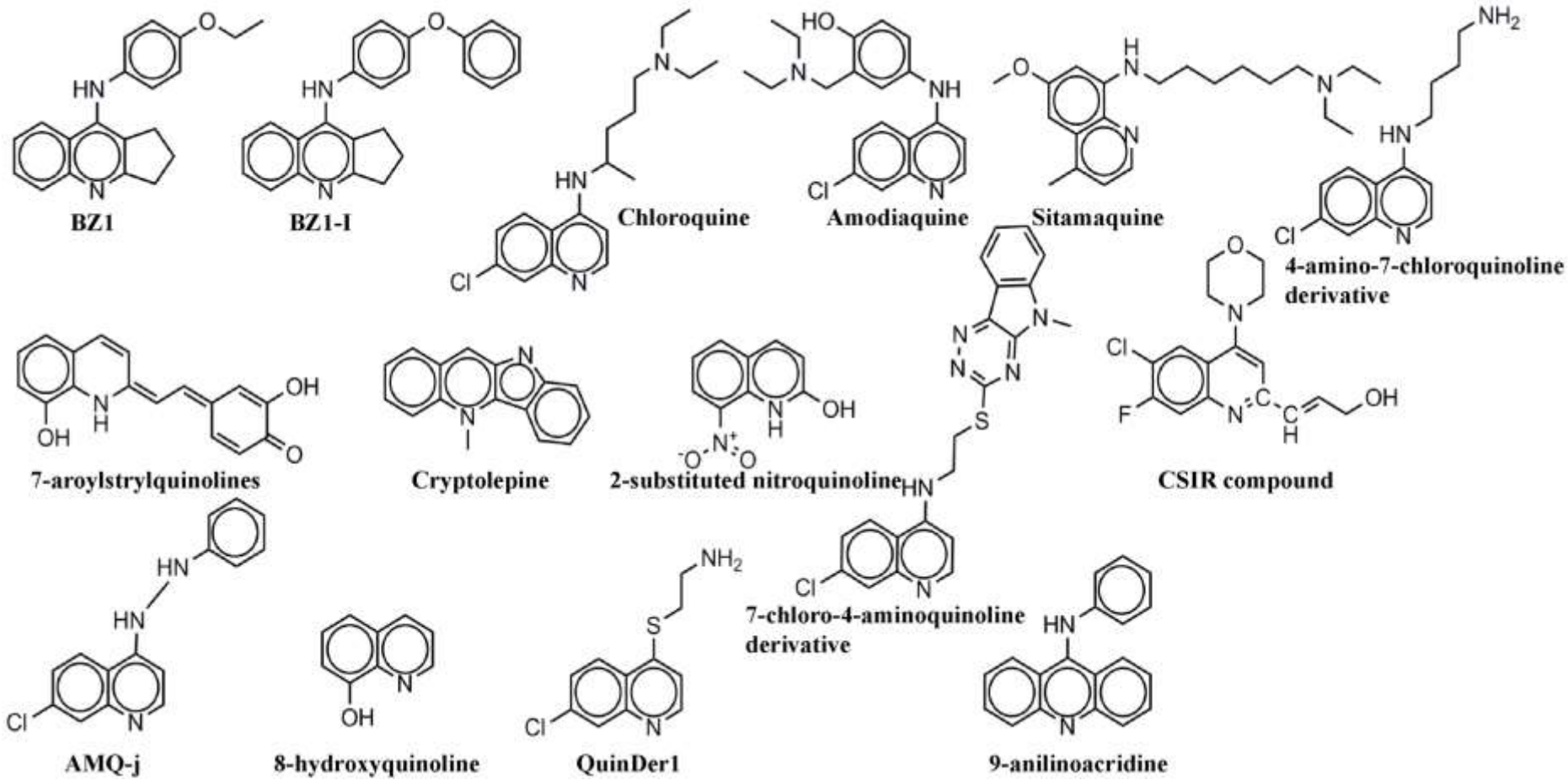

Figure 5.1: Core structures of quinoline derivatives and 9-anilinoacridines.

After the discovery of chloroquine, quinolines attracted considerable interest as anti-leishmanial agents. The anti-leishmanial drug discovery efforts at the Walter Reed Army Institute (USA) led to the discovery of an 8-aminoquinoline analogue termed sitamaquine (WR6026) (Dietze, *et al.*, 2001). Sitamaquine (4-methyl-6-methoxy-8-aminoquinoline) was found to be effective against both Old and New World visceral leishmaniasis in the clinical trials with a variable cure rate of 67-92% (Wasunna, *et al.*, 2005). Like miltefosine, sitamaquine is administered orally with a dose of 1.7-2mg/kg/day for 28 days (Jha, *et al.*, 2005). The mechanism of action of sitamaquine is currently unknown. It was initially proposed that sitamaquine rapidly accumulates into acidocalcisomes (acid vacuoles containing most of the cellular calcium) causing alkalization of the acidic vacuoles, which may have an effect on parasite survival in the host cells (Vercesi, *et al.*, 2000). However, it was subsequently reported that accumulation of the drug in acidocalcisomes is not related to its anti-leishmanial activity (Lopez-Martin, *et al.*, 2008). Coimbra *et al* subsequently demonstrated that the sitamaquine accumulation happens in the cytosol rather than in the acidocalsisomes (Coimbra, *et al.*, 2010). Sitamaquine resistance has been observed in *L. donovani* promastigotes. Sitamaquine was 10 folds more active in the wild strain as compared to the resistant strain Sita-R160. It was proposed that the sitamaquine resistance is related to alteration in choline kinase activity and phosphatidylethanolamine-N-methyl-transferase with a decrease in ergosterol biosynthesis also observed (Imbert, *et al.*, 2014).

Tafenoquine (8-aminoquinoline) was designed as a synthetic analog of primaquine by GlaxoSmithKline, in partnership with Medicines for Malaria Venture. It was found to be active against *Leishmania* both *in vitro* and *in vivo*, demonstrating potential as an oral anti-leishmanial agent (Yardley, Gamarro, and Croft 2010). Tafenoquine has been demonstrated to target mitochondria, leading to an apoptosis-like death in *Leishmania* (Carvalho et al. 2010).

4-amino-7-chloroquinoline derivatives have also been synthesized and evaluated for their anti-leishmanial properties against promastigotes of different *Leishmania* species. Of all the compounds tested, one of the derivatives containing the amino group, was found to be most active with an IC_{50} value of 10 nM against *L. infantum* promastigotes, unfortunately the compounds were not tested for axenic or intracellular

amastigotes (Carmo, *et al.*, 2011). No further progressions of these compounds have been reported.

The *in vitro* anti-leishmanial activity against *L. donovani* DD8 was assessed for 2-substituted series of strylquinolines and 7-aroylstrylquinolines (Loiseau, *et al.*, 2011). The most active compound within the strylquinoline compound class exhibited an IC_{50} of 4.1 µM against intracellular amastigotes with a selectivity of 8.3-fold. The other active compound reported from the 7-aroylstrylquinolines tested exhibited an IC_{50} value of 1.2 µM against intracellular amastigotes with a selectivity of 121.5-fold.

Ablordeppey *et al* isolated an indoloquinoline alkaloid Cryptolepine from a medicinal plant *Cryptolepis sanguinolenta* (Ablordeppey, *et al.*, 1999). Hazara *et al* evaluated the anti-leishmanial properties of cryptolepine and its derivatives against the promastigote form of the *L. donovani* strain (AG83) (Hazra, *et al.*, 2012). Cryptolepine exhibited an IC_{50} of 1.1 ± 0.3 µM, with a selectivity index of 0.7 against mouse peritoneal macrophage cells. In comparison, one of the derivatives, 2,7-dibromocryptolepine, demonstrated better activity (0.5 ± 0.1 µM) and significantly improved selectivity of ~18 fold (Hazra, *et al.*, 2012). This compound was taken forth as a prospective lead due to its activity against the intracellular amastigote forms of two clinical isolates, one of them being an antimony-resistant strain of *L. donovani* (Hazra, *et al.*, 2012). Mechanism of action studies were conducted, that revealed this compound disrupts the mitochondrial membrane integrity in terms of depolarization of membrane potential. It also induces apoptosis within the parasites by degradation of chromosomal DNA into oligonucleosomal fragments, which is a characteristic event of apoptosis (Hazra, *et al.*, 2012).

A novel series of 2-substituted nitroquinolines compounds were synthesized and evaluated for their anti-leishmanial properties against the promastigote and intracellular amastigote forms of *L. donovani*, and promastigote form of *L. infantum* parasite (Paloque, *et al.*, 2012). From this series, the most active compound was 2-hydroxy-8-nitroquinoline, which exhibited low activity for *L. infantum* promastigotes (IC_{50} value of 7.6 µM) and for *L. donovani* promastigotes and intracellular amastigotes IC_{50} values of 6.6 µM and 6.5 µM, respectively. This compound was found to have SI = 16.6 and 13.81 for the parasite when compared with its impact on human HepG2 and murine J774 cell lines, respectively.

R. Sharma *el al* discovered a novel series of 1,2,4-triazino-[5,6b]indole-3-thiones, which were linked covalently with 7-chloro-4-aminoquinoline (Sharma, *et al.*, 2014). The anti-leishmanial activity of these compounds was tested against the intracellular amastigote form of *L. donovani* DD8. One of the compounds demonstrated an IC_{50} value of 0.36 µM, with a ssignificant electivity ≥1111 fold for the parasites over the Vero cell line (Sharma, *et al.*, 2014).

A substituted quinoline compound was reported to have *in vitro* activity (IC_{50} = 0.22 ± 0.06 µM) against the *L. donovani* DD8 intracellular amastigotes and a selectivity index of 187.5 for the parasite over the Vero cells (Gopinath, *et al.*, 2013). This compound was discovered through collaboration between Advinus Therapeutics Ltd- India, CSIR-Central Drug Research Institute- India and Drugs for Neglected Diseases initiative (DNDi) - Switzerland. The compound was shown to have good *in vivo* activity and promising physiochemical propertines (Gopinath, *et al.*, 2013). The same group also performed further investigation of other analogues and reported an additional compound from the same class with an IC_{50} of 0.17 µM (Gopinath, *et al.*, 2014). Last reported the synthesized compounds could not achieve desired metabolic stability in liver microsomes (Gopinath, *et al.*, 2014).

The compound AMQ-j, a 4-aminoquinoline derivative, has shown potential anti-leishmanial activity against promastigote and intracellular amastigotes of *L. amazonensis* exhibiting IC_{50} values of 7.3 and 3.4 µM, respectively (Antinarelli, *et al.*, 2015). It was demonstrated that the mechanism of action of the compound is mitochondrial dysfunction of the parasite associated with reactive oxygen species (ROS) production (Antinarelli, *et al.*, 2015). ROS is produced by host macrophages during the phagocytosis of *Leishmania* parasites which in turn results in parasites death (Carneiro, *et al.*, 2016). To survive this harsh environment *Leishmania* parasites encounter within the host cells, the parasite regulates the lysosomal trafficking (LYST) proteins which result in the formation of parasitophorous vacuoles, within which the parasite resides (Gupta, *et al.*, 2013).

In a recent study conducted by Duarte *et al*, 8-hydroxyquinoline was reported to have anti-leishmanial activity with IC_{50} values of 2.9 ± 0.02, 0.55 ± 0.04 and 4.14 ± 0.06 µM for *L. amazonensis*, *L. infantum* and *L. braziliensis*, respectively (Duarte, *et al.*, 2016). These compounds have also have very good selectivity indices of 328.0, 62.0 and 47.0

in murine macrophages, making them promising candidates for anti-leishmanial drug discovery. It was also confirmed that 8-hydroxyquinolines caused an alteration in the mitochondrial membrane potential of the parasites (Duarte, *et al.*, 2016).

In a separate study, a novel quinoline derivative, QuinDer1, has been shown to be a promising anti-leishmanial hit, with an IC_{50} value of 0.09 μM against intracellular amastigotes of *L. amazonensis* and showing a selectivity index of 1062.8 for the parasite in relation to mouse macrophages (Coimbra, *et al.*, 2016). This compound resulted in the generation of high ROS levels in the macrophages with low alterations in mitochondrial membrane potential of the parasite and maintenance of parasite membrane integrity.

Quinacrine (mepacrine) is an acridine dye derivative and was the first known clinically tested anti-malarial (Valdés, 2011). 9-anilinoacridines have been shown to possess anti-leishmanial activity and novel derivatives were synthesized in order to increase parasite selectivity of the compound compared to the host cells (Mauel, *et al.*, 1993; Mesa-Valle, *et al.*, 1996; Gamage, *et al.*, 1997; Di Giorgio, *et al.*, 2003; Di Giorgio, *et al.*, 2007). The mechanism of action of these 9-Anilinoacridines indicates that they target the Topoisomerase II (Chawla and Madhubala, 2010). Topoisomerases are ubiquitous enzymes that play an important role in genomic stability during DNA recombination and torsional tensions caused during replication and transcription processes. Unfortunately, the pathway in the parasite is no different to that within the mammalian host cells, hence these compounds cause extensive cytotoxicity resulting in poor selectivity, therefore have not been progressed further. For cutaneous leishmaniasis (CL), quinacrine has been administered by intralesional injection or infiltration (Berberian, 1945).

For the 1H-Cyclopenta[b]quinolin-9-amine compounds identified as part of this project (**BZ1** and **BZ1-I**), one of the first parameters studied was the time and concentration dependent susceptibility of these compounds, in addition to mode of action in comparison to known reference compounds / drugs. Compound activity can either be cidal or static in nature. Cidal activity refers to the potential direct killing effect of the compound, whereas the static activity is defined as the effect of the compound to hinder the division process of the parasite, thus delayed response. The time to kill can serve as a determinant of anti-leishmanial compound efficacy relative to the time needed to clear

the infection, ideally as fast as possible. Usually 48 hours treatment is considered the optimal time point to accurately discriminate between fast and slow acting compounds (Tegazzini, *et al.*, 2017). Host cell pre-incubation studies with the compounds were also conducted to see whether the compounds have any immunotherapeutic effect on the transformed THP-1 cells, rather than directly affecting the parasite.

As discussed above, quinoline compounds have been shown to induce apoptosis as a possible mechanism of action (Hazra, *et al.*, 2012; Duarte, *et al.*, 2016). Taking into account the literature regarding the possible mechanism of action of quinolines, we investigated whether the 1H-Cyclopenta[b]quinolin-9-amine compounds induced any apoptotic features, such as externalization of phosphatidylserine and activation of the Caspase-3/7 pathway which are the hallmarks of apoptosis. Cells respond to specific induction signals by initiating intracellular processes that result in characteristic physiological changes. Among these is the externalization of phosphatidylserine (PS) to the cell surface, cleavage and degradation of specific cellular proteins, compaction and fragmentation of nuclear chromatin, plus the loss of membrane integrity (in late stages) (Majno and Joris, 1995). Muse® Caspase-3/7 Assay Kit was used for the quantitative analysis of live, early and late apoptosis, as well as cell death on both the parasites and host cells. The effect of the compounds on the mitochondrial morphology was also determined using MitoTracker Deep Red staining. MitoTracker dyes are a class of cell permeable fluorescent probes that are based on a mildly thiol-reactive chloromethyl moiety specific for staining mitochondria.

Another feature that has been of interest recently in the anti-leishmanial drug discovery field is the efficacy of a compound based on its pH stability crossing from interstitial fluid (pH 7.4) into the parasitopharous vacuole (pH 5.5), in which the parasite resides (Lievin-Le Moal and Loiseau, 2016; Semini and Aebischer, 2017). It is well established that development and proliferation of *Leishmania* intracellular amastigotes is dependent on the acidic niche (pH 4.5-5.5) of the phagolysosomes within the mammalian host cells (Glaser, *et al.*, 1988; Zilberstein and Shapira, 1994) as depicted in Figure 5.2. This raises the question regarding the ability of the parasite to adapt to this harsh environment and maintain a physiological intracellular pH within the acidic

environment of the parasitophorous vacuoles. The other question is how the parasite uses the environment with protons abundantly available to its own benefit?

Transport systems regulating intracellular ion concentrations, such as Na^+, have served as fundamental factors for cell homeostasis for protists (Rodriguez-Navarro and Benito, 2010). The presence of P-type Na^+ ATPases (ENA-ATPases) has been reported in *Trypanosoma cruzi*, *Trypanosoma brucei* and *Leishmania* (Stiles, *et al.*, 2003). The P-type Na^+ ATPases function to induce Na^+ efflux. This has further been proved with the use of the Na^+-ATPase inhibitor furosemide, which kills the promastigotes in *L. amazonensis* (Arruda-Costa, *et al.*, 2017), while the K^+Na^+-ATPase inhibitor ouabain has no effect on them (de Almeida-Amaral, *et al.*, 2008). Other mechanisms have also been reported in which it has been shown that carbonic anhydrase activity is essential for *Leishmania* parasites to maintain successful colonization of the acidic phagolysosome (Pal, *et al.*, 2015).

In this chapter, the stability of the compounds, **BZ1** and **BZ1-I,** within various pH environments was ascertained. Additional potential reasons for the differences in activity of these compounds on the promastigote and intracellular amastigote forms of the parasite have also been investigated.

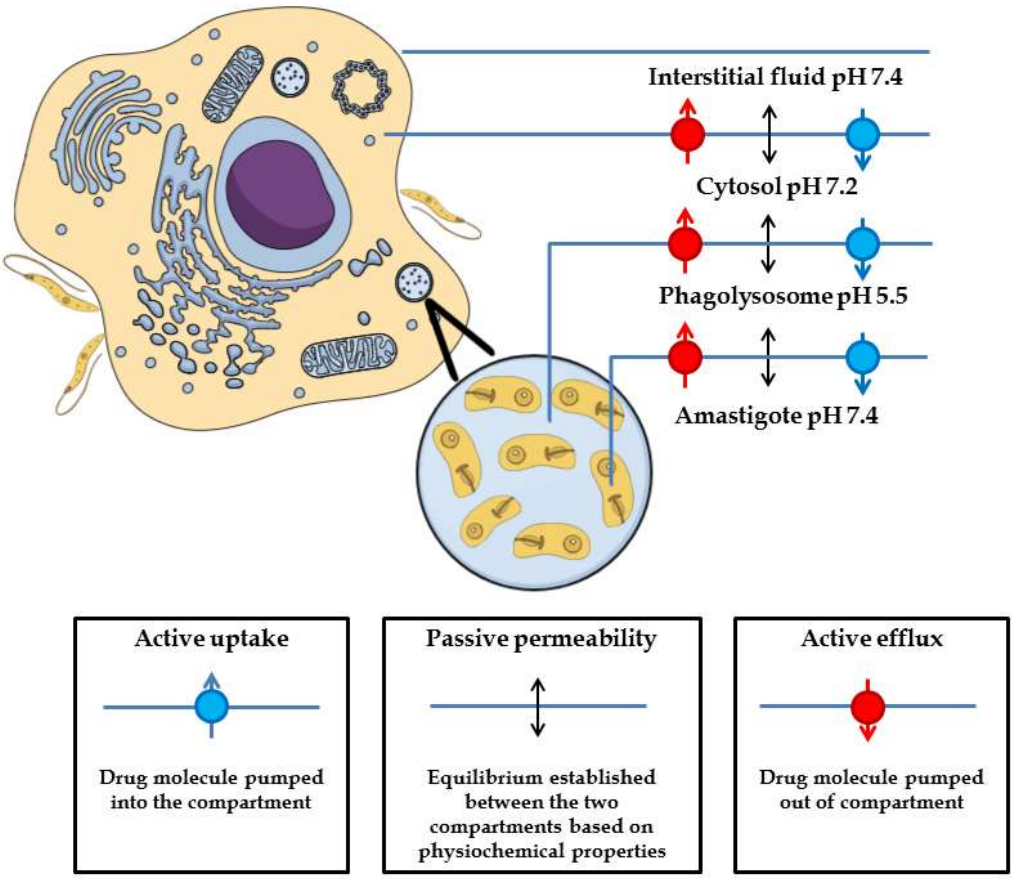

Figure 5.2: The different pH barriers of interstitial fluid, cytosol and phagolysosome which a compound/drug must pass through to reach the *Leishmania* intracellular amastigote.

5.1.1. Drug resistance

Currently, one of the most serious health problems for many diseases, not just *Leishmania*, is drug resistance. The occurrence of drug resistance makes it difficult to control diseases caused by the wide variety of organisms (Ouellette and Ward, 2002). Various approaches, phenotypic genomics, transcriptome and proteomics have been carried out in order to elucidate the mechanisms of resistance present in pathogens (Kaye and Kaye, 2000). However, taking into account the heterogeneity of the population of a particular pathogen, e.g. *Leishmania* spp., *T. cruzi*, or *T. brucei*, or the biological states of that organism (dysgenetic life cycle), not necessarily the same mechanisms of resistance occurs in all organisms of the population present in a certain

endemic region (Field, *et al.*, 2017). Hence, it is of great importance to establish whether the mechanisms of resistance vary with the genotype of the pathogen.

Some conceptual definitions are required to understand the phenomenon of resistance, for example the distinction between failure in the treatment and resistance to the action of a drug. Treatment failure is a multi-factorial clinical phenotype (e.g. immune response and/or pharmacogenetics, among other factors), where the patient does not have an effective response to the drug, while the resistance of the pathogen is a phenotype related to the survival of the parasite to the action of the drug. Treatment failure can also be multi-factorial for example, selected differential genetic expressions, leading to the definitions of intrinsic and acquired resistance. Intrinsic resistance originates from particular biochemical characteristics of the parasite, independent of previous contact with the drug, while the acquired resistance is selected in the presence of the drug. In the case of pathogens such as *Leishmania* spp., given their inter-and intra-specific variability, differences in response to a particular drug is not surprising (Croft, *et al.*, 2006). These differences contribute as important implications in the research and development of new drugs (Field, *et al.*, 2017; Hefnawy, *et al.*, 2017).

The functional validation of genes involved in resistance is decisive in order to establish their role in the mechanism of resistance and therefore potential as markers of resistance (Lamotte, *et al.*, 2017). Using the information generated from the diversity of genome projects of different pathogens, as well as the new technological arsenal, including molecular modelling and computational analysis, new approaches have emerged for the identification and evaluation of old and new drug targets (Dougherty, *et al.*, 2017). This includes the *in silico* evaluation of chemical libraries in the search for new compounds less toxic to the host cells and more effective on the parasites in their action (Liu, *et al.*, 2017).

The possible mechanism conferring amphotericin B resistance in *L. donovani* has been previously reported; and includes mechanisms such as altered membrane composition, up-regulation of thiol metabolic pathways and ABC transporters (Purkait, *et al.*, 2012; Kumar, *et al.*, 2014). It has also been reported that in amphotericin B resistant parasites, ergosterol, which is the main component in parasite membranes, is replaced by one of its precursors cholesta-5,7,24- trien-3-ol, which confer a weak affinity of amphotericin B for such modified membranes (Mbongo, *et al.*, 1998).

Miltefosine resistant promastigotes present a defect in the inward-directed translocation across the plasma membrane through inactivation of the *L. donovani* putative miltefosine-transporter (LdMT) (Pérez-Victoria *et al.* 2003). LdMT localizes to the plasma membrane, and it's overexpression significantly increases the uptake of ^{14}CMIL in *Leishmania tarentolae*, a species non-sensitive to MIL, strongly suggesting that this protein behaves as a true translocase (Pérez-Victoria *et al.* 2003) and/or its beta subunit LdRos3 (Pérez-Victoria *et al.* 2006) or by an increased efflux mediated by the overexpression of ABC-transporter proteins (Castanys-Muñoz *et al.* 2008). Mishra and Singh have shown in their studies that miltefosine resistant cells remained protected against gradual ATP loss, loss of mitochondrial potential and loss of cytochrome c release from mitochondria into the cytosol (Mishra and Singh, 2013). They also reported using comparative transcriptomics that increased expression of Silent Information Regulator 2 (SIR2) and Fe Superoxide dismutase (FeSODA) genes are involved in oxidative stress associated apoptotic cell death.

To investigate the mechanistic aspects of the effect of the newly identified anti-leishmanial compounds, 1H-Cyclopenta[b]quinolin-9-amine, resistant parasites against the two key compounds, **BZ1** and **BZ1-I**, resistant parasites were established. After validation and further biological characterization of these resistant strains, whole genome sequencing analysis will be performed to ascertain the target gene.

The collective outcomes from the mode of action, mechanism of action and resistance studies undertaken for compounds **BZ-1** and **BZ1-I**, will be discussed in this chapter and related to current literature for this class of compounds.

5.2. Materials and Methods

5.2.1. Determination of the cidal action of compounds

To determine the cidal action of the selected compounds, the promastigotes from two different cultures in two separate M199 media (N=2) were seeded at a concentration of $5x10^5$ parasites/mL and volume of 55 µL/well in Greiner 384-well plates using a Bravo liquid handler. A master compound plate was created with the compounds dissolved in 100% DMSO diluted in M199 + 10% HIFBS media using a dilution plate with the final

assay concentration of 66.660, 33.330, 16.660, 6.660, 3.330, 1.660, 0.660, 0.330, 0.160, 0.06, 0.033, 0.016, 0.006 and 0.003 µM. The assay conditions were as previously described in chapter 2 section 2.3.1 following exposure of promastigotes to compounds **BZ1**, **BZ1-I** and reference drugs at the above mentioned concentrations for 24, 48 and 72 hours.

The compounds were dispensed from the master plate to the assay plate in a volume of 5 µL into 55 uL of parasite culture / well. Cell numbers were determined using the method described previously (Sykes, *et al.*, 2012). If no cells were identified at the above concentrations, compounds were considered to have been effectively cidal at that time point.

5.2.2. Time to kill assay

5.2.2.1. Promastigote viability assay

In order to calculate the time to kill for compounds in the promastigote assay the IC_{50} values were determined for compounds BZ1, BZ1-I and reference compounds (amphotericin B and miltefosine) following exposure of the promastigotes to compound and reference drugs for 24, 48 and 72 hours. The starting concentration was 40 µM and the IC_{50} values were determined from a 14 point concentration-response curve. The assay conditions were the same as previously described chapter 2 section 2.3.1 for the promastigote viability assay, except the variation in final compound incubation time (24, 48, 72 and 96 hours).

5.2.2.2. Intracellular amastigote assay

In order to calculate the time to kill for compounds in the intracellular amastigote assay the IC_{50} values were determined for compounds BZ1, BZ1-I and reference drugs (amphotericin B and miltefosine) following incubation for 24, 48 and 72 hours. The starting concentration was 40 µM and the IC_{50} values were determined from a 14 point concentration-response curve. The assay conditions were the same as previously described for the intracellular amastigote assay in chapter 2 section 2.3.2, except for the variation in final compound incubation time (24, 48, 72 and 96 hours).

5.2.3. Host cell and compound pre-incubation studies

A study was performed to assess the percentage infectivity in the host cells after pre-incubation with **BZ1**, **BZ1-I** and reference drugs (amphotericin B and miltefosine) at various time points (12, 24, 48 and 72 hours). THP-1 cells were plated as described previously in chapter 2, section 2.3.2. After 24 hours, cells were washed 3 times with PBS and 45 µL RMPI + 10% HIFBS (v/v) added to the assay plates. The reference compounds and **BZ1** and **BZ1-I** were diluted 1:25 in RPMI with no HIFBS with a final assay concentration in a 14 point concentration response ranging from 80µM to 0.004 µM. Five µL were dispensed into assay plates using a Bravo liquid handler. The assay plates were incubated for 24, 48 and 72 hours at 37°C / 5% CO_2. After 24, 48 and 72 hours the plates were washed 3 times with PBS. The addition of parasites, washing the extracellular parasites away and staining the plates were subsequently performed as mentioned previously (chapter 2, section 2.3.2).

5.2.4. Extent of externalization of phosphatidylserine after exposure with the compounds

To determine the extent of externalization of phosphatidylserine after exposure of the promastigotes with the compounds at different time points (12, 24, 48 and 72 hours) the Muse™ Annexin V & Dead Cell Assay kit was used. The Muse™ Annexin V & Dead Cell Assay allows for the quantitative analysis of parasites which are live, in early or late apoptosis, as well as cell death of both adherent and suspension cell lines on the Muse™.

Four populations of cells were distinguished in this assay:

• Non-apoptotic cells: Annexin V (-) and 7-AAD (-)

• Early apoptotic cells: Annexin V (+) and 7-AAD (-)

• Late stage apoptotic and dead cells: Annexin V (+) and 7-AAD (+)

• Mostly nuclear debris: Annexin V (-) and 7-AAD (+)

Promastigotes were sub-cultured in flasks as previously described in section 2.2.1, following exposure to **BZ1**, **BZ1-I** and reference drugs for 12, 24, 48 and 72 hours. The negative control in this experiment was 0.4% DMSO (vehicle) and the positive control was 5 µM miltefosine. Amphotericin B was added to the cultures at the IC_{50} value of 0.1 µM, **BZ1** at 2.5 µM and **BZ1-I** as 0.5 µM and cultures were incubated for different time points as mentioned above. To determine the extent of externalization of phosphatidylserine after exposure to the compounds, cell counts were performed using a haemocytometer and the parasites were diluted to $1x10^6$ parasites/mL in media containing the same concentration of controls and compounds. 100 µL of diluted culture was added to each sample tube (N=2), followed by the addition of 100 µL of the Muse™ Annexin V & Dead Cell Reagent to each tube. Samples were mixed thoroughly by pipetting up and down or vortexing at a medium speed for 3 to 5 seconds. Samples were stained for 20 minutes at room temperature in the dark and read on the Muse™.

To assess the extent of activation thus externalization of phosphatidylserine after exposure with the compounds and controls in host cells (THP-1) the above procedure was used with a THP-1 cell concentration of $2.5x10^5$ cells/mL.

5.2.5. Activation of Caspase-3/7 pathway

To determine the activation of the Caspase-3/7 pathway after exposure with the compounds at different time points (12, 24, 48 and 72 hours) the Muse™ Caspase-3/7 Kit was used. The Muse™ Caspase-3/7 Kit allows for the facile, rapid, and quantitative measurements of two important cell health parameters simultaneously apoptotic status based on Caspase-3/7 activation, cellular plasma membrane permeabilization and cell death. Four populations of cells can be distinguished:

• (LL) Live cells: Caspase-3/7(–) and 7-AAD(–)

• (LR) Apoptotic cells exhibiting Caspase-3/7 activity: Caspase-3/7 (+) and 7-AAD(–)

• (UR) Late Apoptotic/Dead cells: Caspase-3/7(+) and 7-AAD(+)

• (UL) Necrotic cells: Caspase-3/7(–) and 7-AAD (+)

Promastigotes were sub-cultured in flasks as previously described in section 2.2.2 following exposure to compounds **BZ1**, **BZ1-I** and reference drugs for 12, 24, 48 and 72 hours. The negative control was 0.4% DMSO and the positive control, 5 µM miltefosine. Amphotericin B was added to the cultures at its IC_{50} value of 0.1 µM, **BZ1** at 2.5 µM and **BZ1-I** as 0.5 µM and cultures were incubated for different time points as mentioned in section 2.2.2. The Muse™ Caspase-3/7 Reagent working solution was prepared by diluting the stock solution 1:8 in 1X PBS. Each sample to be tested required 5 µL of the Muse™ Caspase-3/7 working solution. The Muse™ Caspase 7-AAD working solution was prepared by the addition of 2 µL of Muse™ Caspase 7-AAD stock solution to 148 µL of 1X Assay Buffer BA. To determine the activation of Caspase-3/7 pathway after exposure with the compounds, cell counts were performed using a haemocytometer and the parasites were diluted to $1x10^6$ parasites/mL in media containing the same concentration of controls and compounds. 100 µL of diluted culture was added to each sample tube (N=2) and 5 µL of Muse™ Caspase-3/7 Reagent working solution added to each tube. Samples were mixed thoroughly by pipetting up and down or vortexing at a medium speed for 3 to 5 seconds. Sample tubes were loosely caped and incubate for 30 minutes at 37°C with 5% CO_2. After incubation, 150 µL of Muse™ Caspase 7-AAD working solution was added to each tube. Samples were again mixed and then incubated at room temperature for 5 minutes, protected from light and read on MUSE™.

To assess the activation of Caspase-3/7 pathway after exposure with the compounds and controls in host cells (THP-1) the above procedure was used with a cell concentration of $2.5x10^5$ cells/mL.

5.2.6. Compound effect on mitochondrial morphology

To determine the cidal action of compounds, the promastigotes from two different cultures in two separate M199 media (N=2) were seeded at a concentration of $5x10^5$ parasites/mL and volume of 55 µL/well in Greiner 384-well plates using a Bravo liquid handler. Amphotericin B, miltefosine, VL-2098, **BZ1** and **BZ1-I** compounds were added to parasites in a 14-point concentration response format. After 12, 24, 48 and 72 hours incubation at 27ºC, the media/parasite from Greiner 384-well plates was removed and transferred to a collagen I coated 384-well plate. The plates were centrifuged at

3000 rpm for 8 minutes and media was removed, leaving a 10 µL dead volume. The plates were washed twice with PBS ($CaCl_2$ + $MgCl_2$) and centrifuged (3000 rpm/8 minutes) in between each wash. While removing PBS, 10 µL dead volume was left at the bottom of the well after each wash step. MitoTracker™ Red CM-H2Xros was prepared as a 1mM solution and then diluted as a 500 nM solution in media containing no FBS, and 50 µL was added to each well. Plates were incubated for 30 minutes at 37°C in light-protected conditions. Excess Mitotracker Red was removed by washing twice with PBS as above. Hoechst was prepared as a 5 µM solution, and 50 µL of this solution added to each well diluted in 4% PFA at a ratio of 1/500. Unincorporated hoechst was removed by washing twice with PBS as above and 50 µL of media with no FBS added. The positive controls used for the assay are m-chlorocarbonylcyanide phenylhydrazone (CCCP), which is a mitochondrial uncoupler, and valinomycin, a respiratory chain inhibitor. CCCP and valinomycin were added to the control wells in the final assay concentration of 50 µM. The negative control in the assay was 0.4% DMSO.

5.2.7. Selection of resistant parasites

Amphotericin B, miltefosine and compounds **BZ1** and **BZ1-I** were used to select for resistant parasites to assess any differences in THP-1 cell infectivity and whether resistance could be maintained in the intracellular amastigote assay. The promastigotes were cultured in the presence of gradually increasing concentrations of amphotericin B, miltefosine, and either compound **BZ1** or **BZ1-I** beginning at starting concentrations of 0.000135 µM (0.125 µg/mL), 0.03330 µM (13.572 µg/mL), 0.0033 µM (1.004 µg/mL) and 0.0033 µM (1.004 µg/mL) respectively, (a sublethal concentration) to generate drug-resistantstrains. Throughout the process the concentrations for amphotericin B, miltefosine, **BZ1** and **BZ1-I** were increased gradually and only once the cells displayed growth and mobility characteristics after 96 hours incubation comparable to the control cultures grown in the absence of compounds.

Three independent experiments were performed (the promastigotes from three different cultures in three separate M199 media were seeded in 25 cm² flasks at a concentration of $5x10^5$ promastigotes/mL in a volume of 10 mL) with amphotericin B, miltefosine, compounds **BZ1** and **BZ1-I** at sublethal concentrations. These cultures were sub-

cultured every 96 hours with the addition of amphotericin B, miltefosine, compounds **BZ1** and **BZ1-I**.

5.2.7.1. Confirmation of resistant cell lines

For confirming resistance, clonal populations from the resistant parasites were obtained via limiting dilution in a 384-well plate and the confirmation of resistant studies performed on isolated clones.

For confirming resistance, clonal populations from the resistant parasites were obtained via limiting dilution in a 384-well plate and the confirmation of resistant studies performed on isolated clones.

To confirm resistance of these cell lines, a promastigote viability assay was performed (refer to section 2.3.1). Following confirmation that resistance in the promastigotes was achieved, these cultures were used to infect the THP-1 cells and the infectivity of the cells was assessed. In addition, resistance to amphotericin B, miltefosine, compound **BZ1** and **BZ1-I** were also assessed with the intracellular amastigote assay (refer to section 2.3.2).

5.2.7.2. Stability of compound resistance assessed

Following generation of resistant cultures, the sensitivity to the reference drugs (amphotericin B and miltefosine), plus test compounds **BZ1** and **BZ1-I**, were evaluated. In addition, the stability of drug resistance post drug pressure removal throughout time in culture, was assessed. The resistant parasite cultures were grown in the absence of amphotericin B, miltefosine, compounds **BZ1** and **BZ1-I** for 10 passages before the sensitivities of the cultures to these compounds and drugs were retested in the promastigote viability assay and intracellular amastigote assays. This experiment provided an indication as to whether the generated resistance was reversible or not.

5.2.8. pH stability studies for the compounds

Compounds **BZ1** and **BZ1-I** were prepared as 20 mM stock solutions in 100% DMSO and then diluted to a concentration of 0.5 µM in water. Samples were processed using

high-resolution liquid chromatography (Agilent 1100 LC) coupled with Bruker MaXis II QTOF. HRLC separation was performed with a phenomenex Luna C18, 50 x 4.60 mm, 3 u. For the HRLC gradient the mobile phases consisted of two solvents: methanol with 0.1% formic acid and water with 0.1% formic acid, with an injection volume of 20 uL. The gradient profile used was 0-1 min 5% MeOH(with 0.1% FA)/ 95% H2O(with 0.1% FA), 1-10 min gradient to 100% MeOH(with 0.1% FA)/ 0% H2O(with 0.1% FA), 10-11 min gradient to 5% MeOH(with 0.1% FA)/ 95% H2O(with 0.1% FA), 11-12 min 5% MeOH(with 0.1% FA)/ 95% H2O(with 0.1% FA) with a flow rate 1 ml/min with a 1/5 splitting to the QTOF.

5.3. Results

5.3.1. Determining cidal action of compounds

Measurement of the number of promastigotes following exposure to the compounds during 24, 48 and 72 hours are shown in the figure 5.3. A complete lack of viable promastigotes was observed for Amphotericin B, Miltefosine, BZ1 and BZ1-I from 0.33 µM, 6.66 µM, 6.66 µM and 1.66 µM to higher concentrations, respectively.

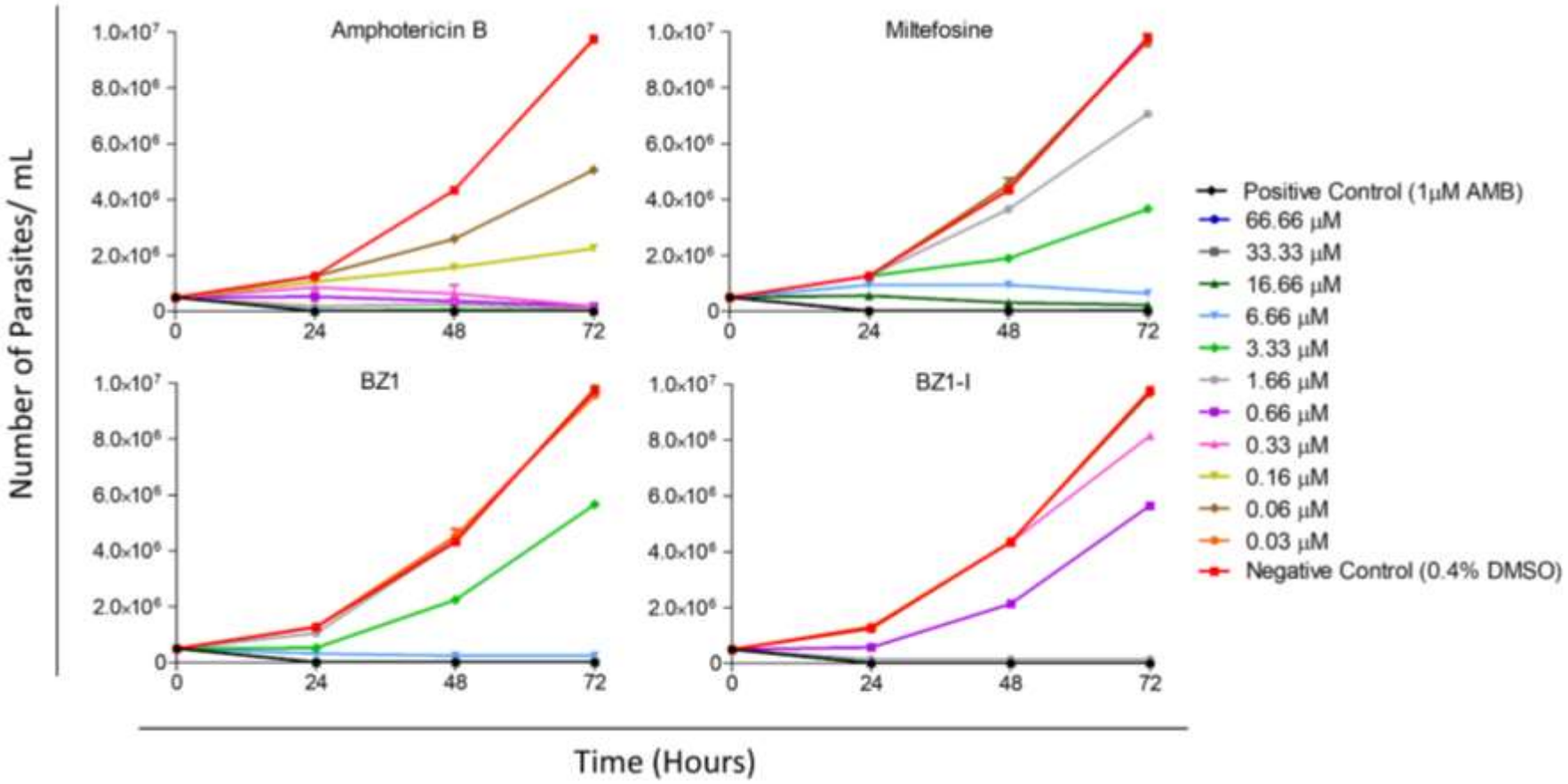

Figure 5.3: Cidal activity of amphotericin B, miltefosine, compound BZ1 and BZ1-I based on various concentrations at different time intervals 24, 48 and 72 hours. Each evaluation was performed in triplicate, for N=2. One way ANOVA P value: 0.42

1

5.3.2. Time to kill assay

5.3.2.1. Promastigote viability assay

Compound **BZ1** was demonstrated to have a stable plateau of activity against the *L. donovani* DD8 promastigotes from 24 hours onwards (Figure 5.4A). In contrast, compound **BZ1-I** was partially active at 24 hours with a stable plateau of activity only achieved after 48, 72 and 96 hours against the *L. donovani* DD8 promastigotes (Figure 5.4B).

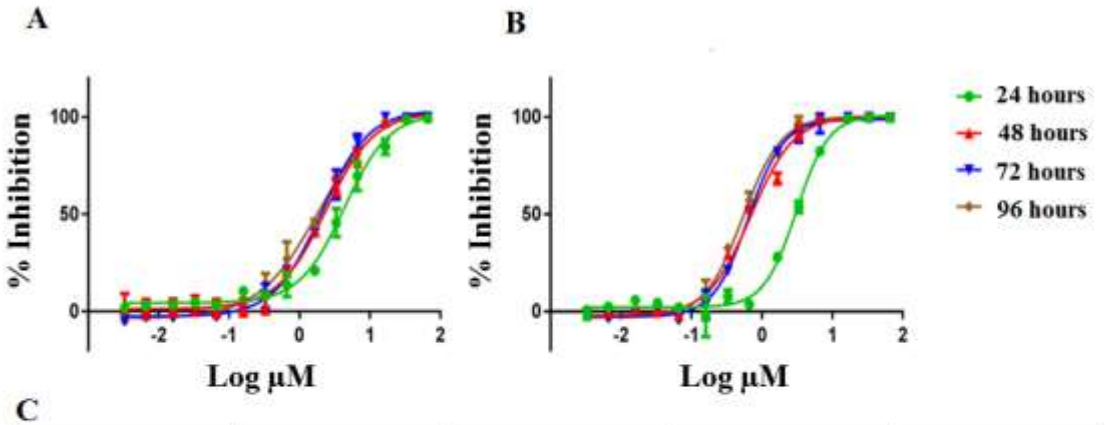

C

	24 Hours IC_{50} µM (Average ± S.D)	48 Hours IC_{50} µM (Average ± S.D)	72 Hours IC_{50} µM (Average ± S.D)	96 Hours IC_{50} µM (Average ± S.D)
BZ1	4.31 ± 0.22	2.37 ± 0.74	2.04 ± 0.77	2.37 ± 0.85
BZ1-I	3.08 ± 1.11	0.69 ± 0.35	0.64 ± 0.16	0.54 ± 0.27

Figure 5.4: Concentration response curve obtained for compounds (A) BZ1 and (B) BZ1-I and (C) IC_{50} values obtained for promastigote viability assay at various time points 24, 48, 72 and 96 hours. Each evaluation was performed in triplicate, for N=2.

5.3.2.2. Intracellular amastigote assay

The compound **BZ1** demonstrated a stable plateau of 100% inhibitory activity against *L. donovani* DD8 intracellular amastigotes following exposure for 48, 72 and 96 hours, as illustrated in figure 5.5A. A stable plateau of activity was not observed for the 24 hour time point. Compound **BZ1-I** was only active against *L. donovani* DD8 intracellular amastigotes at the 72 and 96 hour incubation time points, with a stable plateau of activity shown in the concentration response curve (Figure 5.5B). A stable plateau of activity was not observed for either the 24 or 48 hour time point.

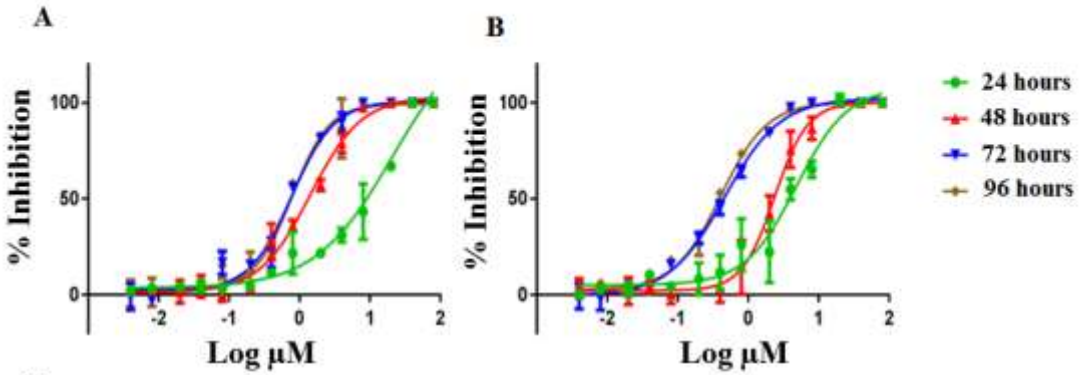

C

	24 Hours IC_{50} µM (Average ± S.D)	48 Hours IC_{50} µM (Average ± S.D)	72 Hours IC_{50} µM (Average ± S.D)	96 Hours IC_{50} µM (Average ± S.D)
BZ1	-	1.43 ± 0.22	0.781 ± 0.27	0.59 ± 0.13
BZ1-I	4.84 ± 0.83	2.38 ± 0.84	0.45 ± 0.28	0.40 ± 0.38

Figure 5.5: Concentration response curve obtained for compounds (A) BZ1 and (B) BZ1-I and (C) IC_{50} values obtained for intracellular amastigote assay at various time points 24, 48, 72 and 96 hours. Each evaluation was performed in triplicate, for N=2.

5.3.3. Compound pre-incubation Studies

Percentage infectivity of the host cells (PMA activated THP-1 cells) with the *L. donovani* DD8 intracellular amastigotes was assessed after pre-incubation of the cells with the reference drugs (amphotericin B and miltefosine) and compounds (BZ1 and BZ1-I) for 12, 24, 48 and 72 hours (Figure 5.6). The data was normalized based on percentage infectivity, rather than number of infected cells. It was observed that a concentration response curve could not be established at 12 or 24 hours for amphotericin B, nor for compounds **BZ1** and **BZ1-I**. For miltefosine a stable concentration response curve was established at 24 hours onwards.

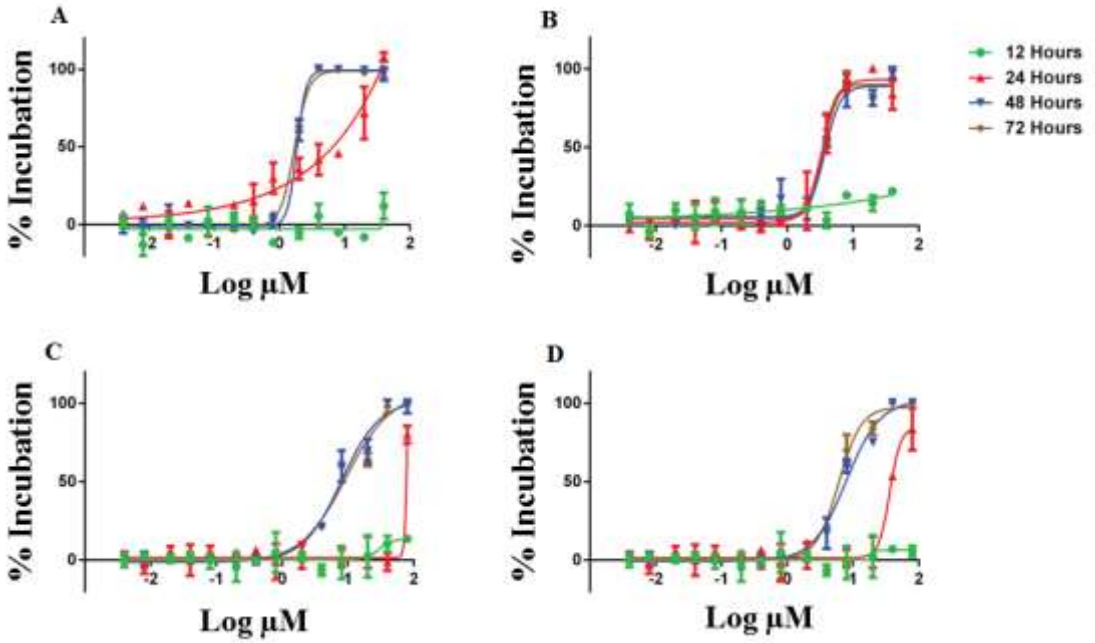

Figure 5.6: Host cell pre-incubation studies. Concentration response curves obtained for (A) amphotericin B, (B) miltefosine and compounds (C) **BZ1** and (D) **BZ1-I** treatment prior to infection in the intracellular amastigote assay at various time points 12, 24, 48 and 72 hours. Each evaluation was performed in triplicate, for N=2.

5.3.4. Extent of externalization of phosphatidylserine

The extent of externalization of phosphatidylserine on *L. donovani* DD8 promastigotes after exposure with the compounds and controls was assessed via a Muse™ Annexin V & Dead Cell Assay. It was observed that 22.68% of the *L. donovani* DD8 promastigotes died after exposure to amphotericin B at the IC_{50} concentration after 12 hours. In addition, the number of promastigote parasites going into early apoptosis starting to increase from 12 hours to 48 hours (9.98% to 30.56%) (Figure 5.7). For the positive control, 5 µM miltefosine, 85% of the promastigote population went into late stage apoptosis at 72 hours. For compounds **BZ1** and **BZ1-I**, 36.34% and 26.34% of the L. donovani DD8 promastigotes population died after 48 hours of exposure with the compounds. The cell populations were significantly reduced after 72 hours of exposure and most likely were counted as debris.

For the THP-1 host cells, 85.78% population went into late apoptotic/death phase with miltefosine (Figure 5.8). There was no effect observed on the host cells for amphotericin B, **BZ1** and **BZ1-I** when compared to negative control, even after 72 hours of exposure.

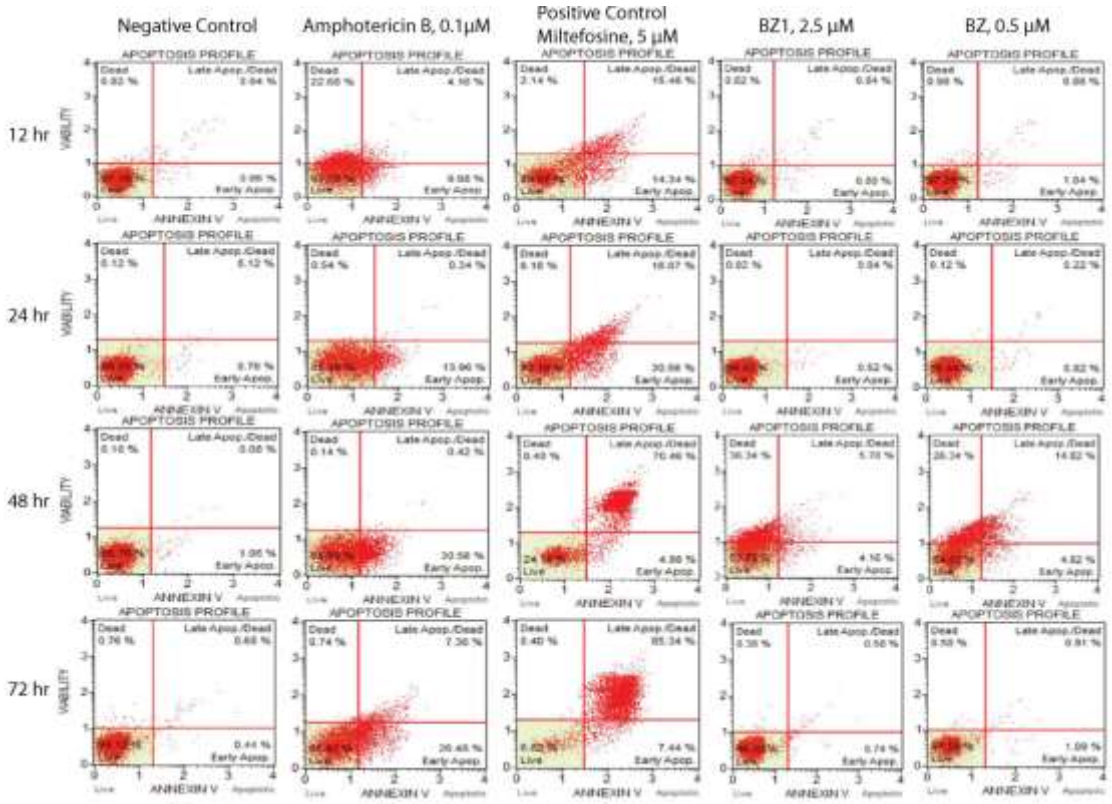

Figure 5.7: Extent of externalization of phosphatidylserine in *L. donovani* parasites after exposure with compounds BZ1, BZ1-I and control compounds at different time points (12, 24, 48 and 72 hours). Each evaluation was performed in duplicate, for N=2.

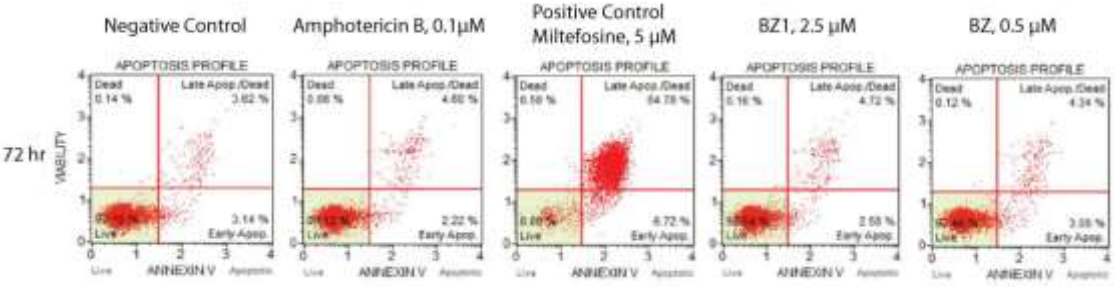

Figure 5.8: Extent of externalization of phosphatidylserine in THP-1 cells after exposure with compounds BZ1, BZ1-I and control compounds at 72 hours. Each evaluation was performed in duplicate, for N=2.

5.3.5. Activation of Caspase-3/7 pathway

The activation of the Caspase-3/7 pathway in *L. donovani* DD8 promastigotes and THP-1 host cells was was assessed after exposure with the compounds and controls via the Muse™ Caspase-3/7 Assay.

It was observed that 49.35% of the intial *L. donovani* DD8 promastigotes initial population died after exposure with concentrations of amphotericin B equivalent to the IC_{50} value (0.01 µM) after 12 hours incubation (Figure 5.9). For the positive control (miltefosine 5 µM), 13.05% of the *L. donovani* DD8 promastigotes went into late stage apoptosis after incubation for 48 hours. For compounds **BZ1** and **BZ1-I**, 32.95% and 25.10% of the *L. donovani* DD8 promastigotes died after 48 hours exposure to the compounds. The *L. donovani* DD8 promastigotes populations were significantly decreased after 72 hours exposure to **BZ1** and **BZ1-I**.

For the THP-1 host cells, 76.85% of the population were identified as being in the late apoptotic/death phase after exposure to miltefosine for 72 hours. This indicated that apoptosis was induced in THP-1 host cells after exposure with miltefosine for 72 hours due to activation of caspase 3/7 pathway (Figure 5.10). There was no effect on the host cells observed for amphotericin B, **BZ1** and **BZ1-I** when compared to the negative control, even after 72 hours of exposure.

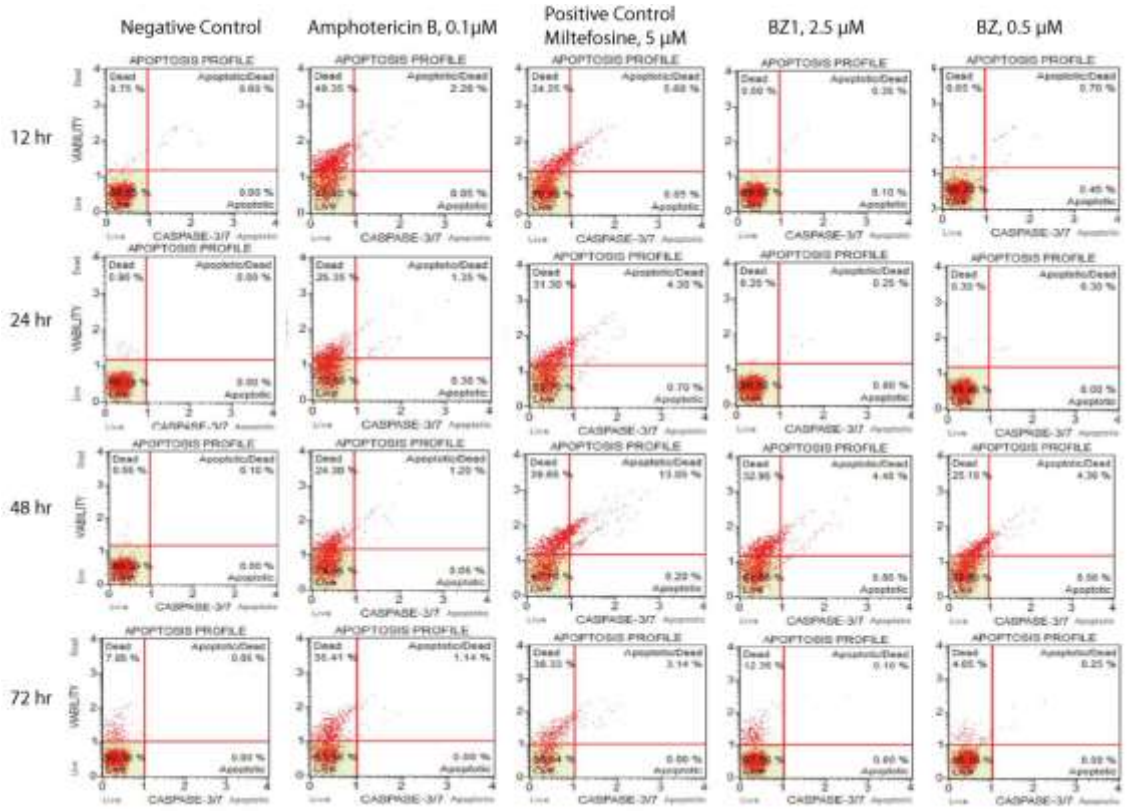

Figure 5.9: Activation of caspase 3/7 pathway in *L. donovani* parasites after exposure with compounds BZ1, BZ1-I and control compounds at different time points (12, 24, 48 and 72 hours). Each evaluation was performed in duplicate, for N=2.

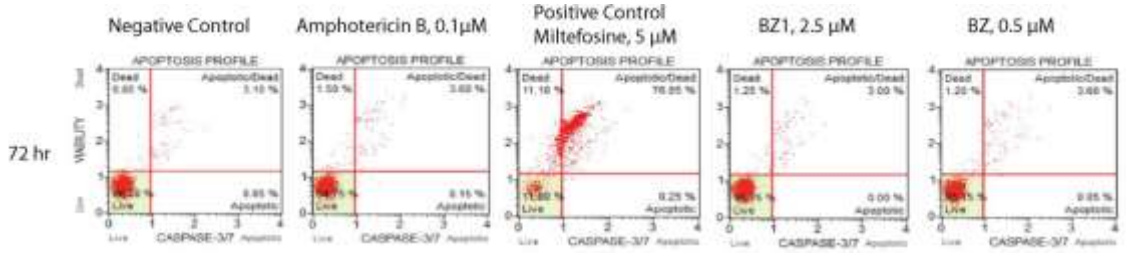

Figure 5.10: Activation of caspase 3/7 pathway in THP-1 cells after exposure with compounds BZ1, BZ1-I and control compounds at 72 hours. Each evaluation was performed in duplicate, for N=2.

5.3.6. Compound effects on mitochondrial morphology

The effect of the compounds **BZ1** and **BZ1-I** on the mitochondrial morphology of L. donovani DD8 promastigotes were assessed using MitoTracker Red CM-H2xRos. The percentage fluorescence per well was calculated after normalizing with the controls. As illustrated in figure 5.11, the positive controls, CCCP and valinomycin, significantly

inhibited the oxidative phosphorylation(P value < 0.001 compared to the negative control of 0.4% DMSO resulting in *L. donovani* DD8 parasite death (Figure 5.12). The reference drugs and compounds, such as amphotericin B, miltefosine and VL-2098, did not affect the mitochondrial morphology when *L. donovani* DD8 promastigotes were exposed to them at their IC_{50} concentrations. Similar results were obtained for compounds **BZ1** and **BZ1-I** at a concentration of 2.5 µM and 0.5 µM, respectively.

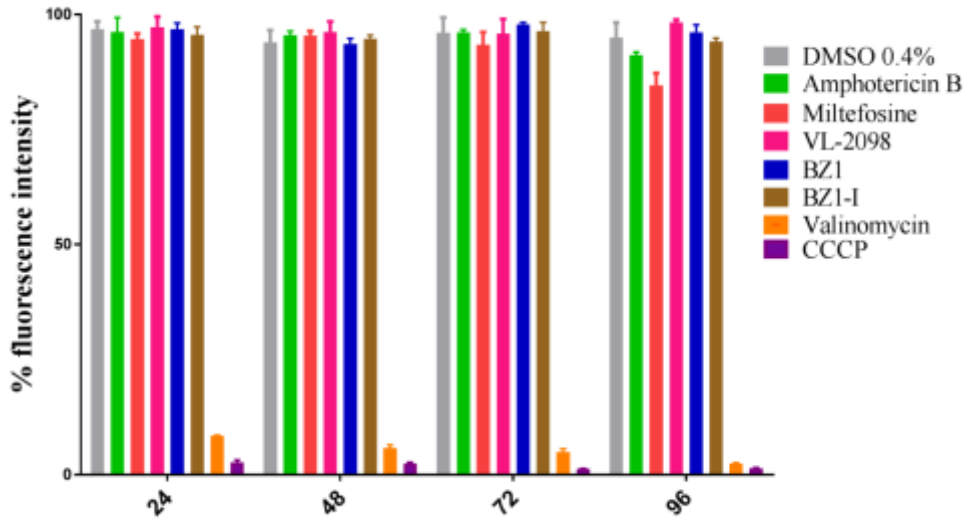

Figure 5.11: Effect of the compounds on the mitochondrial morphology. The positive control for the assay was CCCP and valinomycin both used at a concentration of 50 µM. The negative control for the assay was 0.4% DMSO. Amphotericin B, miltefosine, VL-2098, compound **BZ1** and **BZ1-I** were tested at the following concentrations: 0.1 µM, 3 µM, 0.1 µM, 2.5 µM and 0.5 µM.

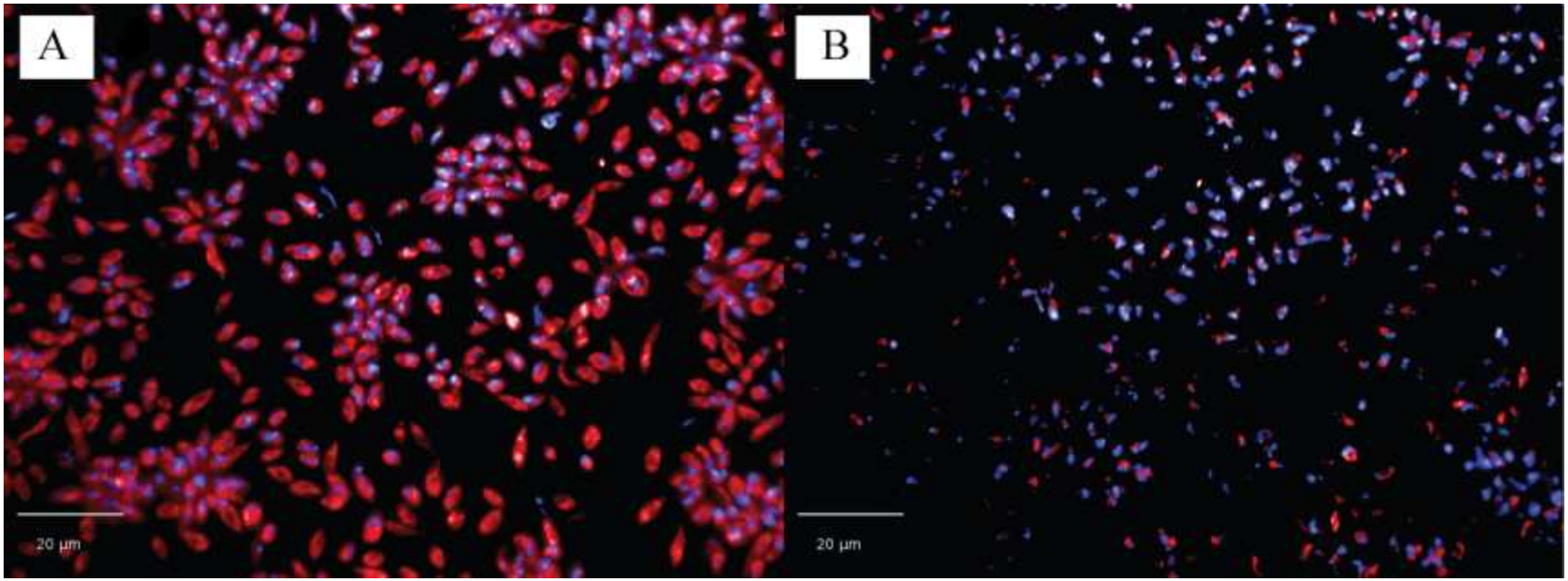

Figure 5.12: Effect of BZ1 and BZ1-I on the mitochondrial morphology measured using MitoTracker to stain the mitochondria and Hoescht to stain the parasite nucleus. (A) Negative control for the assay is 0.4% DMSO, (B) Positive control for the assay is CCCP at a concentration of 50 µM.

5.3.7. Generating resistant cell line

The resistant *L. donovani* parasites cultures were generated for amphotericin B, miltefosine, **BZ1** and **BZ1-I** reaching resistance of the compounds at 420 nM, 40 µM, 11 µM and 5.5 µM, respectively (Figure 5.13). It was observed that resistance in miltefosine was relatively easier to generate when compared to **BZ1**, **BZ1-I** and amphotericin B.

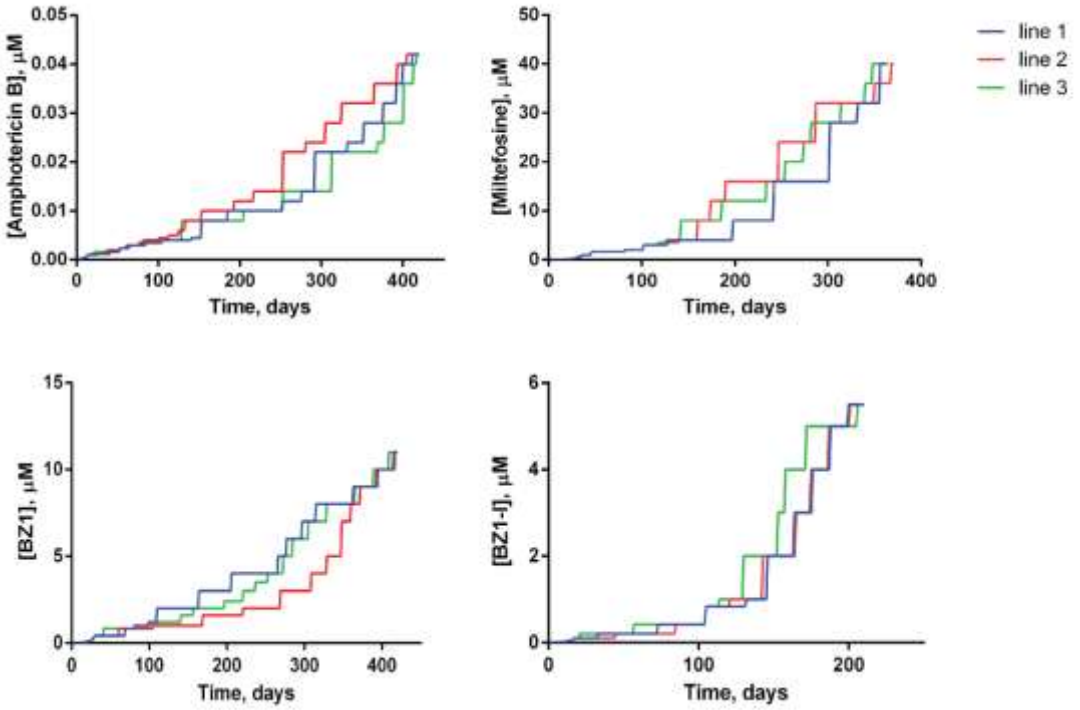

Figure 5.13: Generating resistance during the course of time against amphotericin B, miltefosine, BZ1 and BZ1-I. Line 1,2 and 3 are representative of 3 different clones. Each evaluation was performed as N=3.

5.3.7.1. Confirmation of resistant parasites

Resistance was confirmed in both clones for amphotericin B, miltefosine, **BZ1** and **BZ1-I** using the promastigote viability and intracellular amastigote assay (Figure 5.14). For amphotericin B the IC_{50} value of 0.41 ± 0.01 µM and 0.67 ± 0.09 µM was obtained

for the intracellular amastigote assay and the promastigote viability assay, respectively. An IC_{50} value could not be obtained for miltefosine. Compounds **BZ1** and **BZ1-I** resulted in IC_{50} values of 5.35 ± 0.18 µM, 4.94 ± 0.69 µM and 14.52 ± 0.55 µM, 8.93 ± 0.67 µM for the intracellular amastigote and promastigote viability assays, respectively. The IC_{50} obtained were compared with the control culture of the same passage number (Figure 5.17). It was observed that the level of resistance achieved when compared to the controls for amphotericin B resistant promastigotes and intracellular amastigotes was 13 and 4-fold, respectively. For miltefosine the level of resistance acquired when compared to controls was 16 folds in promastigotes. As no parasite inhibition was observed in the intracellular amastigote assay with the top dose of 40 µM hence the level of resistance must be more than 16-fold. The % inhibition observed at the top doses for miltefosine in Figure 5.14B is because of cytotoxicity of miltefosine on the host cells. For Compounds **BZ1 and BZ1-I** a 5.6 and 16.1-fold resistance was observed in promastigotes, respectively. In intracellular amastigote assay when compared with the control cultures both compounds **BZ1 and BZ1-I** provided a 9.2 and 8.2-fold resistance, respectively.

The control parasite cultures of *L. donovani* DD8 with the same passage number as that of the resistant parasites demonstrated the similar IC_{50} values (Figure 5.15), which were reported previously as described in chapter 4 with IC_{50} values of 0.12 ± 0.01 µM, 3.48 ± 0.26 µM, 2.15 ± 0.14 µM and 0.60 ± 0.04 µM for amphotericin B, miltefosine, compounds BZ1 and BZ1-I in the promastiogote viability assay. Similar IC_{50} values were found in the control cultures as previously reported as described in chapter 4 with IC_{50} values of 0.20 ± 0.02 µM, 2.54 ± 0.57 µM, 0.59 ± 0.04 µM and 0.57 ± 0.52 µM for amphotericin B, miltefosine, compounds BZ1 and BZ1-I in the intracellular amastigoteassay.

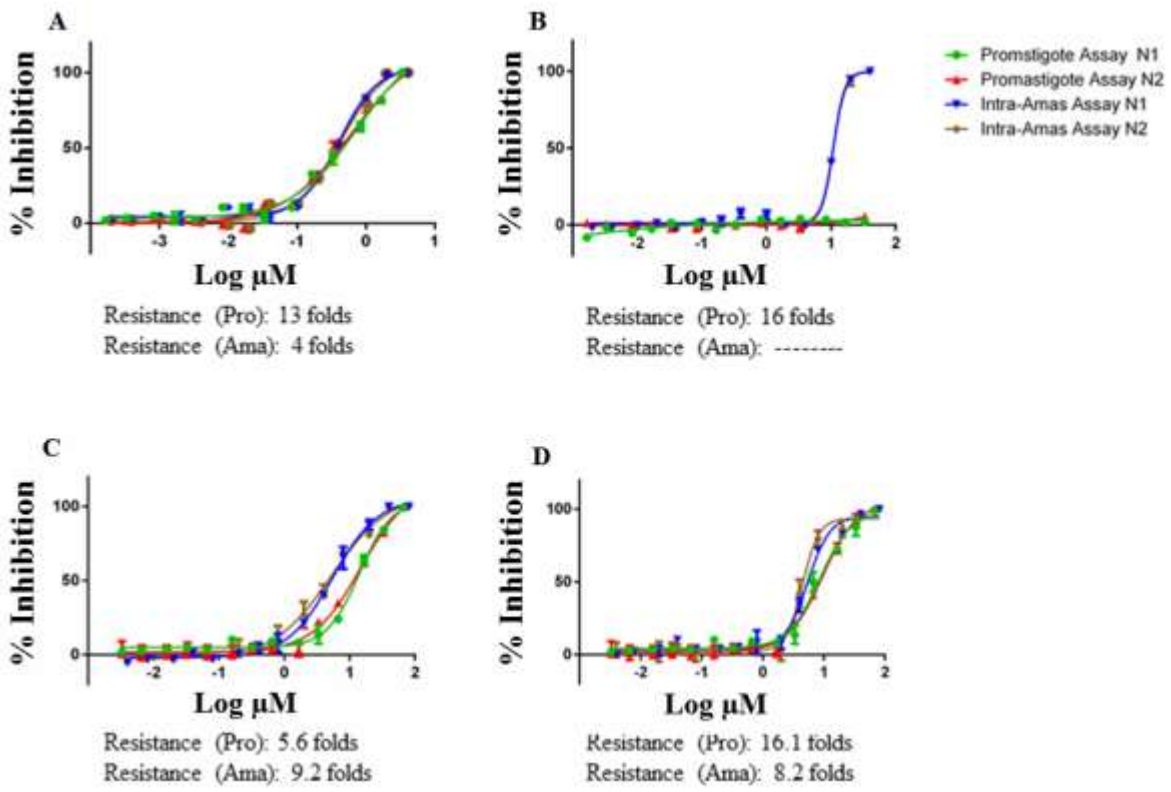

Figure 5.14: Concentration response for confirmation of resistance against (A) amphotericin B, (B) miltefosine, (C) BZ1 and (D) BZ1-I in resistant cultures. Each evaluation was performed as duplicates for N=2.

Table 5.1: IC_{50} values for confirmation of resistance against amphotericin B, miltefosine, BZ1 and BZ1-I. Each evaluation was performed as duplicates for N=2.

	Amphotericin B	Miltefosine	BZ1	BZ1-I
	IC_{50} µM (Average ± S.D)	IC_{50} µM (Average ± S.D)	IC_{50} µM (Average ± S.D)	IC_{50} µM (Average ± S.D)
Intracellular amastigote assay	0.41 ± 0.01 [0.20 ± 0.02]	- [2.54 ± 0.57]	5.35 ± 0.18 [0.59 ± 0.04]	4.94 ± 0.69 [0.57 ± 0.52]
Promastigote assay	0.67 ± 0.09 [0.12 ± 0.01]	- [3.48 ± 0.26]	14.52 ± 0.55 [2.15 ± 0.14]	8.93 ± 0.67 [0.60 ± 0.04]

Values in brackets are IC_{50} values reported on Chapter 4 before selection for resistance.

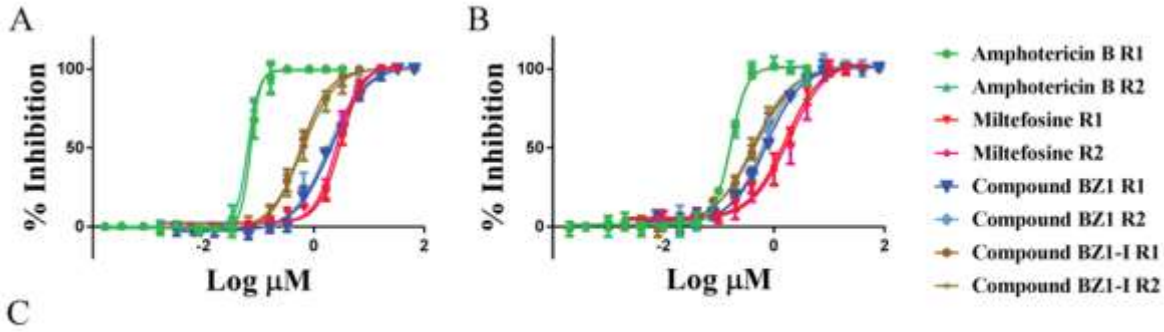

C

	Amphotericin B IC_{50} µM (Average ± S.D)	Miltefosine IC_{50} µM (Average ± S.D)	BZ1 IC_{50} µM (Average ± S.D)	BZ1-I IC_{50} µM (Average ± S.D)
Intracellular amastigote assay	0.16 ± 0.00	1.74 ± 0.15	0.70 ± 0.06	0.43 ± 0.02
Promastigote assay	0.06 ± 0.00	2.86 ± 0.29	1.93 ± 0.15	0.60 ± 0.04

Figure 5.15: Concentration response of reference drugs (amphotericin B and miltefosine) and compounds (BZ1 and BZ1-I) on control cultures in (A) Promastigote assay (B) Intracellular amastigote assay. Each evaluation was performed as duplicates for N=2.

5.3.7.2. Stability of drug resistance assessed

The stability of resistance was also confirmed in both parasite clones for amphotericin B, miltefosine, **BZ1** and **BZ1-I** using the promastigote viability and intracellular amastigote assays (Figure 5.16) and compared with the effect of the compounds on control culture with the same passage number (Figure 5.17).

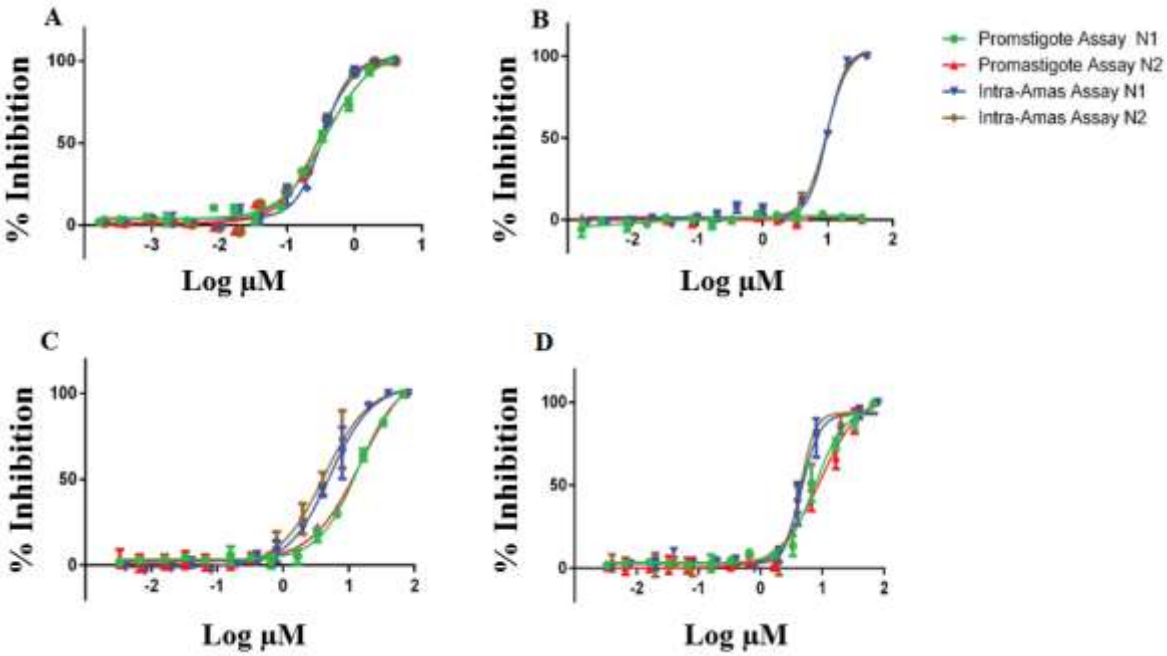

Figure 5.16: Concentration response curves for stability of drug resistance after removal of drug pressure for 10 passages of (A) amophotericin B, (B) miltefosine, compounds (C) BZ1 and (D) BZ1-I in resistant cultures. Each evaluation was performed as duplicates for N=2.

Table 5.2: IC_{50} values for stability of drug resistance after removing drug pressure for 10 passages of compounds BZ1, BZ1-I, amophotericin B and miltefosine.

	Amphotericin B	Miltefosine	BZ1	BZ1-I
	IC_{50} µM (Average ± S.D)	IC_{50} µM (Average ± S.D)	IC_{50} µM (Average ± S.D)	IC_{50} µM (Average ± S.D)
Intracellular amastigote assay	0.31 ± 0.02 [0.20 ± 0.02]	- [2.54 ± 0.57]	4.70 ± 0.67 [0.59 ± 0.04]	4.54 ± 0.19 [0.57 ± 0.52]
Promastigote assay	0.37 ± 0.01 [0.12 ± 0.01]	- [3.48 ± 0.26]	14.8 ± 1.23 [2.15 ± 0.14]	8.46 ± 1.08 [0.60 ± 0.04]

Values in brackets are IC_{50} values reported on Chapter 4 before selection for resistance.

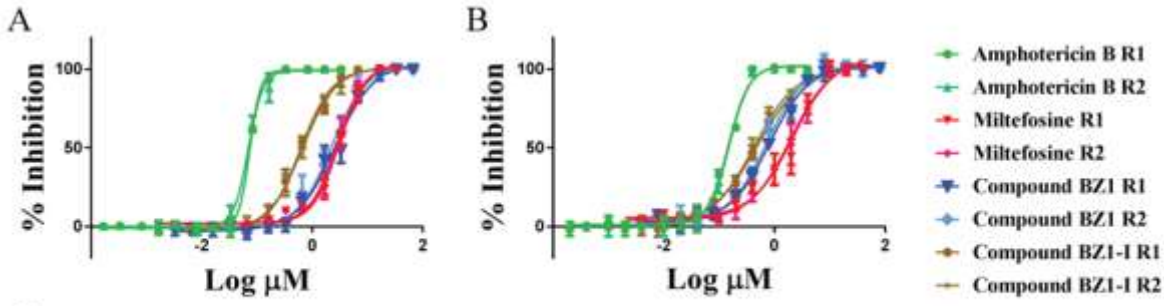

C

	Amphotericin B IC_{50} µM (Average ± S.D)	Miltefosine IC_{50} µM (Average ± S.D)	BZ1 IC_{50} µM (Average ± S.D)	BZ1-I IC_{50} µM (Average ± S.D)
Intracellular amastigote assay	0.15 ± 0.00	2.05 ± 0.15	0.75 ± 0.06	0.45 ± 0.03
Promastigote assay	0.07 ± 0.00	2.97 ± 0.16	2.40 ± 0.29	0.63 ± 0.03

Figure 5.17: Concentration response of reference drugs (amphotericin B and miltefosine) and compounds (BZ1 and BZ1-I) on control cultures in (A) Promastigote assay (B) Intracellular amastigote assay. Each evaluation was performed as duplicates for N=2.

5.3.8. pH stability studies for the compounds

The molecular mass of the **BZ1** is 304 daltons. The pH stability studies undertaken for **BZ1** indicated that the compound breaks into two moieties of molecular weights 242 and 62 daltons at pH values below 6.0 as indicated by the arrows. Data illustrating this are shown for mass spectrophotometry (Figure 5.16) and UV chromatogram (Figure 5.17). The **BZ1** compound only remained stable at pH 7.4. In contrast, compound **BZ1-I** remained stable at all pH tested (5.0, 5.5, 6.0 and 7.4) maintaining a molecular mass of 352 daltons, as shown in figures 5.18 and 5.19.

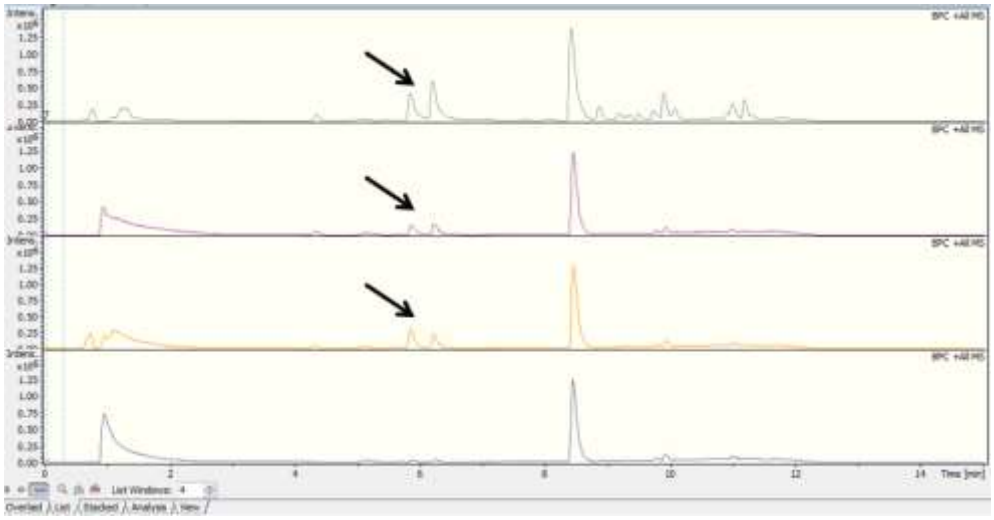

Figure 5.18: Mass spectrogram of compound BZ1 at different pH of 5.0, 5.5, 6.0 and 7.4. Each evaluation was performed as duplicates for N=2.

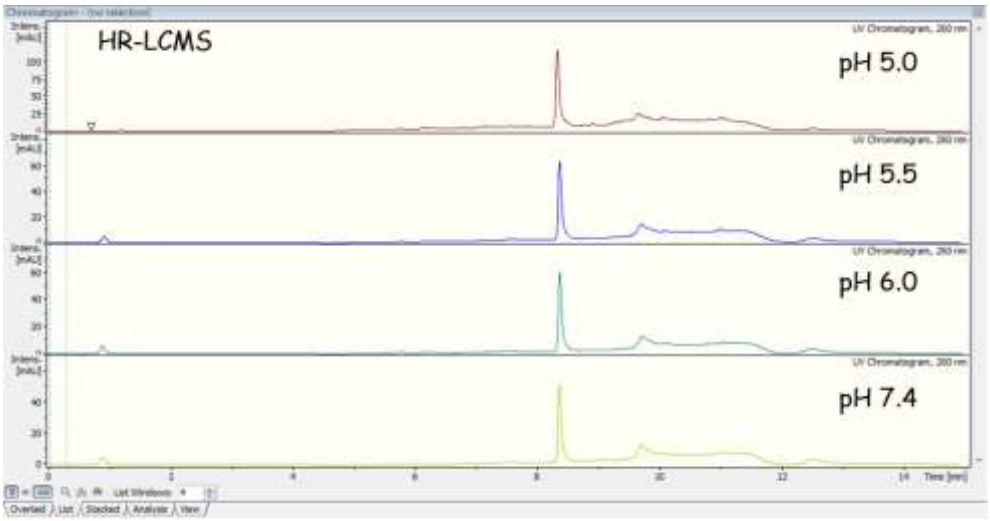

Figure 5.19: Ultraviolet chromatogram of compound BZ1 at different pH of 5.0, 5.5, 6.0 and 7.4. Each evaluation was performed as duplicates for N=2.

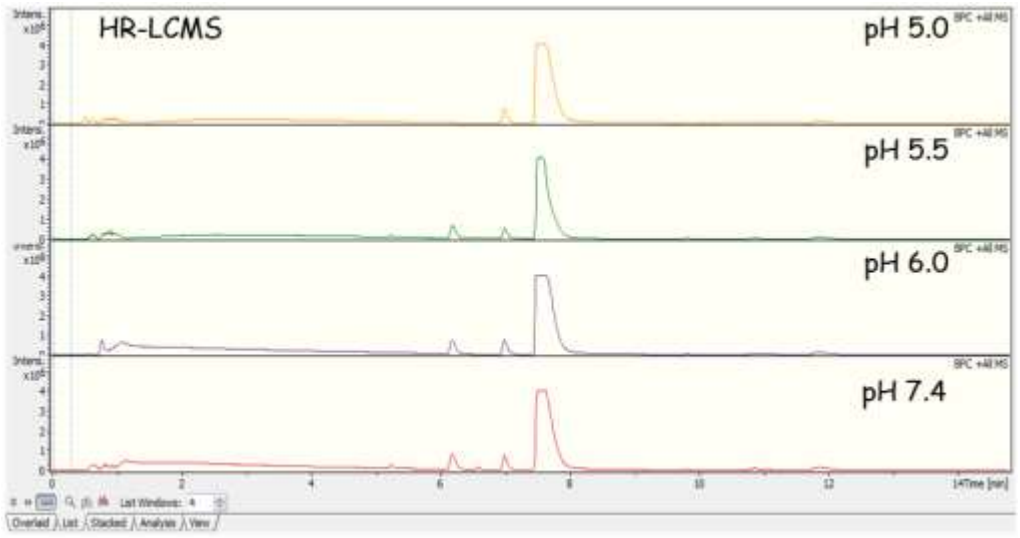

Figure 5.20: Mass spectrogram of compound BZ1-I at different pH of 5.0, 5.5, 6.0 and 7.4. Each evaluation was performed as duplicates for N=2.

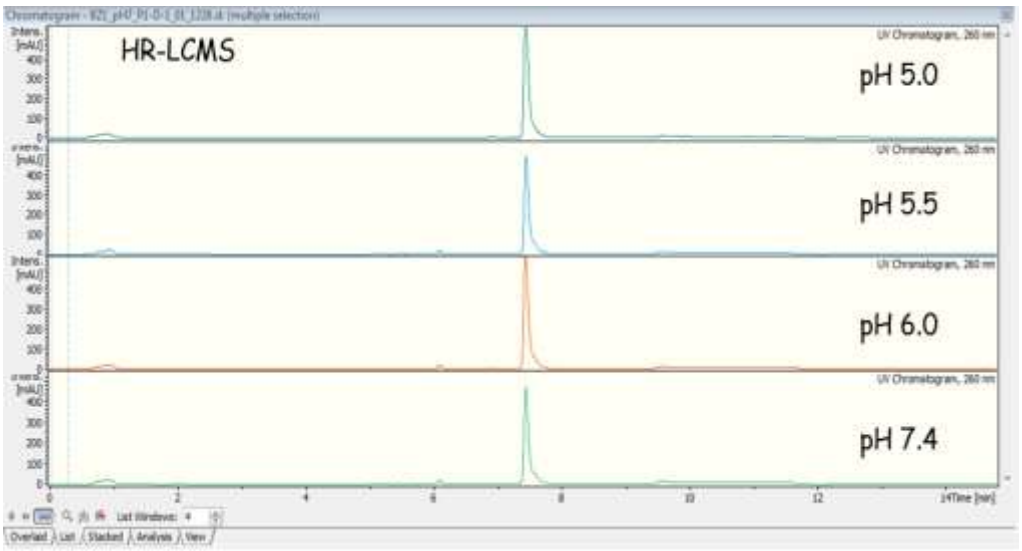

Figure 5.21: Ultraviolet chromatogram of compound BZ1-I at different pH of 5.0, 5.5, 6.0 and 7.4. Each evaluation was performed as duplicates for N=2

5.4. Discussion

Until now the most promising method to discover new hits for leishmaniasis has been unbiased phenotypic screening (Reguera, *et al.*, 2014). Once identified, these hits are progressed into the "hit to lead" programs where in addition to the chemical optimization to become lead molecules their mechanism of action can be elucidated. Unfortunately, the exact mechanism of action of most of the drugs that are currently in

use to treat leishmaniasis have yet to be elucidated. Various mechanisms have been proposed for current drugs, and for new compounds being identified, the target is usually characterized on the basis of an exclusion strategy for possible mechanisms, which takes a considerable amount of time.

Glycolysis is considered a promising target as glycosomes compartmentalize seven of the glycolytic enzymes (e.g. glucose 6-phosphate isomerase, triosephosphate isomerase). Inhibiting these enzymes has a profound effect on promastigotes as they rapidly divide, requiring a greater glucose uptake than amastigotes, which divide at a slower rate. Moreover, it has been reported that amastigotes rely on hexose uptake both *in-vitro* and *in-vivo* (Saunders, *et al.*, 2014). Another key molecule, trypanothione, acts as an inhibitor of oxidative stress in *Leishmania*. It is not unique to the parasite only but helps maintain the cellular redox potential, which is crucial for parasite survival. Gene knockout experiments of this enzyme have confirmed this and suggested it to be an attractive target (Saudagar and Dubey, 2011). Parasites have endogenous folate biosynthesis pathways, as their mammalian host cells cannot synthesize folate and use carriers to transport the folic acid into the cells (Sharma and Chauhan, 2012). In *Leishmania*, DHFR exclusively exists in the form of a complex DHFR-TS with thymidylate synthase, making it an ideal target for selective inhibition (Rajasekaran and Chen, 2012). Another enzyme, pteridine reductase (PTR1), performs the folate reduction in the absence of DHFR-TS, which also makes this an exciting target for anti-leishmanial drug discovery (Hardy *et al.* 1997; Leite, *et al.*, 2017). Rajasekaran and Chen have provided an excellent review regarding the potential therapeutic targets in anti-leishmanial drug discovery (Rajasekaran and Chen, 2015).

To further characterize the compounds identified within this project, mode of action studies were conducted. Cidal/Static assays using promastigote viability assay were conducted to gain insights into the susceptibility of promastigotes to the test and reference compounds. The cidal activities of all compounds are concentration dependent. For the reference drugs, Amphotericin B and Miltefosine, the cidal activity was evident from 0.33 µM and 6.66 µM, respectively. A complete lack of viable promastigotes was observed for BZ1 and BZ1-I from 1.66 to 6.66 µM to higher concentrations, respectively.

To determine the IC_{50} values of compounds to estimate the time to kill for the promastigotes, a resazurin-based assay was used. In the presence of metabolically active cells this dye converts rapidly to a fluorescent end product. Concentration-response curves of **BZ1** activity against promastigotes showed a plateau of activity at 24, 48, 72 and 96 hours (considered as 2 concentrations or more at >90%), suggesting that **BZ1** was able to achieve 100% inhibition after 24 hours (Figure 5.4A). After 48 hours the IC_{50} value of **BZ1** was consistent (2.37 ± 0.74 µM) remaining in the same range for 72 and 96 hours. The same pattern was followed by **BZ1-I** as the IC_{50} value became consistent after 48 hours (0.69 ± 0.35) (Figure 5.4B). This suggested that both compounds were not fast acting compounds.

To determine the time to kill for the intracellular amastigotes, the high content imaging based assay was used. We investigated the effect of the compound after exposing amastigotes to it for 24, 48, 72 and 96 hours. The concentration response curves of **BZ1** showed a plateau of activity (100% inhibition) occurring only beyond the 48 hour time point (Figure 5.5A). However, for **BZ1-I**, the plateau of activity was reached at 24 hours but the IC_{50} value became stable after 48 hours (Figure 5.5B). This delay in activity might be due to potential compound permeability issues, as it has to cross multiple barriers to reach the amastigotes which reside within the parasitophorous vacuoles. Another possible reason includes the conversion of the compound into an active metabolite, which is time dependent. This was further investigated with a series of spectroscopic experiments discussed later on.

In the host preincubation studies, used to determine whether the compounds exert a immunotherapeutic effect on the transformed THP-1 cells, rather than directly affecting the parasite. A plateau of activity was observed for amphotericin B and miltefosine after 48 and 24 hours incubation, respectively. A complete concentration response curve could not be established for compounds **BZ1** and **BZ1-I**. One of the possible reasons for the retention of activity, even after removal of the drug pressure, might be due to the accumulation of amphotericin B (Jahn *et al.*, 1998) and miltefosine (Dohmen *et al.*, 2016) in the transformed macrophages.

Apoptosis, or programmed cell death, is an important and active regulatory pathway of cell growth and proliferation (M. Rudin and B. Thompson, 1997). It has been proposed that limited programmed cell death occurs before infection and this phenomena plays an

important role in establishing the disease (van Zandbergen, *et al.*, 2007; Pal, *et al.*, 2010). It has been reported that antimony compounds, hydrogen peroxide, camptothecin and antimicrobial peptide induce apoptotic like cell death in *Leishmania* (Sudhandiran and Shaha, 2003; Sen, *et al.*, 2004; Kulkarni, *et al.*, 2009). Certain features, such as activation of caspase-3/7-like protease, cytosolic calcium-mediated mitochondrial toxicity and release of mitochondrial apoptotic factors are also termed as hallmarks of apoptosis.

An experiment was performed to assess whether apoptosis in *L. donovani* DD8 promastigotes was induced by either or both **BZ1** and **BZ1-1**, as a similar class of compounds has been shown to induce apoptosis in *Leishmania* parasites (Hazra, *et al.*, 2012; Duarte, *et al.*, 2016). The first aspect determined was externalization of phosphatidylserine (PS) to the cell surface, which is one of the hallmarks of apoptosis. For this purpose the Muse™ Annexin V & dead cell assay kit was used on the Muse™ Cell Analyzer (Merck, USA), which utilizes Annexin V to detect PS on the external membrane of apoptotic cells. A dead cell marker 7-aminoactinomycin D (7-AAD) was used as an indicator of cell membrane structural integrity. 7-AAD is a intercalator that undergoes spectral shift in fluorescence upon association with DNA. It was excluded from live, healthy cells, as well as early apoptotic cells.

In the presence of the positive control (miltefosine 5 µM) 85% of the *L. donovani* DD8 promastigotes went into late stage apoptosis by 72 hours. It has been reported previously that miltefosine induces an apoptosis like death in a time and dose dependent manner in *L. donovani* strain KE-16 parasites (Mishra and Singh, 2013). The primary mode of action of miltefosine is not known, however, various mechanisms have been suggested, such as ether remodeling (Sundar, *et al.*, 2012). Ether-lipids constitute a major portion of the *Leishmania* lipid content mainly found in the glycoproteins and glycosylphosphatidylinositol-anchored glycolipids, which constitute the surface of the parasites (Lux, *et al.*, 2000). Ether remodeling causes a disturbance of glycoproteins and glycosylphosphatidylinositol-anchored glycolipids, which leads to the structural deformity and destabilization of the parasite surface symmetry causing parasite death. Inhibition of cytochrome c oxidase (Luque-Ortega and Rivas, 2007) has also been postulated to have a role in parasite death.

In the presence of amphotericin B (IC_{50} value), 22.68% of the *L. donovani* DD8 promastigotes died after 12 hours exposure, the number of cells entering early apoptosis rising from 12 hours to 48 hours (9.98% to 30.56%) as shown in figure 5.7. Studies have shown that amphotericin B forms complexes with the 24 substituted sterols (Ergosterol) within the biological membrane of the parasite and produces pores within the membrane, which leads to cell death because of ion imbalance (Roberts, *et al.*, 2003). This explains the sudden death of parasites after the 24 hours reading. One of the reasons for toxicity observed with amphotericin B is related to the binding of amphotericin B to the cholesterol on the biological membrane of the mammalian cell causing nephrotoxicity. In addition, it has been proposed that amphotericin B causes cholesterol complexation which hinders the binding of *L. donovani* metacyclic promastigotes to the host cells (Paila, *et al.*, 2010) there by inhibiting their entry into the host cell.

For compounds **BZ1** and **BZ1-I**, 36.34% and 26.34% of *L. donovani* DD8 promastigotes died after 48 hours of exposure. Of the remaining parasites, a small population underwent late stage apoptosis 5.78% and 14.82% with **BZ1** and **BZ1-I**, respectively. The results obtained align with what we have seen in the time to kill assay for promastigotes, where both compounds show inhibitory activity after 48 hours of compound exposure. The cell populations were significantly reduced after 72 hours of exposure resulting in debris. This suggests that the compounds were not inducing apoptosis in the *L. donovani* DD8 promastigotes.

There have been reports suggesting that *Leishmania* can undergo apoptosis in both caspase-dependent and caspase independent pathways during mitochondrial oxidative stress (Arnoult, *et al.*, 2002; Zangger, *et al.*, 2002; BoseDasgupta, *et al.*, 2008). Caspases (cysteinyl-directed aspartate-specific proteases) are cysteine proteases (Riedl and Shi, 2004) that play a central role in propagating the process of programmed cell death (apoptosis) in response to proapoptotic signals. While some caspases primarily act to initiate intracellular event cascade, other caspases called effector caspases act further downstream and direct cellular breakdown through cleavage of structural proteins (Caspase-3, and Caspase-7). Activation of Caspase-3/7 is thus a hallmark of apoptosis (Porter and Jänicke, 1999).

To further assess this phenomena activation of Caspase-3/7 pathway after exposure to the compounds at different time points (12, 24, 48 and 72 hours) was conducted using Muse™ Caspase-3/7 assay. The Muse™ Caspase-3/7 assay reagent contains a DNA binding dye that is linked to a DEVD (Asp-Glu-Val-Asp) peptide substrate. When bound to DEVD the dye is unable to bind DNA. Cleavage by active Caspase-3/7 in the cell results in release of the dye, translocation to the nucleus and binding of the dye to DNA and high fluorescence. Information on the presence of active Caspase-3/7 in the cell is easily obtained when an increase in fluorescence in the Caspase-3/7 parameter is observed. A dead cell marker (7-AAD) is also included in the assay as an indicator of cell membrane structural integrity and cell death. It is excluded from live, healthy cells, as well as early apoptotic cells, but permeates later stage apoptotic and dead cells. Thus dead cells show increased fluorescence in the viability axis.

Our results indicated that a 49.35% reduction in the parasite number was with amphotericin B incubation at the IC_{50} concentration, after a period of 12 hours. For the positive control (miltefosine), 13.05% of the population went into late stage apoptosis at 48 hours. This suggests that miltefosine induces apoptosis within the *L. donovani* DD8 promastigotes via caspase independent pathways. For compounds **BZ1** and **BZ1-I**, 32.95% and 25.10% of the *L. donovani* DD8 promastigotes died after 48 hours of exposure, respectively. The cell populations were significantly reduced after 72 hours of exposure. This data confirms that apoptosis is not induced by compounds **BZ1** and **BZ1-I** via either caspase dependent or caspase independent pathways in *L. donovani* DD8 promastigotes. Interestingly, 76.85% of the host cell (THP-1 cells) population treated with miltefosine went into late apoptotic/death phase after 72 hours indicating activation of caspase 3/7 pathway (Figure 5.10). Previously, Caspase 3/7-like activity has been reported to be induced in a dose-dependent fashion by miltefosine, with 46 µM of this drug inducing stronger activity at 3 h and 6 h than 26 µM miltefosine, as expected (Foucher et al., 2013).

derivatives have been shown to affect the mitochondrial morphology, membrane stability and potential (Hazra, *et al.*, 2012; Antinarelli, *et al.*, 2015; Duarte, *et al.*, 2016). Keeping this notion in perspective, the effect of **BZ1** and **BZ1-I** were assessed for their effect on the mitochondrial membrane morphology and inhibition of oxidative phosphorylation using MitoTracker. The results indicated that both compounds possess

anti-leishmanial activity which is mediated via a different mechanism other than affecting the mitochondrial morphology and membranne potential in *L. donovani* DD8 promastigotes.

Resistance was also generated for both compounds and reference drugs (Figure 5.13). After a duration of 428 days, clones of resistant strains were generated for amphotericin B, miltefosine and **BZ1** that could withstand concentrations of these drugs/ compounds of 420 nM, 40 µM and 11 µM, respectively. Resistant clones were also generated for **BZ1-I** taking 210 days to reach a concentration of 5.5 µM. Thus, was observed that it took less time to attain resistance with **BZ1-I** when compared to **BZ1**.

Resistance in this clonal population was confirmed (Figure 5.14) using the promastigote and the intracellular amastigote assays. For amphotericin B, a 13 fold resistance was observed in the promastigotes, whereas only a 4 fold change was observed in intracellular amastigotes. For miltefosine, resistance up to 40 µM was generated in both promastigotes and intracellular amastigotes providing a 13.3-fold increase in drug required to exert an effect on the promastigotes. In addition, compared to sensitive strain 17-fold increase in drug resistance was found for intracellular amastigotes. However, concentration response curve could not be generated as 40 µM was the top concentration in the assay maintaining 0.4% final assay concentration of DMSO in the assay. A 14-fold increase in drug resistance was obtained for miltefosine (Pérez-Victoria, *et al.*, 2006), and a 20-fold resistance generated for amphotericin B (Mbongo, *et al.*, 1998). Hence, the results we have obtained in the promastigote and intracellular amastigote assays co-align with the previously reported data for miltefosine. Unfortunately, only a 13 fold resistances could be generated for amphotericin B which is less than the previously reported value for *L. donovani* DD8 promastigotes (Mbongo, *et al.*, 1998). Whilst a 5.6-fold resistance to **BZ1** was observed in promastigotes, 9.2 fold increase in resistance was observed in intracellular amastigotes. Similar pattern of activity observed to sensitive parasites with greater impact on amastigotes. For **BZ1-I**, 16.1-fold resistance was observed for promastigotes and 8.2 fold was observed in intracellular amastigotes.

Studies were also conducted to determine the stability of resistance after removing drug pressure for 10 passages (Figure 5.15). This was determined using both the promastigote viability and intracellular amastigote assays. Our results indicated that the

generated resistance is stable even after removing the drug pressure for amphotericin B, miltefosine and compounds **BZ1** and **BZ1-I**. The clones have been frozen and whole genome sequencing is being performed to determine the target gene in future projects.

As previously highlighted the internal environment where the amastigotes reside in the host cell is at a considerably more acidic pH than the external one. A study was therfore conducted to assess the compound stability at various pH levels, as it has been established that *Leishmania* intracellular amastigotes reside within the parasitopharous vacuole at pH 4.5-5.5. A compound does not only have to cross multiple barriers (host cell membrance, parasitopharous vacuole and parasite membrane) but has to remain active throughout significant changes in pH. Hence, compound stability in the presence of extreme pH changes, or conversion to an active form, is highly desirable. The M199 media used for the promastigote assay is pH 6.8, whereas the parasitopharous vacuole where the intracellular amastigote resides is pH 5.5. In order to check whether the compound remains stable or converts into metabolites at this low pH, we assessed the compound stability at varying pH from 5.0, 5.5, 6.0 to 7.4. It appeared that **BZ1** degraded at pH 6.0, 5.5 and 5.0 into two distinct metabolites with molecular masses of 242 and 62 daltons (Figure 5.16). On the other hand, compound **BZ1-I** does not undergo degradation at that pH (Figure 5.18). The degradation of BZ1 at low pH suggests the metabolites formed are influencing activity found in the intracellular amastigote assay where the IC_{50} value of the compound is calculated to be 0.59 ± 0.13 µM, compared to the IC_{50} value of the compound in the promastigote viability assay (2.37 ± 0.85 µM). This will be confirmed by assessing the activity of both the metabolites (242 and 62 daltons) in the promastigote and intracellular amastigote assays. Structure elucidation of these metabolites is in process to confirm theoretical prediction. These metabolites and their analogues will subsequently be obtained and tested in the promastigote and intracellular amastigote models to determine the anti-leishmanial activities.

The possible mechanism of action of the compounds **BZ1** and **BZ1-I** was investigated with initial studies based on the previously reported mechanism of action for similar chemotypes. We found that both the compounds do not induce apoptosis via caspase dependent and caspase independent pathways in the *L. donovani* DD8 promastigotes. In addition, both compounds failed to cause any change to the mitochondrial morphology

or inhibit the mitochondrial membrane, concentrations equivalent to their IC_{50} values in *L. donovani* DD8 promastigotes. Whole geneome sequencing of the resistant clones will hopefully provide us an insight into potential resistance mechanism and thus an indication of the target. This information will help us identify the mechanism through which the compound elicits its anti-leishmanial activity and development of new screening assays for the specific target.

Chapter 6: *In vitro* activity against Old and New World species, DMPK data and cytotoxicity profiling

6.1. Introduction

There exists a significant imbalance in the drug discovery pipeline for leishmaniasis. Many hit and lead molecules have been identified but the models and tools to progress the leads into preclinical stages are still limited (Nagle, *et al.*, 2014; Jain and Sharma, 2017). The variation in compound activity against different *Leishmania* species contributes to different clinical outcomes based on geographical location of the parasite (Stuart, *et al.*, 2008; Rama, *et al.*, 2015; Kamboj, 2016).

Many compounds in the past have exhibited differences in sensitivity to *Leishmania* species, and include antibiotics, organo-metallics, nucleosides and sterol biosynthesis inhibitors (Nelson, *et al.*, 1979; Avila and Casanova, 1982; Neal, *et al.*, 1995; Rangel, *et al.*, 1996). Most of these compounds were not progressed through the drug discovery pipeline due to predicted cytotoxicity to host cells, and a lack of efficacy and safety in *in vivo* models.

Even the currently available treatments for leishmaniasis are facing similar issues. Pentavalent antimonials (Figure 1.13), which still remain the treatment of choice in South America, Africa, Nepal, Bangladesh, and India (except North Bihar) (Haldar, Sen, & Roy, 2011) have demonstrated a difference in *in vitro* sensitivity between the different species in the amastigote macrophage models. It was demonstrated that *L. brasiliensis* and *L. donovani* were three to five fold more sensitive to antimonials compared to *L. tropica*, *L. major* and *L.mexicana* (Croft, *et al.*, 2006; Croft and Olliaro, 2011). Differences in sensitivity were also observed in a controlled trial conducted in Guatemala, where a higher cure rate was obtained for antimonials in cutaneous leishmaniasis patients infected with *L. brasiliensis* (96%) compared to those with *L. mexicana* (57%) lesions (Navin, *et al.*, 1992).

Amphotericin B deoxycholate (Figure 1.14) is considered the second-line therapy in cases that do not respond to antimonials. This drug has been demonstrated to be very effective against visceral leishmaniasis (>90% cure rate) (Sundar and Rai, 2005). A

study by Escobar *et al*, conducted to compare the sensitivity of different species of *Leishmania* to amphotericin B, observed that the rank order of species sensitivities measured in ED_{50} (median effective dose) was *L. mexicana* > *L. aethiopica* > *L. tropica*> *L. major* > *L. panamensis*> *L. donovani* for the promastigote assay and *L. mexicana* > *L. panamensis* > *L. aethiopica* > *L. tropica* > *L. major* > *L. donovani* for the amastigote-macrophage assay (Escobar, *et al.*, 2002). The assay format for the promastigote and the intracellular amastigotes was the same for all the species, so the difference in activity cannot be accounted by the differences in assay format.

Variations in drug sensitivity against different species has also been demonstrated *in vitro* for miltefosine (Figure 1.15) with *L. tropica*, *L. aethiopica*, *L. mexicana*, *L. panamensis* and *L. donovani* using the same assay formats with similar drug exposure times (Croft, *et al.*, 2006). The IC_{50} values obtained for miltefosine varied from 2.63 to 10.63 μM between these different species, whereas the IC_{50} against *L. major* was found to be significantly lower at 37.17 μM (Escobar, *et al.*, 2002). The same pattern has been observed when miltefosine is used against clinical isolates of *L. donovani* from Nepal and *L braziliensis*, *L. guyanensi*, *L. mexicana*, and *L. lainsoni* from Peru (Yardley, *et al.*, 2005).

Paromomycin (Figure 1.16) has been approved by WHO for the treatment of cutaneous leishmaniasis in its topical form (Sinha, *et al.*, 2011). *In vitro* testing suggests that Paromomycin sensitivity of *Leishmania* amastigotes in murine macrophages to paromomycin varies between species. This drug tends to be more effective against *L. tropica* and *L. major* compared to *L. mexicana* and *L. brazaliensis* when compared in the same assay models (Neal, *et al.*, 1995). The drug appears to be intermediately active against all strains of *L. donovani* except *L. donovani* DD8 (Neal, *et al.*, 1995). This suggests that the effect of certain compounds/drugs on different species, as well as strains of *Leishmania* parasite, will be different based on geographical location of the parasite.

In this chapter, variations in activity of 1H-cyclopenta[b]quinolin-9-amine compounds (**BZ1** and **BZ1-I**) against the Old and New World species causing visceral leishmaniasis were investigated (Figure 6.1). Three *Leishmania* were selected, namely *L. donovani* causing visceral leishmaniasis in Asia and Africa, *L. infantum* causing visceral leishmaniasis in the Mediterranean region and *L. infantum*(New World) causing visceral

leishmaniasis in Brazil. The isolate selected to represent *L. donovani* was a WHO reference strain MHOM/IN/80/DD8 (Xu, *et al.*, 1984). The isolate selected to represent *L. infantum* (Old World) was MHOM/MA(BE)/67 (Bañuls, *et al.*, 1999) and the isolate selected to represent *L. infantum* (New World) was MHOM/BR/1972/BH46 (Peruhype-Magalhães, *et al.*, 2005). To compare the strain specific differences *L. donovani* MHOM/SD/62/1S-CL2D, LdBOB was chosen, which is a genetically modified strain, the wild type of which was isolated from Sudanese population. So the cross comparison will be based on visceral leishmaniasis strains causing strains from different geographical locations (Asia and Africa).

A decline has been shown in the reported cases of visceral leishmaniasis caused by *L. infantum* in many foci where living conditions have improved (Ready, 2014). Whereas, visceral leishmaniasis caused by *L. donovani* continues to kill thousands of people in East Africa and Indian subcontinent (Ready, 2014). Based on the impact of the disease we chose to test the compounds between the two strains of *L. donovani*.

High content imaging (HCI) assays have been developed and optimized for *L. donovani* MHOM/IN/80/DD8 (Duffy, *et al.*, 2017), *L. donovani* MHOM/SD/62/1S-CL2D, LdBOB (De Rycker, *et al.*, 2013) and *L. infantum*MHOM/BR/1972/BH46 (Gomes, *et al.*, 2017) using 384-well formats, thus enabling rapid evaluation to be undertaken. A difference still exists in the assay protocols and incubation periods used between these HCI assays which has the potential to contribute to difference in the activities of compounds.

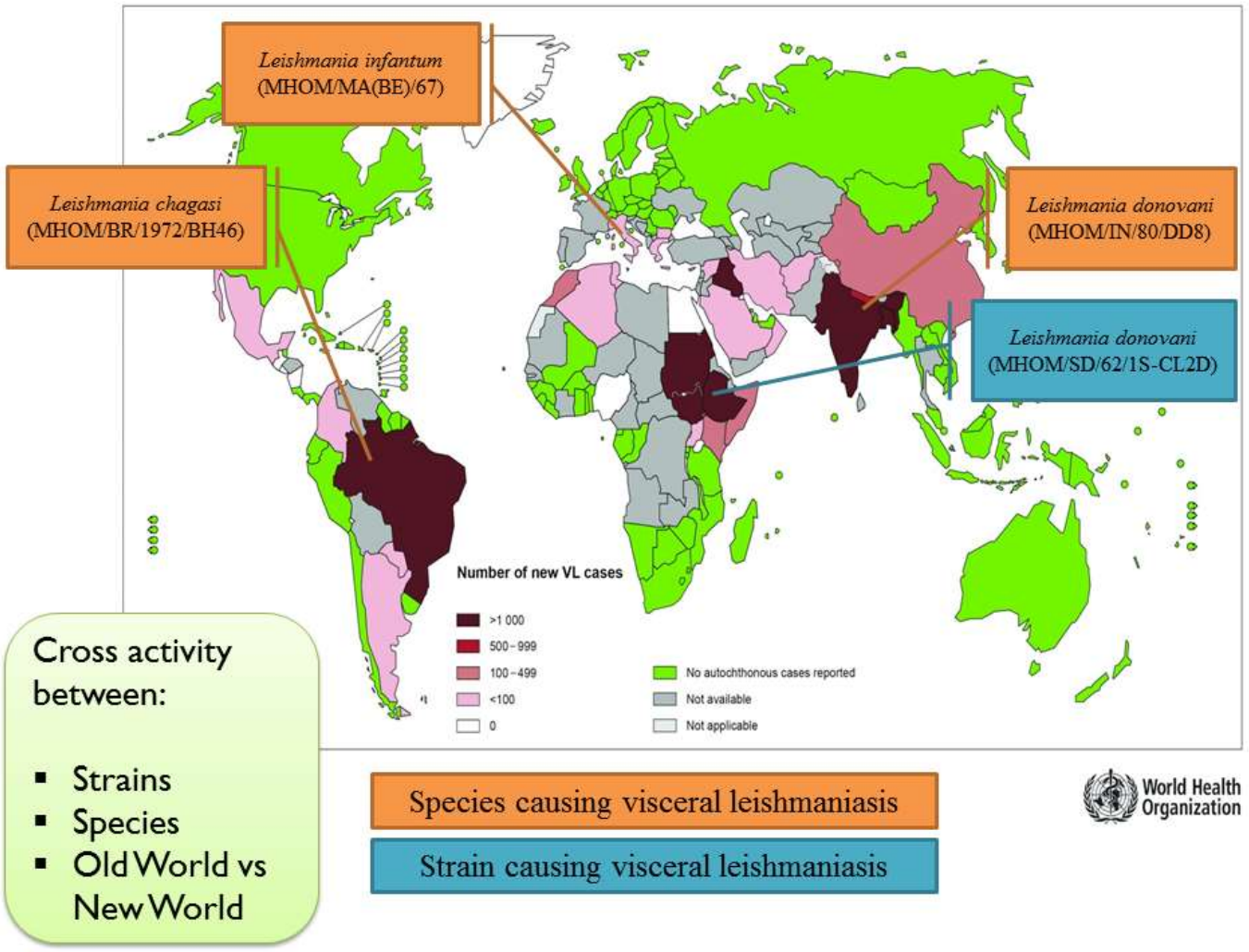

Figure 6.1: Cross activity against different strains and species of *Leishmania* in the Old and New World.

In addition to evaluating **BZ1** and **BZ1-I** activity against Old and New World leishmania, the activity of these two anti-leishmanial compounds was also tested against other trypanosomatid parasites (*T. brucei* species and *T. cruzi*), as well as *Plasmodium falciparum*. It has been reported that molecular mechanisms are often conserved between trypanosomatids and other parasites, including aminoacyl-tRNA synthetases (Pham, *et al.*, 2014), dihydroorotate dehydrogenase (DHODH) (Pinheiro, *et al.*, 2013), Fatty acid acylation (the addition of fatty acid moieties to proteins) (Goldston, *et al.*, 2014), topoisomerases (Balana-Fouce, *et al.*, 2014) and arginine kinase (Pereira, 2014) .

Another aspect which was investigated and will be discussed in this chapter, is the *in vitro* Drug Metabolism and Pharmacokinetics (DMPK) studies. DMPK is an important part of the ADME (Absorption, Distribution, Metabolism, and Elimination) studies (Han and Wang, 2016). These studies provide a basis for choosing lead compounds that have desirable pharmacokinetic and safety profiles required for drug candidate selection in the drug discovery pipeline (Gupta, *et al.*, 2017) (Figure 6.2). Usually at an early stage within hit-to-lead projects *in vitro* DMPK can provide crucial information on liver microsome stability, solubility and permeability. This information can help chemists to identify and select compounds prioritized for *in vivo* DMPK studies (Yamazaki, 2014). In some cases, where the compounds are taken directly into animal models, information pertaining to Log *D* and solubility can be used for selection of suitable formulations (Empfield and Clark, 2014).

The compounds (**BZ1** and **BZ1-I**) were evaluated to determine their *in vitro* DMPK properties to ascertain whether these compounds possessed suitable pharmacokinetic properties to warrant further drug discovery and development studies. *In vitro* DMPK was conducted in collaboration with Professor Susan Charman, Centre for Drug Candidate Optimisation (CDCO), Monash University, Australia. The physiochemical properties such as molecular weight, hydrogen bond donor and acceptor, lipophilicity and solubility in physiological media were investigated. The *in vitro* DMPK studies provided the information regarding the chemical and metabolic stability and pharmacokinetic profile of the compounds.

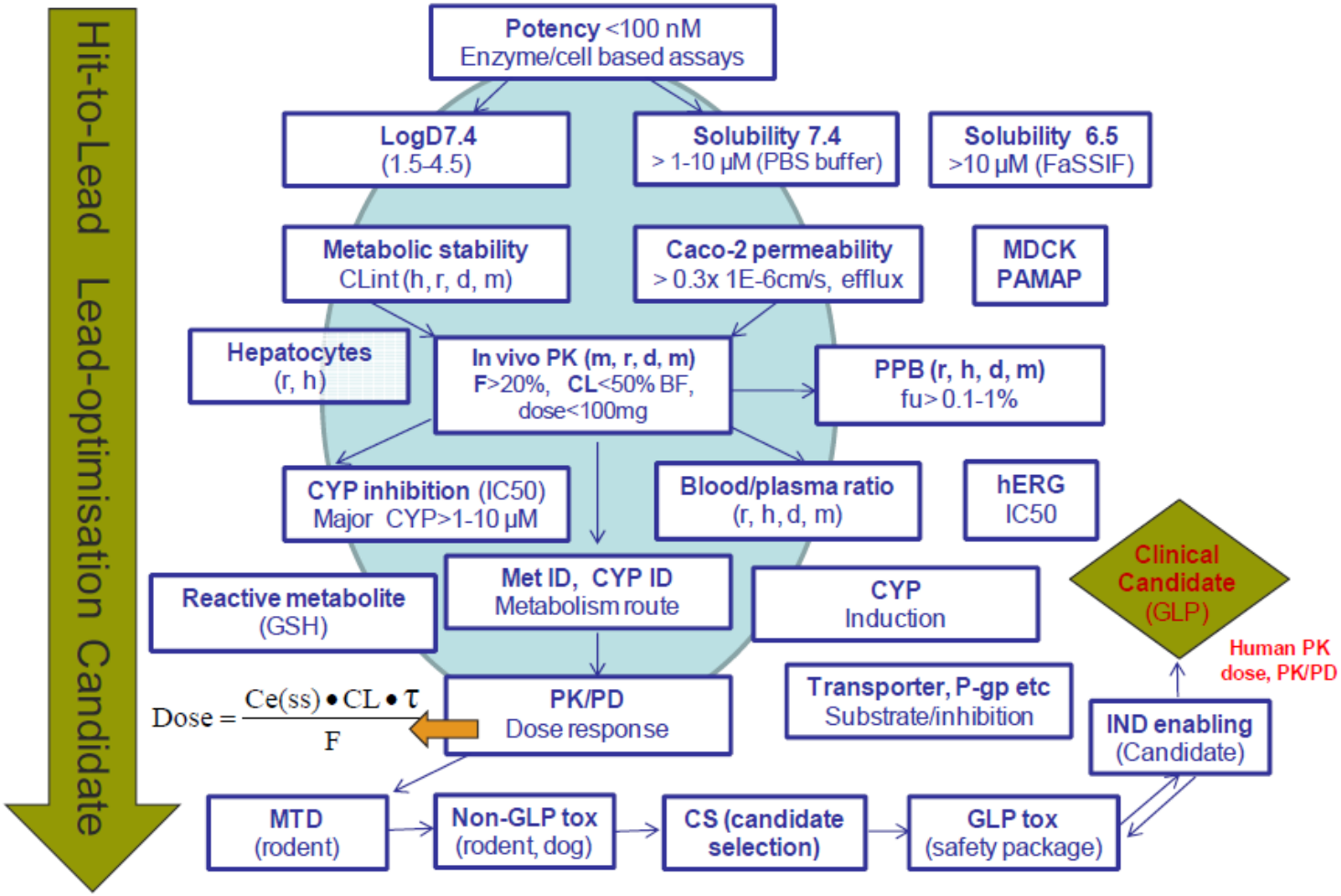

Figure 6.2: Typical ADME/PK screening cascade. Reproduced with permission from Wan H, *What ADME tests should be conducted for preclinical studies?* ADMET & DMPK 1(3) (2013) 19-28.

A cytotoxicity panel comprised of various cell lines from human and mice representing different organ systems was also establish to determine the cytotoxicity profile of these compounds for comparison with the data described in chapter 4. This panel served as a valuable tool to address compound toxicity early in development. The different cell lines included in the panel were HepG2 (human liver cancer cell), HEK-293 (human embryonic kidney cell line), THP-1 (human monocytic cell line), RAW 264.7 and J774.1 (murine macrophages cell lines).

6.2. Materials and Methods

6.2.1. *In vitro* anti-leishmanial assays

6.2.1.1. *L. donovani* MHOM/IN/80/DD8 intracellular amastigotes

The HTS-HCI assay described in chapter 2 (section 2.3.2) was used to determine the IC_{50} value of the compounds against *L. donovani* DD8 intracellular amastigotes. A 14 point concentration response curve was generated using the following concentration range 40 µM to 0.002 µM.

6.2.1.2. *L. donovani* MHOM/SD/62/1S-CL2D, LdBOB intracellular amastigotes

This assay was performed as previously described (De Rycker, *et al.*, 2013) by Dr. De Rycker and colleagues at College of Life Sciences, University of Dundee, United Kingdom. The selectivity of the compounds was assessed using THP-1 host cells. The detailed protocol is described in appendix 3.

6.2.1.3. *L. infantum* MHOM/MA(BE)/67 intracellular amastigotes

This assay as described previously (Cos, *et al.*, 2006) was undertaken at Department of Biomedical Sciences, Laboratory for Microbiology, Parasitology and Hygiene, University of Antwerp, Belgium by Prof. Maes and colleagues. The selectivity of the

compounds was assessed using MRC5 and primary mouse macrophages (PMM). The detailed protocol is described in detail in appendix 1.

6.2.1.4. *L. infantum* MHOM/BR/1972/BH46 intracellular amastigotes

This assay was performed as previously described (Cämmerer, 2016) by Prof. Freitas-Junior and colleagues at National Laboratory of Biosciences, National Center for Research on Energy and Materials, Campinas, São Paulo, Brazil. The cytotoxicity was determined using THP-1 host cells. The detailed protocol is described in appendix 2.

6.2.2. *In vitro* anti-trypanosomal assays

6.2.2.1. *T. b. brucei* 427 strain.

The efficacy of compounds against *T. b. brucei* bloodstream form was evaluated by Dr. Jones using a resazurin- based assay, previously described in the literature (Sykes, *et al.*, 2012).The detailed protocol is described in appendix 4.

6.2.2.2. *T. b. brucei* Squib 427 strain (suramin-sensitive) and *Trypanosoma brucei rhodesiense*.

This assay was performed by Prof. Maes and colleagues at Department of Biomedical Sciences, Laboratory for Microbiology, Parasitology and Hygiene, University of Antwerp, Belgium using the protocol previously decribed (Cos, *et al.*, 2006). The detailed protocol is described in appendix 1.

6.2.2.3. *T. cruzi* Tulahuen intracellular amastigote assay

The efficacy of compounds against *T. cruzi was* undertaken by Dr. Sykes using a phenotypic, high-throughput image-based assay as previously described (Sykes and Avery, 2015). The detailed protocol is described in appendix 4.

6.2.2.4. *T. cruzi* Tulahuen LacZ, clone C4 (nifurtimox-sensitive)

The *T. cruzi* assay undertaken by Prof. Maes and colleagues at Department of Biomedical Sciences, Laboratory for Microbiology, Parasitology and Hygiene, University of Antwerp, Belgium was in accordance to the previously published methodology (Cos, *et al.*, 2006). The detailed protocol is described in appendix 1.

6.2.3. *In vitro* anti-malarial assays

6.2.3.1. 3D7 and Dd2 strains of *P. falciparum*

The 14 point concentration response curves for **BZ1** and **BZ1-1** were generated to determine accurate IC_{50} values for these compounds against *Plasmodium falciparum* 3D7 (Wild type) and Dd2 (Resistant) using a phenotypic, high-throughput imaging assay previously described by (Duffy and Avery, 2012). This assay was performed by Sandra Duffy at Discovery Biology, Griffith Institute for Drug Discovery, Griffith University, Australia.

6.2.3.2. K1 strain of P. falciparum

Evaluation of compounds against the *P. falciparum* K1 strain was undertaken at Department of Biomedical Sciences, Laboratory for Microbiology, Parasitology and Hygiene, University of Antwerp, Belgium by Prof. Maes and colleagues according to the protocol by (Cos, *et al.*, 2006). The detailed protocol is described in appendix 1.

6.2.4. Drug Metabolism and Pharmacokinetics (DMPK) studies

The DMPK studies were conducted by Prof. Charman and colleagues at Centre from Drug Candidate Optimisation, Monash Institute of Pharmaceutical Sciences, Monash University, Australia. The detailed protocol is described in appendix 5.

6.2.5. Cytotoxicity Panel

For all cytotoxicity assays, the assay conditions such as resazurin concentration, DMSO concentration, optimal dilution media, reference compounds and assay reproducibility were optimized as described previously in chapter 3 (section 3.2).

6.2.5.1. HepG2 resazurin viability assay

HepG2 cells is a human liver cancer cell line obtained from the ATCC®, USA (Hep G2-ATCC® HB-8065™) were maintained in DMEM supplemented with 10% (v/v) HIFBS at 37ºC in a humidified atmosphere of 95% air and 5% CO_2. HepG2 cells at 5 x 10^4 cells/mL in DMEM + 10% HIFBS (v/v), were added in a total volume of 55 µL to Greiner™ black 384-well plates using the Multidrop™ liquid handling system. The compounds prepared at 20 mM in 100% DMSO were diluted in DMEM without HIFBS in a ratio 1:25 and 5 µL of the compounds were added to give a final concentration of 0.4% DMSO and desired compound final concentration. The plates were incubated for 48 hours at 37ºC with 5% CO_2. Resazurin was diluted in DMEM+10% HIFBS to give a concentration of 0.49mM. Ten (10) µL of this dilution was added to assay plates, and plates were further incubated for 5 hours at 37ºC/ 5% CO_2, then left at room temperature for 19 hours. The plates were read on the EnVision™ Multilabel plate reader using fluorometry settings with excitation of 530 nm and emission 590 nm. DMSO (0.4%) was used as a negative control and 5µM of Puromycin was used as a positive control.

6.2.5.2. HEK-293 resazurin viability assay

HEK-293 cells is a human embryonic kidney cell line obtained from the ATCC®, USA (HEK-293 CRL-1573™) were maintained in DMEM supplemented with 10% (v/v) HIFBS at 37ºC in a humidified atmosphere of 95% air and 5% CO2. The cells were passaged as they reach 80% confluence. This assay was undertaken as previously described in chapter 2 (section 2.3.2.5.).

6.2.5.3. Macrophage (Induced THP-1) cytotoxicity assay

THP-1 is a human monocytic cell line obtained from the ATCC®, USA (THP-1 TIB-202™). These cells were maintained in RPMI 1640 medium GlutaMAX™ supplemented with 0.05 mM Mercaptoethanol and 10% (v/v) HIFBS at 37ºC in a humidified atmosphere of 95% air and 5% CO_2. This assay was performed as previously described in Chapter 2 (section 2.3.2.4.).

6.2.5.4. RAW-264.7 resazurin viability assay

RAW-264.7 is a murine macrophages cell line derived from Abelson's leukaemia obtained from the ATCC®, USA (RAW 264.7-ATCC® TIB-71™) maintained in DMEM supplemented with 10% (v/v) HIFBS at 37ºC in a humidified atmosphere of 95% air and 5% CO_2. The protocol used was similar to section 2.3.2.5with a slight modification in the number of cells initially seeded per 384 well plate: from 2.5 x 10^5 to 2.0 x 10^4 cells/mL.

6.2.5.5. J774.1 resazurin viability assay

J774.1 cells, a murine macrophages cell line from reticulum cell sarcoma obtained from the ATCC®, USA (J774A.1 -ATCC® TIB-67™)were maintained in DMEM supplemented with 10% (v/v) HIFBS at 37ºC in a humidified atmosphere of 95% air and 5% CO_2.. The protocol used was similar to section 2.3.2.5 with a slight modification in the number of cells initially seeded per 384 well plate: from 2.5 x 10^5 to 4 x 10^4 cells/mL.

6.3. Results

6.3.1. Activity against different strains and species of *Leishmania* in the Old and New World.

The activity of **BZ1** and **BZ1-I** were compared between the different strains and species of *Leishmania* which are representative of Old and New World leishmaniasis (Table 6.1). It was observed that our novel compounds, **BZ1** and **BZ1-I**, demonstrated sub-micromolar activity with IC_{50} values of 0.81 ± 0.25 µM, 0.83 ± 0.34 µM for *L. donovani* (MHOM/SD/62/1S-CL2D, LdBOB), respectively. This value was comparable to the IC_{50} values obtained for the **BZ1** (0.59 ± 0.13 µM) and **BZ1-I** (0.40 ± 0.38 µM) in our *L. donovani* MHOM/IN/80/DD8 intracellular amastigote assay. A slight decline in activity with IC_{50} values 1.56 ± 0.42 µM and 1.19 ± 1.15 µM, respectively was observed for both **BZ1** and **BZ1-I** tested in *L. infantum* MHOM/MA(BE)/67. Both **BZ1** and **BZ1-I** exhibited the least activity for *L. infantum*MHOM/BR/1972/BH46 with IC_{50} values of 6.30 ± 0.14 µM and 5.45 ±1.06 µM, respectively. A threefold difference in selectivity for THP-1 cells was observed for *L. donovani* MHOM/IN/80/DD8 for **BZ1** (>33.89) and **BZ1-I** (>49.12) compared to selectivity for THP-1 in the *L. donovani* MHOM/SD/62/1S-CL2D, LdBOB with **BZ1** (>11.76) and **BZ1-I** (>11.49). A four fold difference in selectivity for THP-1 cells was observed for **BZ1** (>33.89) and **BZ1-I** (>49.12) in *L. donovani* (MHOM/IN/80/DD8) assay when compared to their selectivity for THP-1 in *L. infantum* (MHOM/BR/1972/BH46) [**BZ1** (>15.65) and **BZ1-I** (10.73)]. Both **BZ1** and **BZ1-I** exhibited a selectivity of 3.39 and 5.03 for the MRC5 cells, respectively. Amphotericin B was used as a reference compound exhibiting IC_{50} values of 0.20 ± 0.02 µM and 1.5 ± 0.01 µM µM for *L. donovani* MHOM/IN/80/DD8 and *L. infantum* (MHOM/BR/1972/BH46), respectively. The reported IC_{50} values for miltefosine were 2.54 ± 0.57 µM *L. donovani* MHOM/IN/80/DD8, 10.48 ± 0.10 µM in *L. infantum* MHOM/MA(BE)/67 and 0.80 ± 0.02 µM for *L. infantum* (MHOM/BR/1972/BH46).

6.3.2. Activity against different species of *T. brucei*

The efficacy of **BZ1** and **BZ1-I** was compared between different species of *T. brucei* (*T. b. brucei* Squib 427 strain [suramin-sensitive] and *T. b. rhodesiense*) (Table 6.2). The IC_{50} values obtained for both **BZ1** and **BZ1-I** against the *T. b. brucei* Squib 427 [suramin-sensitive] strain were 2.45 ± 0.73 µM and 1.69 ± 0.06 µM, respectively. The activity of the compounds against the *T. b. rhodesiense* species was IC_{50} values of 2.59 ± 0.45 µM and 1.92 ± 0.01 µM for **BZ1** and **BZ1-I,** respectively. When the assay was performed in our laboratory against *T. b.brucei* bloodstream 427 strain, we obtained the following IC_{50} values of **BZ1:** 3.32 ± 0.15 µM and **BZ1-I** : 2.15 ± 0.58 µM. The selectivity of **BZ1** for *T. b. brucei* Squib 427 [suramin-sensitive] strain and *T. b. rhodesiense* was calculated to be 2.15 and 2.04. Whereas selectivity of **BZ1-I** for *T. b. brucei* Squib 427 [suramin-sensitive] strain and *T. b. rhodesiense* was calculated to be 3.55 and 3.12, respectively. The reference compound suramin, displayed an activity of 0.03 µM and 0.05 µM against the *T. b. brucei* Squib 427 [suramin-sensitive] strain and *T. b. rhodesiense*. The reference compounds pentimidine, diminazene and puromycin exhibited an IC_{50} of 0.002 ± 0.00 µM, 0.05 ± 0.00 µm and 0.06 ± 0.00 µM against the *T. b. brucei* at our laboratory.

Table 6.1: Activity against different strains and species of *Leishmania* in the Old and New World. Each evaluation was performed in triplicate, for N=2 except activity against *Leishmania donovani* (MHOM/SD/62/1S-CL2D, LdBOB) which was performed in triplicate, for N=3.

	Old World			**Old World**		**Old World**			**New World**	
Compounds and Reference Drugs	***Leishmania donovani* (MHOM/IN/80/DD8)**			***Leishmania donovani* (MHOM/SD/62/1S-CL2D, LdBOB)**		***Leishmania infantum* MHOM/MA(BE)/67**			***Leishmania chagasi* (MHOM/BR/1972/BH46)**	
	IC_{50} (µM) [Mean ± SD]	**Selectivity**		**IC_{50} (µM) [Mean ± SD]**	**Selectivity**	**IC_{50} (µM) [Mean ± SD]**	**Selectivity**		**IC_{50} (µM) [Mean ± SD]**	**Selectivity**
		HEK-293 cells	THP-1 cells		THP-1 cells		MRC-5 cells	PMM		THP-1 cells
BZ1	0.59 ± 0.13	>33.72	>33.89	0.85 ± 0.12	>11.76	1.56 ± 0.42	3.39	>41.0	6.30 ± 0.14	>15.65
BZ1-I	0.40 ± 0.38	>24.11	>49.12	0.87 ± 0.24	>11.49	1.19 ± 1.15	5.03	6.72	5.45 ±1.06	10.73
Amphotericin B	0.20 ± 0.02	47.61	10.24	-	-	-	-	-	1.5 ± 0.01	14.74
Miltefosine	2.54 ± 0.57	15.74	7.87	-	-	10.48 ± 0.10	-	-	0.80 ± 0.02	62.72

Table 6.2: Cross activity against different species of *Trypanosoma brucei*. Each evaluation was performed in triplicate, for N=2.

Compounds and Reference Drugs	*Trypanosoma brucei brucei* Squib 427 strain (suramin-sensitive)		*Trypanosoma brucei rhodesiense*		*Trypanosoma brucei brucei* (Discovery Biology laboratory)	
	IC_{50} (µM) [Mean ± SD]	Selectivity (MRC-5 cells)	IC50 (µM) [Mean ± SD]	Selectivity (MRC-5 cells)	IC_{50} (µM) [Mean ± SD]	Selectivity (HEK-293 cells)
Compound BZ1	2.45 ± 0.73	2.15	2.59 ± 0.45	2.04	3.32 ± 0.15	>6.02
Compound BZ1-I	1.69 ± 0.06	3.55	1.92 ± 0.01	3.125	2.15 ± 0.58	>9.30
Pentamidine	-	-	-	-	0.002 ± 0.00	297.78
Diminazene	-	-	-	-	0.05 ± 0.00	29
Puromycin	-	-	-	-	0.06 ± 0.00	1
Suramine	0.03		0.05	-	-	-

6.3.3. Activity against *T. cruzi*

The ability of compounds **BZ1** and **BZ1-I** to have an impact on *T. cruzi* amastigotes was evaluated as described in section 6.2.2. It should be noted that these two assays were performed in different laboratories and their formats are quite different as described in the appendices 1 and 4. . The compounds **BZ1** and **BZ1-I** displayed an IC_{50} of 2.24 ± 0.12 µM and 0.51± 0.01 µM against the *T. cruzi*, Tulahuen LacZ, clone C4 (nifurtimox-sensitive) strain. On the other hand, **BZ1** and **BZ1-I** exhibited an IC_{50} of 15.54 ± 0.59 µM and 3.24 ± 0.14 against *T.cruzi*, Tulahuen strain at our laboratory. The reference compound benznidazole had an IC_{50} values of 1.75 ± 0.07 µM and 4.42 ± 0.80 µM for *T. cruzi*, Tulahuen LacZ, clone C4 (nifurtimox-sensitive) strain and *T.cruzi*, Tulahuen strain at our laboratory. These results are summarized in Table 6.3.

6.3.4. Activity against different *P. falciparum* strains

The activity was compared between the different strains of *P. falciparum* (Table 6.4). Compound **BZ1** exhibited an IC_{50} value of 1.89 ± 0.02 µM and 1.85 ± 0.01 µM against the 3D7 (wild type) and Dd2 (chloroquine resistant) strains of *P. falciparum*. Compound **BZ1** displayed lesser activity (2.98 ± 0.51 µM) against K1 strain of *P. falciparum*. The other compound **BZ1-I** showed an IC_{50} of 2.91 ± 0.06 µM and 3.80 ± 0.11 µM against the the 3D7 and Dd2 strains of *P. falciparum*. On the other hand, when tested against K1 strain of *P. falciparum*, the IC_{50} value for **BZ1** could not be established. The reference compound chloroquine, showed an IC_{50} value of 0.04 ± 0.00 µM in 3D7 and 0.08 ± 0.01 µM for *P. falciparum* K1 strain.

Table 6.3: Cross activity against *Trypanosoma cruzi*. Each evaluation was performed in triplicate, for N=2.

Compounds and Reference Drugs	***Trypanosoma cruzi*, Tulahuen LacZ, clone C4 (nifurtimox-sensitive)**		***Trypanosoma cruzi*, Tulahuen (Discovery Biology laboratory)**	
	IC_{50} (µM) [Mean ± SD]	Selectivity (MRC-5 cells)	IC_{50} (µM) [Mean ± SD]	Selectivity (3T3 cells)
Compound BZ1	2.24 ± 0.12	2.36	15.54 ± 0.59	4.72
Compound BZ1-I	0.51± 0.01	11.74	3.24 ± 0.14	22.59
Nifurtimox	-	-	1.01 ± 0.09	125
Benznidazole	1.75 ± 0.07	-	4.42 ± 0.80	29
Puromycin	-	-	2.03 ± 0.25	1
Posaconazole	-	-	0.003 ± 0.00	349

Table 6.4: Activity against different strains of *Plasmodium falciparum*. Each evaluation was performed in triplicate, for N=2.

	Plasmodium falciparum			***Plasmodium falciparum* K1 strain Resistant to Chloroquine, Pyrimethamine and Cycloguanil.**
Compounds and Reference Drugs	**3D7 IC_{50} µM**	**Dd2 IC_{50} µM**	**Dd2/3D7**	**K1 IC_{50} (µM)**
Compound BZ1	1.89 ± 0.02	1.85 ± 0.01	1.0	2.98 ± 0.51
Compound BZ1-I	2.91 ± 0.06	3.80 ± 0.11	1.3	-
Chloroquine	0.04 ± 0.00	0.44 ± 0.02	11.2	0.08 ± 0.01
Pyrimethamine	0.002 ± 0.00	66% at 40uM	Resistant	
Artesunate	0.001 ± 0.00	0.001 ± 0.00	1.0	

6.3.5. DMPK studies

Both compounds (**BZ1** and **BZ1-I**) share very similar physiochemical properties: low MW (304.39 and 352.44), low PSA (both have 35.4), high lipophilicity cLogP (4.7 and 6.0) and low/moderate solubility at pH 6.5 (12.5-25 and 1.6-3.1 µg/mL) as displayed in table 6.5. The *in vitro* metabolic properties were also similar with both compounds undergoing moderate rates of degradation in human liver microsomes with half live of 47 and 57 min, and a very high rates of metabolism in mouse liver microsomes with half live of <2 minutes (Table 6.6). The predictive clearance *in vitro* in humans was calculated to be 37 µL/min/mg for both compounds; whereas the predictive clearance *in vitro* in mouse models > 866 µL/min/mg.

6.3.6. Cytotoxicity studies

A stable plateau of activity was not observed for either **BZ1** or **BZ1-I** at the top concentration of 80 µM (final assay concentration) hence accurate IC_{50} values could not be determined (Figure 6.2). The compounds face solubility issues at concentrations higher than 80 µM. The compound **BZ1** causes a 50% inhibition at 11.3 ± 0.2 µM, 38.4 ± 0.7 µM, 33.2 ± 0.4 µM, 18.1 ± 1.7 and 18.6 ± 1.4 µM for HepG2, Raw264.7, J774.1, HEK-293 and THP-1 cells, respectively. **BZ1-I** has a slightly reduced safety profile than **BZ1** and causes a 50% inhibition at 9.4 ± 0.7 µM, 40.7 ± 0.1 µM, 45.7 ± 3.1 µM, 11.2 ± 0.9 and 18.2.6 ± 0.3 µM for HepG2, Raw264.7, J774.1, HEK-293 and THP-1 cells, respectively.

Table 6.5: Physicochemical evaluation of BZ1 and BZ1-I. Each evaluation was performed in triplicate, for N=2.

Compound	MW	PSA (Å2)	FRB	HBD	HBA	Arom. Rings	Fsp3	Predicted pKa (0-12 only)	cLogP	cLogD at pH 7.4	gLogD at pH 7.4	Sol 2.0 (µg/mL)	Sol 6.5 (µg/mL)
BZ1	304.39	35.4	4	1	3	3	0.25	Basic: 8.1 Acidic: None	4.7	3.9	5.0	>100	12.5-25
BZ1-I	352.44	35.4	4	1	2	4	0.13	Basic: 8.1 Acidic: None	6.0	5.2	>5.3	25-50	1.6-3.1

Log P: Partition coefficient of a molecule between an aqueous and lipophilic phase, **HBA:** Hydrogen bond acceptors, **HBD:** Hydrogen bond donors, **TPSA:** Topological polar surface area, **Rot Bonds:** Rotational bonds.

Table 6.6: Metabolic evaluation of BZ1 and BZ1-I. Each evaluation was performed in triplicate, for N=2.

Compound	Microsome Species	$T^{1/2}$ (min)	CLint, in vitro (µL/min/ mg protein)	Predicted CL int, *in vivo* (mL/min/kg)	Predicted CLblood (mL/min/kg)	Predicted EH	Clearance Classification
BZ1	Human	47	37	30	12	0.59	Intermediate
	Mouse	<2	> 866	> 2235	> 113	> 0.94	very high
BZ1-I	Human	57	37	25	11	0.55	Intermediate
	Mouse	<2	> 866	> 2235	> 113	> 0.94	very high

T1/2: Half life of compound, **CL:** Hepatic blood clearance, **EH:** Hepatic extraction ratio.

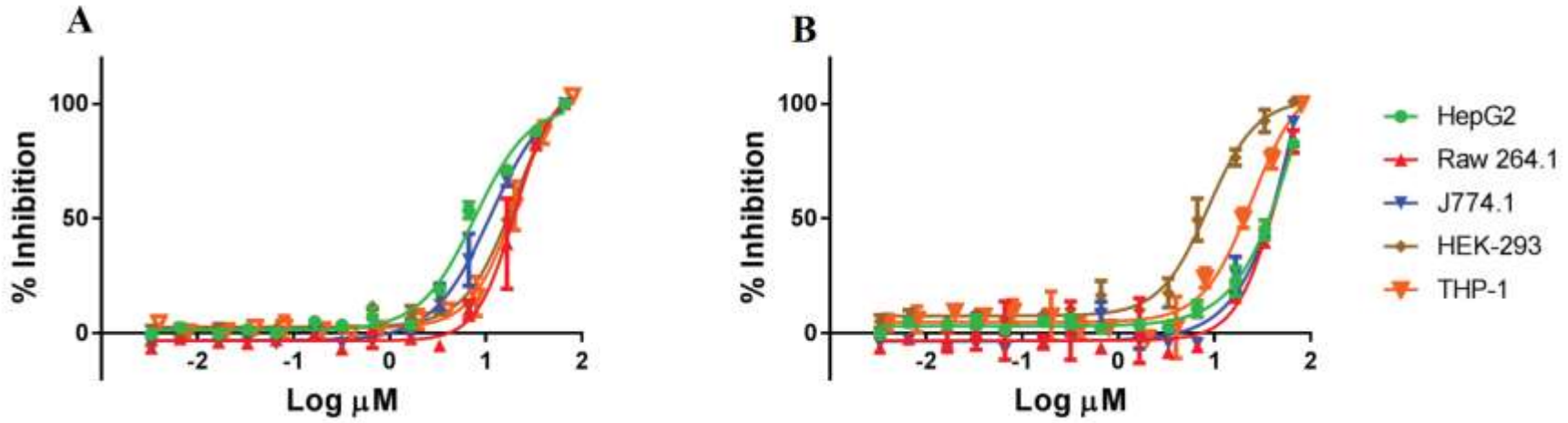

Figure 6.3: Concentration response curve against cytotoxicity panel for compounds BZ1 (A) and BZ1-I (B). Each evaluation was performed in triplicate, for N=2. The plates were read on the EnVision™ Multilabel plate reader using fluorometry settings with excitation of 530 nm and emission 590 nm.

6.4. Discussion

The taxonomic classification for the genus *Leishmania* is based on the molecular and biochemical characterization of each species (Akhoundi, *et al.*, 2016). These differences contribute for the variable sensitivity of compounds and may present important clinical implications (Croft and Coombs, 2003). It has been reported that therapeutic efficiency of drugs is dependent on the species of *Leishmania*, geographic region and clinical manifestations therefore; experimental and clinical data should not be generalized (Croft and Olliaro, 2011; Kevric, *et al.*, 2015).

Previous work has shown that the activity of a particular drug or candidate molecule can be variable based on its activity for different *Leishmania* species and strains. This variation was noted even for reference compounds, as demonstrated by Escobar *et al.*, 2002, where the values of IC_{50} values obtained for miltefosine varied from 2.6 to 37.1 µM, within different species of *Leishmania* (Escobar, *et al.*, 2002). The same profile was observed for a panel of leishmanial strains including *L. amazonensis* and *L. braziliensis*, when treated with amphotericin B (Miguel, *et al.*, 2011). A better understanding of the variation in susceptibility/drug tolerance, considering different strains and species, may have important clinical implications, as demonstrated by Faraut–Gambarelli and collaborators (Faraut-Gambarelli, *et al.*, 1997). There was a significant correlation between the *in vitro* results and the clinical success or failure of the treatment: all strains related to therapeutic failures require greater concentration of miltefosine to eliminate the infection in the trials (Faraut-Gambarelli, *et al.*, 1997). In another more recent study, carried out in endemic regions of Colombia, it was shown that susceptibility to antimonial compounds and miltefosine differed between strains of the same species and among different species, isolated from different geographical regions at different periods of time (Fernandez, *et al.*, 2014).

To verify whether a variation of activity exists for the compounds of interest here, the activity of **BZ-1** and **BZ1-1** compounds were compared for three different parameters, which are as follows:

1. Variation between the different strains of *Leishmania*.
2. Variation between the different species of *Leishmania*.
3. Variation between the Old and New World species of *Leishmania*.

A variation in activity was observed for compounds **BZ1** and **BZ1-I** following the pattern of increased activity with *L. donovani* (MHOM/IN/80/DD8) > *L. donovani* (MHOM/SD/62/1S-CL2D, LdBOB) > *L. infantum* (MHOM/MA(BE)/67) > *L. infantum* (MHOM/BR/1972/BH46).

The data suggested that the variation of compound activity determined between the species was substantial when compared to the differences in the activity between the strains (Table 6.1). This was evident in the case of *L. donovani* (MHOM/IN/80/DD8) and *L. infantum* (MHOM/BR/1972/BH46), with a 10-fold difference in activity. There may be a number of reasons for the difference in activity observed between the two species. One contributing factor for this difference was the assay conditions. For the *L. donovani* (MHOM/IN/80/DD8) amastigote assay the infection ratio was 1:5, thus one host cell per five parasites, whereas for *L. infantum* (MHOM/BR/1972/BH46), the infection ratio was 1:50 (host cell : parasite). The 10-fold increase in parasite number per cell would appear to correlate with the observed differences in compound activity. Another reason which may have impact upon the activity of the compounds was the incubation period with compounds. For the *L. infantum* (MHOM/BR/1972/BH46) intracellular amastigote assay the incubation periods after the addition of compounds was 48 hours, whereas for the *L. donovani* (MHOM/IN/80/DD8) intracellular amastigote assay the incubation period after addition of compounds was 96 hours. A similar pattern can be observed in the marked decrease in activity of amphotericin B from 0.20 ± 0.02 µM in *L. donovani* (MHOM/IN/80/DD8) to 1.5 ± 0.01 µM in *L. infantum* (MHOM/BR/1972/BH46) as demonstrated in table 1. One theory to describe this difference between the sensitivity of these species may also be to the impact of the different type and concentration of sterols present in the membranes of the different species of *Leishmania* (Croft, *et al.*, 2002). Previously, different concentrations of sterols have been reported in different species of *Leishmania* (Beach, *et al.*, 1988). A similar variation was observed for miltefosine with IC_{50} values 0.80 ± 0.02, 2.54 ± 0.57, 10.48 ± 0.10 in *L. infantum*(MHOM/BR/1972/BH46), *L. donovani*

(MHOM/IN/80/DD8) and *L. infantum* (MHOM/MA(BE)/67), respectively. It has been reported in the past that there was a three to five fold intrinsic variation in drug sensitivity among *Leishmania* species for antimonials, azoles, miltefosine and Paromomycin (Croft, *et al.*, 2006; Croft and Olliaro, 2011; Rama, *et al.*, 2015).

A variation in selectivity of the compounds for the THP-1 host cells in the different assays is evident with a 3 to 4-fold difference, as illustrated in table 6.1. Once again the variation may be due to the difference in assay conditions, as well as the different concentrations of PMA used to differentiate the THP-1 cells into macrophages. It has been reported in the past that the profile of infection, as well as the anti-leishmanial activity of compounds, can be dependent on the host cell, which could have major implications for the process of selecting anti-leishmanial molecules (Seifert, *et al.*, 2010). THP-1 cells are used as an alternative to the primary mouse macrophages. Primary mouse macrophages are rarely used in the initial screening processes, since they are a heterogeneous population of cells with different rates of cellular division, which could impact the reproducibility of the assays. In addition, ready access to large quantities of primary cells is limited. Once differentiated, the THP-1 cells form a homogeneous monolayer of cells that do not divide *in vitro* (Tsuchiya, *et al.*, 1980). These activated THP-1 cells have been used as a gold standard for a variety of high-throughput assays in the past (Siqueira-Neto, *et al.*, 2012; Dagley, *et al.*, 2015; Pena, *et al.*, 2015; Khare, *et al.*, 2016).

Both the compounds **BZ1** and **BZ1-I** displayed IC_{50} values of < 5 μM for the different species of *T. b. brucei* and *T. b. rhodesiense*, as shown in table 6.2. The compound **BZ1** exhibited an activity pattern as follows : *T. b. brucei* Squib 427 (suramin-sensitive) strain > *T. b. rhodesiense* > *T. b. brucei* strain (our laboratory). **BZ1-I** exhibited an inhibitory activity with similar pattern as **BZ1**: *T. b. brucei* Squib 427 (suramin-sensitive) strain > *T. b. rhodesiense* > *T. b. brucei* strain (our laboratory). All assays used to determine activity against *Tryopanosoma brucei* used colorimetric evaluation with similar assay formats.

To evaluate the activity of both **BZ1** and **BZ1-I** against *Trypanosoma cruzi*, the compounds were tested both by Prof. Maes laboratory at Department of Biomedical Sciences, Laboratory for Microbiology, Parasitology and Hygiene, University of Antwerp, Belgium and in a well validated assay in our laboratory. A 6-fold difference in

activity was observed for *T. cruzi*, Tulahuen and *T. cruzi*, Tulahuen LacZ Clone 4 strain for **BZ1** and **BZ1-I** as illustrated in table 6.3. There are a number of potential reasons for the differences in activity observed for the compounds obtained from these two independent laboratories. The reason is the difference in assay format. The assay for *T. cruzi*, Tulahuen undertaken by Dr. M Sykes (Discovery Biology, Griffith University) is a high-throughput image based assay, whereas the assay at Prof. Maes laboratory uses the T. *cruzi*, Tulahuen LacZ Clone 4 strain and is a lower throughput colorimetric assay. The second potential cause for discrepancy might be associated with the different incubation periods used for the two assays. The Sykes image based assay (Sykes and Avery, 2015) has an incubation period of 48 hours, whereas in the colorimetric assay the compound exposure was for 7 days. The possibility also exists that the compounds are relatively slow acting, hence why they have shown more activity following the longer incubation periods. As increased activity with increased exposure, is not uncommon. Lastly, a variation associated with the host cells could have had an impact on the compound activity. The colorimetric assays used *T. cruzi*, Tulahuen LacZ Clone 4 strain infected MRC-5 cells (human lung fibroblasts cells), whereas the imaging assay used *T. cruzi*, Tulahuen infected 3T3 cells (mouse embryonic fibroblast cells). Variations in compound susceptibility for *T. cruzi* based on host cells, genetic origin and geographical location have been reported in the past (Revollo, *et al.*, 1998; Luna, *et al.*, 2009). Previously, Moraes *et al.*,2014, also reported a differences of activity of nitroheterocyclic compounds for a panel of strains and clones (Dm28c, Y, ARMA13 cl1, ERA cl2, 92-80 cl2, CL Brener and Tulahuen) of *T. cruzi* (Moraes, *et al.*, 2014). Recently a study was conducted to assess the difference in activity between two strains of the wildlife trypanosomes, *Trypanosoma copemani* (G1 and G2 strains) with *T.cruzi*, the results indicated that all reference drugs (benznidazole and posaconazole) and pyridine derivatives were more active on *T. copemani* than against *T.cruzi* (Botero, *et al.*, 2017), An intra-strain difference in activity was observed for all the drugs and compounds against the *T. copemani* G1 and G2 strains signifying physiological and infectivity differences between both strains (Botero, *et al.*, 2017).

A target candidate profile (TCP) (Don and Ioset, 2014) has been established by DND*i* to classify a compound as an active hit against *Leishmania, T. b. brucei* and *T. cruzi*. Using this criteria, specifically in terms of *in vitro* efficacy being IC_{50} value<10 µM as the classification of a potential anti-kinetoplastid hit, compounds which underwent

screening were selected as hit compounds. Based on the criteria proposed by DND*i*, both compounds **BZ1** and **BZ1-I**, were classified as having anti-kinetoplastid activity.

In order to investigate whether the compounds have anti-plasmodial activity against the different strains of *P. falciparum* the compounds were tested on the Dd2 and 3D7 strains of *P. falciparum* by Sandra Duffy (Discovery Biology, Griffith university) using a phenotypic, high-throughput high-content assay previously described (Duffy and Avery, 2012). The compounds were also sent to Prof. Maes laboratory to be assessed for activity against K1 strain. Compound **BZ1** showed somewhat similar activities on all of the strains of *P. falciparum* (K1, Dd2 and 3D7) tested with IC_{50} values of 2.98 ± 0.51 µM, 1.85 ± 0.01 µM and 1.89 ± 0.02 µM, respectively (Table 6.4). On the other hand, the IC_{50} value could not be calculated for the compound **BZ1-I** as the concentration response curve did not reach the plateau. It would be worthwhile to test the other analogues to identify a compound showing sub-micromolar activity. It is believed that compounds that have anti-plasmodial activity with unknown mechanisms of actions could be used as suitable starting points for medicinal chemists and can be used as chemical probes to reveal previous mechanisms and unstudied targets for parasite survival (Duffy, *et al.*, 2017).

Our data indicated that both **BZ1** and **BZ1-I** have demonstrated promising anti-leishmanial activity and further characterization and biological profiling of these compounds should be conducted. For this purpose these compounds were sent to Centre for Drug Candidate Optimisation Monash Institute of Pharmaceutical Sciences, Monash University, Australia for DMPK studies. Compounds **BZ1** and **BZ1-I** were evaluated for their physicochemical properties (Table 6.5). The physicochemical evaluation of the compounds **BZ1** and **BZ1-I** suggests that both the molecules have lead-like properties. Lead-like properties are physiochemical characteristics of a compound such as cLogP, molecular weight and polar surface area (PSA), which can predict optimization problems and toxicity on later phases of drug discovery (Di and Kerns, 2015; Cernak, *et al.*, 2016). Since many cases of failures are related to poor physicochemical properties (i.e toxicity), restricting these properties values helps to decide which compounds are goods starting points for optimization.

The solubility of a compound is an important parameter to identify the activity of a compound at a specific concentration in *in vitro* experiments. Precise inhibitory

concentrations cannot be calculated for compounds displaying poor solubility hence usually discontinued or chemical modifications (like complexation, derivatization and salt formation) are recommended to enhance solubility. Later in drug development phases solubility is required to achieve desired concentration of drug in systemic circulation to provide the pharmacological response. The solubility of the compounds was analysed via a Nephelometry method using standard test buffers (pH 2.0 and pH 6.5). Both the compounds exhibited moderate solubility based on solubility being from >100 at pH 2.0 to 12.5-25 at pH 6.5 for **BZ1**. Compound **BZ1-I** demonstrated lesser solubility as it changed from 25-50 at pH 2.0 to 1.6-3.1 at pH 6.5. Both the compounds have displayed moderate solubility.

The next objective was to determine the *in vitro* metabolic stability of these two compounds using human and mouse liver microsomes as a preliminary indication of their likely *in vivo* metabolic clearance and potential metabolic products. Both of the compounds **BZ1** and **BZ1-I**, demonstrated intermediate clearance in human microsomes but rapid clearance in mouse microsomes suggesting rapid degradation as illustrated in table 6.6. It has been previously reported that *in vitro* hepatocyte models and liver microsomes fail to predict the *in vivo* metabolism. In these cases usually *in vivo* PK studies are recommended (Wan, 2013). The intermediate clearance in human microsomes suggests that *in vivo* metabolic stability should be further investigated in golden Syrian hamster model. Future research in progressing these compounds should involve *in vivo* DMPK studies. This result will be critical to proceed with *in vivo* testing of compounds **BZ1** and **BZ1-I** as golden Syrian hamster model is standard model used for visceral leishmaniasis (Hendrickx, *et al.*, 2015; Sacks and Melby, 2015; Rouault, *et al.*, 2017).

The cytotoxicity panel was also established to compare and evaluate the cytotoxicity of compound using a broad range of cell lines which represent different species and origins (Figure 6.2). The cytotoxicity panel was established using HepG2, HEK-293, J774.1 and Raw 264.7 cells, all of which are proliferating cell lines. On the other hand, THP-1 induced into macrophages using PMA as described in chapter 2 (section 2.3.3.1) were also included. These induced THP-1 machophages (Chanput, *et al.*, 2014) are non-dividing, hence collectively the panel provides a profile of the toxicity of both proliferating cells and non-dividing cells. The cell lines chosen represent different organ systems from mouse or human origin and are routinely used for cytotoxicity testings,

HepG2 [human liver cancer cell line] (Sahu, *et al.*, 2014), HEK-293 [embryonic kidney cell line] (Reddy, *et al.*, 2010), J774.1 (Yamaori, *et al.*, 2013) and Raw 264.7 (Tripathy, *et al.*, 2014) are murine macrophages. When **BZ1** and **BZ1-I** were tested, the plateau of activity could not be established at a top concentration of 80 µM, hence an exact IC_{50} values could not be calculated for either compound. The cytotoxicity panel established here represent cell types from a variety of organs and also accounts for the effect of the compounds on heterogeneous cell types. Hence, it is predictive, and therefore highly recommended for evaluating compounds destined for the drug discovery process.

Table 6.7: Difference between the anti-leishmanial intracellular amastigote assays performed for compound BZ1 and BZ1-I.

	GRIDD intracellular amastigote assay	De Rycker and colleagues intracellular amastigote assay	Freitas-Junior and colleagues intracellular amastigote assay
Parasite	*L. donovani* MHOM/IN/80/DD8	*L. donovani* MHOM/SD/62/1S-CL2D, LdBOB	*L. infantum* MHOM/BR/1972/BH46
Host cells	THP-1 human monocytes	THP-1 human monocytes	THP-1 human monocytes
Format	384-well	384-well	384-well
Number of Cells/wells	12,500 cells/well	8000 cells/well	7000 cells/well
PMA differentiation of THP-1	25 ng/mL of PMA for 24 hours	10 ng/mL of PMA for 75 hours	50 ng/mL of PMA for 48 hours
Washing Step to remove PMA prior infection	Yes.	Yes.	No.
Infection	Late stationary phase promastigotes	Axenic amastigotes 5 parasites per each THP-1 cell	Late stationary phase promastigotes 50 parasites per each THP-1 cell
Washing Step to remove extracellular parasites	Yes. PMA is re-added after washing.	Yes. PMA is not added after washing.	No.
Compounds	added 24 h post-infection	added 24 h post-infection	added 24 h post-infection
Total treatment period	96 h	72h	48h
Dyes	SYBR® Green (1:10,000) and CellMask Deep Red (1:25,000)	DAPI (1:1000) Cellmask Deep Red (1:20,000)	Draq-5 (1:1000)
HCS system	Opera (PerkinElmer)	IN Cell 1000 or IN Cell 2000 (GE)	Operetta (PerkinElmer)

There are no platforms currently available which can test the compounds against various parasite species and strains taking into account the assay conditions and duration of compound exposure. Table 6.7 demonstrates the differences between the anti-leishmanial intracellular amastigtote assays performed for compound BZ1 and BZ1-I. This would have been ideal to ensure consistency and direct comparability of results. Thus, there exists an urgent and yet unmet need to expand the *in vitro* assay portfolio to incorporate such a panel to provide data to better understand activity of the candidate molecule and improved prioritization of candidates.

Both the compounds **BZ1** and **BZ1-I** demonstrated promising *in vitro* activity against *Leishmania* intracellular amastigotes from the Old and New World species and strains causing visceral leishmaniasis. Both compounds **BZ1** and **BZ1-I** were nanomolar active on *L. donovani* DD8 intracellular amastigotes with IC_{50} values of 0.59 ± 0.13 µM and 0.40 ± 0.38 µM. The DMPK studies sugguest that the compounds have lead like properties based on physiochemical properties and metabolic evaluation on human microsomes. The promising *in vitro* activity, selectivity in the cytotoxicity panel and DMPK studies warrants further *in vivo* investigation in animal models for compounds **BZ1** and **BZ1-I**.

Chapter 7: General discussion and future prospects

7.1. Significance of the research

Visceral, cutaneous and mucocutaneous leishmaniasis remains some of, the most devastating neglected tropical diseases, each with a high unmet medical need. Sadly, within the past century the available treatment options only have marginally improved for these diseases. The treatment regime faces therapeutic limitations largely due to emerging resistance (Sundar, 2001); extensive toxicity for current drugs (Bhargava and Singh, 2012) and limited efficacy to particular geographical locations. It is therefore imperative that new chemical starting points for drug discovery and development are identified. Thus, new assays need to be developed for screening compounds for anti-leishmanial properties. These assays should be cost effective, robust, accurate, precise and automated to minimize the risk associated with human error. They should be able to simultaneously assess multiple compounds. Critical is that these assays reflect the true *in vivo* disease state and thus facilitate translation into the clinic. The path for a new chemical entity from discovery to registration is long and costly with considerable attrition rates, thus high risk. Thus, rather than these difficulties defer us, they should be used to foster creativity and innovation in *Leishmania* drug discovery, it is necessary to continue searching for new active compounds.

The research presented here aimed to develop, optimize and validate a screening cascade of phenotypic HTS compatible anti-leishmanial assays against the different forms of the parasite. This cascade was inclusive of using promastigote viability and an intracellular amastigote assays with complementary cytotoxicity assays. Novel compounds active on both forms of the parasite were identified using this approach to screen libraries of synthetic and natural products. Active hit compounds as defined by the DND*i* target candidate profile were identified, which were selective for the parasite and had minimal effect on host cells. Of note, these compounds demonstrated activity across multiple species and strains of *Leishmania* parasite representative of both the Old and New World. The ability to simultaneously screen compounds against extracellular and intracellular parasite forms, from multiple *Leishmania* strains and species provides a unique activity profile for prioritizing compounds.

7.2. Development, optimization and validation of the anti-leishmanial screening cascade assays

We have successfully developed, optimized and validated a HTS promastigote viability assay which was used in combination with the HTS-HCI intracellular amastigote assay to identify compounds with anti-leishmanial activity. In addition, a cytotoxicity panel incorporating a variety of cell types was also established to evaluate compounds cyto-toxicological profile. While establishing a HTS assay is a laborious process, it is necessary to find the best conditions and thus potential for identifying molecules, which have real activity, not artefacted. Considerable automatic and operational procedures are involved in the screening process. Appropriate data processing tools for data quality assessment and statistical analysis are essential as is technical expertise. Large data sets are generated in a considerably short period of time, making data storage and rapid data analysis a challenging task. When combined with HCI, consistency and reproducibility of an HTS campaign is even more challenging. In order to validate the screening cascade, reference drugs and pre-clinical compounds were utilized. Both assays developed and described here are robust and reproducible, presenting good standard statistical parameters, such as Z' factor and coefficient of variance.

7.3. Screening of synthetic scaffold and natural product libraries

The 384-well phenotypic HTS promastigote and intracellular amastigote assays were used to profile the activity of two libraries against the *L. donovani* DD8 parasite. Namely, a synthetic scaffold library and the DOANP natural product library. The libraries were selected for two different reasons. The synthetic library has not previously been screened against *Leishmania*, it was also chosen to enable more rapid progression of compounds as synthetic stocks were readily available, as were analogues. The natural product library is comprised of bioactive molecules that have previously shown promising anti-bacterial (Yin, *et al.*, 2011), anti-fungal (Davis, *et al.*, 2004), anti-malarial (Davis, *et al.*, 2010) and recently reported anthelmintic activity (Preston, *et al.*, 2017) but had not been tested for anti-leishmanial and anti-trypanosomal activity. Thus later library provided an alternative source of diversity.

From the DOANP natural product library of 472 compounds, a pan active compound **NP1** (Lissoclinotoxin E) was identified having activity <5 µM against both forms of *L. donovani* DD8, *T. b. brucei* and *T. cruzi* parasites.

From the synthetic scaffold library (5560 compounds), two novel compounds **BZ1** and **BZ1-I** were identified with relatively potent activity against both the extracellular and intracellular forms of the *L. donovani* DD8 parasite. Compound **BZ1** exhibited an IC_{50} value of 0.59 ± 0.13 µM against the intracellular form (amastigote) of the parasite and IC_{50} value of 2.37 ± 0.85 µM against the extracellular form (promastigote). The second compound **BZ1-I** (an analogue of compound **BZ1**) was demonstrated to have an IC_{50} of 0.57 ± 0.17 µM against intracellular amastigotes and an IC_{50} value of 0.60 ± 1.12 µM against promastigotes. The low cytotoxicity observed for **BZ1** and **BZ1-I** in conjuction with their anti-leishmanial activity, prioritized them for more extensive profiling.

7.4. Mechanism of action studies

Further investigations performed with **BZ1** compound and its analogue **BZ1-I** included (1) time to kill and (2) host cell pre-incubation studies. These illustrated quite clearly that the speed of killing was not fast and that pre-incubation with the host cell prior to the infection did not cause any immunotherapeutic effect. Based on the previously reported mechanism of action of similar chemotypes the ability of these compounds to induce apoptosis and affect the mitochondrial integrity of the *Leishmania* parasite were assessed. The results indicated that **BZ1** and **BZ1-I** do not induce apoptosis via either the caspase dependent or independent pathways (externalization of phosphatidylserineto the cell surface was not observed). It was also shown that both compounds have no effect on mitochondrial morphology and failed to inhibit the mitochondrial membrane potential. Thus one can conclude that the mechanism of action of these compounds on *Leishmania* parasite is not through the mechanism previously observed for similar chemotypes.

An interesting finding, and unexpected, was the reduced activity observed on the promastiogtes compared with the amastigotes. This is in contrast to what one would expect as often compound activity is reduced against intracellular compounds as multiple membrances must be crossed and the low acidic pH is often detrimental to

compound integrity.To assess the reason, for these differences in activity, pH stability studies were conducted. The results suggested that **BZ1** undergoes degradation within parasitopharous vacuole which has (pH 5.5). **BZ1** is forming two metabolites, whereas to clarify whether the increased activity is associated specifically with one metabolite, future studies will investigate this. **BZ1-I** remains intact and the change in pH doesn't affect it. Resistant clones were also generated for both compounds and clinically used reference drugs (amphotericin B and miltefosine). Clones showed resistance up to concentration of 11 μM, 5.5 μM, 420 nM and 40 μM for **BZ1**, **BZ1-I**, amphotericin B and miltefosine, respectively for promastigotes. Thus the parasites were able to survive in 13-fold, 16-fold, 5.6-fold and 16.1-fold more concentration than their IC_{50} values for amphotericin B, miltefosine, **BZ1** and **BZ1-I**, respectively. The resistant clones demonstrated stability in maintaining in the resistance even after removal of drug/compound pressure after 10 passages.

7.5. Efficacy against Old and New World *Leishmania* strains/species causing visceral leishmaniasis; anti-trypanosomal and antiplasmodial activity.

After assessing the anti-leishmanial, ant-trypanosomal and anti-plasmodial activity of the compounds, cross comparative analysis was undertaken in other laboratories. The data we obtained from our collaborators enabled comparison of activity against different *Leishmania* strains and species, providing an independent validation of our initial results. **BZ1** and **BZ1-I** demonstrated activity against the Old World and New World strains and species of visceral leishmaniasis resulting in IC_{50} values < 6.3 μM (*L. donovani* MHOM/IN/80/DD8 promastigotes and intracellular amastigote, *L. donovani* (MHOM/SD/62/1S-CL2D, LdBOB) intracellular amastigote, *L. infantum* (MHOM/MA(BE)/67) intracellular amastigotes and *L. infantum* (MHOM/BR/1972/BH46) intracellular amastigote. The compounds also showed IC_{50} < 3.3 μM for *T. b. brucei* , *T. b. rhodesiense*, and *T. cruzi* Tulahuen LacZ, clone C4 _ nifurtimox-sensitive) species and strain, with the exception of *T. cruzi* Tulahuen intracellular amastigote. The lower activity observed in the *T. cruzi* Tulahuen intracellular amastigote assay may be explained by the shorter incubation period (48 hours) after compound exposure. In addition, **BZ1** and **BZ1-I** compounds were shown

to have *in vitro* activity with IC_{50} < 3.8 μM against 3d7 (wild type), Dd2 (resistant) and K1 (resistant) strains of *P. falciparum* strains.

7.6. Downstream processing in drug discovery

The physicochemical evaluation of **BZ1** and **BZ1-I** suggested that both the molecules have lead-like properties. The *in vitro* metabolic evaluation of **BZ1** and **BZ1-I** using human microsomes looked promising; however both compounds demonstrated rapid clearance in mouse microsomes. This will be further assessed with *in vivo* DMPK studies to be undertaken in the hamster models. The cytotoxicity profile of these compounds was assessed for a range of cell lines including HepG2 Raw264,7, J774.1, HEK-293 and THP-1 cells. It was observed that both compounds show minimal cytotoxicity against mammalian cells resulting in a selectivity indices of <10 for all the cell lines.

7.7. Future prospects

In the current juncture, in which DND*i* pipeline presents only 7 new chemical entities for leishmaniasis, identifying new compounds is crucial to provide essential new molecules to accommodate potential attrition due to unforeseen problems with current candidates. Leishmaniasis is responsible for high mortality and morbidity in developing countries and presents a severe economic impact in the affected regions. But as we know, the drug discovery and development processes demand high investment and this disease does not represent a substantial profitable market. Thus the majority of the pharmaceutical industry has little interest in this field. From the 850 new therapeutic products licensed between 2000-2011, only 4% were exclusively driven for neglected diseases, including: 25 new indications/formulation, 8 vaccines or other biological products (e.g. immunoglobulins) and 4 new chemical entities (Pedrique, *et al.*, 2013). The development of new chemical entities in the neglected disease sector has primarily focused on the treatment of malaria, cryptosporidiosis and giardiasis. With respect to Leishmaniasis, only miltefosine and paromomycin have been approved for treatment during this period, both resulting from repurposing of an existing therapeutic for the treatment of an unrelated disease (Pedrique *et al*. 2013).

The anti-kinetoplastid agents that we have identified (**BZ1** and **BZ1-I**) are promising hit compounds awaiting testing in *in vivo* disease models, with good physico-chemical properties and potential for further development. They are not only active on all kinetoplastids, against multiple life cycle stages but have also demonstrated good selectivity for the parasites over the human host. *In vivo* DMPK in hamster models would provide an indication of metabolic stability of the compounds relevant to the *in vivo* disease models used for determining efficacy. Access to these studies is, however, limited due to restrictions imposed for the utilization of hamsters. Thus, a reliance on extrapolation of data from alternative rodent models has been undertaken to date. Three additional **BZ1** analogues, **BZ1-F**, **BZ1-S** and **BZ1-d** will be further profiled in the cytotoxicity panel with testing undertaken at greater concentrations to ascertain their IC_{50} values. These compounds will be subsequently progressed to *in vitro* DMPK studies.

Next-generation sequencing is being carried out on the resistant clones in order to determine the mutation / potential target and elucidate the drug resistance mechanism of the compounds, **BZ1** and **BZ1-I**. This information is crucial to identify the mechanism of action of the chemotype identified. Structure elucidation of the metabolites of **BZ1** will also be conducted and these metabolites will be tested in the screening cascade to determine whether one of the metabolites is actually the active component. Additional analogues of these metabolites will also be investigated.

The natural compound **NP1** which showed <5 μM activity against all kinetoplastids tested was not progressed into mechanism of action studies because of its low selectivity of ~2.5 for *L. donovani* DD8 and *T. cruzi* intracellular amastigotes.

The identification of novel anti-leishmanial compounds illustrates the utility of the anti-leishmanial screening cascade assays. Since the description of the first HCI assay for intracellular amastigotes (Siqueira-Neto *et al.* 2012), different protocols have been established, each attempting to improve upon the former (De Rycker *et al.* 2013; Dagley *et al.* 2015; Tegazzini *et al.* 2016). The differences between these assays include variations in host cells type, parasite species and strains, as well as parasite form used to infect cells (metacyclic promastigotes or axenic amastigotes), incubation times and the fluorophores used for detection of the intracellular amastigotes. All of these assays have allowed the testing of a considerable number of samples. There has been great

engagement of screening research groups, allowing the identification of new active, selective and bioavailable compounds, which are now progressing into the development pipeline (DND*i* 2016). However, despite the advances in drug discovery phenotypic assays for *Leishmania* parasites, image-based assays need to be frequently optimized in order to provide a more reliable and robust selection (Tegazzini *et al*. 2016).

Often leishmaniasis is treated as a single disease, whereas it is a group of diseases in different geographical locations, different causative parasite species of *Leishmania*, clinical manifestations of the disease and even the regimen used to treat the disease. Experimental and clinical outcomes cannot be generalized for the treatments available as has been demonstrated with clinical trial results. In particular, data relating to therapeutic clinical trials for *L. donovani* causing visceral leishmaniasis in India are not directly applicable to visceral leishmaniasis caused by other species, nor to *L. donovani* in other geographic locations, or for the treatment of mucosal and cutaneous leishmaniasis. Attention thus needs to be made in addressing this issue.

Expanding the assay repertoire to include additional species is therefore warranted. Usually, the screening assays are established with only one species of *Leishmania*, traditionally a visceral leishmaniasis species. Large libraries of compounds are screened and activity against cutaneous leishmaniasis species is evaluated on the compounds effective against visceral leishmaniasis in more advanced steps in the discovery pipeline. The major problem with this approach is the intrinsic variation in drug sensitivity of the more than 17 *Leishmania* species known to infect humans (Croft and Olliaro, 2011). Thus, species specific compounds can be lost in the process.

Due to the limited resources available for the development of new drugs against neglected diseases, cutaneous leishmaniasis is not part of the R&D agenda of many foundations, partnerships or the industrial sector; the scientific community has focused on the screening of compounds against visceral species, since it has a higher mortality rate (Mohapatra, 2014). However, cutaneous leishmaniasis has an estimated 700,000 - 1,300,000 cases per year and it is present in over 98 countries and 3 territories on 5 continents (de Vries, *et al.*, 2015). In addition, mucocutanoues leishmaniasis are highly disfiguring, thus associated social stigmatization can have significant negative effects on psychological well-being (Handler, *et al.*, 2015). Efforts are therefore required to deal with the alarming prevalence of cutaneous and mucocutaneous leishmaniasis

among children and women, who are the most neglected and highest risk groups (Al-Kamel, *et al*, 2016). Few treatments exist specifically for cutaneous leishmaniasis (Hailu, *et al.*, 2016). Many are visceral leishmaniasis treatments used for cutaneous leishmaniasis, and their effectiveness or safety has often not been tested in cutaneous leishmaniasis patients. Therefore, regarding the limitations with current therapies, and the lack of advanced candidates specifically for cutaneous leishmaniasis in the drug discovery pipeline, the identification of active compounds against tegumentary leishmaniasis is essential for the development of new, safe, efficacious and more affordable treatment. To facilitate this, dedicated platforms are therefore required.

REFERENCES

Abdullah S. M., Flath B. and Presber H. W., (1999), Comparison of different staining procedures for the flow cytometric analysis of U-937 cells infected with different *Leishmania* -species, *J Microbiol Methods*, **37**, 123-138.

Ablordeppey S. Y., Fan P., Clark A. M. and Nimrod A., (1999), Probing the N-5 region of the indoloquinoline alkaloid, cryptolepine for anticryptococcal activity, *Bioorganic & medicinal chemistry*, **7**, 343-349.

Adak S. and Datta R., (2015), *Leishmania: Current Biology and Control*Caister Academic Press.

Adaui, V., Lye, L.-F., Akopyants, N. S., Zimic, M., Llanos-Cuentas, A., Garcia, L., Beverley, S. M., (2016), Association of the Endobiont Double-Stranded RNA Virus LRV1 With Treatment Failure for Human Leishmaniasis Caused by Leishmania braziliensis in Peru and Bolivia, *The Journal of Infectious Diseases*, **213**, 112–21

Aft R. L. and Mueller G., (1983), Hemin-mediated DNA strand scission, *Journal of Biological Chemistry*, **258**, 12069-12072.

Aggarwal BB, Eessalu TE, Hass PE. (1985). Characterization of receptors for human tumour necrosis factor and their regulation by gamma-interferon. *Nature* **318**,665-7.

Akhoundi M., Kuhls K., Cannet A., Votypka J., Marty P., Delaunay P. and Sereno D., (2016), A Historical Overview of the Classification, Evolution, and Dispersion of *Leishmania* Parasites and Sandflies, *PLoS neglected tropical diseases*, **10**, e0004349.

Akopyants N. S., Kimblin N., Secundino N., Patrick R., Peters N., Lawyer P., Dobson D. E., Beverley S. M. and Sacks D. L., (2009), Demonstration of genetic exchange during cyclical development of *Leishmania* in the sand fly vector, *Science*, **324**, 265-268.

Alawieh A, Musharrafieh U, Jaber A, Berry A, Ghosn N, Bizri AR.., (2014), Revisiting leishmaniasis in the time of war: the Syrian conflict and the Lebanese outbreak. *Int J Infect Dis* **29**,115-9.

Alexander B. and Maroli M., (2003), Control of phlebotomine sandflies, *Medical and veterinary entomology*, **17**, 1-18.

Al-Kamel MA. 2016. Impact of leishmaniasis in women: a practical review with an update on my ISD-supported initiative to combat leishmaniasis in Yemen (ELYP). International Journal of Women's Dermatology 2:93-101.

Althaus J. B., Malyszek C., Kaiser M., Brun R. and Schmidt T. J., (2017), Alkamides from Anacyclus pyrethrum L. and Their in Vitro Antiprotozoal Activity, *Molecules*, **22**.

Alvar J., Croft S. and Olliaro P., (2006), Chemotherapy in the treatment and control of Leishmaniasis, *Adv Parasitol*, **61**, 223-274.

Alvar J., Velez I. D., Bern C., Herrero M., Desjeux P., Cano J., Jannin J. and den Boer M., (2012), Leishmaniasis worldwide and global estimates of its incidence, *PLoS One*, **7**, e35671.

Amato V. S., Tuon F. F., Imamura R., Abegao de Camargo R., Duarte M. I. and Neto V. A., (2009), Mucosal Leishmaniasis: description of case management approaches and analysis of risk factors for treatment failure in a cohort of 140 patients in Brazil, *J Eur Acad Dermatol Venereol*, **23**, 1026-1034.

Ambit A., Woods K. L., Cull B., Coombs G. H. and Mottram J. C., (2011), Morphological events during the cell cycle of *Leishmania* major, *Eukaryot Cell*, **10**, 1429-1438.

Annang F., Pérez-Moreno G., García-Hernández R., Cordon-Obras C., Martín J., Tormo J., Rodríguez L., De Pedro N., Gómez-Pérez V. and Valente M., (2015), High-Throughput Screening Platform for Natural Product–Based Drug Discovery Against 3 Neglected Tropical Diseases: Human African Trypanosomiasis, Leishmaniasis, and Chagas Disease, *Journal of biomolecular screening*, **20**, 82-91.

Antinarelli L. M., Dias R. M., Souza I. O., Lima W. P., Gameiro J., da Silva A. D. and Coimbra E. S., (2015), 4-Aminoquinoline Derivatives as Potential Anti*Leishmania*l Agents, *Chem Biol Drug Des*, **86**, 704-714.

Antinori S., Longhi E., Bestetti G., Piolini R., Acquaviva V., Foschi A., Trovati S., Parravicini C., Corbellino M. and Meroni L., (2007), Post-kala-azar dermal Leishmaniasis as an immune reconstitution inflammatory syndrome in a patient with acquired immune deficiency syndrome, *British Journal of Dermatology*, **157**, 1032-1036.

Armson A., Kamau S. W., Grimm F., Reynoldson J. A., Best W. M., MacDonald L. M. and Thompson R. C., (1999), A comparison of the effects of a benzimidazole and the dinitroanilines against *Leishmania* infantum, *Acta Trop*, **73**, 303-311.

Arnoult D., Akarid K., Grodet A., Petit P., Estaquier J. and Ameisen J., (2002), On the evolution of programmed cell death: apoptosis of the unicellular eukaryote *Leishmania* major involves cysteine proteinase activation and mitochondrion permeabilization, *Cell death and differentiation*, **9**, 65.

Arruda-Costa N., Escrivani D., Almeida-Amaral E. E., Meyer-Fernandes J. R. and Rossi-Bergmann B., (2017), Anti-parasitic effect of the diuretic and Na+-ATPAse inhibitor furosemide in cutaneous Leishmaniasis, *Parasitology*, **144**, 1375-1383.

Ashkan M. M. and Rahim K. M., (2008), Visceral leishmanisis in paediatrics: a study of 367 cases in southwest Iran, *Trop Doct*, **38**, 186-188.

Ashutosh, Gupta S., Ramesh, Sundar S. and Goyal N., (2005), Use of *Leishmania* donovani field isolates expressing the luciferase reporter gene in in vitro drug screening, *Antimicrob Agents Chemother*, **49**, 3776-3783.

Assefa D., Worku Y. and Skoglund G., (1995), Protein kinase activities in *Leishmania* aethiopica: control by growth, transformation and inhibitors, *Biochim Biophys Acta*, **1270**, 157-162.

Aulner N., Danckaert A., Rouault-Hardoin E., Desrivot J., Helynck O., Commere P. H., Munier-Lehmann H., Spath G. F., Shorte S. L., Milon G. and Prina E., (2013), High content analysis of primary macrophages hosting proliferating *Leishmania* amastigotes: application to anti-*Leishmania*l drug discovery, *PLoS Negl Trop Dis*, **7**, e2154.

Avila J. and Casanova M., (1982), Comparative effects of 4-aminopyrazolopyrimidine, its 2'-deoxyriboside derivative, and allopurinol on in vitro growth of American *Leishmania* species, *Antimicrobial agents and chemotherapy*, **22**, 380-385.

Awasthi A., Mathur R. K. and Saha B., (2004), Immune response to *Leishmania* infection, *Indian Journal of Medical Research*, **119**, 238.

Bacellar, O., Lessa, H., Schriefer, A., Machado, P., Ribeiro de Jesus, A., Dutra, W. O., Carvalho, E. M., (2002), Up-regulation of Th1-type responses in mucosal leishmaniasis patients, *Infection and Immunity*, **70**, 6734–40.

Baell JB., (2016), Feeling Nature's PAINS: Natural Products, Natural Product Drugs, and Pan Assay Interference Compounds (PAINS). *J Nat Prod* **79**,616-28.

Baell JB, Nissink JWM., (2018), Seven Year Itch: Pan-Assay Interference Compounds (PAINS) in 2017-Utility and Limitations. *ACS Chem Biol* **13**,36-44.

Baiocco P., Poce G., Alfonso S., Cocozza M., Porretta G. C., Colotti G., Biava M., Moraca F., Botta M. and Yardley V., (2013), Inhibition of *Leishmania infantum* Trypanothione Reductase by Azole-Based Compounds: a Comparative Analysis with Its Physiological Substrate by X-ray Crystallography, *ChemMedChem*, **8**, 1175-1183.

Balana-Fouce R., Alvarez-Velilla R., Fernandez-Prada C., Garcia-Estrada C. and Reguera R. M., (2014), Trypanosomatids topoisomerase re-visited. New

structural findings and role in drug discovery, *International journal for parasitology. Drugs and drug resistance*, **4**, 326-337.

Balasegaram M, Ritmeijer K, Lima MA, Burza S, Ortiz Genovese G, Milani B, Gaspani S, Potet J, Chappuis F. 2012. Liposomal amphotericin B as a treatment for human leishmaniasis. Expert Opin Emerg Drugs 17:493-510.

Bañuls A.-L., Brisse S., Sidibé I., Noël S. and Tibayrenc M., (1999), A phylogenetic analysis by multilocus enzyme electrophoresis and multiprimer random amplified polymorphic DNA fingerprinting of the *Leishmania* genome project Friedlin reference strain, *Folia parasitologica*, **46**, 10-14.

Banuls A. L., Hide M. and Prugnolle F., (2007), *Leishmania* and the *Leishmania*ses: a parasite genetic update and advances in taxonomy, epidemiology and pathogenicity in humans, *Adv Parasitol*, **64**, 1-109.

Barak E., Amin-Spector S., Gerliak E., Goyard S., Holland N. and Zilberstein D., (2005), Differentiation of *Leishmania* donovani in host-free system: analysis of signal perception and response, *Mol Biochem Parasitol*, **141**, 99-108.

Barnes E. C., Kumar R. and Davis R. A., (2016), The use of isolated natural products as scaffolds for the generation of chemically diverse screening libraries for drug discovery, *Natural product reports*, **33**, 372-381.

Barnes E. C., Said N. A. B., Williams E. D., Hooper J. N. and Davis R. A., (2010), Ecionines A and B, two new cytotoxic pyridoacridine alkaloids from the Australian marine sponge, Ecionemia geodides, *Tetrahedron*, **66**, 283-287.

Barrett M. P., Boykin D. W., Brun R. and Tidwell R. R., (2007), Human African trypanosomiasis: pharmacological re-engagement with a neglected disease, *British Journal of Pharmacology*, **152**, 1155-1171.

Barrett M. P. and Croft S. L., (2012), Management of trypanosomiasis and Leishmaniasis, *Br Med Bull*, **104**, 175-196.

Bates P., (1993), Axenic culture of *Leishmania* amastigotes, *Parasitology Today*, **9**, 143-146.

Bates P. A., (1993), Characterization of developmentally-regulated nucleases in promastigotes and amastigotes of *Leishmania* mexicana, *FEMS Microbiol Lett*, **107**, 53-58.

Beach D. H., Goad L. J. and Holz G. G., Jr., (1988), Effects of antimycotic azoles on growth and sterol biosynthesis of *Leishmania* promastigotes, *Mol Biochem Parasitol*, **31**, 149-162.

Beattie L. and Kaye P. M., (2011), *Leishmania* –host interactions: what has imaging taught us?, *Cellular microbiology*, **13**, 1659-1667.

Ben-Shimol S., Sagi O., Horev A., Avni Y. S., Ziv M. and Riesenberg K., (2016), Cutaneous Leishmaniasis caused by *Leishmania* infantum in Southern Israel, *Acta Parasitol*, **61**, 855-858.

Ben-Shimol S., Sagi O., Schwartz E. and Greenberg D., (2012), [Cutaneous Leishmaniasis treated with ambisome (liposomal amphotericin B)], *Harefuah*, **151**, 458-460, 498.

Berberian, D. A., (1945), cutaneous leishmaniasis (oriental sore), *Archives of Dermatology and Syphilology*, **52**, 26.

Berg K., Zhai L., Chen M., Kharazmi A. and Owen T. C., (1994), The use of a water-soluble formazan complex to quantitate the cell number and mitochondrial function of *Leishmania* major promastigotes, *Parasitol Res*, **80**, 235-239.

Berman J., (2015), Amphotericin B formulations and other drugs for visceral Leishmaniasis, *Am J Trop Med Hyg*, **92**, 471-473.

Berman J. D., (1997), Human Leishmaniasis: clinical, diagnostic, and chemotherapeutic developments in the last 10 years, *Clin Infect Dis*, **24**, 684-703.

Bermudez J., Davies C., Simonazzi A., Real J. P. and Palma S., (2016), Current drug therapy and pharmaceutical challenges for Chagas disease, *Acta Trop*, **156**, 1-16.

Bessho T., Morii S., Kusumoto T., Shinohara T., Noda M., Uchiyama S., Shuto S., Nishimura S., Djikeng A. and Duszenko M., (2013), Characterization of the novel Trypanosoma brucei inosine 5′-monophosphate dehydrogenase, *Parasitology*, **140**, 735-745.

Bhandari V., Kulshrestha A., Deep D. K., Stark O., Prajapati V. K., Ramesh V., Sundar S., Schonian G., Dujardin J. C. and Salotra P., (2012), Drug susceptibility in *Leishmania* isolates following miltefosine treatment in cases of visceral Leishmaniasis and post kala-azar dermal Leishmaniasis, *PLoS Negl Trop Dis*, **6**, e1657.

Bhargava P. and Singh R., (2012), Developments in diagnosis and anti*Leishmania*l drugs, *Interdiscip Perspect Infect Dis*, **2012**, 626838.

Bhuniya D., Mukkavilli R., Shivahare R., Launay D., Dere R. T., Deshpande A., Verma A., Vishwakarma P., Moger M., Pradhan A., Pati H., Gopinath V. S., Gupta S., Puri S. K. and Martin D., (2015), Aminothiazoles: Hit to lead development to identify anti*Leishmania*l agents, *Eur J Med Chem*, **102**, 582-593.

Bickle M., (2010), The beautiful cell: high-content screening in drug discovery, *Analytical and bioanalytical chemistry*, **398**, 219-226.

Biswas S., Subramanian A., ELMojtaba I. M., Chattopadhyay J. and Sarkar R. R., (2017), Optimal combinations of control strategies and cost-effective analysis for visceral Leishmaniasis disease transmission, *PloS one*, **12**, e0172465.

Bodley A. L., McGarry M. W. and Shapiro T. A., (1995), Drug cytotoxicity assay for African trypanosomes and *Leishmania* species, *J Infect Dis*, **172**, 1157-1159.

Bogdan C., Donhauser N., Doring R., Rollinghoff M., Diefenbach A. and Rittig M. G., (2000), Fibroblasts as host cells in latent leishmaniosis, *J Exp Med*, **191**, 2121-2130.

Bogyo M. and Rudd P. M., (2013), New technologies and their impact on 'omics' research, *Curr Opin Chem Biol*, **17**, 1-3.

Boiani M., Piacenza L., Hernández P., Boiani L., Cerecetto H., González M. and Denicola A., (2010), Mode of action of Nifurtimox and N-oxide-containing heterocycles against Trypanosoma cruzi: Is oxidative stress involved?, *Biochemical Pharmacology*, **79**, 1736-1745.

Bourreau, E., Ginouves, M., Prévot, G., Hartley, M.-A., Gangneux, J.-P., Robert-Gangneux, F., Ronet, C., (2016), Presence of Leishmania RNA Virus 1 in Leishmania guyanensis Increases the Risk of First-Line Treatment Failure and Symptomatic Relapse, *The Journal of Infectious Diseases*, **213**, 105–11.

BoseDasgupta S., Das B., Sengupta S., Ganguly A., Roy A., Dey S., Tripathi G., Dinda B. and Majumder H. K., (2008), The caspase-independent algorithm of programmed cell death in *Leishmania* induced by baicalein: the role of LdEndoG, LdFEN-1 and LdTatD as a DNA'degradesome', *Cell death and differentiation*, **15**, 1629.

Botero A., Keatley S., Peacock C. and Thompson R. A., (2017), In vitro drug susceptibility of two strains of the wildlife trypanosome, Trypanosoma copemani: A comparison with Trypanosoma cruzi, *International Journal for Parasitology: Drugs and Drug Resistance*, **7**, 34-41.

Breuning A., Degel B., Schulz F., Buchold C., Stempka M., Machon U., Heppner S., Gelhaus C., Leippe M., Leyh M., Kisker C., Rath J., Stich A., Gut J., Rosenthal P. J., Schmuck C. and Schirmeister T., (2010), Michael acceptor based antiplasmodial and antitrypanosomal cysteine protease inhibitors with unusual amino acids, *J Med Chem*, **53**, 1951-1963.

Buchanan M. S., Carroll A. R., Fechner G. A., Boyle A., Simpson M. M., Addepalli R., Avery V. M., Hooper J. N., Su N., Chen H. and Quinn R. J., (2007),

Spermatinamine, the first natural product inhibitor of isoprenylcysteine carboxyl methyltransferase, a new cancer target, *Bioorg Med Chem Lett*, **17**, 6860-6863.

Buckner F. S., Kateete D. P., Lubega G. W., Van Voorhis W. C. and Yokoyama K., (2002), Trypanosoma brucei prenylated-protein carboxyl methyltransferase prefers farnesylated substrates, *Biochemical Journal*, **367**, 809-816.

Bustamante J. M., Park H. J., Tarleton R. L. and The Chagas Drug Discovery C., (2011), Report of the 2nd Chagas Drug Discovery Consortium meeting, held on 3 November 2010; Atlanta GA, USA, *Expert Opin Drug Discov*, **6**, 965-973.

Bystry R. S., Aluvihare V., Welch K. A., Kallikourdis M. and Betz A. G., (2001), B cells and professional APCs recruit regulatory T cells via CCL4, *Nature immunology*, **2**, 1126.

Callahan H. L., Kelley C., Pereira T. and Grogl M., (1996), Microtubule inhibitors: structure-activity analyses suggest rational models to identify potentially active compounds, *Antimicrobial agents and chemotherapy*, **40**, 947-952.

Callahan H. L., Portal A. C., Devereaux R. and Grogl M., (1997), An axenic amastigote system for drug screening, *Antimicrob Agents Chemother*, **41**, 818-822.

Calvo-Álvarez E., Guerrero N. A., Álvarez-Velilla R., Prada C. F., Requena J. M., Punzón C., Llamas M. Á., Arévalo F. J., Rivas L. and Fresno M., (2012), Appraisal of a *Leishmania* major strain stably expressing mCherry fluorescent protein for both in vitro and in vivo studies of potential drugs and vaccine against cutaneous Leishmaniasis, *PLoS neglected tropical diseases*, **6**, e1927.

Calvo-Álvarez E., Stamatakis K., Punzón C., Álvarez-Velilla R., Tejería A., Escudero-Martínez J. M., Pérez-Pertejo Y., Fresno M., Balaña-Fouce R. and Reguera R. M., (2015), Infrared fluorescent imaging as a potent tool for in vitro, ex vivo and in vivo models of visceral Leishmaniasis, *PLoS neglected tropical diseases*, **9**, e0003666.

Cameron M. M., Acosta-Serrano A., Bern C., Boelaert M., Den Boer M., Burza S., Chapman L. A., Chaskopoulou A., Coleman M. and Courtenay O., (2016), Understanding the transmission dynamics of *Leishmania* donovani to provide robust evidence for interventions to eliminate visceral Leishmaniasis in Bihar, India, *Parasites & vectors*, **9**, 25.

Cämmerer S. B., (2016), N-[4-[Benzyloxy] benzyl]-benzenemethaneamines with High Biological Activity against Intracellular Trypanosoma cruzi and *Leishmania* infantum Amastigotes, *Int. J. Chem, Pharm, Sci*, **4**, 570-578.

Campos-Varela I., Len O., Castells L., Tallada N., Ribera E., Dopazo C., Vargas V., Gavalda J. and Charco R., (2008), Visceral Leishmaniasis among liver transplant recipients: an overview, *Liver Transplantation*, **14**, 1816-1819.

Cao S., Aboge G. O., Terkawi M. A., Zhou M., Luo Y., Yu L., Li Y., Goo Y., Kamyingkird K. and Masatani T., (2013), Cloning, characterization and validation of inosine 5′-monophosphate dehydrogenase of Babesia gibsoni as molecular drug target, *Parasitology international*, **62**, 87-94.

Cardo L. J., (2006), *Leishmania*: risk to the blood supply, *Transfusion*, **46**, 1641-1645.

Carmo A. M., Silva F. M., Machado P. A., Fontes A. P., Pavan F. R., Leite C. Q., Sergio R. d. A., Coimbra E. S. and Da Silva A. D., (2011), Synthesis of 4-aminoquinoline analogues and their platinum (II) complexes as new anti*Leishmania*l and antitubercular agents, *Biomedicine & Pharmacotherapy*, **65**, 204-209.

Carneiro P. P., Conceicao J., Macedo M., Magalhaes V., Carvalho E. M. and Bacellar O., (2016), The Role of Nitric Oxide and Reactive Oxygen Species in the Killing of *Leishmania* braziliensis by Monocytes from Patients with Cutaneous Leishmaniasis, *PLoS One*, **11**, e0148084.

Carrasco L., Fresno M. and Vazquez D., (1975), Narciclasine: an antitumour alkaloid which blocks peptide bond formation by eukaryotic ribosomes, *FEBS letters*, **52**, 236-239.

Carvalho, E. M., Barral, A., Costa, J. M., Bittencourt, A., & Marsden, P., (1994), Clinical and immunopathological aspects of disseminated cutaneous leishmaniasis, *Acta Tropica*, **56**, 315–25.

Carvalho L, Luque-Ortega JR, Manzano JI, Castanys S, Rivas L, Gamarro F., (2010), Tafenoquine, an antiplasmodial 8-aminoquinoline, targets leishmania respiratory complex III and induces apoptosis, *Antimicrob. Agents Chemother.*, **54**, 5344–51

Castanys-Muñoz, E., Pérez-Victoria, J. M., Gamarro, F. & Castanys, S., (2008) Characterization of an ABCG-like transporter from the protozoan parasite Leishmania with a role in drug resistance and transbilayer lipid movement. *Antimicrob. Agents Chemother*. **52**, 3573–9.

Castilla J. J., Sanchez-Moreno M., Mesa C. and Osuna A., (1995), *Leishmania* donovani: in vitro culture and [1H] NMR characterization of amastigote-like forms, *Mol Cell Biochem*, **142**, 89-97.

Cavalli A., Lizzi F., Bongarzone S., Brun R., Luise Krauth-Siegel R. and Bolognesi M. L., (2009), Privileged structure-guided synthesis of quinazoline derivatives as inhibitors of trypanothione reductase, *Bioorg Med Chem Lett*, **19**, 3031-3035.

Ceriotti G., (1967), Narciclasine: an antimitotic substance from Narcissus bulbs, *Nature*, **213**, 595-596.

Cernak T., Dykstra K. D., Tyagarajan S., Vachal P. and Krska S. W., (2016), The medicinal chemist's toolbox for late stage functionalization of drug-like molecules, *Chemical Society Reviews*, **45**, 546-576.

Chan-Bacab M. J., Balanza E., Deharo E., Munoz V., Garcia R. D. and Pena-Rodriguez L. M., (2003), Variation of leishmanicidal activity in four populations of Urechites andrieuxii, *J Ethnopharmacol*, **86**, 243-247.

Chan M. M., Bulinski J. C., Chang K. P. and Fong D., (2003), A microplate assay for *Leishmania* amazonensis promastigotes expressing multimeric green fluorescent protein, *Parasitol Res*, **89**, 266-271.

Chan S. L., Lee M. C., Tan K. O., Yang L. K., Lee A. S., Flotow H., Fu N. Y., Butler M. S., Soejarto D. D., Buss A. D. and Yu V. C., (2003), Identification of chelerythrine as an inhibitor of BclXL function, *J Biol Chem*, **278**, 20453-20456.

Chang K.-P., (1979), *Leishmania* donovani: promastigote-macrophage surface interactions in vitro, *Experimental parasitology*, **48**, 175-189.

Chanput W., Mes J. J. and Wichers H. J., (2014), THP-1 cell line: an in vitro cell model for immune modulation approach, *International immunopharmacology*, **23**, 37-45.

Chappuis F., Sundar S., Hailu A., Ghalib H., Rijal S., Peeling R. W., Alvar J. and Boelaert M., (2007), Visceral Leishmaniasis: what are the needs for diagnosis, treatment and control?, *Nat Rev Microbiol*, **5**, 873-882.

Charest H. and Matlashewski G., (1994), Developmental gene expression in *Leishmania* donovani: differential cloning and analysis of an amastigote-stage-specific gene, *Mol Cell Biol*, **14**, 2975-2984.

Chatelain E. and Ioset J. R., (2011), Drug discovery and development for neglected diseases: the DNDi model, *Drug Des Devel Ther*, **5**, 175-181.

Chawla B. and Madhubala R., (2010), Drug targets in *Leishmania*, *Journal of Parasitic Diseases: Official Organ of the Indian Society for Parasitology*, **34**, 1-13.

Choomuenwai V., Andrews K. T. and Davis R. A., (2012), Synthesis and antimalarial evaluation of a screening library based on a tetrahydroanthraquinone natural product scaffold, *Bioorg Med Chem*, **20**, 7167-7174.

Choomuenwai V., Andrews K. T. and Davis R. A., (2012), Synthesis and antimalarial evaluation of a screening library based on a tetrahydroanthraquinone natural product scaffold, *Bioorganic & medicinal chemistry*, **20**, 7167-7174.

Choomuenwai V., Beattie K. D., Healy P. C., Andrews K. T., Fechner N. and Davis R. A., (2015), Entonalactams A-C: Isoindolinone derivatives from an Australian rainforest fungus belonging to the genus Entonaema, *Phytochemistry*, **117**, 10-16.

Choomuenwai V., Schwartz B. D., Beattie K. D., Andrews K. T., Khokhar S. and Davis R. A., (2013), The discovery, synthesis and antimalarial evaluation of natural product-based polyamine alkaloids, *Tetrahedron Letters*, **54**, 5188-5191.

Coimbra E. S., Antinarelli L. M., Silva N. P., Souza I. O., Meinel R. S., Rocha M. N., Soares R. P. and da Silva A. D., (2016), Quinoline derivatives: Synthesis, leishmanicidal activity and involvement of mitochondrial oxidative stress as mechanism of action, *Chemico-biological interactions*, **260**, 50-57.

Coimbra E. S., Libong D., Cojean S., Saint-Pierre-Chazalet M., Solgadi A., Le Moyec L., Duenas-Romero A. M., Chaminade P. and Loiseau P. M., (2010), Mechanism of interaction of sitamaquine with *Leishmania* donovani, *J Antimicrob Chemother*, **65**, 2548-2555.

Coleman M., Foster G. M., Deb R., Pratap Singh R., Ismail H. M., Shivam P., Ghosh A. K., Dunkley S., Kumar V., Coleman M., Hemingway J., Paine M. J. and Das P., (2015), DDT-based indoor residual spraying suboptimal for visceral Leishmaniasis elimination in India, *Proceedings of the National Academy of Sciences of the United States of America*, **112**, 8573-8578.

Coleman M., Foster G. M., Deb R., Singh R. P., Ismail H. M., Shivam P., Ghosh A. K., Dunkley S., Kumar V. and Coleman M., (2015), DDT-based indoor residual spraying suboptimal for visceral Leishmaniasis elimination in India, *Proceedings of the National Academy of Sciences*, **112**, 8573-8578.

Copeland N. K. and Aronson N. E., (2015), Leishmaniasis: treatment updates and clinical practice guidelines review, *Current opinion in infectious diseases*, **28**, 426-437.

Corona P., Gibellini F., Cavalli A., Saxena P., Carta A., Loriga M., Luciani R., Paglietti G., Guerrieri D., Nerini E., Gupta S., Hannaert V., Michels P. A., Ferrari S. and Costi P. M., (2012), Structure-based selectivity optimization of piperidine-pteridine derivatives as potent *Leishmania* pteridine reductase inhibitors, *J Med Chem*, **55**, 8318-8329.

Corral M. J., Gonzalez-Sanchez E., Cuquerella M. and Alunda J. M., (2014), In vitro synergistic effect of amphotericin B and allicin on *Leishmania* donovani and L. infantum, *Antimicrob Agents Chemother*, **58**, 1596-1602.

Corral M. J., Gonzalez E., Cuquerella M. and Alunda J. M., (2013), Improvement of 96-well microplate assay for estimation of cell growth and inhibition of *Leishmania* with Alamar Blue, *J Microbiol Methods*, **94**, 111-116.

Cos P., Vlietinck A. J., Berghe D. V. and Maes L., (2006), Anti-infective potential of natural products: how to develop a stronger in vitro 'proof-of-concept', *Journal of ethnopharmacology*, **106**, 290-302.

Couper K. N., Blount D. G. and Riley E. M., (2008), IL-10: the master regulator of immunity to infection, *J Immunol*, **180**, 5771-5777.

Croft S. L., (2008), PKDL--a drug related phenomenon?, *Indian J Med Res*, **128**, 10-11.

Croft S. L. and Coombs G. H., (2003), Leishmaniasis–current chemotherapy and recent advances in the search for novel drugs, *Trends in parasitology*, **19**, 502-508.

Croft S.L. and Engel J., (2006), Miltefosine--discovery of the antileishmanial activity of phospholipid derivatives, *Trans R Soc Trop Med Hyg*, **100 Suppl**, S4-8.

Croft S. and Olliaro P., (2011), Leishmaniasis chemotherapy—challenges and opportunities, *Clinical Microbiology and Infection*, **17**, 1478-1483.

Croft S. L., Seifert K. and Yardley V., (2006), Current scenario of drug development for Leishmaniasis, *Indian J Med Res*, **123**, 399-410.

Croft S. L., Sundar S. and Fairlamb A. H., (2006), Drug resistance in Leishmaniasis, *Clin Microbiol Rev*, **19**, 111-126.

Croft S. L., Yardley V. and Kendrick H., (2002), Drug sensitivity of *Leishmania* species: some unresolved problems, *Trans R Soc Trop Med Hyg*, **96 Suppl 1**, S127-129.

Cunningham, (1885), On the presence of peculiar parasitic organisms in the tissue of a specimen of Delhi boil, *Sci Mem Med Offic Army India* **1**, 21-31.

Dagley M. J., Saunders E. C., Simpson K. J. and McConville M. J., (2015), High-Content Assay for Measuring Intracellular Growth of *Leishmania* in Human Macrophages, *Assay Drug Dev Technol*, **13**, 389-401.

Dantas-Torres F. and Otranto D., (2016), Best practices for preventing vector-borne diseases in dogs and humans, *Trends in parasitology*, **32**, 43-55.

Dantas-Torres F., Solano-Gallego L., Baneth G., Ribeiro V. M., de Paiva-Cavalcanti M. and Otranto D., (2012), Canine leishmaniosis in the Old and New Worlds: unveiled similarities and differences, *Trends in parasitology*, **28**, 531-538.

Das S., Mandal R., Rabidas V. N., Verma N., Pandey K., Ghosh A. K., Kesari S., Kumar A., Purkait B., Lal C. S. and Das P., (2016), Chronic Arsenic Exposure and Risk of Post Kala-azar Dermal Leishmaniasis Development in India: A Retrospective Cohort Study, *PLoS Negl Trop Dis*, **10**, e0005060.

Das V. N. R., Ranjan A., Pandey K., Singh D., Verma N., Das S., Lal C. S., Sinha N. K., Verma R. B. and Siddiqui N. A., (2012), Clinical Epidemiologic Profile of a Cohort of Post–Kala-Azar Dermal Leishmaniasis Patients in Bihar, India, *The American journal of tropical medicine and hygiene*, **86**, 959-961.

Das V. N. R., Siddiqui N. A., Pal B., Lal C. S., Verma N., Kumar A., Verma R. B., Kumar D., Das P. and Pandey K., (2017), To evaluate efficacy and safety of amphotericin B in two different doses in the treatment of post kala-azar dermal Leishmaniasis (PKDL), *PloS one*, **12**, e0174497.

Davies C. R., Kaye P., Croft S. L. and Sundar S., (2003), Leishmaniasis: new approaches to disease control, *BMJ (Clinical research ed.)*, **326**, 377-382.

Davis R. A., (2005), Isolation and structure elucidation of the new fungal metabolite (-)-xylariamide A, *J Nat Prod*, **68**, 769-772.

Davis R. A., Duffy S., Avery V. M., Camp D., Hooper J. N. and Quinn R. J., (2010), (+)-7-Bromotrypargine: an antimalarial β-carboline from the Australian marine sponge Ancorina sp, *Tetrahedron Letters*, **51**, 583-585.

Davis R. A., Duffy S., Fletcher S., Avery V. M. and Quinn R. J., (2013), Thiaplakortones A-D: antimalarial thiazine alkaloids from the Australian marine sponge Plakortis lita, *J Org Chem*, **78**, 9608-9613.

Davis R. A., Mangalindan G. C., Bojo Z. P., Antemano R. R., Rodriguez N. O., Concepcion G. P., Samson S. C., De Guzman D., Cruz L. J. and Tasdemir D., (2004), Microcionamides A and B, bioactive peptides from the Philippine sponge Clathria (Thalysias) abietina, *The Journal of organic chemistry*, **69**, 4170-4176.

Davis R. A., Sandoval I. T., Concepcion G. P., da Rocha R. M. and Ireland C. M., (2003), Lissoclinotoxins E and F, novel cytotoxic alkaloids from a Philippine didemnid ascidian, *Tetrahedron*, **59**, 2855-2859.

Davis R. A., Sykes M., Avery V. M., Camp D. and Quinn R. J., (2011), Convolutamines I and J, antitrypanosomal alkaloids from the bryozoan Amathia tortusa, *Bioorg Med Chem*, **19**, 6615-6619.

de Almeida-Amaral E. E., Caruso-Neves C., Pires V. M. and Meyer-Fernandes J. R., (2008), *Leishmania* amazonensis: characterization of an ouabain-insensitive Na+-ATPase activity, *Exp Parasitol*, **118**, 165-171.

de Menezes J. P., Guedes C. E., Petersen A. L., Fraga D. B. and Veras P. S., (2015), Advances in Development of New Treatment for Leishmaniasis, *Biomed Res Int*, **2015**, 815023.

De Muylder G., Ang K. K., Chen S., Arkin M. R., Engel J. C. and McKerrow J. H., (2011), A screen against *Leishmania* intracellular amastigotes: comparison to a promastigote screen and identification of a host cell-specific hit, *PLoS Negl Trop Dis*, **5**, e1253.

De Muylder G., Vanhollebeke B., Caljon G., Wolfe A. R., McKerrow J. and Dujardin J. C., (2016), Naloxonazine, an Amastigote-Specific Compound, Affects *Leishmania* Parasites through Modulation of Host-Encoded Functions, *PLoS neglected tropical diseases*, **10**, e0005234.

De Rycker M., Hallyburton I., Thomas J., Campbell L., Wyllie S., Joshi D., Cameron S., Gilbert I. H., Wyatt P. G. and Frearson J. A., (2013), Comparison of a high-throughput high-content intracellular *Leishmania* donovani assay with an axenic amastigote assay, *Antimicrobial agents and chemotherapy*, **57**, 2913-2922.

de Vries H. J., Reedijk S. H. and Schallig H. D., (2015), Cutaneous Leishmaniasis: recent developments in diagnosis and management, *American journal of clinical dermatology*, **16**, 99-109.

Debrabant A., Joshi M. B., Pimenta P. F. and Dwyer D. M., (2004), Generation of *Leishmania* donovani axenic amastigotes: their growth and biological characteristics, *International journal for parasitology*, **34**, 205-217.

del Giudice P., Marty P., Lacour J. P., Perrin C., Pratlong F., Haas H., Dellamonica P. and Le Fichoux Y., (1998), Cutaneous Leishmaniasis due to *Leishmania* infantum. Case reports and literature review, *Arch Dermatol*, **134**, 193-198.

Delgado G., Puentes F., Moreno A. and Patarroyo M. E., (2001), Flow cytometry, a useful tool for detecting the lethal effect of pentamidine on *Leishmania* viannia complex promastigote forms, *Pharmacol Res*, **44**, 281-286.

Denton H., McGregor J. C. and Coombs G. H., (2004), Reduction of anti-*Leishmania*l pentavalent antimonial drugs by a parasite-specific thiol-dependent reductase, TDR1, *Biochem J*, **381**, 405-412.

Desjeux P., Ghosh R. S., Dhalaria P., Strub-Wourgaft N. and Zijlstra E. E., (2013), Report of the Post Kala-Azar Dermal Leishmaniasis (PKDL) consortium meeting, New Delhi, India, 27–29 June 2012, *Parasites & Vectors*, **6**, 196.

Desjeux P. and Ramesh V., (2011), in *Kala Azar in South Asia*Springer, pp. 111-124.

Di Giorgio C., Delmas F., Filloux N., Robin M., Seferian L., Azas N., Gasquet M., Costa M., Timon-David P. and Galy J.-P., (2003), In vitro activities of 7-substituted 9-chloro and 9-amino-2-methoxyacridines and their bis-and tetra-acridine complexes against *Leishmania* infantum, *Antimicrobial agents and chemotherapy*, **47**, 174-180.

Di Giorgio C., Shimi K., Boyer G., Delmas F. and Galy J.-P., (2007), Synthesis and anti*Leishmania*l activity of 6-mono-substituted and 3, 6-di-substituted acridines obtained by acylation of proflavine, *European journal of medicinal chemistry*, **42**, 1277-1284.

Di Giorgio C., Shimi K., Boyer G., Delmas F. and Galy J. P., (2007), Synthesis and anti*Leishmania*l activity of 6-mono-substituted and 3,6-di-substituted acridines obtained by acylation of proflavine, *Eur J Med Chem*, **42**, 1277-1284.

Di L. and Kerns E. H., (2015), *Drug-like properties: concepts, structure design and methods from ADME to toxicity optimization*Academic press.

Dietze R., Carvalho S., Valli L., Berman J., Brewer T., Milhous W., Sanchez J., Schuster B. and Grogl M., (2001), Phase 2 trial of WR6026, an orally administered 8-aminoquinoline, in the treatment of visceral Leishmaniasis caused by *Leishmania* chagasi, *The American journal of tropical medicine and hygiene*, **65**, 685-689.

DND*i*, (2015), Anfoleish. Available at: http://www.dndi.org/diseases-projects/portfolio/anfoleish-cl.html.

DND*i*, (2015), Available at: http://www.dndi.org/diseases-projects/diseases/vl/current-treatment.html.

DND*i*, (2015), VL-2098. Available at: http://www.dndi.org/diseases-projects/portfolio/completed-projects/vl-2098/.

DND*i*, Target Product Profile for Visceral Leishmaniasis. Available at: http://www.dndi.org/diseases-projects/Leishmaniasis/tpp-vl/).

DND*i*, (2017), Aminopyrazoles. Available at: https://www.dndi.org/diseases-projects/portfolio/aminopyrazoles/. Accessed on: 9th October, 2017.

DND*i*, (2017), CpG-D35. Available at: https://www.dndi.org/diseases-projects/portfolio/cpg-d35/. Accessed on: 9th Oct, 2017.

DND*i*, (2017), DNDi-0690. Available at:https://www.dndi.org/diseases-projects/portfolio/nitroimidazole/. Accessed on: 9th October, 2017.

DND*i*, Fexinidazole (HAT). Available at: http://www.dndi.org/diseases-projects/portfolio/fexinidazole/.).

DND*i*, (2017), Oxaboroles. Available at: https://www.dndi.org/diseases-projects/portfolio/oxaleish/. Accessed on: 9th October, 2017.

Dobson D. E., Kamhawi S., Lawyer P., Turco S. J., Beverley S. M. and Sacks D. L., (2010), *Leishmania* major survival in selective Phlebotomus papatasi sand fly vector requires a specific SCG-encoded lipophosphoglycan galactosylation pattern, *PLoS pathogens*, **6**, e1001185.

Don R. and Ioset J. R., (2014), Screening strategies to identify new chemical diversity for drug development to treat kinetoplastid infections, *Parasitology*, **141**, 140-146.

Donovan, (1903), The etiology of the heterogeneous fevers in India, *Br Med J* **2**, 1401.

Dorlo T. P., Rijal S., Ostyn B., de Vries P. J., Singh R., Bhattarai N., Uranw S., Dujardin J. C., Boelaert M., Beijnen J. H. and Huitema A. D., (2014), Failure of miltefosine in visceral Leishmaniasis is associated with low drug exposure, *J Infect Dis*, **210**, 146-153.

Dostalova A. and Volf P., (2012), *Leishmania* development in sand flies: parasite-vector interactions overview, *Parasit Vectors*, **5**, 276.

Dougherty B. V., Moutinho Jr T. J. and Papin J., (2017), Accelerating the Drug Development Pipeline with Genome-Scale Metabolic Network Reconstructions, *Systems Biology*, **6**.

Du R, Hotez PJ, Al-Salem WS, Acosta-Serrano A., (2016). Old World Cutaneous Leishmaniasis and Refugee Crises in the Middle East and North Africa. *PLoS Negl Trop Dis* **10**:e0004545.

Duarte M. C., dos Reis Lage L. M., Lage D. P., Mesquita J. T., Salles B. C. S., Lavorato S. N., Menezes-Souza D., Roatt B. M., Alves R. J. and Tavares C. A. P., (2016), An effective in vitro and in vivo anti*Leishmania*l activity and mechanism of action of 8-hydroxyquinoline against *Leishmania* species causing visceral and tegumentary Leishmaniasis, *Veterinary parasitology*, **217**, 81-88.

Duarte M. C., Lage L. M., Lage D. P., Martins V. T., Carvalho A. M., Roatt B. M., Menezes-Souza D., Tavares C. A., Alves R. J., Barichello J. M. and Coelho E. A., (2016), Treatment of murine visceral Leishmaniasis using an 8-hydroxyquinoline-containing polymeric micelle system, *Parasitology international*, **65**, 728-736.

Dube A., Gupta R. and Singh N., (2009), Reporter genes facilitating discovery of drugs targeting protozoan parasites, *Trends in parasitology*, **25**, 432-439.

Duffy S. and Avery V. M., (2012), Development and Optimization of a Novel 384-Well Anti-Malarial Imaging Assay Validated for High-Throughput Screening, *The American Journal of Tropical Medicine and Hygiene*, **86**, 84-92.

Duffy S., Sykes M. L., Jones A. J., Shelper T. B., Simpson M., Lang R., Poulsen S.-A., Sleebs B. E. and Avery V. M., (2017), Screening the Medicines for Malaria Venture Pathogen Box across multiple pathogens reclassifies starting points for open-source drug discovery, *Antimicrobial agents and chemotherapy*, **61**, e00379-00317.

Dufour J. H., Dziejman M., Liu M. T., Leung J. H., Lane T. E. and Luster A. D., (2002), IFN-γ-inducible protein 10 (IP-10; CXCL10)-deficient mice reveal a role for IP-10 in effector T cell generation and trafficking, *The Journal of Immunology*, **168**, 3195-3204.

Duque G. A. and Descoteaux A., (2015), *Leishmania* survival in the macrophage: where the ends justify the means, *Current opinion in microbiology*, **26**, 32-40.

Durieu E., Prina E., Leclercq O., Oumata N., Gaboriaud-Kolar N., Vougogiannopoulou K., Aulner N., Defontaine A., No J. H., Ruchaud S., Skaltsounis A. L., Galons H., Spath G. F., Meijer L. and Rachidi N., (2016), From Drug Screening to Target Deconvolution: a Target-Based Drug Discovery Pipeline Using *Leishmania* Casein Kinase 1 Isoform 2 To Identify Compounds with Anti*Leishmania*l Activity, *Antimicrob Agents Chemother*, **60**, 2822-2833.

El-Sayed N. M., Myler P. J., Blandin G., Berriman M., Crabtree J., Aggarwal G., Caler E., Renauld H., Worthey E. A., Hertz-Fowler C., Ghedin E., Peacock C., Bartholomeu D. C., Haas B. J., Tran A. N., Wortman J. R., Alsmark U. C., Angiuoli S., Anupama A., Badger J., Bringaud F., Cadag E., Carlton J. M., Cerqueira G. C., Creasy T., Delcher A. L., Djikeng A., Embley T. M., Hauser C., Ivens A. C., Kummerfeld S. K., Pereira-Leal J. B., Nilsson D., Peterson J., Salzberg S. L., Shallom J., Silva J. C., Sundaram J., Westenberger S., White O., Melville S. E., Donelson J. E., Andersson B., Stuart K. D. and Hall N., (2005), Comparative genomics of trypanosomatid parasitic protozoa, *Science*, **309**, 404-409.

Elfaituri S. S., Matoug I., Elsalheen H., Belrasali Y. and Emaetig F., (2015), Letter to the Editor: Mucocutaneous Leishmaniasis in an 11-year-old girl with ataxia telangectasia case report, *Libyan Journal of Medicine*, **10**.

Empfield J. R. and Clark M. P., (2014), *Reducing Drug Attrition*Springer.

Engwerda C. R., Ato M., Stäger S., Alexander C. E., Stanley A. C. and Kaye P. M., (2004), Distinct roles for lymphotoxin-α and tumor necrosis factor in the control of *Leishmania* donovani infection, *The American journal of pathology*, **165**, 2123-2133.

Engwerda CR, Ato M, Kaye PM., (2004), Macrophages, pathology and parasite persistence in experimental visceral leishmaniasis. *Trends Parasitol* **20**,524-30.

Escobar P., Matu S., Marques C. and Croft S. L., (2002), Sensitivities of *Leishmania* species to hexadecylphosphocholine (miltefosine), ET-18-OCH(3) (edelfosine) and amphotericin B, *Acta Trop*, **81**, 151-157.

Faleiro R. J., Kumar R., Hafner L. M. and Engwerda C. R., (2014), Immune regulation during chronic visceral Leishmaniasis, *PLoS Negl Trop Dis*, **8**, e2914.

Faraut-Gambarelli F., Piarroux R., Deniau M., Giusiano B., Marty P., Michel G., Faugere B. and Dumon H., (1997), In vitro and in vivo resistance of *Leishmania* infantum to meglumine antimoniate: a study of 37 strains collected from patients with visceral Leishmaniasis, *Antimicrob Agents Chemother*, **41**, 827-830.

Feng Y., Davis R. A., Sykes M. L., Avery V. M. and Quinn R. J., (2012), Iotrochamides A and B, antitrypanosomal compounds from the Australian marine sponge Iotrochota sp, *Bioorg Med Chem Lett*, **22**, 4873-4876.

Fernandez O., Diaz-Toro Y., Valderrama L., Ovalle C., Valderrama M., Castillo H., Perez M. and Saravia N. G., (2012), Novel approach to in vitro drug susceptibility assessment of clinical strains of *Leishmania* spp, *J Clin Microbiol*, **50**, 2207-2211.

Fernandez O. L., Diaz-Toro Y., Ovalle C., Valderrama L., Muvdi S., Rodriguez I., Gomez M. A. and Saravia N. G., (2014), Miltefosine and antimonial drug susceptibility of *Leishmania* Viannia species and populations in regions of high transmission in Colombia, *PLoS Negl Trop Dis*, **8**, e2871.

Field M. C., Horn D., Fairlamb A. H., Ferguson M. A., Gray D. W., Read K. D., De Rycker M., Torrie L. S., Wyatt P. G. and Wyllie S., (2017), Anti-trypanosomatid drug discovery: an ongoing challenge and a continuing need, *Nature Reviews Microbiology*, **15**, 217-231.

Figueiro-Filho E. A., Duarte G., El-Beitune P., Quintana S. M. and Maia T. L., (2004), Visceral Leishmaniasis (kala-azar) and pregnancy, *Infectious diseases in obstetrics and gynecology*, **12**, 31-40.

Fontenot J. D., Gavin M. A. and Rudensky A. Y., (2003), Foxp3 programs the development and function of CD4+ CD25+ regulatory T cells, *Nature immunology*, **4**, 330-336.

Foucher, A. L., Rachidi, N., Gharbi, S., Blisnick, T., Bastin, P., Pemberton, I. K., & Späth, G. F., (2013), Apoptotic marker expression in the absence of cell death in staurosporine-treated Leishmania donovani, *Antimicrobial Agents and Chemotherapy*, **57**, 1252–61.

Freitas-Junior L. H., Chatelain E., Kim H. A. and Siqueira-Neto J. L., (2012), Visceral Leishmaniasis treatment: what do we have, what do we need and how to deliver

it?, *International Journal for Parasitology: Drugs and Drug Resistance*, **2**, 11-19.

Freitas-Junior L. H., Chatelain E., Kim H. A. and Siqueira-Neto J. L., (2012), Visceral Leishmaniasis treatment: What do we have, what do we need and how to deliver it?, *Int J Parasitol Drugs Drug Resist*, **2**, 11-19.

Gabrielsen B., Monath T. P., Huggins J. W., Kirsi J. J., Hollingshead M., Shannon W. M. and Pettit G. R., (1992), in *Natural Products as Antiviral Agents*Springer, pp. 121-135.

Galvez R., Descalzo M. A., Miro G., Jimenez M. I., Martin O., Dos Santos-Brandao F., Guerrero I., Cubero E. and Molina R., (2010), Seasonal trends and spatial relations between environmental/meteorological factors and leishmaniosis sand fly vector abundances in Central Spain, *Acta Trop*, **115**, 95-102.

Gamage S. A., Figgitt D. P., Wojcik S. J., Ralph R. K., Ransijn A., Mauel J., Yardley V., Snowdon D., Croft S. L. and Denny W. A., (1997), Structure− activity relationships for the anti*Leishmania*l and antitrypanosomal activities of 1 '-substituted 9-anilinoacridines, *Journal of medicinal chemistry*, **40**, 2634-2642.

Ganguly S., Das N. K., Barbhuiya J. N. and Chatterjee M., (2010), Post-kala-azar dermal Leishmaniasis--an overview, *Int J Dermatol*, **49**, 921-931.

Gaspar R., Opperdoes F. R., Preat V. and Roland M., (1992), Drug targeting with polyalkylcyanoacrylate nanoparticles: in vitro activity of primaquine-loaded nanoparticles against intracellular *Leishmania* donovani, *Ann Trop Med Parasitol*, **86**, 41-49.

Gilbert I. H., (2013), Drug discovery for neglected diseases: molecular target-based and phenotypic approaches, *J Med Chem*, **56**, 7719-7726.

Glaser T. A., Baatz J. E., Kreishman G. P. and Mukkada A. J., (1988), pH homeostasis in *Leishmania* donovani amastigotes and promastigotes, *Proceedings of the National Academy of Sciences*, **85**, 7602-7606.

Gluenz E., Ginger M. L. and McKean P. G., (2010), Flagellum assembly and function during the *Leishmania* life cycle, *Current opinion in microbiology*, **13**, 473-479.

Goldston A. M., Sharma A. I., Paul K. S. and Engman D. M., (2014), Acylation in trypanosomatids: an essential process and potential drug target, *Trends in parasitology*, **30**, 350-360.

Gomes M. N., Alcântara L. M., Neves B. J., Melo-Filho C. C., Freitas-Junior L. H., Moraes C. B., Ma R., Franzblau S. G., Muratov E. and Andrade C. H., (2017), Computer-aided discovery of two novel chalcone-like compounds active and

selective against *Leishmania* infantum, *Bioorganic & medicinal chemistry letters*, **27**, 2459-2464.

Gonzalez U., Pinart M., Sinclair D., Firooz A., Enk C., Velez I. D., Esterhuizen T. M., Tristan M. and Alvar J., (2015), Vector and reservoir control for preventing Leishmaniasis, *Cochrane Database Syst Rev*, **8**, CD008736.

Gopinath V. S., Pinjari J., Dere R. T., Verma A., Vishwakarma P., Shivahare R., Moger M., Goud P. S. K., Ramanathan V. and Bose P., (2013), Design, synthesis and biological evaluation of 2-substituted quinolines as potential anti*Leishmania*l agents, *European journal of medicinal chemistry*, **69**, 527-536.

Gopinath V. S., Rao M., Shivahare R., Vishwakarma P., Ghose S., Pradhan A., Hindupur R., Sarma K. D., Gupta S. and Puri S. K., (2014), Design, synthesis, ADME characterization and anti*Leishmania*l evaluation of novel substituted quinoline analogs, *Bioorganic & medicinal chemistry letters*, **24**, 2046-2052.

Gossage, S. M., Rogers, M. E. and Bates, P. A., (2003), Two separate growth phases during the development of Leishmania in sand flies: implications for understanding the life cycle, *International journal for parasitology*, **33**,1027-34.

Goto, H., & Lindoso, J. A. L., (2004), Immunity and immunosuppression in experimental visceral leishmaniasis, *Brazilian Journal of Medical and Biological*, **37**, 615–23

Goto H. and Lindoso J. A. L., (2010), Current diagnosis and treatment of cutaneous and mucocutaneous Leishmaniasis, *Expert review of anti-infective therapy*, **8**, 419-433.

Gradoni L., (2015), Canine *Leishmania* vaccines: still a long way to go, *Veterinary parasitology*, **208**, 94-100.

Guerra J. A., Prestes S. R., Silveira H., Coelho L. I., Gama P., Moura A., Amato V., Barbosa M. and Ferreira L. C., (2011), Mucosal Leishmaniasis caused by *Leishmania* (Viannia) braziliensis and *Leishmania* (Viannia) guyanensis in the Brazilian Amazon, *PLoS Negl Trop Dis*, **5**, e980.

Guglielmo S., Bertinaria M., Rolando B., Crosetti M., Fruttero R., Yardley V., Croft S. L. and Gasco A., (2009), A new series of amodiaquine analogues modified in the basic side chain with in vitro anti*Leishmania*l and antiplasmodial activity, *European journal of medicinal chemistry*, **44**, 5071-5079.

Gupta A., Jat R., Shrimal N., Sharma P. and Kharb M., (2017), A REVIEW: FACTORS THAT IMPACT THE DEVELOPABILITY OF DRUG CANDIDATES, *International Journal of Drug Research and Technology*, **2**, 4.

Gupta G., Oghumu S. and Satoskar A. R., (2013), Mechanisms of Immune Evasion in Leishmaniasis, *Advances in applied microbiology*, **82**, 155-184.

Gupta S., (2011), Visceral Leishmaniasis: experimental models for drug discovery, *Indian J Med Res*, **133**, 27-39.

Gupta S., Yardley V., Vishwakarma P., Shivahare R., Sharma B., Launay D., Martin D. and Puri S. K., (2015), Nitroimidazo-oxazole compound DNDI-VL-2098: an orally effective preclinical drug candidate for the treatment of visceral Leishmaniasis, *J Antimicrob Chemother*, **70**, 518-527.

Hailu A., Dagne D. A. and Boelaert M., (2016), in *Neglected Tropical Diseases-Sub-Saharan Africa*Springer, pp. 87-112.

Haldar A. K., Sen P. and Roy S., (2011), Use of antimony in the treatment of Leishmaniasis: current status and future directions, *Mol Biol Int*, **2011**, 571242.

Han C. and Wang B., (2016), Factors that impact the developability of drug candidates, *Drug Delivery: Principles and Applications, Second Edition*, 1-18.

Handler M. Z., Patel P. A., Kapila R., Al-Qubati Y. and Schwartz R. A., (2015), Cutaneous and mucocutaneous Leishmaniasis: differential diagnosis, diagnosis, histopathology, and management, *Journal of the American Academy of Dermatology*, **73**, 911-926.

Handman E., (1999), Cell biology of *Leishmania*, *Advances in parasitology*, **44**, 1-39.

Handman E. and Bullen D. V., (2002), Interaction of *Leishmania* with the host macrophage, *Trends Parasitol*, **18**, 332-334.

Hardie D. G., (1999), *Protein phosphorylation : a practical approach / edited by D.G. Hardie.*, England: Oxford ; New York : Oxford University Press, c1999.

Hart D. T. and Coombs G. H., (1982), *Leishmania* mexicana: energy metabolism of amastigotes and promastigotes, *Exp Parasitol*, **54**, 397-409.

Harvey A. L., (2008), Natural products in drug discovery, *Drug Discov Today*, **13**, 894-901.

Harvey A. L., Edrada-Ebel R. and Quinn R. J., (2015), The re-emergence of natural products for drug discovery in the genomics era, *Nat Rev Drug Discov*, **14**, 111-129.

Hasnain M. G., Shomik M. S., Ghosh P., Rashid M. O., Hossain M. S., Hamano S. and Mondal D., (2016), Post-Kala-Azar Dermal Leishmaniasis without Previous History of Visceral Leishmaniasis, *Am J Trop Med Hyg*.

Hawgood B. J., (2001), Alexander Russell (1715-1768) and Patrick Russell (1727-1805): physicians and natural historians of Aleppo, *J Med Biogr*, **9**, 1-6.

Hayward R., Saliba K. J. and Kirk K., (2006), The pH of the digestive vacuole of Plasmodium falciparum is not associated with chloroquine resistance, *Journal of cell science*, **119**, 1016-1025.

Hazra S., Ghosh S., Debnath S., Seville S., Prajapati V. K., Wright C. W., Sundar S. and Hazra B., (2012), Anti*Leishmania*l activity of cryptolepine analogues and apoptotic effects of 2, 7-dibromocryptolepine against *Leishmania* donovani promastigotes, *Parasitology research*, **111**, 195-203.

Hefnawy A., Berg M., Dujardin J.-C. and De Muylder G., (2017), Exploiting knowledge on *Leishmania* drug resistance to support the quest for new drugs, *Trends in parasitology*, **33**, 162-174.

Heitman J., (2006), Sexual reproduction and the evolution of microbial pathogens, *Current Biology*, **16**, R711-R725.

Hempelmann E., (2007), Hemozoin biocrystallization in Plasmodium falciparum and the antimalarial activity of crystallization inhibitors, *Parasitology research*, **100**, 671-676.

Hendrickx S., Eberhardt E., Mondelaers A., Rijal S., Bhattarai N. R., Dujardin J. C., Delputte P., Cos P. and Maes L., (2015), Lack of correlation between the promastigote back-transformation assay and miltefosine treatment outcome, *J Antimicrob Chemother*, **70**, 3023-3026.

Hendrickx S., Mondelaers A., Eberhardt E., Delputte P., Cos P. and Maes L., (2015), In Vivo Selection of Paromomycin and Miltefosine Resistance in *Leishmania* donovani and L. infantum in a Syrian Hamster Model, *Antimicrob Agents Chemother*, **59**, 4714-4718.

Hertzberg R. P. and Pope A. J., (2000), High-throughput screening: new technology for the 21st century, *Curr Opin Chem Biol*, **4**, 445-451.

Herwaldt B. L., (1999), Leishmaniasis, *Lancet*, **354**, 1191-1199.

Hodiamont C. J., Kager P. A., Bart A., de Vries H. J., van Thiel P. P., Leenstra T., de Vries P. J., van Vugt M., Grobusch M. P. and van Gool T., (2014), Species-directed therapy for Leishmaniasis in returning travellers: a comprehensive guide, *PLoS Negl Trop Dis*, **8**, e2832.

Holzer T. R., McMaster W. R. and Forney J. D., (2006), Expression profiling by whole-genome interspecies microarray hybridization reveals differential gene expression in procyclic promastigotes, lesion-derived amastigotes, and axenic amastigotes in *Leishmania* mexicana, *Mol Biochem Parasitol*, **146**, 198-218.

Hsieh E. and Liu J. P., (2008), On statistical evaluation of the linearity in assay validation, *J Biopharm Stat*, **18**, 677-690.

Hughes J., Rees S., Kalindjian S. and Philpott K., (2011), Principles of early drug discovery, *Br J Pharmacol*, **162**, 1239-1249.

Hardy, L. W., Matthews, W., Nare, B. & Beverley, S. M., (1997) Biochemical and genetic tests for inhibitors of Leishmania pteridine pathways. *Exp. Parasitol.* **87**, 157–69.

Hynes J., Hill R. and Papkovsky D. B., (2006), The use of a fluorescence-based oxygen uptake assay in the analysis of cytotoxicity, *Toxicol In Vitro*, **20**, 785-792.

Imbert L., Cojean S., Libong D., Chaminade P. and Loiseau P. M., (2014), Sitamaquine-resistance in *Leishmania* donovani affects drug accumulation and lipid metabolism, *Biomed Pharmacother*, **68**, 893-897.

Ingolfsson HI, Thakur P, Herold KF, Hobart EA, Ramsey NB, Periole X, de Jong DH, Zwama M, Yilmaz D, Hall K, Maretzky T, Hemmings HC, Jr., Blobel C, Marrink SJ, Kocer A, Sack JT, Andersen OS., (2014). Phytochemicals perturb membranes and promiscuously alter protein function. *ACS Chem Biol* **9**,1788-98.

Ivens A. C., Peacock C. S., Worthey E. A., Murphy L., Aggarwal G., Berriman M., Sisk E., Rajandream M. A., Adlem E., Aert R., Anupama A., Apostolou Z., Attipoe P., Bason N., Bauser C., Beck A., Beverley S. M., Bianchettin G., Borzym K., Bothe G., Bruschi C. V., Collins M., Cadag E., Ciarloni L., Clayton C., Coulson R. M., Cronin A., Cruz A. K., Davies R. M., De Gaudenzi J., Dobson D. E., Duesterhoeft A., Fazelina G., Fosker N., Frasch A. C., Fraser A., Fuchs M., Gabel C., Goble A., Goffeau A., Harris D., Hertz-Fowler C., Hilbert H., Horn D., Huang Y., Klages S., Knights A., Kube M., Larke N., Litvin L., Lord A., Louie T., Marra M., Masuy D., Matthews K., Michaeli S., Mottram J. C., Muller-Auer S., Munden H., Nelson S., Norbertczak H., Oliver K., O'Neil S., Pentony M., Pohl T. M., Price C., Purnelle B., Quail M. A., Rabbinowitsch E., Reinhardt R., Rieger M., Rinta J., Robben J., Robertson L., Ruiz J. C., Rutter S., Saunders D., Schafer M., Schein J., Schwartz D. C., Seeger K., Seyler A., Sharp S., Shin H., Sivam D., Squares R., Squares S., Tosato V., Vogt C., Volckaert G., Wambutt R., Warren T., Wedler H., Woodward J., Zhou S., Zimmermann W., Smith D. F., Blackwell J. M., Stuart K. D., Barrell B. and Myler P. J., (2005), The genome of the kinetoplastid parasite, *Leishmania* major, *Science*, **309**, 436-442.

Ives, A., Ronet, C., Prevel, F., Ruzzante, G., Fuertes-Marraco, S., Schutz, F., Masina, S., (2011), Leishmania RNA virus controls the severity of mucocutaneous leishmaniasis, *Science*, **331**, 775–8.

Jain V. and Sharma A., (2017), Repurposing of Potent Drug Candidates for Multiparasite Targeting, *Trends in parasitology*, **33**, 158-161.

Jha T. K., Sundar S., Thakur C. P., Felton J. M., Sabin A. J. and Horton J., (2005), A phase II dose-ranging study of sitamaquine for the treatment of visceral Leishmaniasis in India, *Am J Trop Med Hyg*, **73**, 1005-1011.

Jhingran A., Chawla B., Saxena S., Barrett M. P. and Madhubala R., (2009), Paromomycin: uptake and resistance in *Leishmania* donovani, *Mol Biochem Parasitol*, **164**, 111-117.

Jimenez-Ruiz A, Alzate JF, Macleod ET, Luder CG, Fasel N, Hurd H., (2010). Apoptotic markers in protozoan parasites. *Parasit Vectors* **3**,104.

John D. T., Petri W. A., Markell E. K. and Voge M., (2006), *Markell and Voge's medical parasitology*Elsevier Health Sciences.

Jones A. J. and Avery V. M., (2015), Future treatment options for human African trypanosomiasis, *Expert Rev Anti Infect Ther*, **13**, 1429-1432.

Jones A. J., Grkovic T., Sykes M. L. and Avery V. M., (2013), Trypanocidal activity of marine natural products, *Marine drugs*, **11**, 4058-4082.

Jones D. C., Hallyburton I., Stojanovski L., Read K. D., Frearson J. A. and Fairlamb A. H., (2010), Identification of a kappa-opioid agonist as a potent and selective lead for drug development against human African trypanosomiasis, *Biochem Pharmacol*, **80**, 1478-1486.

Jung H. J. and Kwon H. J., (2015), Target deconvolution of bioactive small molecules: the heart of chemical biology and drug discovery, *Arch Pharm Res*, **38**, 1627-1641.

Kamau S. W., Nunez R. and Grimm F., (2001), Flow cytometry analysis of the effect of allopurinol and the dinitroaniline compound (Chloralin) on the viability and proliferation of *Leishmania* infantum promastigotes, *BMC Pharmacol*, **1**, 1.

Kamboj A. K., (2016), Leishmaniasis: A public health issue, *Journal of Alternative Medicine Research*, **8**, 297.

Kamhawi S., (2006), Phlebotomine sand flies and *Leishmania* parasites: friends or foes?, *Trends in parasitology*, **22**, 439-445.

Kamhawi S., Modi G. B., Pimenta P. F., Rowton E. and Sacks D. L., (2000), The vectorial competence of Phlebotomus sergenti is specific for *Leishmania* tropica and is controlled by species-specific, lipophosphoglycan-mediated midgut attachment, *Parasitology*, **121 (Pt 1)**, 25-33.

Kar K., Mukerji K., Naskar K., Bhattacharya A. and Ghosh D. K., (1990), *Leishmania* donovani: a chemically defined medium suitable for cultivation and cloning of

promastigotes and transformation of amastigotes to to promastigotes, *J Protozool*, **37**, 277-279.

Kassi M., Kassi M., Afghan A. K., Rehman R. and Kasi P. M., (2008), Marring Leishmaniasis: the stigmatization and the impact of cutaneous Leishmaniasis in Pakistan and Afghanistan, *PLoS Negl Trop Dis*, **2**, e259.

Katara G. K., Ansari N. A., Verma S., Ramesh V. and Salotra P., (2011), Foxp3 and IL-10 expression correlates with parasite burden in lesional tissues of post kala azar dermal Leishmaniasis (PKDL) patients, *PLoS Negl Trop Dis*, **5**, e1171.

Katsuno K., Burrows J. N., Duncan K., Van Huijsduijnen R. H., Kaneko T., Kita K., Mowbray C. E., Schmatz D., Warner P. and Slingsby B., (2015), Hit and lead criteria in drug discovery for infectious diseases of the developing world, *Nature reviews. Drug discovery*, **14**, 751.

Kaufer A., Ellis J., Stark D. and Barratt J., (2017), The evolution of trypanosomatid taxonomy, *Parasites & vectors*, **10**, 287.

Kaye K. S. and Kaye D., (2000), Multidrug-resistant pathogens: mechanisms of resistance and epidemiology, *Current infectious disease reports*, **2**, 391-398.

Kevric I., Cappel M. A. and Keeling J. H., (2015), New World and Old World *Leishmania* Infections, *Dermatologic clinics*, **33**, 579-593.

Kevric I., Cappel M. A. and Keeling J. H., (2015), New World and Old World *Leishmania* Infections: A Practical Review, *Dermatol Clin*, **33**, 579-593.

Khan K. M., Rasheed M., Zia U., Hayat S., Kaukab F., Choudhary M. I., Atta ur R. and Perveen S., (2003), Synthesis and in vitro leishmanicidal activity of some hydrazides and their analogues, *Bioorg Med Chem*, **11**, 1381-1387.

Khare S., Nagle A. S., Biggart A., Lai Y. H., Liang F., Davis L. C., Barnes S. W., Mathison C. J., Myburgh E., Gao M. Y., Gillespie J. R., Liu X., Tan J. L., Stinson M., Rivera I. C., Ballard J., Yeh V., Groessl T., Federe G., Koh H. X., Venable J. D., Bursulaya B., Shapiro M., Mishra P. K., Spraggon G., Brock A., Mottram J. C., Buckner F. S., Rao S. P., Wen B. G., Walker J. R., Tuntland T., Molteni V., Glynne R. J. and Supek F., (2016), Proteasome inhibition for treatment of Leishmaniasis, Chagas disease and sleeping sickness, *Nature*, **537**, 229-233.

Khalil EA, Weldegebreal T, Younis BM, Omollo R, Musa AM, Hailu W, Abuzaid AA, Dorlo TP, Hurissa Z, Yifru S, Haleke W, Smith PG, Ellis S, Balasegaram M, AM EL-H, Schoone GJ, Wasunna M, Kimutai R, Edwards T, Hailu A., (2014). Safety and efficacy of single dose versus multiple doses of AmBisome for treatment of visceral leishmaniasis in eastern Africa: a randomised trial. *PLoS Negl Trop Dis* **8**,e2613.

Killick-Kendrick R., (1990), Phlebotomine vectors of the *Leishmania*ses: a review, *Med Vet Entomol*, **4**, 1-24.

Killick-Kendrick R., (1985), Some epidemiological consequences of the evolutionary fit between leishmaniae and their phlebotomine vectors, *Bull Soc Path Exot*, **78**: 747-755

Kloehn J., Saunders E. C., O'Callaghan S., Dagley M. J. and McConville M. J., (2015), Characterization of metabolically quiescent *Leishmania* parasites in murine lesions using heavy water labeling, *PLoS Pathog*, **11**, e1004683.

Knasmuller S., Mersch-Sundermann V., Kevekordes S., Darroudi F., Huber W. W., Hoelzl C., Bichler J. and Majer B. J., (2004), Use of human-derived liver cell lines for the detection of environmental and dietary genotoxicants; current state of knowledge, *Toxicology*, **198**, 315-328.

Kroidl A., Kroidl I., Bretzel G. and Loscher T., (2014), Non-healing old world cutaneous Leishmaniasis caused by L. infantum in a patient from Spain, *BMC Infect Dis*, **14**, 206.

Kubitscheck U., (2017), *Fluorescence microscopy: from principles to biological applications*John Wiley & Sons.

Kulkarni M. M., McMaster W. R., Kamysz W. and McGwire B. S., (2009), Antimicrobial peptide-induced apoptotic death of *Leishmania* results from calcium-de pend ent, caspase-independent mitochondrial toxicity, *Journal of Biological Chemistry*, **284**, 15496-15504.

Kumar A., Das S., Purkait B., Sardar A. H., Ghosh A. K., Dikhit M. R., Abhishek K. and Das P., (2014), Ascorbate peroxidase, a key molecule regulating amphotericin B resistance in clinical isolates of *Leishmania* donovani, *Antimicrobial agents and chemotherapy*, **58**, 6172-6184.

Lackovic K., Parisot J. P., Sleebs N., Baell J. B., Debien L., Watson K. G., Curtis J. M., Handman E., Street I. P. and Kedzierski L., (2010), Inhibitors of *Leishmania* GDP-mannose pyrophosphorylase identified by high-throughput screening of small-molecule chemical library, *Antimicrobial agents and chemotherapy*, **54**, 1712-1719.

Lamotte S., Späth G. F., Rachidi N. and Prina E., (2017), The enemy within: Targeting host–parasite interaction for anti*Leishmania*l drug discovery, *PLOS Neglected Tropical Diseases*, **11**, e0005480.

Landires, E. A. G., Andrial, M., Hosokawa, A., Nonaka, S. & Hashiguchi, Y., (1995), Oral treatment of new world cutaneous leishmaniasis with anti-malarial drugs in Ecuador: a preliminary clinical trial, *Jpn J Trop Med Hyg*, **23**, 151–157.

Lang T., Goyard S., Lebastard M. and Milon G., (2005), Bioluminescent *Leishmania* expressing luciferase for rapid and high throughput screening of drugs acting on amastigote-harbouring macrophages and for quantitative real-time monitoring of parasitism features in living mice, *Cell Microbiol*, **7**, 383-392.

Lasserre R., (1979), Treatment of amoebiasis, *Phil J Microbiol Infect Dis*, **8**, 1.

Leishman, (1903), On the possibility of the occurrence of trypanosomiasis in India, *Br Med J* **1**, 1252-1254.

Leite F. H. A., Froes T. Q., da Silva S. G., de Souza E. I. M., Vital-Fujii D. G., Trossini G. H. G., Pita S. and Castilho M. S., (2017), An integrated approach towards the discovery of novel non-nucleoside *Leishmania* major pteridine reductase 1 inhibitors, *Eur J Med Chem*, **132**, 322-332.

Lemmens-Gruber R., Karkhaneh A., Studenik C. and Heistracher P., (1996), Cardiotoxicity of emetine dihydrochloride by calcium channel blockade in isolated preparations and ventricular myocytes of guinea-pig hearts, *British journal of pharmacology*, **117**, 377-383.

Lessa H. A., Machado P., Lima F., Cruz A. A., Bacellar O., Guerreiro J. and Carvalho E. M., (2001), Successful treatment of refractory mucosal Leishmaniasis with pentoxifylline plus antimony, *Am J Trop Med Hyg*, **65**, 87-89.

Levrier C., Balastrier M., Beattie K. D., Carroll A. R., Martin F., Choomuenwai V. and Davis R. A., (2013), Pyridocoumarin, aristolactam and aporphine alkaloids from the Australian rainforest plant Goniothalamus australis, *Phytochemistry*, **86**, 121-126.

Lewis D. J., (1971), Phlebotomid sandflies, *Bull World Health Organ*, **44**, 535-551.

Lievin-Le Moal V. and Loiseau P. M., (2016), *Leishmania* hijacking of the macrophage intracellular compartments, *FEBS J*, **283**, 598-607.

Liu D. and Uzonna J. E., (2012), The early interaction of *Leishmania* with macrophages and dendritic cells and its influence on the host immune response, *Frontiers in cellular and infection microbiology*, **2**.

Liu R., Li X. and Lam K. S., (2017), Combinatorial chemistry in drug discovery, *Current Opinion in Chemical Biology*, **38**, 117-126.

Loiseau P. M., Cojean S. and Schrevel J., (2011), Sitamaquine as a putative anti*Leishmania*l drug candidate: from the mechanism of action to the risk of drug resistance, *Parasite*, **18**, 115-119.

Loiseau P. M., Gupta S., Verma A., Srivastava S., Puri S., Sliman F., Normand-Bayle M. and Desmaele D., (2011), In vitro activities of new 2-substituted quinolines against *Leishmania* donovani, *Antimicrobial agents and chemotherapy*, **55**, 1777-1780.

Lombardo F., Shalaeva M. Y., Tupper K. A. and Gao F., (2001), ElogD(oct): a tool for lipophilicity determination in drug discovery. 2. Basic and neutral compounds, *J Med Chem*, **44**, 2490-2497.

Lopez-Martin C., Perez-Victoria J. M., Carvalho L., Castanys S. and Gamarro F., (2008), Sitamaquine sensitivity in *Leishmania* species is not mediated by drug accumulation in acidocalcisomes, *Antimicrob Agents Chemother*, **52**, 4030-4036.

Luna K. P., Hernandez I. P., Rueda C. M., Zorro M. M., Croft S. L. and Escobar P., (2009), In vitro susceptibility of Trypanosoma cruzi strains from Santander, Colombia, to hexadecylphosphocholine (miltefosine), nifurtimox and benznidazole, *Biomedica : revista del Instituto Nacional de Salud*, **29**, 448-455.

Luque-Ortega J. R. and Rivas L., (2007), Miltefosine (hexadecylphosphocholine) inhibits cytochrome c oxidase in *Leishmania* donovani promastigotes, *Antimicrob Agents Chemother*, **51**, 1327-1332.

Luque-Ortega J. R. and Rivas L., (2007), Miltefosine (hexadecylphosphocholine) inhibits cytochrome c oxidase in *Leishmania* donovani promastigotes, *Antimicrobial agents and chemotherapy*, **51**, 1327-1332.

Lux H., Heise N., Klenner T., Hart D. and Opperdoes F. R., (2000), Ether--lipid (alkyl-phospholipid) metabolism and the mechanism of action of ether--lipid analogues in *Leishmania*, *Molecular and biochemical parasitology*, **111**, 1-14.

M. Rudin M., PhD, Charles and B. Thompson M., Craig, (1997), Apoptosis and disease: regulation and clinical relevance of programmed cell death, *Annual review of medicine*, **48**, 267-281.

Maarouf M., de Kouchkovsky Y., Brown S., Petit P. X. and Robert-Gero M., (1997), In vivo interference of paromomycin with mitochondrial activity of *Leishmania*, *Exp Cell Res*, **232**, 339-348.

Machado P. R., Rosa M. E., Guimaraes L. H., Prates F. V., Queiroz A., Schriefer A. and Carvalho E. M., (2015), Treatment of Disseminated Leishmaniasis With Liposomal Amphotericin B, *Clin Infect Dis*, **61**, 945-949.

Mackey Z. B., Baca A. M., Mallari J. P., Apsel B., Shelat A., Hansell E. J., Chiang P. K., Wolff B., Guy K. R., Williams J. and McKerrow J. H., (2006), Discovery of trypanocidal compounds by whole cell HTS of Trypanosoma brucei, *Chem Biol Drug Des*, **67**, 355-363.

Maia C. and Campino L., (2011), Can domestic cats be considered reservoir hosts of zoonotic Leishmaniasis?, *Trends in parasitology*, **27**, 341-344.

Maia C. and Cardoso L., (2015), Spread of *Leishmania* infantum in Europe with dog travelling, *Veterinary parasitology*, **213**, 2-11.

Majno G. and Joris I., (1995), Apoptosis, oncosis, and necrosis. An overview of cell death, *The American journal of pathology*, **146**, 3.

Mandal G., Mandal S., Sharma M., Charret K. S., Papadopoulou B., Bhattacharjee H. and Mukhopadhyay R., (2015), Species-specific antimonial sensitivity in *Leishmania* is driven by post-transcriptional regulation of AQP1, *PLoS Negl Trop Dis*, **9**, e0003500.

Mandell M. A. and Beverley S. M., (2017), Continual renewal and replication of persistent *Leishmania* major parasites in concomitantly immune hosts, *Proceedings of the National Academy of Sciences of the United States of America*, **114**, E801-E810.

Marr J. and Muller M., (1995), *Biochemistry and molecular biology of parasites*Academic Press.

Masmoudi A., Hariz W., Marrekchi S., Amouri M. and Turki H., (2013), Old World cutaneous Leishmaniasis: diagnosis and treatment, *J Dermatol Case Rep*, **7**, 31-41.

Matoussi N., Ameur H. B., Amor S. B., Fitouri Z. and Becher S. B., (2007), [Cardiotoxicity of n-methyl-glucamine antimoniate (Glucantime). A case report], *Med Mal Infect*, **37 Suppl 3**, S257-259.

Matthews H., Usman-Idris M., Khan F., Read M. and Nirmalan N., (2013), Drug repositioning as a route to anti-malarial drug discovery: preliminary investigation of the in vitro anti-malarial efficacy of emetine dihydrochloride hydrate, *Malaria journal*, **12**, 359.

Mauricio IL, Stothard JR, Miles MA., (2000). The strange case of *Leishmania chagasi*. *Parasitol Today* **16**,188-9.

Mauel J., Denny W., Gamage S., Ransijn A., Wojcik S., Figgitt D. and Ralph R., (1993), 9-Anilinoacridines as potential anti*Leishmania*l agents, *Antimicrobial agents and chemotherapy*, **37**, 991-996.

Mauel J. and Ransijn A., (1997), *Leishmania* spp.: mechanisms of toxicity of nitrogen oxidation products, *Exp Parasitol*, **87**, 98-111.

Mbongo N., Loiseau P. M., Billion M. A. and Robert-Gero M., (1998), Mechanism of Amphotericin B Resistance in *Leishmania* donovani Promastigotes, *Antimicrobial Agents and Chemotherapy*, **42**, 352-357.

McConville M. J., Schnur L. F., Jaffe C. and Schneider P., (1995), Structure of *Leishmania* lipophosphoglycan: inter- and intra-specific polymorphism in Old World species, *Biochem J*, **310 (Pt 3)**, 807-818.

McMaster W. R., Morrison C. J., MacDonald M. H. and Joshi P. B., (1994), Mutational and functional analysis of the *Leishmania* surface metalloproteinase GP63: similarities to matrix metalloproteinases, *Parasitology*, **108 Suppl**, S29-36.

Meade J. C., Glaser T. A., Bonventre P. F. and Mukkada A. J., (1984), Enzymes of carbohydrate metabolism in *Leishmania* donovani amastigotes, *J Protozool*, **31**, 156-161.

Mesa-Valle C., Castilla-Calvente J., Sanchez-Moreno M., Moraleda-Lindez V., Barbe J. and Osuna A., (1996), Activity and mode of action of acridine compounds against *Leishmania* donovani, *Antimicrobial agents and chemotherapy*, **40**, 684-690.

Miguel D. C., Zauli-Nascimento R. C., Yokoyama-Yasunaka J. K., Pereira L. I., Jeronimo S. M., Ribeiro-Dias F., Dorta M. L. and Uliana S. R., (2011), Clinical isolates of New World *Leishmania* from cutaneous and visceral Leishmaniasis patients are uniformly sensitive to tamoxifen, *Int J Antimicrob Agents*, **38**, 93-94.

Mikus J. and Steverding D., (2000), A simple colorimetric method to screen drug cytotoxicity against *Leishmania* using the dye Alamar Blue, *Parasitology international*, **48**, 265-269.

Millán J., Ferroglio E. and Solano-Gallego L., (2014), Role of wildlife in the epidemiology of *Leishmania* infantum infection in Europe, *Parasitology research*, **113**, 2005-2014.

Mishra J., Saxena A. and Singh S., (2007), Chemotherapy of Leishmaniasis: past, present and future, *Curr Med Chem*, **14**, 1153-1169.

Mishra J. and Singh S., (2013), Miltefosine resistance in *Leishmania* donovani involves suppression of oxidative stress-induced programmed cell death, *Experimental parasitology*, **135**, 397-406.

Mohapatra S., (2014), Drug resistance in Leishmaniasis: Newer developments, *Tropical parasitology*, **4**, 4.

Molina R., Ghosh D., Carrillo E., Monnerat S., Bern C., Mondal D. and Alvar J., (2017), Infectivity of Post-Kala-azar Dermal Leishmaniasis Patients to Sand

Flies: Revisiting a Proof of Concept in the Context of the Kala-azar Elimination Program in the Indian Subcontinent, *Clinical Infectious Diseases*, **65**, 150-153.

Monge-Maillo B, Lopez-Velez R., (2013). Therapeutic options for old world cutaneous leishmaniasis and new world cutaneous and mucocutaneous leishmaniasis. *Drugs* **73**,1889-920.

Moraes C. B., Giardini M. A., Kim H., Franco C. H., Araujo-Junior A. M., Schenkman S., Chatelain E. and Freitas-Junior L. H., (2014), Nitroheterocyclic compounds are more efficacious than CYP51 inhibitors against Trypanosoma cruzi: implications for Chagas disease drug discovery and development, *Sci Rep*, **4**, 4703.

Moradi M, Rassi Y, Abai MR, Zahraei Ramazani A, Mohebali M, Rafizadeh S., (2018). Some epidemiological aspects of cutaneous leishmaniasis with emphasis on vectors and reservoirs of disease in the borderline of Iran and Iraq. *J Parasit Dis* **42**,243-251.

Morais-Teixeira E., Damasceno Q. S., Galuppo M. K., Romanha A. J. and Rabello A., (2011), The in vitro leishmanicidal activity of hexadecylphosphocholine (miltefosine) against four medically relevant *Leishmania* species of Brazil, *Memorias do Instituto Oswaldo Cruz*, **106**, 475-478.

Mowbray C. E., Braillard S., Speed W., Glossop P. A., Whitlock G. A., Gibson K. R., Mills J. E., Brown A. D., Gardner J. M., Cao Y., Hua W., Morgans G. L., Feijens P. B., Matheeussen A. and Maes L. J., (2015), Novel Amino-pyrazole Ureas with Potent In Vitro and In Vivo Anti*Leishmania*l Activity, *J Med Chem*, **58**, 9615-9624.

Mowbray C. E., Braillard S. p., Speed W., Glossop P. A., Whitlock G. A., Gibson K. R., Mills J. E., Brown A. D., Gardner J. M. F. and Cao Y., (2015), Novel amino-pyrazole ureas with potent in vitro and in vivo anti*Leishmania*l activity, *Journal of medicinal chemistry*, **58**, 9615-9624.

Mpamhanga C. P., Spinks D., Tulloch L. B., Shanks E. J., Robinson D. A., Collie I. T., Fairlamb A. H., Wyatt P. G., Frearson J. A., Hunter W. N., Gilbert I. H. and Brenk R., (2009), One scaffold, three binding modes: novel and selective pteridine reductase 1 inhibitors derived from fragment hits discovered by virtual screening, *J Med Chem*, **52**, 4454-4465.

Mukhopadhyay D., Dalton J. E., Kaye P. M. and Chatterjee M., (2014), Post kala-azar dermal Leishmaniasis: an unresolved mystery, *Trends in parasitology*, **30**, 65-74.

Mukkavilli R., Pinjari J., Patel B., Sengottuvelan S., Mondal S., Gadekar A., Verma M., Patel J., Pothuri L., Chandrashekar G., Koiram P., Harisudhan T., Moinuddin A., Launay D., Vachharajani N., Ramanathan V. and Martin D., (2014), In vitro

metabolism, disposition, preclinical pharmacokinetics and prediction of human pharmacokinetics of DNDI-VL-2098, a potential oral treatment for Visceral Leishmaniasis, *Eur J Pharm Sci*, **65**, 147-155.

Mullard A., (2015), The phenotypic screening pendulum swings, *Nature reviews. Drug discovery*, **14**, 807.

Muñoz D. L., Robledo S. M., Kolli B. K., Dutta S., Chang K. P. and Muskus C., (2009), *Leishmania* (Viannia) panamensis: an in vitro assay using the expression of GFP for screening of anti*Leishmania*l drug, *Experimental parasitology*, **122**, 134-139.

Musa A., Khalil E., Hailu A., Olobo J., Balasegaram M., Omollo R., Edwards T., Rashid J., Mbui J., Musa B., Abuzaid A. A., Ahmed O., Fadlalla A., El-Hassan A., Mueller M., Mucee G., Njoroge S., Manduku V., Mutuma G., Apadet L., Lodenyo H., Mutea D., Kirigi G., Yifru S., Mengistu G., Hurissa Z., Hailu W., Weldegebreal T., Tafes H., Mekonnen Y., Makonnen E., Ndegwa S., Sagaki P., Kimutai R., Kesusu J., Owiti R., Ellis S. and Wasunna M., (2012), Sodium stibogluconate (SSG) & paromomycin combination compared to SSG for visceral Leishmaniasis in East Africa: a randomised controlled trial, *PLoS Negl Trop Dis*, **6**, e1674.

Mushtaque M. and Shahjahan, (2015), Reemergence of chloroquine (CQ) analogs as multi-targeting antimalarial agents: a review, *European journal of medicinal chemistry*, **90**, 280-295.

Myskova J., Svobodova M., Beverley S. M. and Volf P., (2007), A lipophosphoglycan-independent development of *Leishmania* in permissive sand flies, *Microbes and infection*, **9**, 317-324.

Naderer T. and McConville M. J., (2011), Intracellular growth and pathogenesis of *Leishmania* parasites, *Essays Biochem*, **51**, 81-95.

Nagata S., (2018). Apoptosis and Clearance of Apoptotic Cells. *Annu Rev Immunol* **36**,489-517.

Nagle A. S., Khare S., Kumar A. B., Supek F., Buchynskyy A., Mathison C. J., Chennamaneni N. K., Pendem N., Buckner F. S., Gelb M. H. and Molteni V., (2014), Recent developments in drug discovery for Leishmaniasis and human African trypanosomiasis, *Chemical reviews*, **114**, 11305-11347.

Naiff R. D., Talhari S. and Barrett T. V., (1988), Isolation of *Leishmania* guyanensis from lesions of the nasal mucosa, *Mem Inst Oswaldo Cruz*, **83**, 529-530.

Nakayama G. R., Caton M. C., Nova M. P. and Parandoosh Z., (1997), Assessment of the Alamar Blue assay for cellular growth and viability in vitro, *J Immunol Methods*, **204**, 205-208.

Navin T. R., Arana B. A., Arana F. E., Berman J. D. and Chajon J. F., (1992), Placebo-controlled clinical trial of sodium stibogluconate (Pentostam) versus ketoconazole for treating cutaneous Leishmaniasis in Guatemala, *The Journal of infectious diseases*, **165**, 528-534.

Neal R., Allen S., McCoy N., Olliaro P. and Croft S., (1995), The sensitivity of *Leishmania* species to aminosidine, *Journal of Antimicrobial Chemotherapy*, **35**, 577-584.

Neal R. A., Allen S., McCoy N., Olliaro P. and Croft S. L., (1995), The sensitivity of *Leishmania* species to aminosidine, *J Antimicrob Chemother*, **35**, 577-584.

Nelson D., La Fon S. and Tuttle J., (1979), Al-lopurinol ribonucleoside as an anti*Leishmania*l agent, *Biol Chem J*, **254**, 11544-11549.

Neuber H., (2008), Leishmaniasis, *J Dtsch Dermatol Ges*, **6**, 754-765.

Newman D. J. and Cragg G. M., (2016), Natural Products as Sources of New Drugs from 1981 to 2014, *J Nat Prod*, **79**, 629-661.

No J. H., (2016), Visceral Leishmaniasis: Revisiting current treatments and approaches for future discoveries, *Acta tropica*, **155**, 113-123.

Noel G. J., (1999), Liposomal amphotericin B for empirical therapy in patients with persistent fever and neutropenia, *J Pediatr*, **135**, 399.

Nuhs A., De Rycker M., Manthri S., Comer E., Scherer C. A., Schreiber S. L., Ioset J. R. and Gray D. W., (2015), Development and Validation of a Novel *Leishmania* donovani Screening Cascade for High-Throughput Screening Using a Novel Axenic Assay with High Predictivity of Leishmanicidal Intracellular Activity, *PLoS Negl Trop Dis*, **9**, e0004094.

O'Brien J., Wilson I., Orton T. and Pognan F., (2000), Investigation of the Alamar Blue (resazurin) fluorescent dye for the assessment of mammalian cell cytotoxicity, *Eur J Biochem*, **267**, 5421-5426.

Okuno T., Goto Y., Matsumoto Y., Otsuka H. and Matsumoto Y., (2003), Applications of recombinant *Leishmania* amazonensis expressing egfp or the beta-galactosidase gene for drug screening and histopathological analysis, *Exp Anim*, **52**, 109-118.

Oryan, A., (2015), Plant-derived compounds in treatment of leishmaniasis. *Iran. J. Vet. Res.*, **16**, 1–19.

Osorio Y., Travi B. L., Renslo A. R., Peniche A. G. and Melby P. C., (2011), Identification of small molecule lead compounds for visceral Leishmaniasis

using a novel ex vivo splenic explant model system, *PLoS Negl Trop Dis*, **5**, e962.

Otigbuo I. N. and Onabanjo A. O., (1992), The in vitro and in vivo effects of mefloquine on Trypanosoma brucei brucei, *J Hyg Epidemiol Microbiol Immunol*, **36**, 191-199.

Ouellette M., Drummelsmith J. and Papadopoulou B., (2004), Leishmaniasis: drugs in the clinic, resistance and new developments, *Drug Resist Updat*, **7**, 257-266.

Ouellette M. and Ward S., (2002), *Drug resistance in parasites*Academic Press.

Paila Y. D., Saha B. and Chattopadhyay A., (2010), Amphotericin B inhibits entry of *Leishmania* donovani into primary macrophages, *Biochem Biophys Res Commun*, **399**, 429-433.

Pal D. S., Mondal D. K. and Datta R., (2015), Identification of metal dithiocarbamates as a novel class of anti*Leishmania*l agents, *Antimicrob Agents Chemother*, **59**, 2144-2152.

Pal S., Dolai S., Yadav R. K. and Adak S., (2010), Ascorbate peroxidase from *Leishmania* major controls the virulence of infective stage of promastigotes by regulating oxidative stress, *PloS one*, **5**, e11271.

Paloque L., Verhaeghe P., Casanova M., Castera-Ducros C., Dumètre A., Mbatchi L., Hutter S., Kraiem-M'Rabet M., Laget M. and Remusat V., (2012), Discovery of a new anti*Leishmania*l hit in 8-nitroquinoline series, *European journal of medicinal chemistry*, **54**, 75-86.

Pardo R. H., Santamaria E. and Cabrera O. L., (2017), Entering and exiting behaviour of the phlebotomine sand fly Lutzomyia longiflocosa (Diptera: Psychodidae) in rural houses of the sub-Andean region of Colombia, *Mem Inst Oswaldo Cruz*, **112**, 19-30.

Park E. K., Mak S. K., Kultz D. and Hammock B. D., (2007), Evaluation of cytotoxicity attributed to thimerosal on murine and human kidney cells, *J Toxicol Environ Health A*, **70**, 2092-2095.

Pathak M. K. and Yi T., (2001), Sodium stibogluconate is a potent inhibitor of protein tyrosine phosphatases and augments cytokine responses in hemopoietic cell lines, *J Immunol*, **167**, 3391-3397.

Pedrique B., Strub-Wourgaft N., Some C., Olliaro P., Trouiller P., Ford N., Pécoul B. and Bradol J.-H., (2013), The drug and vaccine landscape for neglected diseases (2000–11): a systematic assessment, *The Lancet Global Health*, **1**, e371-e379.

Pena I., Pilar Manzano M., Cantizani J., Kessler A., Alonso-Padilla J., Bardera A. I., Alvarez E., Colmenarejo G., Cotillo I., Roquero I., de Dios-Anton F., Barroso V., Rodriguez A., Gray D. W., Navarro M., Kumar V., Sherstnev A., Drewry D. H., Brown J. R., Fiandor J. M. and Julio Martin J., (2015), New compound sets identified from high throughput phenotypic screening against three kinetoplastid parasites: an open resource, *Scientific reports*, **5**, 8771.

Pereira C. A., (2014), Arginine kinase: a potential pharmacological target in trypanosomiasis, *Infectious disorders drug targets*, **14**, 30-36.

Pérez-Victoria, F. J., Gamarro, F., Ouellette, M. & Castanys, S., (2003), Functional cloning of the miltefosine transporter. A novel P-type phospholipid translocase from Leishmania involved in drug resistance. *J. Biol. Chem*. **278**, 49965–71

Pérez-Victoria F. J., Sánchez-Cañete M. P., Seifert K., Croft S. L., Sundar S., Castanys S. and Gamarro F., (2006), Mechanisms of experimental resistance of *Leishmania* to miltefosine: implications for clinical use, *Drug Resistance Updates*, **9**, 26-39.

Perry M., Wyllie S., Prajapati V., Menten J., Raab A., Feldmann J., Chakraborti D., Sundar S., Boelaert M., Picado A. and Fairlamb A., (2015), Arsenic, antimony, and *Leishmania*: has arsenic contamination of drinking water in India led to treatment- resistant kala-azar?, *Lancet*, **385 Suppl 1**, S80.

Perry M. R., Prajapati V. K., Menten J., Raab A., Feldmann J., Chakraborti D., Sundar S., Fairlamb A. H., Boelaert M. and Picado A., (2015), Arsenic exposure and outcomes of antimonial treatment in visceral Leishmaniasis patients in Bihar, India: a retrospective cohort study, *PLoS Negl Trop Dis*, **9**, e0003518.

Perry M. R., Wyllie S., Raab A., Feldmann J. and Fairlamb A. H., (2013), Chronic exposure to arsenic in drinking water can lead to resistance to antimonial drugs in a mouse model of visceral Leishmaniasis, *Proc Natl Acad Sci U S A*, **110**, 19932-19937.

Peruhype-Magalhães V., Martins-Filho O. d. A., Prata A., Silva D. A., Rabello A., Teixeira-Carvalho A., Figueiredo R. M., Guimarães-Carvalho S., Ferrari T. C. d. A. and Correa-Oliveira R., (2005), Immune response in human visceral Leishmaniasis: analysis of the correlation between innate immunity cytokine profile and disease outcome, *Scandinavian journal of immunology*, **62**, 487-495.

Pescher P., Blisnick T., Bastin P. and Spath G. F., (2011), Quantitative proteome profiling informs on phenotypic traits that adapt *Leishmania* donovani for axenic and intracellular proliferation, *Cellular microbiology*, **13**, 978-991.

Peters NC, Egen JG, Secundino N, Debrabant A, Kimblin N, Kamhawi S, Lawyer P., Fay M. P., Germain R. N. and Sacks D., (2008), In vivo imaging reveals an

essential role for neutrophils in leishmaniasis transmitted by sand flies. *Science*, **321**: 970–4.

Pham J. S., Dawson K. L., Jackson K. E., Lim E. E., Pasaje C. F., Turner K. E. and Ralph S. A., (2014), Aminoacyl-tRNA synthetases as drug targets in eukaryotic parasites, *International journal for parasitology. Drugs and drug resistance*, **4**, 1-13.

Pigott D. M., Bhatt S., Golding N., Duda K. A., Battle K. E., Brady O. J., Messina J. P., Balard Y., Bastien P., Pratlong F., Brownstein J. S., Freifeld C. C., Mekaru S. R., Gething P. W., George D. B., Myers M. F., Reithinger R. and Hay S. I., (2014), Global distribution maps of the *Leishmania*ses, *Elife*, **3**.

Pimenta P. F., Saraiva E. M., Rowton E., Modi G. B., Garraway L. A., Beverley S. M., Turco S. J. and Sacks D. L., (1994), Evidence that the vectorial competence of phlebotomine sand flies for different species of *Leishmania* is controlled by structural polymorphisms in the surface lipophosphoglycan, *Proc Natl Acad Sci U S A*, **91**, 9155-9159.

Pinheiro M. P., Emery Fda S. and Nonato M. C., (2013), Target sites for the design of anti-trypanosomatid drugs based on the structure of dihydroorotate dehydrogenase, *Current pharmaceutical design*, **19**, 2615-2627.

Pinto M. C., Campbell-Lendrum D. H., Lozovei A. L., Teodoro U. and Davies C. R., (2001), Phlebotomine sandfly responses to carbon dioxide and human odour in the field, *Med Vet Entomol*, **15**, 132-139.

Planer J. D., Hulverson M. A., Arif J. A., Ranade R. M., Don R. and Buckner F. S., (2014), Synergy testing of FDA-approved drugs identifies potent drug combinations against Trypanosoma cruzi, *PLoS Negl Trop Dis*, **8**, e2977.

Podinovskaia M. and Descoteaux A., (2015), *Leishmania* and the macrophage: a multifaceted interaction, *Future microbiology*, **10**, 111-129.

Pollmeier M. and Blair J. L., (2017), Method for treating and curing leishmaniosis using fexinidazole, *Journal*.

Porter A. G. and Jänicke R. U., (1999), Emerging roles of caspase-3 in apoptosis, *Cell death & differentiation*, **6**.

Prajapati V. K., Sharma S., Rai M., Ostyn B., Salotra P., Vanaerschot M., Dujardin J. C. and Sundar S., (2013), In vitro susceptibility of *Leishmania* donovani to miltefosine in Indian visceral Leishmaniasis, *The American journal of tropical medicine and hygiene*, **89**, 750-754.

Pral E. M., Bijovsky A. T., Balanco J. M. and Alfieri S. C., (1993), *Leishmania* mexicana: proteinase activities and megasomes in axenically cultivated amastigote-like forms, *Exp Parasitol*, **77**, 62-73.

Preston S., Jiao Y., Baell J. B., Keiser J., Crawford S., Koehler A. V., Wang T., Simpson M. M., Kaplan R. M., Cowley K. J., Simpson K. J., Hofmann A., Jabbar A. and Gasser R. B., (2017), Screening of the 'Open Scaffolds' collection from Compounds Australia identifies a new chemical entity with anthelmintic activities against different developmental stages of the barber's pole worm and other parasitic nematodes, *International journal for parasitology. Drugs and drug resistance*, **7**, 286-294.

Pulido S. A., Muñoz D. L., Restrepo A. M., Mesa C. V., Alzate J. F., Vélez I. D. and Robledo S. M., (2012), Improvement of the green fluorescent protein reporter system in *Leishmania* spp. for the in vitro and in vivo screening of anti*Leishmania*l drugs, *Acta tropica*, **122**, 36-45.

Purkait B., Kumar A., Nandi N., Sardar A. H., Das S., Kumar S., Pandey K., Ravidas V., Kumar M. and De T., (2012), Mechanism of amphotericin B resistance in clinical isolates of *Leishmania* donovani, *Antimicrobial agents and chemotherapy*, **56**, 1031-1041.

Purkait B., Kumar A., Nandi N., Sardar A. H., Das S., Kumar S., Pandey K., Ravidas V., Kumar M., De T., Singh D. and Das P., (2012), Mechanism of amphotericin B resistance in clinical isolates of *Leishmania* donovani, *Antimicrob Agents Chemother*, **56**, 1031-1041.

Quinnell R. J. and Courtenay O., (2009), Transmission, reservoir hosts and control of zoonotic visceral Leishmaniasis, *Parasitology*, **136**, 1915-1934.

Rajao M. A., Furtado C., Alves C. L., Passos-Silva D. G., de Moura M. B., Schamber-Reis B. L., Kunrath-Lima M., Zuma A. A., Vieira-da-Rocha J. P., Garcia J. B. F., Mendes I. C., Pena S. D. J., Macedo A. M., Franco G. R., de Souza-Pinto N. C., de Medeiros M. H. G., Cruz A. K., Motta M. C. M., Teixeira S. M. R. and Machado C. R., (2014), Unveiling benznidazole's mechanism of action through overexpression of DNA repair proteins in Trypanosoma cruzi, *Environ Mol Mutagen*, **55**, 309-321.

Rajasekaran R. and Chen Y.-P. P., (2015), Potential therapeutic targets and the role of technology in developing novel anti*Leishmania*l drugs, *Drug discovery today*, **20**, 958-968.

Rajasekaran R. and Chen Y. P., (2012), Probing the structure of *Leishmania* major DHFR TS and structure based virtual screening of peptide library for the identification of anti-*Leishmania*l leads, *J Mol Model*, **18**, 4089-4100.

Rajasekaran R. and Chen Y. P., (2015), Potential therapeutic targets and the role of technology in developing novel anti*Leishmania*l drugs, *Drug discovery today*, **20**, 958-968.

Ralton J. E., Mullin K. A. and McCONVILLE M. J., (2002), Intracellular trafficking of glycosylphosphatidylinositol (GPI)-anchored proteins and free GPIs in *Leishmania* mexicana, *Biochemical Journal*, **363**, 365-375.

Rama M., Kumar N. V. A. and Balaji S., (2015), A comprehensive review of patented anti*Leishmania*l agents.

Ramesh V., Singh R. and Salotra P., (2007), Short communication: post-kala-azar dermal Leishmaniasis--an appraisal, *Trop Med Int Health*, **12**, 848-851.

Rangel H., Dagger F., Hernandez A., Liendo A. and Urbina J. A., (1996), Naturally azole-resistant *Leishmania* braziliensis promastigotes are rendered susceptible in the presence of terbinafine: comparative study with azole-susceptible *Leishmania* mexicana promastigotes, *Antimicrob Agents Chemother*, **40**, 2785-2791.

Raz B., Iten M., Grether-Buhler Y., Kaminsky R. and Brun R., (1997), The Alamar Blue assay to determine drug sensitivity of African trypanosomes (T.b. rhodesiense and T.b. gambiense) in vitro, *Acta tropica*, **68**, 139-147.

Ready P. D., (2014), Epidemiology of visceral Leishmaniasis, *Clinical Epidemiology*, **6**, 147-154.

Reddy A. R. N., Reddy Y. N., Krishna D. R. and Himabindu V., (2010), Multi wall carbon nanotubes induce oxidative stress and cytotoxicity in human embryonic kidney (HEK293) cells, *Toxicology*, **272**, 11-16.

Reguera R. M., Calvo-Álvarez E., Álvarez-Velilla R. and Balaña-Fouce R., (2014), Target-based vs. phenotypic screenings in *Leishmania* drug discovery: A marriage of convenience or a dialogue of the deaf?, *International Journal for Parasitology: Drugs and Drug Resistance*, **4**, 355-357.

Reithinger R., Coleman P. G., Alexander B., Vieira E. P., Assis G. and Davies C. R., (2004), Are insecticide-impregnated dog collars a feasible alternative to dog culling as a strategy for controlling canine visceral Leishmaniasis in Brazil?, *International journal for parasitology*, **34**, 55-62.

Reithinger R., Mohsen M. and Leslie T., (2010), Risk factors for anthroponotic cutaneous Leishmaniasis at the household level in Kabul, Afghanistan, *PLoS neglected tropical diseases*, **4**, e639.

Revollo S., Oury B., Laurent J. P., Barnabe C., Quesney V., Carriere V., Noel S. and Tibayrenc M., (1998), Trypanosoma cruzi: impact of clonal evolution of the parasite on its biological and medical properties, *Exp Parasitol*, **89**, 30-39.

Ribeiro-Gomes FL, Sacks D., (2012) The influence of early neutrophil-Leishmania interactions on the host immune response to infection. *Front Cell Infect Microbiol.*; **2**: 59.

Riedl S. J. and Shi Y., (2004), Molecular mechanisms of caspase regulation during apoptosis, *Nature reviews. Molecular cell biology*, **5**, 897-907.

Rijal S., Bhandari S., Koirala S., Singh R., Khanal B., Loutan L., Dujardin J. C., Boelaert M. and Chappuis F., (2010), Clinical risk factors for therapeutic failure in kala-azar patients treated with pentavalent antimonials in Nepal, *Trans R Soc Trop Med Hyg*, **104**, 225-229.

Rioux J.A., Lanotte G., Serres E., Pratlong F., Bastien P., Perieres J., (1990), Taxonomy of Leishmania. Use of isoenzymes. Suggestions for a new classification, *Ann Parasitol Hum Comp*, **65**, 111-125.

Ritter U., Frischknecht F. and van Zandbergen G., (2009), Are neutrophils important host cells for *Leishmania* parasites?, *Trends Parasitol*, **25**, 505-510.

Roberts C., McLeod R., Rice D., Ginger M., Chance M. L. and Goad L. J., (2003), Fatty acid and sterol metabolism: potential antimicrobial targets in apicomplexan and trypanosomatid parasitic protozoa, *Molecular and biochemical parasitology*, **126**, 129-142.

Roberts C. W., McLeod R., Rice D. W., Ginger M., Chance M. L. and Goad L. J., (2003), Fatty acid and sterol metabolism: potential antimicrobial targets in apicomplexan and trypanosomatid parasitic protozoa, *Mol Biochem Parasitol*, **126**, 129-142.

Roberts M. T., (2005), Current understandings on the immunology of Leishmaniasis and recent developments in prevention and treatment, *British medical bulletin*, **75-76**, 115-130.

Rocha M. N., Correa C. M., Melo M. N., Beverley S. M., Martins-Filho O. A., Madureira A. P. and Soares R. P., (2013), An alternative in vitro drug screening test using *Leishmania* amazonensis transfected with red fluorescent protein, *Diagn Microbiol Infect Dis*, **75**, 282-291.

Rocha V. P. C., Nonato F. R., Guimarães E. T., de Freitas L. A. n. R. and Soares M. B. P., (2013), Activity of antimalarial drugs in vitro and in a murine model of cutaneous Leishmaniasis, *Journal of medical microbiology*, **62**, 1001-1010.

Rodgers M. R., Popper S. J. and Wirth D. F., (1990), Amplification of kinetoplast DNA as a tool in the detection and diagnosis of *Leishmania*, *Experimental parasitology*, **71**, 267-275.

Rodrigues V, Cordeiro-da-Silva A, Laforge M, Silvestre R, Estaquier J., (2016). Regulation of immunity during visceral *Leishmania* infection. *Parasit Vectors* **9**,118.

Rodriguez-Navarro A. and Benito B., (2010), Sodium or potassium efflux ATPase a fungal, bryophyte, and protozoal ATPase, *Biochim Biophys Acta*, **1798**, 1841-1853.

Rogers M. E., (2012), The role of *Leishmania* proteophosphoglycans in sand fly transmission and infection of the mammalian host, *Frontiers in microbiology*, **3**.

Rogers M. E., Chance M. L. and Bates P. A., (2002), The role of promastigote secretory gel in the origin and transmission of the infective stage of *Leishmania* mexicana by the sandfly Lutzomyia longipalpis, *Parasitology*, **124**, 495-507.

Rosenkranz V. and Wink M., (2008), Alkaloids induce programmed cell death in bloodstream forms of trypanosomes (Trypanosoma b. brucei), *Molecules*, **13**, 2462-2473.

Rouault E., Lecoeur H., Meriem A. B., Minoprio P., Goyard S. and Lang T., (2017), Imaging visceral Leishmaniasis in real time with golden hamster model: Monitoring the parasite burden and hamster transcripts to further characterize the immunological responses of the host, *Parasitology international*, **66**, 933-939.

Rougeron V., De Meeus T., Hide M., Waleckx E., Bermudez H., Arevalo J., Llanos-Cuentas A., Dujardin J. C., De Doncker S., Le Ray D., Ayala F. J. and Banuls A. L., (2009), Extreme inbreeding in *Leishmania* braziliensis, *Proc Natl Acad Sci U S A*, **106**, 10224-10229.

Roy G., Dumas C., Sereno D., Wu Y., Singh A. K., Tremblay M. J., Ouellette M., Olivier M. and Papadopoulou B., (2000), Episomal and stable expression of the luciferase reporter gene for quantifying *Leishmania* spp. infections in macrophages and in animal models, *Mol Biochem Parasitol*, **110**, 195-206.

Sacks D. and Kamhawi S., (2001), Molecular aspects of parasite-vector and vector-host interactions in Leishmaniasis, *Annual review of microbiology*, **55**, 453-483.

Sacks D. L. and Melby P. C., (2015), Animal models for the analysis of immune responses to Leishmaniasis, *Current protocols in immunology*, **108**, 19 12 11-24.

Sacks D. L. and Perkins P. V., (1984), Identification of an infective state of *Leishmania* promastigotes, *Science*, **223**, 1417-1420.

Sahu S. C., Zheng J., Graham L., Chen L., Ihrie J., Yourick J. J. and Sprando R. L., (2014), Comparative cytotoxicity of nanosilver in human liver HepG2 and colon Caco2 cells in culture, *Journal of Applied Toxicology*, **34**, 1155-1166.

Sakthianandeswaren A, Elso CM, Simpson K, Curtis JM, Kumar B, Speed TP, Handman E, Foote SJ., (2005). The wound repair response controls outcome to cutaneous leishmaniasis. *Proc Natl Acad Sci U S A* **102**,15551-6.

Salem M. M. and Werbovetz K. A., (2005), Antiprotozoal compounds from Psorothamnus polydenius, *J Nat Prod*, **68**, 108-111.

Salih M. A., Fakiola M., Abdelraheem M. H., Younis B. M., Musa A. M., ElHassan A. M., Blackwell J. M., Ibrahim M. E. and Mohamed H. S., (2014), Insights into the possible role of IFNG and IFNGR1 in Kala-azar and Post Kala-azar Dermal Leishmaniasis in Sudanese patients, *BMC Infect Dis*, **14**, 662.

Salih M. A., Ibrahim M. E., Blackwell J. M., Miller E. N., Khalil E. A., ElHassan A. M., Musa A. M. and Mohamed H. S., (2007), IFNG and IFNGR1 gene polymorphisms and susceptibility to post-kala-azar dermal Leishmaniasis in Sudan, *Genes Immun*, **8**, 75-78.

Salotra P., Kaushal H. and Ramesh V., (2016), in *Kala Azar in South Asia*Springer, pp. 7-21.

Sangshetti J. N., Khan F. A. K., Kulkarni A. A., Arote R. and Patil R. H., (2015), Anti*Leishmania*l drug discovery: comprehensive review of the last 10 years, *Rsc Advances*, **5**, 32376-32415.

Saudagar P. and Dubey V. K., (2011), Cloning, expression, characterization and inhibition studies on trypanothione synthetase, a drug target enzyme, from *Leishmania* donovani, *Biol Chem*, **392**, 1113-1122.

Saunders E. C., Ng W. W., Kloehn J., Chambers J. M., Ng M. and McConville M. J., (2014), Induction of a stringent metabolic response in intracellular stages of *Leishmania* mexicana leads to increased dependence on mitochondrial metabolism, *PLoS Pathog*, **10**, e1003888.

Savoia D., (2015), Recent updates and perspectives on Leishmaniasis, *The Journal of Infection in Developing Countries*, **9**, 588-596.

Savoia D., (2015), Recent updates and perspectives on Leishmaniasis, *J Infect Dev Ctries*, **9**, 588-596.

Scheuer P. J., (2013), *Marine natural products: chemical and biological perspectives*Academic Press.

Schirle M. and Jenkins J. L., (2016), Identifying compound efficacy targets in phenotypic drug discovery, *Drug discovery today*, **21**, 82-89.

Schroder J., Noack S., Marhofer R. J., Mottram J. C., Coombs G. H. and Selzer P. M., (2013), Identification of semicarbazones, thiosemicarbazones and triazine nitriles as inhibitors of *Leishmania* mexicana cysteine protease CPB, *PLoS One*, **8**, e77460.

Schwartz B. D., Coster M. J., Skinner-Adams T. S., Andrews K. T., White J. M. and Davis R. A., (2015), Synthesis and Antiplasmodial Evaluation of Analogues Based on the Tricyclic Core of Thiaplakortones A-D, *Mar Drugs*, **13**, 5784-5795.

Schwartz B. D., Skinner-Adams T. S., Andrews K. T., Coster M. J., Edstein M. D., MacKenzie D., Charman S. A., Koltun M., Blundell S., Campbell A., Pouwer R. H., Quinn R. J., Beattie K. D., Healy P. C. and Davis R. A., (2015), Synthesis and antimalarial evaluation of amide and urea derivatives based on the thiaplakortone A natural product scaffold, *Org Biomol Chem*, **13**, 1558-1570.

Scott P, Novais FO., (2016). Cutaneous leishmaniasis: immune responses in protection and pathogenesis. *Nat Rev Immunol* **16**,581-92.

Seethala R. and Zhang L., (2016), *Handbook of drug screening*CRC Press.

Seifert K., Escobar P. and Croft S. L., (2010), In vitro activity of anti-*Leishmania*l drugs against *Leishmania* donovani is host cell dependent, *J Antimicrob Chemother*, **65**, 508-511.

Seifert K., Matu S., Javier Perez-Victoria F., Castanys S., Gamarro F. and Croft S. L., (2003), Characterisation of *Leishmania* donovani promastigotes resistant to hexadecylphosphocholine (miltefosine), *Int J Antimicrob Agents*, **22**, 380-387.

Semini G. and Aebischer T., (2017), Phagosome proteomics to study *Leishmania*'s intracellular niche in macrophages, *International journal of medical microbiology : IJMM*.

Sen N., Das B., Ganguly A., Mukherjee T., Tripathi G., Bandyopadhyay S., Rakshit S., Sen T. and Majumder H., (2004), Camptothecin induced mitochondrial dysfunction leading to programmed cell death in unicellular hemoflagellate *Leishmania* donovani, *Cell death and differentiation*, **11**, 924.

Sereno D., Da Silva A. C., Mathieu-Daude F. and Ouaissi A., (2007), Advances and perspectives in *Leishmania* cell based drug-screening procedures, *Parasitology international*, **56**, 3-7.

Sereno D. and Lemesre J. L., (1997), Axenically cultured amastigote forms as an in vitro model for investigation of anti*Leishmania*l agents, *Antimicrob Agents Chemother*, **41**, 972-976.

Shahian M. and Alborzi A., (2009), Effect of meglumine antimoniate on the pancreas during treatment of visceral Leishmaniasis in children, *Med Sci Monit*, **15**, CR290-293.

Sharma M. and Chauhan P. M., (2012), Dihydrofolate reductase as a therapeutic target for infectious diseases: opportunities and challenges, *Future Med Chem*, **4**, 1335-1365.

Sharma R., Pandey A. K., Shivahare R., Srivastava K., Gupta S. and Chauhan P. M., (2014), Triazino indole–quinoline hybrid: A novel approach to anti*Leishmania*l agents, *Bioorganic & medicinal chemistry letters*, **24**, 298-301.

Showler A. J. and Boggild A. K., (2015), Cutaneous Leishmaniasis in travellers: a focus on epidemiology and treatment in 2015, *Curr Infect Dis Rep*, **17**, 489.

Silva J. R., Ramos Ade S., Machado M., de Moura D. F., Neto Z., Canto-Cavalheiro M. M., Figueiredo P., do Rosario V. E., Amaral A. C. and Lopes D., (2011), A review of antimalarial plants used in traditional medicine in communities in Portuguese-speaking countries: Brazil, Mozambique, Cape Verde, Guinea-Bissau, Sao Tome and Principe and Angola, *Mem Inst Oswaldo Cruz*, **106 Suppl 1**, 142-158.

Simonsen P., Cook G. and Zumla A., (2009), Manson's tropical diseases.

Sindermann H. and Engel J., (2006), Development of miltefosine as an oral treatment for Leishmaniasis, *Transactions of the Royal Society of Tropical Medicine and Hygiene*, **100**, S17-S20.

Sinderson, HC., (1924), Emetine hydrochloride in the treatment of oriental sore, *Trans Soc Trop Med Hyg*., **18**:108–110.

Singh N., Gupta R., Jaiswal A. K., Sundar S. and Dube A., (2009), Transgenic *Leishmania* donovani clinical isolates expressing green fluorescent protein constitutively for rapid and reliable ex vivo drug screening, *The Journal of antimicrobial chemotherapy*, **64**, 370-374.

Singh N., Mishra B. B., Bajpai S., Singh R. K. and Tiwari V. K., (2014), Natural product based leads to fight against Leishmaniasis, *Bioorganic & medicinal chemistry*, **22**, 18-45.

Singh O. P., Gidwani K., Kumar R., Nylen S., Jones S. L., Boelaert M., Sacks D. and Sundar S., (2012), Reassessment of immune correlates in human visceral

Leishmaniasis as defined by cytokine release in whole blood, *Clin Vaccine Immunol*, **19**, 961-966.

Singh O. P., Singh B., Chakravarty J. and Sundar S., (2016), Current challenges in treatment options for visceral Leishmaniasis in India: a public health perspective, *Infect Dis Poverty*, **5**, 19.

Singh P. S. and Kumar M., (2017), Current treatment of visceral Leishmaniasis (Kala-azar): an overview, *International Journal of Research in Medical Sciences*, **2**, 810-817.

Sinha P. K. and Bhattacharya S., (2014), Single-dose liposomal amphotericin B: an effective treatment for visceral Leishmaniasis, *Lancet Glob Health*, **2**, e7-8.

Sinha P. K., Jha T. K., Thakur C. P., Nath D., Mukherjee S., Aditya A. K. and Sundar S., (2011), Phase 4 pharmacovigilance trial of paromomycin injection for the treatment of visceral Leishmaniasis in India, *J Trop Med*, **2011**, 645203.

Siqueira-Neto J. L., Moon S., Jang J., Yang G., Lee C., Moon H. K., Chatelain E., Genovesio A., Cechetto J. and Freitas-Junior L. H., (2012), An image-based high-content screening assay for compounds targeting intracellular *Leishmania* donovani amastigotes in human macrophages, *PLoS Negl Trop Dis*, **6**, e1671.

Siqueira-Neto J. L., Song O. R., Oh H., Sohn J. H., Yang G., Nam J., Jang J., Cechetto J., Lee C. B., Moon S., Genovesio A., Chatelain E., Christophe T. and Freitas-Junior L. H., (2010), Anti*Leishmania*l high-throughput drug screening reveals drug candidates with new scaffolds, *PLoS Negl Trop Dis*, **4**, e675.

Sirenko O., Mitlo T., Hesley J., Luke S., Owens W. and Cromwell E. F., (2015), High-content assays for characterizing the viability and morphology of 3D cancer spheroid cultures, *Assay Drug Dev Technol*, **13**, 402-414.

Slater A. F., (1993), Chloroquine: mechanism of drug action and resistance in Plasmodium falciparum, *Pharmacology & therapeutics*, **57**, 203-235.

Somanna A., Mundodi V. and Gedamu L., (2002), In vitro cultivation and characterization of *Leishmania* chagasi amastigote-like forms, *Acta Tropica*, **83**, 37-42.

Soto, J., Arana, B. A., Toledo, J., Rizzo, N., Vega, J. C., Diaz, A., Sindermann, H., (2004), Miltefosine for new world cutaneous leishmaniasis, *Clinical Infectious Diseases : An Official Publication of the Infectious Diseases Society of America*, **38**, 1266–72.

Soto, J., Rea, J., Balderrama, M., Toledo, J., Soto, P., Valda, L., & Berman, J. D., (2008), Efficacy of miltefosine for Bolivian cutaneous leishmaniasis, *The American Journal of Tropical Medicine and Hygiene,* **78**, 210–1

Souza T. D., Turchetti A. P., Fujiwara R. T., Paixão T. A. and Santos R. L., (2014), Visceral Leishmaniasis in zoo and wildlife, *Veterinary parasitology*, **200**, 233-241.

Spath GF, Beverley SM. 2001. A lipophosphoglycan-independent method for isolation of infective Leishmania metacyclic promastigotes by density gradient centrifugation. Exp Parasitol 99:97-103.

Srivastava P., Gidwani K., Picado A., Van der Auwera G., Tiwary P., Ostyn B., Dujardin J. C., Boelaert M. and Sundar S., (2013), Molecular and serological markers of *Leishmania* donovani infection in healthy individuals from endemic areas of Bihar, India, *Trop Med Int Health*, **18**, 548-554.

Stanley A. C. and Engwerda C. R., (2007), Balancing immunity and pathology in visceral Leishmaniasis, *Immunol Cell Biol*, **85**, 138-147.

Stiles J. K., Kucerova Z., Sarfo B., Meade C. A., Thompson W., Shah P., Xue L. and Meade J. C., (2003), Identification of surface-membrane P-type ATPases resembling fungal K(+)- and Na(+)-ATPases, in Trypanosoma brucei, Trypanosoma cruzi and *Leishmania* donovani, *Ann Trop Med Parasitol*, **97**, 351-366.

Stockdale L. and Newton R., (2013), A review of preventative methods against human Leishmaniasis infection, *PLoS neglected tropical diseases*, **7**, e2278.

Stuart K., Brun R., Croft S., Fairlamb A., Gurtler R. E., McKerrow J., Reed S. and Tarleton R., (2008), Kinetoplastids: related protozoan pathogens, different diseases, *J Clin Invest*, **118**, 1301-1310.

Stuart K., Brun R., Croft S., Fairlamb A., Gürtler R. E., McKerrow J., Reed S. and Tarleton R., (2008), Kinetoplastids: related protozoan pathogens, different diseases, *The Journal of clinical investigation*, **118**, 1301.

Subramanian A, Sarkar RR., (2017), Revealing the mystery of metabolic adaptations using a genome scale model of *Leishmania infantum*. *Sci Rep* **7**,10262.

Sudhandiran G. and Shaha C., (2003), Antimonial-induced increase in intracellular Ca2+ through non-selective cation channels in the host and the parasite is responsible for apoptosis of intracellular *Leishmania* donovani amastigotes, *Journal of Biological Chemistry*, **278**, 25120-25132.

Suganuma K., Sarwono A. E., Mitsuhashi S., Jakalski M., Okada T., Nthatisi M., Yamagishi J., Ubukata M. and Inoue N., (2016), Mycophenolic Acid and Its Derivatives as Potential Chemotherapeutic Agents Targeting Inosine Monophosphate Dehydrogenase in Trypanosoma congolense, *Antimicrob Agents Chemother*, **60**, 4391-4393.

Sullivan W. J., Dixon S. E., Li C., Striepen B. and Queener S. F., (2005), IMP dehydrogenase from the protozoan parasite Toxoplasma gondii, *Antimicrobial agents and chemotherapy*, **49**, 2172-2179.

Sundar S., (2001), Drug resistance in Indian visceral Leishmaniasis, *Trop Med Int Health*, **6**, 849-854.

Sundar S. and Chakravarty J., (2013), Leishmaniasis: an update of current pharmacotherapy, *Expert Opin Pharmacother*, **14**, 53-63.

Sundar S. and Chakravarty J., (2015), An update on pharmacotherapy for Leishmaniasis, *Expert opinion on pharmacotherapy*, **16**, 237-252.

Sundar S. and Goyal N., (2007), Molecular mechanisms of antimony resistance in *Leishmania*, *Journal of Medical Microbiology*, **56**, 143-153.

Sundar S., Jha T. K., Thakur C. P., Mishra M., Singh V. P. and Buffels R., (2003), Single-dose liposomal amphotericin B in the treatment of visceral Leishmaniasis in India: a multicenter study, *Clin Infect Dis*, **37**, 800-804.

Sundar S., Jha T. K., Thakur C. P., Sinha P. K. and Bhattacharya S. K., (2007), Injectable paromomycin for Visceral Leishmaniasis in India, *N Engl J Med*, **356**, 2571-2581.

Sundar S., More D. K., Singh M. K., Singh V. P., Sharma S., Makharia A., Kumar P. C. and Murray H. W., (2000), Failure of pentavalent antimony in visceral Leishmaniasis in India: report from the center of the Indian epidemic, *Clin Infect Dis*, **31**, 1104-1107.

Sundar S. and Olliaro P. L., (2007), Miltefosine in the treatment of Leishmaniasis: Clinical evidence for informed clinical risk management, *Ther Clin Risk Manag*, **3**, 733-740.

Sundar S., Pandey K., Thakur C. P., Jha T. K., Das V. N., Verma N., Lal C. S., Verma D., Alam S. and Das P., (2014), Efficacy and safety of amphotericin B emulsion versus liposomal formulation in Indian patients with visceral Leishmaniasis: a randomized, open-label study, *PLoS Negl Trop Dis*, **8**, e3169.

Sundar S. and Rai M., (2005), Treatment of visceral Leishmaniasis, *Expert Opin Pharmacother*, **6**, 2821-2829.

Sundar S., Rai M., Chakravarty J., Agarwal D., Agrawal N., Vaillant M., Olliaro P. and Murray H. W., (2008), New treatment approach in Indian visceral Leishmaniasis: single-dose liposomal amphotericin B followed by short-course oral miltefosine, *Clin Infect Dis*, **47**, 1000-1006.

Sundar S. and Singh A., (2016), Recent developments and future prospects in the treatment of visceral Leishmaniasis, *Therapeutic advances in infectious disease*, **3**, 98-109.

Sundar S., Singh A., Agarwal D., Rai M., Agrawal N. and Chakravarty J., (2009), Safety and efficacy of high-dose infusions of a preformed amphotericin B fat emulsion for treatment of Indian visceral Leishmaniasis, *Am J Trop Med Hyg*, **80**, 700-703.

Sundar S., Singh A., Chakravarty J. and Rai M., (2015), Efficacy and safety of miltefosine in treatment of post-kala-azar dermal Leishmaniasis, *The Scientific World Journal*, **2015**.

Sundar S., Singh A., Rai M., Prajapati V. K., Singh A. K., Ostyn B., Boelaert M., Dujardin J. C. and Chakravarty J., (2012), Efficacy of miltefosine in the treatment of visceral Leishmaniasis in India after a decade of use, *Clin Infect Dis*, **55**, 543-550.

Sundar S., Sinha P., Jha T. K., Chakravarty J., Rai M., Kumar N., Pandey K., Narain M. K., Verma N., Das V. N., Das P., Berman J. and Arana B., (2013), Oral miltefosine for Indian post-kala-azar dermal Leishmaniasis: a randomised trial, *Trop Med Int Health*, **18**, 96-100.

Sundar S., Sinha P. K., Rai M., Verma D. K., Nawin K., Alam S., Chakravarty J., Vaillant M., Verma N., Pandey K., Kumari P., Lal C. S., Arora R., Sharma B., Ellis S., Strub-Wourgaft N., Balasegaram M., Olliaro P., Das P. and Modabber F., (2011), Comparison of short-course multidrug treatment with standard therapy for visceral Leishmaniasis in India: an open-label, non-inferiority, randomised controlled trial, *Lancet*, **377**, 477-486.

Svárovská A., Ant T. H., Seblová V., Jecná L., Beverley S. M. and Volf P., (2010), *Leishmania* major glycosylation mutants require phosphoglycans (lpg2−) but not lipophosphoglycan (lpg1−) for survival in permissive sand fly vectors, *PLoS neglected tropical diseases*, **4**, e580.

Swinney D. C. and Anthony J., (2011), How were new medicines discovered?, *Nat Rev Drug Discov*, **10**, 507-519.

Sykes M. L. and Avery V. M., (2009), Development of an Alamar Blue viability assay in 384-well format for high throughput whole cell screening of Trypanosoma brucei brucei bloodstream form strain 427, *The American journal of tropical medicine and hygiene*, **81**, 665-674.

Sykes M. L. and Avery V. M., (2015), Development and application of a sensitive, phenotypic, high-throughput image-based assay to identify compound activity against Trypanosoma cruzi amastigotes, *Int J Parasitol Drugs Drug Resist*, **5**, 215-228.

Sykes M. L., Baell J. B., Kaiser M., Chatelain E., Moawad S. R., Ganame D., Ioset J. R. and Avery V. M., (2012), Identification of compounds with anti-proliferative activity against Trypanosoma brucei brucei strain 427 by a whole cell viability based HTS campaign, *PLoS Negl Trop Dis*, **6**, e1896.

Tegazzini D., Cantizani J., Peña I., Martín J. and Coterón J. M., (2017), Unravelling the rate of action of hits in the *Leishmania* donovani box using standard drugs amphotericin B and miltefosine, *PLOS Neglected Tropical Diseases*, **11**, e0005629.

Tegazzini D., Diaz R., Aguilar F., Pena I., Presa J. L., Yardley V., Martin J. J., Coteron J. M., Croft S. L. and Cantizani J., (2016), A replicative in vitro assay for drug discovery against *Leishmania* donovani, *Antimicrob Agents Chemother*.

Thakur C. P., Sinha G. P., Pandey A. K., Kumar N., Kumar P., Hassan S. M., Narain S. and Roy R. K., (1998), Do the diminishing efficacy and increasing toxicity of sodium stibogluconate in the treatment of visceral Leishmaniasis in Bihar, India, justify its continued use as a first-line drug? An observational study of 80 cases, *Ann Trop Med Parasitol*, **92**, 561-569.

Thalhofer C. J., Graff J. W., Love-Homan L., Hickerson S. M., Craft N., Beverley S. M. and Wilson M. E., (2010), In vivo imaging of transgenic *Leishmania* parasites in a live host, *Journal of visualized experiments : JoVE*.

Tibayrenc M., Ben Abderrazak S., Guerrini F. and Banuls A., (1993), *Leishmania* and the clonal theory of parasitic protozoa, *Arch Inst Pasteur Tunis*, **70**, 375-382.

Tiuman T. S., Santos A. O., Ueda-Nakamura T., Filho B. P. and Nakamura C. V., (2011), Recent advances in Leishmaniasis treatment, *Int J Infect Dis*, **15**, e525-532.

Torrie L. S., Brand S., Robinson D. A., Ko E. J., Stojanovski L., Simeons F. R. C., Wyllie S., Thomas J., Ellis L., Osuna-Cabello M., Epemolu O., Nuhs A., Riley J., MacLean L., Manthri S., Read K. D., Gilbert I. H., Fairlamb A. H. and De Rycker M., (2017), Chemical Validation of Methionyl-tRNA Synthetase as a Druggable Target in *Leishmania* donovani, *ACS infectious diseases*, **3**, 718-727.

Traore K., Trush M. A., George M., Jr., Spannhake E. W., Anderson W. and Asseffa A., (2005), Signal transduction of phorbol 12-myristate 13-acetate (PMA)-induced growth inhibition of human monocytic leukemia THP-1 cells is reactive oxygen dependent, *Leuk Res*, **29**, 863-879.

Tripathy N., Hong T.-K., Ha K.-T., Jeong H.-S. and Hahn Y.-B., (2014), Effect of ZnO nanoparticles aggregation on the toxicity in RAW 264.7 murine macrophage, *Journal of hazardous materials*, **270**, 110-117.

Tsuchiya S., Kobayashi Y., Goto Y., Okumura H., Nakae S., Konno T. and Tada K., (1982), Induction of maturation in cultured human monocytic leukemia cells by a phorbol diester, *Cancer Res*, **42**, 1530-1536.

Tsuchiya S., Yamabe M., Yamaguchi Y., Kobayashi Y., Konno T. and Tada K., (1980), Establishment and characterization of a human acute monocytic leukemia cell line (THP-1), *Int J Cancer*, **26**, 171-176.

Turk, J. L., & Bryceson, A. D., (1971), Immunological phenomena in leprosy and related diseases, *Advances in Immunology*, **13**, 209–66.

Turco S. J., Späth G. F. and Beverley S. M., (2001), Is lipophosphoglycan a virulence factor? A surprising diversity between *Leishmania* species, *Trends in parasitology*, **17**, 223-226.

Vacchina P. and Morales M. A., (2014), In vitro screening test using *Leishmania* promastigotes stably expressing mCherry protein, *Antimicrobial agents and chemotherapy*, **58**, 1825-1828.

Valdés, A. F.-C., (2011), Acridine and acridinones: old and new structures with antimalarial activity, *The Open Medicinal Chemistry Journal*, **5**, 11–20.

van den Berg H., (2009), Global status of DDT and its alternatives for use in vector control to prevent disease, *Environmental health perspectives*, **117**, 1656-1663.

van den Bogaart E., Schoone G. J., England P., Faber D., Orrling K. M., Dujardin J. C., Sundar S., Schallig H. D. and Adams E. R., (2014), Simple colorimetric trypanothione reductase-based assay for high-throughput screening of drugs against *Leishmania* intracellular amastigotes, *Antimicrob Agents Chemother*, **58**, 527-535.

van Zandbergen G., Solbach W. and Laskay T., (2007), Apoptosis driven infection: Minireview, *Autoimmunity*, **40**, 349-352.

Vargas-Inchaustegui D. A., Hogg A. E., Tulliano G., Llanos-Cuentas A., Arevalo J., Endsley J. J. and Soong L., (2010), CXCL10 production by human monocytes in response to *Leishmania* braziliensis infection, *Infection and immunity*, **78**, 301-308.

Vargas-Inchaustegui D. A., Hogg A. E., Tulliano G., Llanos-Cuentas A., Arevalo J., Endsley J. J. and Soong L., (2010), CXCL10 production by human monocytes in response to *Leishmania* braziliensis infection, *Infect Immun*, **78**, 301-308.

Vercesi A. E., Rodrigues C. O., Catisti R. and Docampo R., (2000), Presence of a Na(+)/H(+) exchanger in acidocalcisomes of *Leishmania* donovani and their alkalization by anti-*Leishmania*l drugs, *FEBS Lett*, **473**, 203-206.

Vincent F., Loria P., Pregel M., Stanton R., Kitching L., Nocka K., Doyonnas R., Steppan C., Gilbert A. and Schroeter T., (2015), Developing predictive assays: the phenotypic screening "rule of 3", *Science translational medicine*, **7**, 293ps215-293ps215.

Vogel H. G. and Vogel W. H., (2013), *Drug discovery and evaluation: pharmacological assays*Springer Science & Business Media.

Volf P. and Myskova J., (2007), Sand flies and *Leishmania*: specific versus permissive vectors, *Trends in parasitology*, **23**, 91-92.

Volf P., Nogueira P. M., Myskova J., Turco S. J. and Soares R. P., (2014), Structural comparison of lipophosphoglycan from *Leishmania* turanica and L. major, two species transmitted by Phlebotomus papatasi, *Parasitology international*, **63**, 683-686.

Von Stebut E., (2015), Leishmaniasis, *J Dtsch Dermatol Ges*, **13**, 191-200; quiz 201.

Wan H., (2013), What ADME tests should be conducted for preclinical studies?, *ADMET and DMPK*, **1**, 19-28.

Wasunna M. K., Rashid J. R., Mbui J., Kirigi G., Kinoti D., Lodenyo H., Felton J. M., Sabin A. J., Albert M. J. and Horton J., (2005), A phase II dose-increasing study of sitamaquine for the treatment of visceral Leishmaniasis in Kenya, *Am J Trop Med Hyg*, **73**, 871-876.

Wheeler R. J., Gluenz E. and Gull K., (2011), The cell cycle of *Leishmania*: morphogenetic events and their implications for parasite biology, *Molecular microbiology*, **79**, 647-662.

WHO, (1990), Control of the *Leishmania*ses. Report of a WHO Expert Committee, *World Health Organ Tech Rep Ser*, **793**, 1-158.

WHO, (2010), Control of the *Leishmania*ses: report of a meeting of the WHO Expert Commitee on the Control of *Leishmania*ses, Geneva, 22-26 March 2010.

WHO, (2010), World Health Organization. Global Health Estimates (GHE). Available at: http://www.who.int/healthinfo/global_burden_disease/en/.

WHO, (2014), World Health Organization. Vector-borne disease. Available at: http://www.who.int/kobe_centre/mediacentre/vbdfactsheet.pdf.

WHO, (2015), World Health Organization, Leishmaniasis fact sheet. Available at: http://www.who.int/mediacentre/factsheets/fs375/en/

WHO, (2016), Leishmaniasis in high-burden countries: an epidemiological update based on data reported in 2014, *Wkly Epidemiol Rec*, **91**, 287-296.

Wilson A. L., Dhiman R. C., Kitron U., Scott T. W., van den Berg H. and Lindsay S. W., (2014), Benefit of insecticide-treated nets, curtains and screening on vector borne diseases, excluding malaria: a systematic review and meta-analysis, *PLoS neglected tropical diseases*, **8**, e3228.

Wingard J. R., Kubilis P., Lee L., Yee G., White M., Walshe L., Bowden R., Anaissie E., Hiemenz J. and Lister J., (1999), Clinical significance of nephrotoxicity in patients treated with amphotericin B for suspected or proven aspergillosis, *Clin Infect Dis*, **29**, 1402-1407.

Wu X., Cao S., Goh S., Hsu A. and Tan B. K., (2002), Mitochondrial destabilisation and caspase-3 activation are involved in the apoptosis of Jurkat cells induced by gaudichaudione A, a cytotoxic xanthone, *Planta medica*, **68**, 198-203.

Wyllie S., Patterson S., Stojanovski L., Simeons F. R., Norval S., Kime R., Read K. D. and Fairlamb A. H., (2012), The anti-trypanosome drug fexinidazole shows potential for treating visceral Leishmaniasis, *Science translational medicine*, **4**, 119re111.

Xu Z. B., Le Blancq S., Evans D. A. and Peters W., (1984), The characterization by isoenzyme electrophoresis of *Leishmania* isolated in the People's Republic of China, *Trans R Soc Trop Med Hyg*, **78**, 689-693.

Yamaori S., Ishii H., Chiba K., Yamamoto I. and Watanabe K., (2013), Δ 8-Tetrahydrocannabinol induces cytotoxicity in macrophage J774-1 cells: Involvement of cannabinoid receptor 2 and p38 MAPK, *Toxicology*, **314**, 254-261.

Yamazaki H., (2014), Drug-induced liver toxicity studies: research into human metabolites clarifies their role in drug development, *Drug metabolism and pharmacokinetics*, **29**, 111-111.

Yang X., Davis R. A., Buchanan M. S., Duffy S., Avery V. M., Camp D. and Quinn R. J., (2010), Antimalarial bromotyrosine derivatives from the Australian marine sponge Hyattella sp, *J Nat Prod*, **73**, 985-987.

Yang X., Feng Y., Duffy S., Avery V. M., Camp D., Quinn R. J. and Davis R. A., (2011), A new quinoline epoxide from the Australian plant Drummondita calida, *Planta Med*, **77**, 1644-1647.

Yao C., Donelson J. E. and Wilson M. E., (2003), The major surface protease (MSP or GP63) of *Leishmania* sp. Biosynthesis, regulation of expression, and function, *Molecular and biochemical parasitology*, **132**, 1-16.

Yardley V., Croft S. L., De Doncker S., Dujardin J. C., Koirala S., Rijal S., Miranda C., Llanos-Cuentas A. and Chappuis F., (2005), The sensitivity of clinical isolates

of *Leishmania* from Peru and Nepal to miltefosine, *Am J Trop Med Hyg*, **73**, 272-275.

Yardley V, Gamarro F, Croft SL., (2010) Antileishmanial and antitrypanosomal activities of the 8-aminoquinoline tafenoquine. *Antimicrob Agents Chemother.;* **54:** 5356–8.

Yin S., Davis R. A., Shelper T., Sykes M. L., Avery V. M., Elofsson M., Sundin C. and Quinn R. J., (2011), Pseudoceramines A-D, new antibacterial bromotyrosine alkaloids from the marine sponge Pseudoceratina sp, *Org Biomol Chem*, **9**, 6755-6760.

Yin S., Davis R. A., Shelper T., Sykes M. L., Avery V. M., Elofsson M., Sundin C. and Quinn R. J., (2011), Pseudoceramines A–D, new antibacterial bromotyrosine alkaloids from the marine sponge Pseudoceratina sp, *Organic & biomolecular chemistry*, **9**, 6755-6760.

Zaghloul I. Y. and Al-Jasser M., (2004), Effect of renal impairment on the pharmacokinetics of antimony in hamsters, *Ann Trop Med Parasitol*, **98**, 793-800.

Zanella F., Lorens J. B. and Link W., (2010), High content screening: seeing is believing, *Trends in biotechnology*, **28**, 237-245.

Zangger H., Mottram J. and Fasel N., (2002), Cell death in *Leishmania* induced by stress and differentiation: programmed cell death or necrosis?, *Cell death and differentiation*, **9**, 1126.

Zhang H.-Z., Kasibhatla S., Wang Y., Herich J., Guastella J., Tseng B., Drewe J. and Cai S. X., (2004), Discovery, characterization and SAR of gambogic acid as a potent apoptosis inducer by a HTS assay, *Bioorganic & medicinal chemistry*, **12**, 309-317.

Zhang J. H., Chung T. D. and Oldenburg K. R., (1999), A Simple Statistical Parameter for Use in Evaluation and Validation of High Throughput Screening Assays, *J Biomol Screen*, **4**, 67-73.

Zhou Y., Messier N., Ouellette M., Rosen B. P. and Mukhopadhyay R., (2004), *Leishmania* major LmACR2 is a pentavalent antimony reductase that confers sensitivity to the drug pentostam, *J Biol Chem*, **279**, 37445-37451.

Zhu X., Pandharkar T. and Werbovetz K., (2012), Identification of new anti*Leishmania*l leads from hits obtained by high-throughput screening, *Antimicrob Agents Chemother*, **56**, 1182-1189.

Zijlstra E. E., (2016), The immunology of post-kala-azar dermal Leishmaniasis (PKDL), *Parasites & vectors*, **9**, 464.

Zijlstra E. E., Musa A. M., Khalil E. A., el-Hassan I. M. and el-Hassan A. M., (2003), Post-kala-azar dermal Leishmaniasis, *Lancet Infect Dis*, **3**, 87-98.

Zilberstein D. and Shapira M., (1994), The role of pH and temperature in the development of *Leishmania* parasites, *Annual Reviews in Microbiology*, **48**, 449-470.

Zulfiqar B., Shelper T. B. and Avery V. M., (2017), Leishmaniasis drug discovery: recent progress and challenges in assay development, *Drug discovery today*. 22(10), 1516-1531.

Zulfiqar B., Jones, A. J., Sykes, M. L., Shelper, T. B., Davis, R. A., & Avery, V. M. (2017). Screening a Natural Product-Based Library against Kinetoplastid Parasites. Molecules, 22(10), 1715.

APPENDIX 1

Assays undertaken by Prof. Maes and colleagues at Department of Biomedical Sciences, Laboratory for Microbiology, Parasitology and Hygiene, University of Antwerp, Belgium.

- ***In vitro L. infantum* MHOM/MA(BE)/67**

Primary peritoneal mouse macrophages (PMM) were used as host cells and were collected 2 days after peritoneal stimulation with a 2% potato starch suspension from Golden Hamster infected with *L. infantum* MHOM/MA(BE)/67. The assay was performed in 96-well microtiter round bottom plates, each well containing 10 µL of the compound dilutions in a 8 point concentration response curve with a top concentration of 64 µM together with 190 µL of macrophage-parasite inoculum ($3x10^5$ cells + $3x10^5$ parasites/well in RPMI-1640 + 5% FBS). After 5 days incubation, total amastigote burden was microscopically assessed using Giemsa staining. The results are expressed as % reduction in parasite burden compared to untreated control wells and an IC_{50} (50% inhibitory concentration) was calculated. miltefosine (IC_{50} = 5.2 + 0.8 µM) was included as reference drug. A concentration response curve was plotted for the compounds **BZ1** and **BZ1-I** to determine their IC_{50} values against *L. infantum* amastigotes.

- ***In vitro T. b. brucei* Squib 427 strain (suramin-sensitive) and *T. b. rhodesiense*.**

T. b. brucei Squib 427 and *T. b. rhodesiense* were maintained in HMI-9 medium, supplemented with 10% FBS. Assay was performed in 96-well microtiter plates, each well containing 10 µL of the compound dilutions in an 8 point concentration response curve with a top concentration of 64 µM together with 190 µL of the parasite suspension (7×10^4 parasites/mL). After 3 days incubation, parasite growth was assessed fluorometrically after addition of resazurin. Fluorescence was measured (excitation 550 nm and emission 590 nm) after 24 hours incubation at 37°C. The results were expressed as % reduction in parasite growth/viability compared to control wells

and an IC_{50} value was calculated. Suramin was included as the reference drug (IC_{50} = 0.12 + 0.07 nM). A concentration response was plotted to determine the IC_{50} of the compounds.

- ***In vitro T. cruzi* Tulahuen LacZ, clone C4 (nifurtimox-sensitive)**

The Tulahuen LacZ, clone C4 (nifurtimox-sensitive) strain was maintained on MRC-5SV2 (human lung fibroblast) cells in MEM medium, supplemented with 200 mM L-glutamine, 16.5 mM NaHC03, and 5% FBS. All cultures and assays were conducted at 37°C under an atmosphere of 5% $C0_2$. Assays were performed in sterile 96-well microtiter round bottom plates, each well containing 10 µL of the compound dilutions in a 8 point with highest concentration of 64 µM with 190 µL of MRC-5 cell/parasite inoculum (2 x 10^4 cells/mL + 2 x 10^5 parasites/mL). Parasite growth was compared to untreated-infected controls (100% growth) and non-infected controls (0% growth) after 7 days incubation. Parasite burdens were assessed after the addition of the substrate CPRG (chlorophenolred ß-D-galactopyranoside): 50µL/well of a stock solution containing 15.2 mg CPRG + 250 µl Nonidet in 100 mL PBS. The change in colour was measured at 540 nm after 4 hours incubation at 37 °C. The results were expressed as % reduction in parasite burdens compared to control wells and an IC_{50} was calculated. Nifurtimox (IC_{50} = 0.845 + 0.2 µM) was included as a reference drug. A concentration response curve was plotted for the compounds **BZ1** and **BZ1-I** to determine the IC_{50} values.

- ***In vitro* K1 strain of *P. falciparum***

Plasmodium falciparum K1 strain (P.falK1) was used which was isolated in Thailand and multidrug resistant to chloroquine, pyrimethamine and cycloguanil. The parasites were maintained in RPMI-1640 medium supplemented with 0.37 mM hypoxanthine, 25 mM Hepes, 25 mM NaHC03, and 10% O^+ human serum together with 2% washed human O^+ erythrocytes. All cultures and assays were conducted under an atmosphere of 4% $C0_2$, 3% 0_2 and 93% N_2. The assay was performed in 96-well microtiter plates, each well containing 10 µL of the watery compound dilutions together with 190 µL of the malaria parasite inoculum (1% parasitaemia, 2% HCT). After 72h incubation, plates were frozen and stored at –20°C. After thawing, 20 µL of each well is transferred into

another 96 well round bottom plate together with 100 µL Malstat® reagent and 20 µL of a 1/1 mixture of PES (phenazine ethosulfaat, 0.1 mg/mL) and NBT (Nitro Blue Tetrazolium Grade III, 2 mg/mL). A change in colour from was measured spectrophotometrically at 655 nm. The results were expressed as % reduction in parasitaemia compared to control wells. Artesunate (IC_{50} = 0.005 + 0.004 µM) and chloroquine (IC_{50}: 0.05 ± 0.08 µM) are included as reference drugs.

APPENDIX 2

Assays undertaken by Prof. Freitas-Junior and colleagues at National Laboratory of Biosciences, National Center for Research on Energy and Materials, Campinas, São Paulo, Brazil.

- ***In vitro L. infantum*** **(MHOM/BR/1972/BH46)**

The efficacy of compounds against *L. infantum* (MHOM/BR/1972/BH46) intracellular amastigotes were tested in dose response (10-point, 2-fold-dilution). THP-1 cells were plated onto 384-well plates (7000 cells/well) in RPMI-1640 medium containing 50 ng/mL phorbol 12-myristate 13-acetate (PMA), and incubated for 48 h. Then, 6 day-old promastigotes were added, at a ratio of 50 parasites per each THP-1 cell seeded earlier. After 24h of infection, negative controls (0.5% DMSO), positive controls (10 μM amphotericin B) or compounds were added to the plate. Assay plates were incubated for 48h, and then fixed with 4% paraformaldehyde and stained with Draq-5. The Operetta high-content automated imaging system was used to acquire images and the Harmony Software was optimized to quantify the host cell number, the infection ratio and the number of parasites per infected cell. The ratio between infected cells and total number of cells was then calculated, and defined as the Infection Ratio (IR). The raw data for IR values were normalized to negative-DMSO (mock)-treated infected cells and positive (noninfected cells) controls to determine the normalized anti-parasitic activity. A concentration response curve was plotted to determine the IC50 of the compounds [2016, N-[4-[Benzyloxy] benzyl]-benzenemethaneamines with High Biological Activity against Intracellular Trypanosoma cruzi and Leishmania infantum Amastigotes].

APPENDIX 3

Assays undertaken by by Dr. De Rycker and colleagues at College of Life Sciences, University of Dundee, United Kingdom.

- ***In vitro L. donovani*** **(MHOM/SD/62/1S-CL2D, LdBOB)**

The concentration response curve was plotted to determine IC_{50} against *L. donovani* (MHOM/SD/62/1S-CL2D, LdBOB) intracellular amastigotes using a phenotypic, high-throughput image-based assay as previously described (De Rycker, *et al.*, 2013).

The efficacy of compounds against *L. donovani* (MHOM/SD/62/1S-CL2D, LdBOB) intracellular amastigotes were tested in dose response. THP-1 cells were plated onto 384-well plates (8,000 per well, 50 µl) in medium containing 10 ng/mL phorbol 12-myristate 13-acetate (PMA), and incubated for 75 h. Then, the cells were washed with PBS supplemented with 1 mM CaCl2, 0.5 mM MgCl2, 0.1% (w/v) bovine serum albumin (PBS-A) and amastigotes (eGFP expressing LdBOB axenic amastigotes) were added, at a ratio of 5 parasites per each THP-1 cell seeded earlier. After 16h of infection, extracellular amastigotes were removed by washing the plates with PBS-A, followed by addition of the compound pre-dilutions and controls (0.5% DMSO_no effect control; 2 µM amphotericin B_maximum effect control). Assay plates were incubated for 72h, and then washed with PBS-A and fixed with 4% paraformaldehyde. After fixation, the wells were washed with PBS, stained (10 µg ml-1 DAPI, 0.4 µg ml-1 HCS Cellmask Deep Red in PBS + 0.1% (v/v) Triton X-100, 30 min, room temperature) and washed with PBS. Then, PBS + 0.05% (v/v) thimerosal was added to the wells and the plates were sealed. The GE IN Cell 1000 or GE IN Cell 2000 automated imaging system was used to acquire images and the GE IN Cell Analyzer 1000 Workstation quantified THP-1 cell count and average number of amastigotes per cell using the "Multi Target Analysis" module. Percent inhibitions was calculated through raw data linear regression by setting the high-inhibition control as 100% and the no-inhibition control as 0%.

APPENDIX 4

Assays undertaken at Discovery Biology, Griffith Institute for Drug Discovery, Griffith University, Australia.

- ***In vitro T. b. brucei* 427 strain.**

The efficacy of compounds against *T. b. brucei* bloodstream form was performed by Dr. Jones using a resazurin- based assay, previously described in the literature (Sykes, *et al.*, 2012). *Trypanosoma brucei brucei* parasites were kindly supplied by Dr. Achim Schnaufer (University of Edinburgh, Edinburgh, Scotland), while at the Seattle Biomedical Research Institute (Seattle, WA). *T. b. brucei* were cultivated in HMI-9 media supplemented with 10% HIFBS, maintained in log-phase growth in 25 cm^2 vented tissue culture flasks by sub-culturing at 48-hour intervals. Cells were grown by incubating in a humidified atmosphere of 5% CO_2 at 37°C.

A volume of 55 µL of 1200 cells/mL *T. b. brucei* cultivated in HMI-9 medium + 10% FBS were added to black, clear bottom 384-well plates (Greiner-bio-one®) and incubated for 24 hours at 37°C/ 5% CO_2. The stocks were diluted 1:21 in high glucose DMEM media without HIFBS using a MiniTrak™ robotic liquid handler (PerkinElmer, Waltham, MA, USA). Compounds were dispensed 1:12, 5 µL in 55 µL using a Minitrack robotic liquid handler and plates incubated for an additional 48 hours at 37°C/ 5% CO_2. Then 10 µL of 0.49 mM resazurin diluted in HMI-9 media was added to the plates using a Multidrop™ 384 Reagent Dispenser (Thermo Scientific®, Newington, NH) and incubated for 2 hours at 37°C/ 5% CO_2 and then incubated in dark for 22 hours at room temperature. The plates were read on an EnVision™ Multilabel plate reader using fluorometry settings with excitation of 530 nm and emission 590 nm.

- ***T. cruzi* Tulahuen intracellular amastigote assay**

The efficacy of compounds against *T. cruzi was* undertaken by Dr. Skyes using a phenotypic, high-throughput image-based assay as previously described (Sykes and Avery, 2015).

Trypanosoma cruzi Tulahuen strain epimastigotes were provided by Professor Frederick Buckner (Washington University, USA). Epimastigotes of *T. cruzi* strains were cultured in liver infusion tryptone (LIT) medium, supplemented with 10% HIFBS and 100IU/mL penicillin/ streptomycin, in 25 cm^2 flasks, in 10 mL, with phenolic, non-vented lids (Corning, NY, USA). Cells were cultured at 28ºC. LIT medium contained 68.4 mM NaCl, 5.37 mM KCl, 45.10 mM Na_2HPO_4, 11.10 mM D- glucose, 50g/L liver extract, 50 g/L tryptone and 50 mg/L hemin. The medium was adjusted to pH 7.2 before autoclaving at 121ºC for 40 minutes. To differentiate epimastigotes to metacyclic trypomastigotes, cells were adjusted to a density of $1x10^6$ cells/mL in LIT medium. Following incubation for 6 days, when cells were estimated to be at the end of the log phase of growth, flasks were harvested by centrifugation at 3000 g for 8 minutes. Epimastigotes were washed twice in PBS, by centrifugation, and resuspended at a density of $5x10^8$ cells in 15 mL centrifuge tubes (Falcon-Corning, USA) in approximately 2-4 mL of artificial triatomine urine (TAU), supplemented with L-proline, L-glutamate, L-aspartate, glucose and 100 IU/mL penicillin/ streptomycin (TAU3AAG). Cells were incubated for 2 hours at 28ºC and subsequently following, were adjusted to $5x10^6$ cells per mL in TAU3AAG.

Briefly, 3T3 (CCL-92, ATCC) host cells in 50 µL of RPMI 1640 growth medium supplemented with 100 IU/mL penicillin/streptomycin and 10% FBS were added to a 384-well collagen I coated plate (CellCarrier, Perkin Elmer, WA, USA), at 1×10^3 cells/well. After 24 hours at 37 °C and 5% CO2, trypomastigotes, from the supernatant of a previously infected culture of 3T3 cells, were added at a multiplicity of infection (MOI) of 5:1 trypomastigotes: host cells. Following 24 hours infection, the medium was removed from plates in a PC2 biosafety cabinet by inverting the plate into a plastic reservoir, followed by the addition of 50 µL of PBS with a Multidrop™ 384 Reagent Dispenser (Thermo Scientific®, Newington, NH). The volume was removed again by inverting the plate. Two wash steps were then undertaken on a Bravo liquid handler (Agilent, USA), by addition and removal of 50 µL of PBS. Compounds in DMSO were pre-diluted 1:21 in water with a MiniTrak™ robotic liquid handler (PerkinElmer, Waltham, MA, USA) and 5 µL of this volume was added to assay plates. The positive controls used to determine the compound activity against the intracellular amastigote form of the parasite and the 3T3 host cell were Nifurtimox and Puromycin, respectively, and the negative control was 0.4 % DMSO. Plates were incubated for 48 hours, the

medium was removed and wells were washed before the addition of 20 µL of 4% paraformaldehyde, containing 0.1% Triton X-100 (Sigma-Aldrich, St Louis, MO, USA) and 0.01 mg/mL Hoescht 3342 (Life Technologies) and incubated for 30 mins at room temperature. Following, 0.05 µg/mL HCS CellMask Green™ (Life Technologies) diluted in RPMI 1640 was added and incubated for 30 min. After a final wash, 20 µL of RPMI 1640 containing 100 IU/mL penicillin/streptomycin was added and plates read by the Opera (Perkin Elmer). Images were captured on an Opera imaging system (PerkinElmer, Waltham, MA, USA), on the Hoechst 3342 and Alexa Fluor 488 channels, at 20× magnification for *T.cruzi* intracellular amastigotes. A script was developed, using the building block commands in the Operetta Imaging system Harmony Software (PerkinElmer, USA).

APPENDIX 5

DMPK studies conducted by Prof. Charman and colleagues at Centre from Drug Candidate Optimisation Monash Institute of Pharmaceutical Sciences, Monash University, Australia.

- **Calculated physicochemical parameters using ChemAxon JChem software**

A range of physicochemical properties evaluating drug-likeness and oral absorption characteristics were calculated using the ChemAxon chemistry cartridge via JChem for Excel software (version 16.4.11). A brief description of each parameter is provided below, along with a suggested ideal range based on research reported in the ADME literature from key industry and academic sources.

MW (< 500): Molecular Weight.

PSApH 7.4 (< 140 Å2): Polar surface area also inversely correlates with membrane permeability.

HBD (< 5) & HBA (< 10): Number of hydrogen bond donors and acceptors gives an indication of the hydrogen bonding capacity, which is inversely related to membrane permeability.

FRB (<10): Number of freely rotating bonds represent the flexibility of a molecule's conformation.

Aromatic Rings (< 4): Total number of aromatic and heteroaromatic rings is also related to molecular flexibility.

Fsp3 (> 0.3): Fraction of sp3 carbons to total carbons indicates the complexity of a molecule's 3D structure.

cpKa: Ionisation constants impact solubility and permeability. Only physiologically relevant predicted values are provided here (i.e. $0 < pKa < 12$).

cLogP/cLogDpH (< 5): Partition coefficients reflect the lipophilic character of the neutral structure, while distribution coefficients reflect the partitioning properties of the ionised molecule at a specific pH.

- **Kinetic Solubility Estimation using Nephelometry (SolpH)**

Compounds were prepared in DMSO and were spiked into either pH 6.5 phosphate buffer or 0.01 M HCl (approx pH 2.0) with the final DMSO concentration being 1%. After 30 minutes had elapsed, samples were analysed via Nephelometry to determine a solubility range.

- **Distribution Coefficient Estimation using Chromatography (gLogDpH)**

Partition coefficient values (LogD) of the test compounds were estimated at pH 7.4 by correlation of their chromatographic retention properties against the characteristics of a series of standard compounds with known and well validated partition coefficient values. The method employed utilised a gradient HPLC based derivation of the method developed by Lombardo *et al* 2001 (Lombardo, *et al.*, 2001).

- ***In vitro* Metabolic Stability**

The metabolic stability assay was performed by incubating each test compound in liver microsomes at 37°C and a protein concentration of 0.4 mg/mL. The metabolic reaction was initiated by the addition of an NADPH-regenerating system and quenched at various time points over a 60 minute incubation period by the addition of acetonitrile containing diazepam as an internal standard. Control samples (containing no NADPH) were included (and quenched at 2, 30 and 60 minutes) to monitor for potential degradation in the absence of cofactor. The human and mouse liver microsomes used in this experiment were supplied by XenoTech. Microsomal incubations were performed at a substrate concentration of 0.5 μM.

APPENDIX 6

Publications arising from research undertaken as part of this Ph.D. listed below are attached with this thesis:

- Zulfiqar, B., Shelper, T. B., & Avery, V. M. (2017). Leishmaniasis drug discovery: recent progress and challenges in assay development. *Drug Discovery Today*. *22*(10), 1516-1531.

- Zulfiqar, B., Jones, A. J., Sykes, M. L., Shelper, T. B., Davis, R. A., & Avery, V. M. (2017). Screening a Natural Product-Based Library against Kinetoplastid Parasites. *Molecules*, *22*(10), 1715.

In order to comply with copyright these articles have not been published here.